Volatile Organic Compounds as Breathomic Biomarkers of Malignant Mesothelioma

Liam David Little

A thesis submitted in partial fulfilment of the requirements of
Sheffield Hallam University
for the degree of Doctor of Philosophy

August 2022

Candidate Declaration

I hereby declare that:

- I have not been enrolled for another award of the University, or other academic or professional organisation, whilst undertaking my research degree.
- None of the material contained in the thesis has been used in any other submission for an academic award.
- I am aware of and understand the University's policy on plagiarism and certify that this thesis is my own work. The use of all published or other sources of material consulted have been properly and fully acknowledged.
- The work undertaken towards the thesis has been conducted in accordance with the SHU Principles of Integrity in Research and the SHU Research Ethics Policy.
- Chapter 4 and 5 were performed in collaboration with Professor Judy Coulson and her lab (University of Liverpool, Department of Cellular and Molecular Physiology). Sections completed by others are specifically referenced in these chapters.
- The word count of the thesis is……37,715

Name	Liam David Little
Award	PhD
Date of Submission	7th August 2022
Faculty	Health and Wellbeing
Director(s) of Studies	Dr Sarah Haywood-Small

Acknowledgements

I would like to start by thanking my supervisory team, my director of studies, Sarah Haywood-Small, Vikki Carolan, Liz Allen, and Laura Cole for all of their support and guidance throughout my PhD. I would also like to thank my collaborators at the University of Liverpool, Judy Coulson, Sarah Barnett, and Martina Tripari, for their help and resources throughout this project. Special thanks to Sue Campbell for your support over the past year. Additionally, thank you to all other staff at Sheffield Hallam University and within the BMRC.

A very big thank you to every single PhD student that I've met over the past few years, without whom the PhD experience would have been completely different. Honorary mention to Katie Kennedy. I met Katie on my very first day and I couldn't have asked for anyone better to go through this with. Thank you for everything and always being there at every step along the way, I couldn't have done this without you.

To all of my friends back home and elsewhere, thank you for everything over the past few years. This experience has made me appreciate how important you all are to me, and I love you all. I would also like to say thank you to all of my family for all of the support and everything else you have given me.

To my Mam, Dawn, and my Dad, Paul, thank you for believing in me more than I could ever believe in myself, I love you both.

Ed infine, l'amore della mia vita, Sonia. Senza di te, non c'è niente. Grazie di tutto, mi porti felicità ogni giorno. Ti amerò per sempre.

Abstract

Malignant pleural mesothelioma (MPM) is an aggressive and incurable cancer with an extremely poor 5-year survival rate. The majority of MPM cases are associated with past exposure to asbestos and the most common route of exposure is through occupation. Current diagnostic methods are invasive, leading to patient discomfort, and often are not capable of diagnosing MPM in the early stages. Most MPM patients are therefore diagnosed at a late stage when treatment options are limited, and overall survival is approximately 12 months. Novel diagnostic methods are required to reliably detect MPM at an early stage, where prognosis and treatment options can be improved. Analysis of volatile organic compounds (VOCs) in exhaled breath has shown the potential to identify MPM patients and therefore provide a non-invasive method of detection through a diagnostic breath test. A VOC based breath test for MPM diagnosis has not yet reached clinical practice. The aim of the current project was to explore *in vitro* VOC analysis within mesothelioma to identify candidate VOC biomarkers at a cellular level and accelerate MPM breath analysis.

To achieve this aim, a gas chromatography-mass spectrometry (GC-MS) method was developed to identify VOCs released from cell cultures. GC-MS was used to detect and identify VOCs in the headspace gas of a panel of MPM and control cell lines, statistical analysis associated specific compounds with MPM. The GC-MS methodology was then used to identify changes in VOC profiles caused by mutations in the BAP1 gene, the most commonly mutated gene in MPM. Finally, GC-MS was used to analyse the headspace gas of MPM cell xenografts generated using a chorioallantoic membrane (CAM) model. This was the first time

that VOCs had been identified from CAM xenografts and represents a progression of pre-clinical VOC analysis methods. The current results show that VOC analysis models are important tools in the progression of MPM breath analysis. Further development of these findings has the potential to lead to a clinical impact and the development of a diagnostic breath test within MPM.

Contents

List of Figures

List of Tables

Abbreviations

2D	Two dimensional
3D	Three dimensional
a.m.u	Atomic mass unit
AAV	Adeno associated viral vector
ADH	Alcohol dehydrogenase
AEx	Previous asbestos exposure
ARD	Asbestos related disease
ATCC	American Type Culture Collection
AUC	Area under the curve
BAP1	BRCA1 associated protein 1
BCA	Bicinchoninic acid
BLD	Benign lung disease
CAM	Chorioallantoic membrane
CAR	Carboxen
CDKN2A	Cyclin dependent kinase inhibitor 2A
CO_2	Carbon dioxide
CT	Computed tomography
DFA	Discriminant function analysis
DVB	Divinylbenzene
EGF	Epidermal growth factor
EGFR	Epidermal growth factor receptor
e-Nose	Electronic-nose
EVOC	Exogenous volatile organic compound
FBS	Foetal bovine serum
FDR	False discovery rate
FID	Flame ionisation detector
GC	Gas chromatography
GC-MS	Gas chromatography-mass spectrometry
H_2O_2	Hydrogen peroxide
HBEC	Human bronchial epithelial cell
HC	Healthy control
HEPES	N-2-hydroxyethylpiperazine-N-2-ethane sulfonic acid

HMGB1	High mobility group box protein 1
HSE	Health and safety executive
IABR	International association of breath research
IASLC	International association for the study of lung cancer
ICI	Immune checkpoint inhibitor
MCC-IMS	Multi-capillary column-ion mobility spectrometry
miRNA	microRNA
MPM	Malignant Pleural Mesothelioma
MRI	Magnetic resonance imaging
NIH	National institutes of health
NIST	National institute of standards and technology
NSCLC	non-small cell lung cancer
NTD	Needle trap device
O_2	Oxygen
$OH^{\cdot}$	Hydroxyl radical
ONS	Office for national statistics
OPLS-DA	Orthogonal partial least squares-discriminant analysis
PBS	Phosphate buffered saline
PCA	Principal component analysis
PD-(L)1	Programmed death ligand 1
PDMS	Polydimethylsiloxane
pen/strep	Penicillin/streptomycin
PET-CT	Positron emission tomography-computed tomography
PLS-DA	Partial least squares-discriminant analysis
ppb	Parts per billion
ppt	Parts per trillion
PTEN	Phosphatase and tensin homolog
PTFE	Polytetrafluoroethylene
PTR-MS	Proton-transfer-reaction mass spectrometry
ROC	Receiver operating characteristic
ROS	Reactive oxygen species
RT	Retention time
SDS-PAGE	Sodium dodecyl-sulphate polyacrylamide gel electrophoresis
SIFT-MS	Selected-in flow-tube mass spectrometry

SMRP	Soluble mesothelin-related peptide
SPME	Solid-phase microextraction
SV40	Simian virus 40
TD	Thermal desorption
TNM	Tumour, node, metastasis
TP53	Tumour protein 53
TSG	Tumour suppressor gene
ULA	Ultra-low adhesion
v/v	Volume/volume
VOC	Volatile organic compound
WHO	World Health Organisation

1 General Introduction

1.1 Introduction to Cancer

Cancer is an umbrella term for a vast variety of diseases that can occur in cells, tissues and organs across the entire human body. Cancer is one of the leading causes of mortality worldwide, accountable for almost 10 million deaths caused in 2020 according to the World Health Organisation (WHO). The leading sites of cancer associated with mortality include lung, colorectal, liver, stomach and breast cancer (Siegel et al., 2022). Although they can occur in different sites, diseases that are defined as cancer share the same biological traits – the uncontrolled division of genetically mutated cells (Torre et al., 2016). In the development of cancer, normal healthy cells develop genetic mutations which drive tumourigenesis, leading to malignant transformation and tumour development (Crosby et al., 2022). Hereditary germline mutations can result in individuals being more susceptible to developing certain types of cancer (Carbone et al., 2020). The risk of cancer development also depends on external factors including lifestyle, diet, alcohol use, cigarette smoking, UV exposure and infection with cancer-associated viruses (human papilloma virus, simian virus 40) (Wu et al., 2018). Often, risk of cancer combines both extrinsic factors as well as intrinsic genetic factors (Wu et al., 2018).

As well as uncontrolled proliferation, the biological capabilities that all cancers develop during tumourigenesis have been presented as the hallmarks of cancer (Hanahan & Weinberg, 2011). These include six fundamental hallmarks: sustaining proliferative signalling, evading growth suppressors, resisting cell death, enabling replicative immortality, inducing angiogenesis and activating invasion and metastasis (Hanahan & Weinberg, 2011). The original hallmarks have been updated to include four tumour enabling characteristics including:

genome instability and mutation, tumour-promoting inflammation, deregulating cellular energetics and avoiding immune destruction (Hanahan & Weinberg, 2011). Recently, these biological capabilities have been updated even further to include unlocking phenotypic plasticity, non-mutational epigenetic reprogramming, polymorphic microbiomes and senescent cells (Hanahan, 2022). These hallmarks provide a framework for the study of cancer and are important considerations when conducting research regarding any tumour type.

1.2 Malignant Mesothelioma

1.2.1 General Introduction to Mesothelioma

Malignant mesothelioma is an extremely aggressive and incurable malignancy which arises from pathological transformation of mesothelial cells forming the lining of the body's internal organs (Figure 1.1). These serous membranes surrounding the pleura, peritoneum, pericardium and tunica vaginalis provide a lubricated, non-adhesive surface due to their double monolayer structure (Hiriart et al., 2019). Malignant pleural mesothelioma (MPM) is the most common form of mesothelioma, with peritoneal, pericardial and tunica vaginalis tumours occurring at a much lower incidence (Abdel-Rahman, 2018). Mesothelioma has a long-established causative link to previous exposure to asbestos, a group of naturally occurring silicate mineral fibres (Wagner et al., 1960). The risk of mesothelioma development has been found to be increased in areas that previously saw high production and use of asbestos, such as northwest Europe (Wilk & Krówczyńska, 2021). Non-asbestos causes of mesothelioma include other mineral fibres such as erionite, previous radiotherapy, carbon nanotubes and SV40 infection (Attanoos et al., 2018).

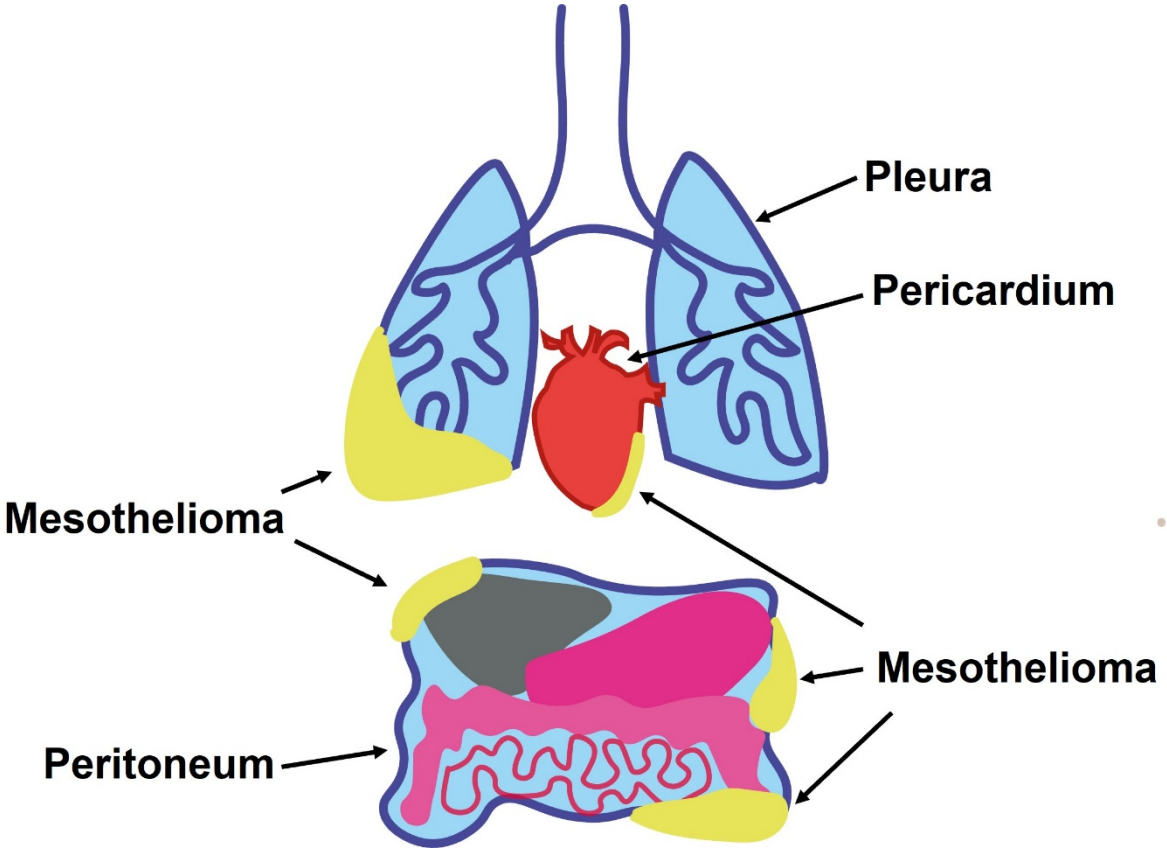

Figure 1.1: Original figure - Mesothelioma is a malignancy that occurs in the serous membranes surrounding the lungs (pleura), the abdomen (peritoneum), heart (pericardium) and tunica vaginalis (not shown).

Mesothelioma is an inflammatory cancer – asbestos fibres generate reactive oxygen species (ROS), causing oxidative stress, chronic inflammation and frustrated phagocytosis (Brusselmans et al., 2018). Due to the bio-persistence of fibres, this inflammatory response is not resolved, which over a prolonged period of time leads to DNA mutations and chromosomal aberrations (Yap et al., 2017). This environment supports the growth of mesothelial cells that have acquired genetic mutations and ultimately leads to the development of mesothelioma (Carbone et al., 2019). Although the precise series of mutations leading to mesothelioma development is not as well defined as some other cancers, mesothelioma is still underpinned by the accumulation of genetic damage and a number of associated genes have been identified (Carbone et al., 2019). Several of the well-established tumour-suppressor genes (TSG) include BAP1 (Wang, A. et al., 2016), CDKN2A (Hylebos et al., 2016), TP53 and PTEN (Sementino et al., 2018). A lack of oncogenic driver mutations may in part explain mesothelioma's prolonged incubation period, of up to 50 years, from the initial exposure to asbestos (Carbone et al., 2019). Instead, the development of mesothelioma may rely on the slower accumulation of TSG mutations, which over time fulfil the hallmarks of cancer and lead to malignancy.

Clinically, the most significant gene associated with mesothelioma development is BAP1 (Carbone et al., 2020). Germline mutations in the BAP1 gene are associated with the tumour predisposition syndrome, which was discovered in families with a high hereditary burden of mesothelioma (Carbone et al., 2007). Carriers of germline BAP1 mutations are much more likely to develop multiple cancers throughout their lifetime, including mesothelioma (Carbone et al., 2020).

Individuals with BAP1 mutations are also more sensitive to asbestos, with lower levels of exposure capable of initiating mesothelioma development (Carbone et al., 2019).

The extended asbestos incubation period also explains why mesothelioma is still prominent, even though legislation was introduced in the mid-1980's to control the use of asbestos. In countries that saw widespread asbestos use in the 20th century such as the UK, USA, Australia and Western Europe, mesothelioma incidence has increased, with these countries having some of the highest age-standardised incidence rates in the world (Carbone et al., 2019). As well as this, approximately 80% of the global population live in countries without strict asbestos controls (Abdel-Rahman, 2018; Yap et al., 2017), highlighting mesothelioma as a prominent worldwide public health issue for potentially years to come.

1.2.1.1 Mesothelioma Demographics

Worldwide mesothelioma is a relatively rare cancer with 30,443 new cases and 25,576 deaths reported in 2018 (Sung et al., 2021). According to the Health and Safety Executive (HSE), there were 2369 mesothelioma deaths in Great Britain in 2019 and approximately the same number of new cases (Mesothelioma statistics for Great Britain, 2021). Historically, mesothelioma was strongly associated with males, rather than females, because of the link to occupational asbestos exposure (Røe & Stella, 2015). This is reflected in the current statistics; male deaths still make up the majority, however, this number has decreased recently, and the number of female deaths has remained at a similar level (Mesothelioma statistics for Great Britain, 2021). A consequence of the

prevalence of asbestos in the UK, the total number of deaths caused by mesothelioma has increased rapidly over the past 50 years (Figure 1.2A). Mesothelioma cases are expected to reach a plateau and potentially decline over the coming years due to the effects of the control of asbestos (Figure 1.2B). Although the incidence and deaths attributed to mesothelioma are relatively rare compared to other cancers, the survival rate is estimated to be the lowest of all cancer types (Mutti et al., 2018). According to the Office of National Statistics, the 5-year survival rate for all persons diagnosed with mesothelioma is just 6.5% (ONS, UK).

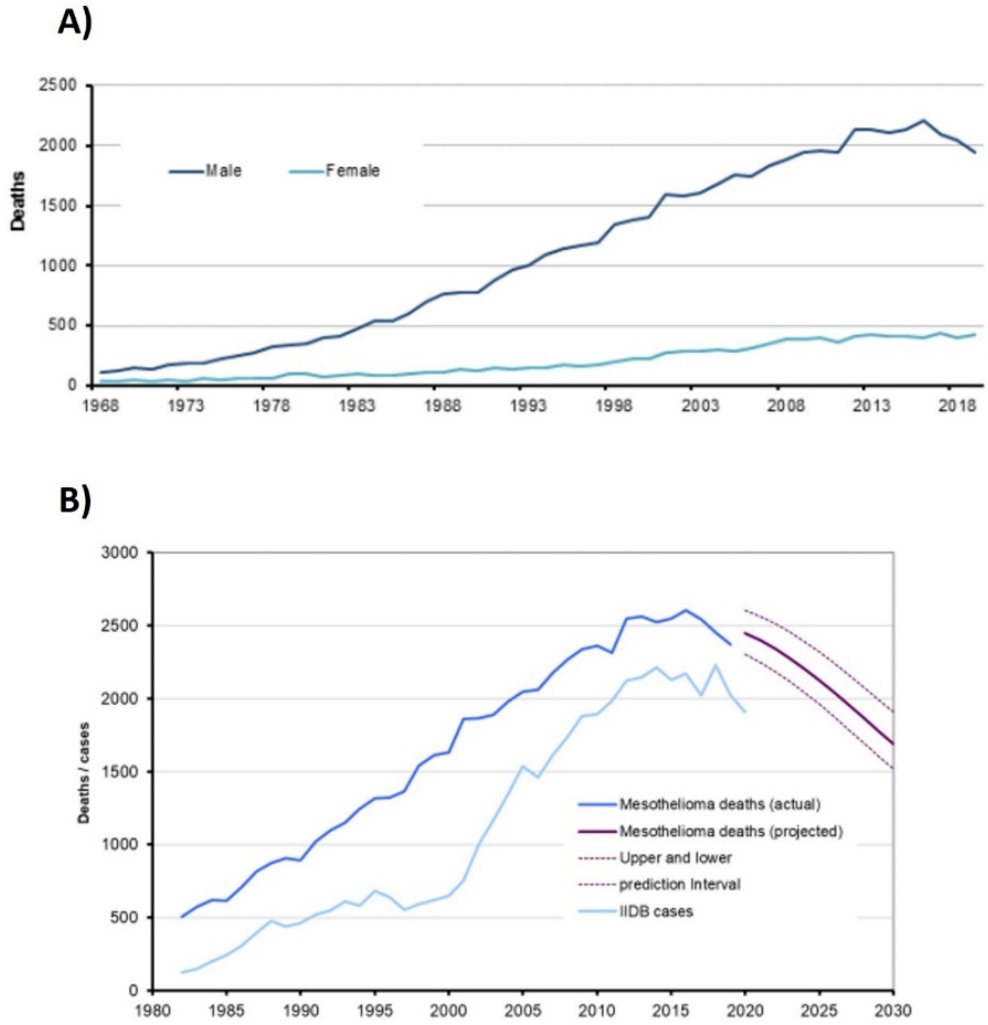

Figure 1.2: A) Mesothelioma annual deaths for Great Britain. B) Mesothelioma annual deaths and projected future deaths to 2030 in Great Britain. Figures taken from HSE.gov.uk Mesothelioma statistics for Great Britain, 2021. IIDB: Industrial Injuries Disablement Benefit.

1.2.1.2 Mesothelioma Classification

MPM is the most common form of mesothelioma, arising in the mesothelial cells of the pleura, surrounding the lungs (Hiriart et al., 2019). MPM represents between 70-90% of total mesothelioma cases (Hiriart et al., 2019). Approximately 20% of mesothelioma cases occur in the peritoneum, with the remainder occurring in the pericardium, testis and tunica vaginalis at much lower levels (Mezei et al., 2017). Mesothelial cells have the capacity to differentiate into cells with several phenotypes with characteristics from fibroblasts, smooth muscle and endothelial cells (Lansley et al., 2011). Following this, it is possible for mesothelioma tumours to contain multiple cell phenotypes. The three mesothelioma subtypes are epithelioid, sarcomatoid and biphasic, which is a combination of both epithelioid and sarcomatoid (Galateau-Salle et al., 2016). Epithelioid is the most common subtype and offers the best prognosis with sarcomatoid having the worst prognosis (Galateau-Salle et al., 2016). The prognosis of biphasic mesothelioma can change depending on the percentage of epithelioid and sarcomatoid cells present (Meyerhoff et al., 2015).

MPM has an official staging system: Stage I – the cancer is localised on a single layer of the pleura; Stage II – the cancer has spread to a single lung and lymph nodes; Stage III – the cancer has spread into nearby organs and deeper tissues in the chest wall; Stage IV – the cancer has metastasised to sites such as the chest, abdomen, neck and bones (Berzenji et al., 2018). The International Association for the Study of Lung Cancer (IASLC) also recommends a tumour, node, metastasis (TNM) grading system to help with staging in MPM diagnosis.

1.2.2 Asbestos

The majority of mesothelioma cases are still linked to some form of previous asbestos exposure, most commonly through occupational exposure in the workplace (Hiriart et al., 2019). However, it is possible to be exposed to asbestos in other ways. For example: fibres incorporated into the structure of buildings constructed in the 20th century may still contain asbestos which can be released due to damage or incorrect removal and levels of asbestos may be present in the environment in some areas (Alpert et al., 2020). Firefighters also have a higher incidence of asbestos exposure and large volumes of fibres have been released into the environment during catastrophic events such as the September 11th terror attack (de la Hoz et al., 2019).

Asbestos is the common name for a group of naturally occurring silicate mineral fibres that saw widespread use in the 20th century within construction and manufacturing industries (Røe & Stella, 2015). Asbestos fibres possess high tensile strength as well as insulating properties against heat, fire and corrosion (van Zandwijk et al., 2020). This, combined with their fibrous nature, led to the incorporation of asbestos fibres into material for construction and shipbuilding, motor parts and many other commercially available products including jewellery and cigarette filters (Røe & Stella, 2015). Asbestos fibres can be classified into two main groups based on their structure: amphibole fibres and serpentine fibres (Solbes & Harper, 2018). Serpentine fibres, which consist of chrysotile alone, have a short and curved structure in contrast to amphibole fibres, which are straight and long (van Zandwijk et al., 2020). The amphibole class consists of more than one fibre type including crocidolite, amosite, tremolite, anthophyllite and actinolite (Solbes & Harper, 2018). Asbestos fibres were commonly identified

based on their colour: chrysotile as “white asbestos”, crocidolite as “blue asbestos” and amosite as “brown asbestos” (Bononi et al., 2015).

1.2.2.1 Asbestos Linked Mesothelioma Pathogenesis

Despite previous discussion surrounding the carcinogenic capacity of serpentine vs amphibole asbestos, both fibre types have now been classified as carcinogenic with the ability to induce genetic mutations and chromosomal aberrations (Yap et al., 2017). The most common route for asbestos fibres entering the body is via inhalation through the lungs. Once inhaled, fibres can enter the lymphatic system, resulting in transportation around the body and deposition in the serous membranes – most commonly the pleura (Hiriart et al., 2019). Once lodged in mesothelial cells, asbestos fibres initiate the production of ROS, cycles of chronic inflammation and frustrated phagocytosis which are unable to be resolved due to the fibre’s bio-persistence (Yap et al., 2017). This creates an environment which favours both the development of genetic mutations and the proliferation of mesothelial cells with genetic abnormalities (Brusselmans et al., 2018). As previously mentioned, this causes mutations in key TSGs including BAP1, CDKN2A, TP53, PTEN and others until the development of MPM is reached (Hylebos et al., 2016; Sementino et al., 2018; Wang et al., 2016).

1.3 Malignant Pleural Mesothelioma

MPM is the most common form of mesothelioma accounting for 70-90% of mesothelioma cases (Hiriart et al., 2019) and has a poor median survival of between 9 and 12 months (Brims, 2021). Between 1994 and 2016 almost 50,000 MPM deaths were recorded in Europe, accounting for 54% of total malignant

mesothelioma deaths worldwide (Brims, 2021). Current issues within MPM include early diagnosis and effective treatment options. Research into these areas is critical for the progression of MPM, leading to the detection of patients at an earlier stage when therapeutic intervention would have more of an impact.

1.3.1 Malignant Pleural Mesothelioma Diagnosis

Obtaining an effective diagnosis is one of the main issues faced clinically with MPM. It is currently extremely difficult to identify the disease in its early stages, in part due to the prolonged incubation period since initial asbestos exposure (Carbone et al., 2019). Symptoms often only present once the cancer has progressed to a very late stage; at this point the signs of MPM are not very specific including breathlessness, chest pains and pleural effusions (Blyth & Murphy, 2018). After a patient presents these symptoms, definitive MPM diagnosis must be confirmed through invasive methods including chest CT scan and biopsy followed by histological examination (Brusselmans et al., 2018). Similarities to lung carcinomas, combined with the multiple epithelioid, sarcomatoid and biphasic subtypes, can lead to the misdiagnosis of MPM and inappropriate treatment regimens (Yap et al., 2017).

A typical MPM diagnostic workflow is presented in Figure 1.3. After presenting with general symptoms, MPM is investigated through imaging procedures starting with chest X-ray before moving on to others including CT scan and MRI scan (Bianco et al., 2018). Definitive diagnosis of MPM requires invasive procedures, including biopsy and fine-needle aspiration, to obtain the tumour tissue samples required for histological and molecular analysis (Bianco et al., 2018). The

invasiveness of the definitive diagnostic procedures (Figure 1.3) result in extreme discomfort for the MPM patients. As these workflows also currently struggle to diagnose MPM patients at an early stage, it is important to explore novel diagnostic methods that can identify patients earlier and with less discomfort.

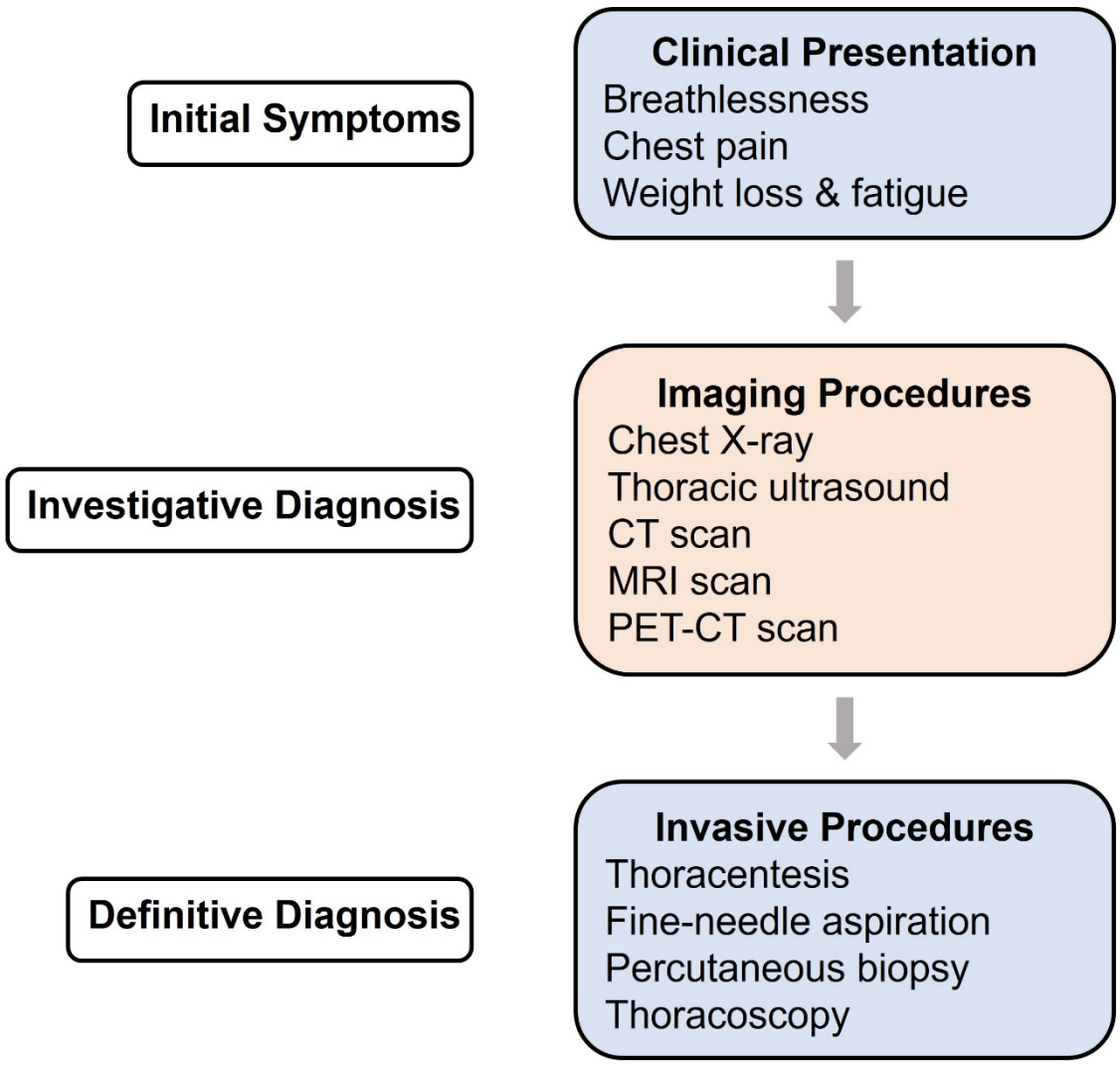

Figure 1.3: A typical MPM diagnostic workflow, adapted from Bianco *et al.*, (2018).

1.3.1.1 Malignant Pleural Mesothelioma Treatment

Inefficient diagnosis methods combined with the prolonged incubation period result in MPM patients often being diagnosed at a very late stage, with only palliative treatment options available (Zalcman et al., 2015). Prognosis at the point of diagnosis is poor, with an overall survival of just 12-14 months following combined pemetrexed and platinum compound therapy (Zalcman et al., 2015). An additional compound, bevacizumab, has also been shown to provide a limited additional benefit on top of pemetrexed and platinum therapy (Zalcman et al., 2015). Research into the use of other immunotherapies is also being pursued within MPM, with clinical trials publishing results of PD-(L)1 and CTLA-4 inhibitors both individually and in combination (de Gooijer et al., 2020). There appears to be a group of MPM patients that stand to benefit from this type of immunotherapy, with further research required to understand the role of immunotherapy in MPM treatment in the future (de Gooijer et al., 2020). Surgery within MPM is also a possibility when macroscopic complete resection can be achieved (Bueno & Opitz, 2018).

In order to improve patient survival and treatment options, an increased number of patients must be identified to enrol onto clinical trials (Cherrie et al., 2018). Most importantly, patients with early stage MPM must be identified to allow for long term monitoring of disease progression and improvements in treatment response (Cherrie et al., 2018).

1.3.2 Malignant Pleural Mesothelioma Biomarker Development

An ideal biomarker needs to provide sensitive and specific biological information about a particular disease. Within cancer, clinically used biomarkers are based on genes, proteins and other molecules to build a picture of each tumour and inform prognosis and treatment options (Goossens et al., 2015). The requirement for novel diagnostic methods within MPM has led to research into potentially suitable candidate biomarkers identified in biological samples such as blood or pleural effusions (Lagniau et al., 2017). One of the most extensively studied biomarkers is the protein mesothelin and its counterpart soluble mesothelin-related peptide (SMRP) (Schillebeeckx et al., 2021). Mesothelin is usually expressed on mesothelial cells and is involved in cell-to-cell interactions and cellular adhesion (Lagniau et al., 2017). Although mesothelin has shown some promising results in the identification of MPM, it is not sensitive enough to be used as a single diagnostic biomarker (Schillebeeckx et al., 2021). Analysing mesothelin and SMRP in combination with other proteins such as osteopontin and megakaryocyte potentiating factor in order to improve diagnostic accuracy within MPM has been explored (Lagniau et al., 2017). Other candidate biomarkers have also been studied including high mobility group box protein 1 (HMGB1) and microRNAs (miRNA), and current results suggest a biomarker panel may be necessary to identify MPM at the sensitivity and specificity required (Schillebeeckx et al., 2021)

The search for suitable biomarkers has led to the development of breathomics and breath analysis within MPM, which may solve sensitivity issues and provide a non-invasive method of diagnosis.

1.4 Breath Analysis

1.4.1 History

Breath analysis is a relatively recent field of research; however, the association of an unusual or distinctive odour on an individual's breath and the presence of a particular disease has been recognised since ancient times. Hippocrates described *fetor oris* and *fetor hepaticus,* associating breath odour with disease (Dweik & Amann, 2008). Following this, the breath of those with diabetes was described as having the scent of decaying apple as early as 1798 (Dweik & Amann, 2008; Ruzsányi & Péter Kalapos, 2017). This was later shown in the 1800s to be caused by the presence of acetone in the breath of diabetic individuals (Dweik & Amann, 2008; Ruzsányi & Péter Kalapos, 2017). These early developments underline the basic principles of breath analysis: the ability to identify specific signals in exhaled breath which may produce a particular "scent" and are indicative of the presence of disease. In theory, this could make the process of identifying and diagnosing diseases as easy and as non-invasive as measuring the composition of someone's breath. In 1971, 250 compounds were detected in exhaled breath using gas-liquid partition chromatography (Pauling et al., 1971). This major development within breath analysis signified the era of modern breath analysis, which is also often called "Breathomics".

1.4.2 Modern Breath Analysis

The field of breath analysis has progressed alongside the development of more complex analytical methods such as gas chromatography-mass spectrometry (GC-MS) (Amann et al., 2014). In addition to the expected gases – oxygen, carbon dioxide (CO_2), nitrogen and water vapour – thousands of other compounds have also been identified in exhaled breath (Amann et al., 2014;

Dweik & Amann, 2008). Compounds present in human breath include other gases such as nitric oxide and carbon monoxide, but the vast majority of breath molecules are organic chemicals known as volatile organic compounds (VOCs) (Amann et al., 2014). A single exhaled breath can contain hundreds of different VOCs (Issitt et al., 2022). Exhaled breath also consists of a liquid phase known as exhaled breath condensate which consists of aerosol droplets containing other non-volatile molecules such as proteins, amino acids, nucleic acids and peptides (Campanella et al., 2019). The balance of research and progression within breath analysis does however lean towards VOCs and as such the current project aimed to focus on these compounds.

1.4.3 Volatile Organic Compounds

VOCs are a highly diverse group of organic chemicals with high vapour pressure and a molecular weight of less than 350 a.m.u which therefore exist in a gaseous state at human body temperature (Issitt et al., 2022). VOCs have been identified in exhaled breath, urine, faeces, saliva, skin, sweat and also released from human cell lines cultured *in vitro* (Amann et al., 2014; Filipiak et al., 2016; Monedeiro et al., 2020). The total composition of VOCs released from the human body has been termed the “volatilome” and an online database cataloguing these compounds has over 1000 individual entries at the time of writing (Pleil & Williams, 2019). Research into the use of VOCs in disease diagnosis and monitoring has expanded rapidly and breath analysis has shown promise in multiple types of cancer (Einoch Amor et al., 2019), asthma (Brinkman et al., 2020) and other inflammatory conditions (Christiansen et al., 2016).

The exact mechanisms underlying the production and release of VOCs has not been fully elucidated, however much progress has been made in understanding the biology of these compounds. At a cellular level, VOCs are both released and taken up by cells in all tissues and organs within the body (Issitt et al., 2022). VOCs can diffuse into and out of blood circulation, leading to the transportation of compounds around the body and eventual release in breath via gas exchange in the lungs (Brusselmans et al., 2018; Issitt et al., 2022). VOCs present in breath can come from either endogenous or exogenous sources (Issitt et al., 2022). Endogenous compounds are produced and released by cells in the body and are highly researched as they are considered to be candidate biomarkers that can provide important information relating to diseases (Gaude et al., 2019). The suggested mechanisms responsible for the production of VOCs involve oxidative stress and lipid peroxidation (Ratcliffe et al., 2020). Normal cells produce ROS such as hydrogen peroxide (H_2O_2) and hydroxyl radicals ($OH^{\cdot}$) which are also frequently elevated in response to disease conditions (Ratcliffe et al., 2020). Lipid peroxidation caused by ROS oxidative attack has been mechanistically shown to be able to produce a large number of VOCs that are present in breath (Ratcliffe et al., 2020).

In contrast exogenous VOCs derive from external sources such as diet and environmental exposure. They enter the body, are subject to circulatory transportation and cellular metabolism before leaving the body again in exhaled breath (Gaude et al., 2019). The metabolic relationships that exogenous VOCs exhibit suggest that these compounds may be used to measure metabolic function through the administration of “EVOC probes” (Gaude et al., 2019; Murgia et al., 2021). For example, there appears to be an association between breath

limonene levels and liver dysfunction, leading to the possibility of measuring the metabolism of an EVOC limonene probe in the detection of chronic liver diseases (Murgia et al., 2021). Focussing on the response to one particular VOC target has been suggested to provide more valuable information regarding metabolism, rather than measuring total breath output which contains many VOC signals and can be influenced by multiple confounding factors (Gaude et al., 2019).

1.4.3.1 VOC Sampling and Analysis

Exhaled breath is an abundant biological matrix, however due to the gaseous nature of samples, specialised collection and storage methods are required for VOC analysis. In the past, Tedlar® bags have provided a straightforward and economic method of exhaled breath collection and they maintain stable VOC levels over short storage periods (Beauchamp et al., 2008). Subsequently, numerous publications have used Tedlar® bags to collect breath (Altomare et al., 2013; de Gennaro et al., 2010; Di Gilio et al., 2020; Lamote et al., 2017), resulting in this methodology becoming the most prominently used for the sampling of VOCs from exhaled breath (Di Gilio et al., 2020b). Sampling procedures with Tedlar® bags involve an equilibration period where patients breathe tidally through a mouthpiece that contains a VOC filter to remove exogenous VOCs (Altomare et al., 2013; de Gennaro et al., 2010). After this, a single deep inspiration is taken followed by exhalation of full vital capacity volume (total air exhaled) into the Tedlar® bag – this process can be repeated in order to fill the volume of the bag (Altomare et al., 2013; de Gennaro et al., 2010; Di Gilio et al., 2020; Lamote et al., 2017).

The concentrations of VOCs released in breath have been reported in the low parts per billion (ppb) to parts per trillion (ppt) levels, meaning that a pre-concentration step is necessary to obtain an adequate analysis (Brusselmans et al., 2018). Common methods of VOC concentration involve solid-phase microextraction (SPME) and thermal desorption (TD) tubes (Issitt et al., 2022). VOCs have been transferred from a Tedlar bag to a SPME fibre simply by exposing the fibre to the inside of the bag for a short period of time (Papaefstathiou et al., 2020). In a similar manner, the contents of Tedlar bags have been transferred directly to TD tubes, thereby concentrating the sampled VOCs (Di Gilio et al., 2020b). Needle trap devices (NTD) are also an alternative micro-extraction technique for the pre-concentration of VOCs from breath which can be used with standard GC-MS systems (Bellagambi et al., 2020). More recently, improved systems for the collection of VOCs in exhaled breath have been developed including the ReCIVA device from Owlstone medical (Abderrahman, 2019). This custom face mask aims to standardise breath sampling, aiding reproducibility by controlling variables such as flow rate and collecting VOCs directly onto TD tubes (Abderrahman, 2019).

After breath sampling and pre-concentration, VOCs must be detected and identified using an analytical technique. GC-MS is still considered the gold standard for VOC analysis and is frequently used in breath analysis studies (Di Gilio et al., 2020). With GC-MS, separation of a complex mixture of VOCs can be achieved along with simultaneous tentative identification through mass spectra matching to the NIST library database (Sparkman et al., 2011). GC-MS sample introduction is compatible with SPME, TD tubes and NTD (Sugita & Sato, 2021). Alternatives to GC-MS are also available including proton-transfer-reaction mass

spectrometry (PTR-MS), selected-ion flow-tube mass spectrometry (SIFT-MS) and multi-capillary column-ion mobility spectrometry (MCC-IMS), which all provide real time on-line analysis of exhaled breath (Henderson et al., 2020; Lamote et al., 2017b). Pattern recognition using chemical sensors such as electronic-Noses (e-Noses) have also been explored as a point-of-care analysis option within breath analysis; these devices react to the complete profile of VOCs in a sample but do not identify specific compounds (Lamote et al., 2017).

1.5 Mesothelioma Breath Analysis

Breath analysis provides an attractive option for MPM diagnosis – a reliable source of biological information that can be non-invasively collected could potentially solve the issues currently faced clinically. Over the past two decades, a number of studies have been published focusing on breath analysis within mesothelioma, using a range of different analytical techniques (Table 1.4).

Table 1.4: Publications researching breathomics, breath analysis or volatile organic compounds within the diagnosis of malignant mesothelioma. e-Nose: electronic nose, GC-MS: gas chromatography mass spectrometry, MCC-IMS: multi-capillary column-ion mobility spectrometry.

Article Reference	VOC Analysis Method
Disselhorst et al., 2021	e-Nose
Di Gilio et al., 2020	GC-MS
Lamote et al., 2017	GC-MS/e-Nose
Lamote et al., 2017b	MCC-IMS
Lamote et al., 2016	MCC-IMS
Chapman et al., 2012	e-Nose
Dragonieri et al., 2011	e-Nose
De Gennaro et al., 2010	GC-MS

These techniques include GC-MS, MCC-IMS and e-Nose, with each having their own set of advantages and disadvantages when it comes to the analysis of VOCs (Figure 1.4). Despite being not as well developed as lung cancer research, MPM VOC analysis studies have explored different areas of breath analysis and provided a strong foundation for research into a mesothelioma breath test.

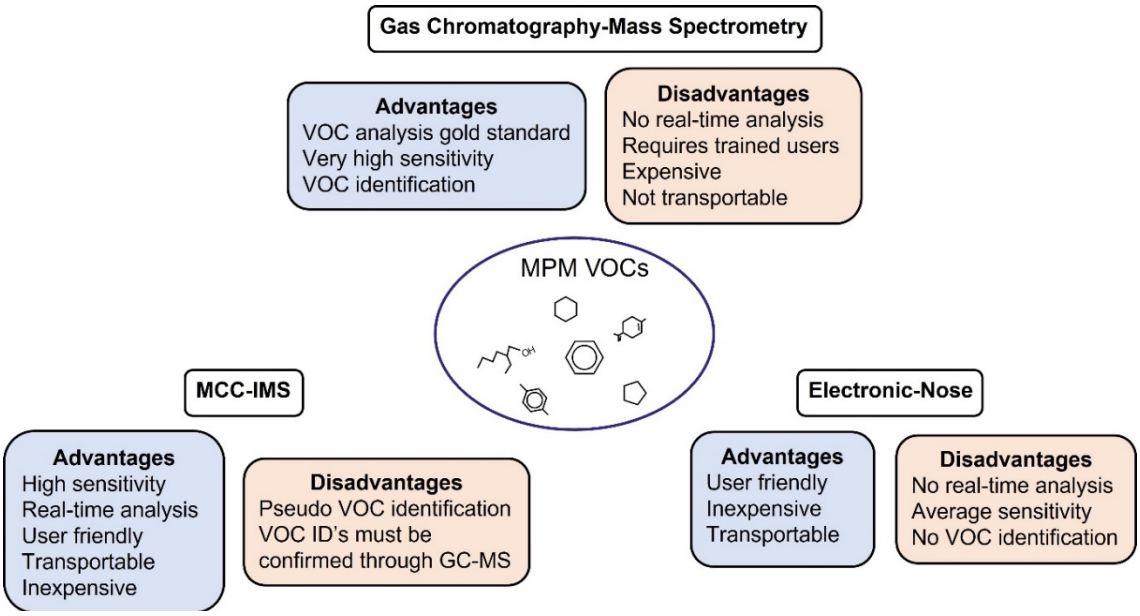

Figure 1.4: Analytical techniques that have been used for MPM VOC detection and identification. Advantages and Disadvantages adapted from Brusselmans *et al.,* (2018).

1.5.1 GC-MS Analysis

GC-MS is an analytical technique used for the identification and quantification of VOCs (Catino et al., 2019); several studies used GC-MS to analyse MPM patient breath (Table 1.4). Encouragingly, all studies that used GC-MS as an analysis method used the same method for sample collection – breath sampling in a Tedlar® bag, transfer to TD tubes and analysis with GC-MS (de Gennaro et al., 2010; Di Gilio et al., 2020; Lamote et al., 2017). Differences in GC-MS systems, TD tube sorbent material, GC column and oven temperature programming meant that the analysis was not exactly the same between the three studies (de Gennaro et al., 2010; Di Gilio et al., 2020; Lamote et al., 2017), but comparisons between the results can still be made in some cases.

All studies sampled breath from MPM patients, healthy controls (HC) and previously asbestos-exposed (AEx) groups (de Gennaro et al., 2010; Di Gilio et al., 2020; Lamote et al., 2017); one study also included an asbestos related diseases (ARD) group consisting of patients with well-defined benign asbestos-related diseases such as pleural plaques and asbestosis (Lamote et al., 2017). De Gennaro *et al.,* specified that the AEx group consisted of individuals with long-term professional exposure to asbestos whereas the other two studies described this group as asymptomatic former asbestos exposed (Di Gilio et al., 2020; Lamote et al., 2017). Regardless of these definitions, asbestos-exposed individuals have an increased risk of developing MPM, with the AEx group representing those that could benefit the most from the early diagnosis of MPM with a breath test (de Gennaro et al., 2010; Di Gilio et al., 2020; Lamote et al., 2017).

The breath VOCs from the MPM group were compared to those from the other clinical groups. Following data reduction and visualisation, principal component analysis (PCA) showed separation between MPM, AEx and HC groups based on VOC profiles which was also confirmed through discriminant function analysis (DFA) achieving complete separation of the groups (de Gennaro et al., 2010). After these initial results, GC-MS data was used to make several different comparisons between the groups: receiver operating characteristic (ROC) curves were generated and the sensitivity and specificity of each model was determined (Lamote et al., 2017). MPM vs HC had a sensitivity of 64.3% and a specificity of 78.6%, MPM vs AEx a sensitivity of 92.9% and a specificity of 100%, and MPM vs ARD a sensitivity of 78.6% and specificity of 80.0% (Lamote et al., 2017). MPM was compared to both AEx and ARD combined with a sensitivity of 100% and a specificity of 91.2% (Lamote et al., 2017). AEx and ARD groups were the most similar to each other with the model showing a sensitivity of 60.0% and a specificity of 42.1% (Lamote et al., 2017).

ROC curves were again generated to determine the discrimination between different MPM and HC groups, achieving a 93% accuracy (Di Gilio et al., 2020). In contrast to the other studies, the third paper used the data from the AEx group as an independent validation of the MPM vs HC model by processing the AEx samples blindly and assessing their prediction to either MPM or HC (Di Gilio et al., 2020). The prediction model showed average performance: after further diagnosis with CT scan, two cases that were predicted to be HC were proved to be healthy and one case that was predicted as MPM proved to be MPM (Di Gilio et al., 2020). However, the remaining AEx cases were classified as MPM by the

prediction model, with the presence of pleural plaques as the suggested cause of this (Di Gilio et al., 2020).

The differences in statistical analysis methods shown within the studies is reflective of the complexity of the data that is produced using GC-MS analysis. A single GC-MS run can achieve the separation and detection of several hundred VOCs with associated chromatographic data including RTs and peak areas, as well as MS data for compound identification (Töreyin et al., 2020). A single unified method for analysis of GC-MS VOC data has yet to be accepted; all three studies used different statistical methods which did, however, follow the same general path of data reduction and then visualisation of the differences between groups (de Gennaro et al., 2010; Di Gilio et al., 2020; Lamote et al., 2017). Concordantly, all studies showed that discrimination was possible between MPM groups and HCs based on the analysis of breath VOCs (de Gennaro et al., 2010; Di Gilio et al., 2020; Lamote et al., 2017). These findings suggested that MPM VOC profiles are distinctive from HCs and forms the basis of using a diagnostic breath test within mesothelioma. The inclusion of other clinical groups such as AEx and ARD were also important validation steps as these groups commonly need to be distinguished from MPM patients clinically.

The use of GC-MS as an analytical method meant that a number of the VOCs used for the discrimination between the different groups were able to be tentatively identified (Table 1.5). Lamote *et al.,* also reported compounds that were unable to be identified but were still used in discrimination models by reporting the Kovats retention index of each unidentified VOC (Lamote et al., 2017).

Table 1.5: Mesothelioma breath analysis studies that used GC-MS as an analytical method and the potentially important candidate VOCs that were identified. Compounds highlighted in bold were identified across more than one study.

Article Reference	Important VOCs Identified with GC-MS
Di Gilio et al., 2020	benzene, **benzonitrile**, p-benzoquinone, **2-ethyl-1-hexanol**, ethylbenzene, 2,2,4,6,6-pentamethyl-heptane, **α-pinene**, 1-propanol, **toluene**
Lamote et al., 2017	**benzonitrile**, bromobenzene, chloroform, **cyclohexane**, 1,2-dichlorobenzene, 1,3-dichlorobenzene, diethyl ether, ethanol, **2-ethyl-1-hexanol**, furfural, hexamethyldisiloxane, hexane, isoprene, isothiocyanato-n-butylbenzene, **limonene**, linalole, methylbenzoate, methyl-cyclopentane, 3-methylpentane, 2-methyl-1-propanol, naphthalene, nonanal, nonane, phenol, **β-pinene**, propylbenzene, 1,2,3-trichlorobenzene, 1,2,4-trichlorobenzene, 2,2,4-trimethyl-pentane, tert-butylbenzene, **xylene**
De Gennaro et al., 2010	acetophenone, benzaldehyde, **cyclohexane**, cyclopentane, decane, dimethylnonane, dodecane, **limonene**, methylcyclohexane, methyl-octane, 1,2-pentadiene, **α-pinene**, **β-pinene**, styrene, trimethylbenzene, **toluene**, **xylene**

Again, the three studies used different criteria for determining which compounds were the most important for MPM discrimination, but α-pinene, β-pinene, 2-ethyl-1-hexanol, benzonitrile, toluene, cyclohexane, limonene and xylene were identified across multiple studies (Table 1.5). Unfortunately, there were no compounds that were present in all three studies (de Gennaro et al., 2010; Di Gilio et al., 2020; Lamote et al., 2017). However, it is encouraging that even from a limited number of studies, the same VOCs have begun to be identified as important in the discrimination of MPM. In order to progress the development of a MPM breath test, it is important to understand the biological origins of compounds such as these, if they are specific to MPM, and if the identification of MPM depends on the analysis of singular VOCs or the profiles of a more comprehensive VOC panel.

1.5.2 On-line Breath Analysis

MCC-IMS was used as an alternative to GC-MS for the analysis of MPM patient breath samples (Lamote et al., 2016; Lamote et al., 2017b). Using this methodology, breath was sampled in real time and directed to an MCC-IMS for immediate analysis (Lamote et al., 2016); meaning that pre-concentration and sample transfer processes weren't required. Initial results showed discrimination between MPM, AEx and HC groups, however MCC-IMS does not specify VOC identities meaning that a comparison to GC-MS data could not be performed (Lamote et al., 2016). This also does not rule out the possibility that the same VOCs were analysed both by MCC-IMS and GC-MS (Lamote et al., 2016). Further groups were then included for MCC-IMS analysis, including ARD, primary

lung cancer and benign lung diseases unrelated to asbestos exposure (BLD) (Lamote et al., 2017b). The sensitivity and specificity for MPM identification was in line with what was previously reported; however, good discrimination was also observed in identifying MPM patients from lung cancer and BLD groups (Lamote et al., 2017b). MPM can often be mistaken for carcinomas of the lung, leading to incorrect diagnosis and inappropriate treatment (Yap et al., 2017). Other groups such as AEx and ARD are at an increased risk of MPM development (Lamote et al., 2017b). The results from these studies are important in showing that MPM patient breath is distinct from other common malignancies and at-risk individuals, providing evidence for the high specificity required for a breath test to become a viable option in clinical practice.

1.5.3 Electronic-Noses

e-Noses are chemical sensing devices that can react to patterns of VOCs in a gaseous sample (Dragonieri et al., 2017). In contrast to other analytical methods, e-Noses do not analyse individual VOCs but react to the overall pattern of compounds within a sample, providing on-line analysis with real-time discrimination of “breathprints” from different groups (Dragonieri et al., 2017). The use of e-Noses has been explored within MPM (Table 1.4) as these devices may provide a cost-effective and easy, point-of-care solution for MPM breath analysis.

The Cyranose 320, a commonly used handheld e-Nose, was used to analyse the breath of MPM, AEx, ARD and HC patients (Chapman et al., 2010; Dragonieri et al., 2011). A change in the e-Nose sensor resistance was caused by the breath

of each patient, resulting in a unique sensor response and distinct breathprint (Chapman et al., 2010; Dragonieri et al., 2011). PCA score plots generated from e-Nose data showed discrimination between MPM, AEx and HC groups; the strongest differentiation was between MPM and AEx individuals (Dragonieri et al., 2011). These results were replicated, whilst also considering ARD samples, and a sensitivity of 90% and specificity of 88% was observed for the discrimination between MPM, ARD and HC groups (Chapman et al., 2012). This specificity was increased to 91% when identifying MPM patients from HCs alone (Chapman et al., 2012). These studies showed that despite the lack of VOC identification associated with e-Noses, these sensors were still able to detect changes in the breath of MPM patients compared to other groups.

A direct comparison was also performed between e-Nose and GC-MS; the same discrimination between groups was observed, with a slightly lower sensitivity and specificity when using e-Nose (Lamote et al., 2017). The validation of e-Nose against the gold standard GC-MS was an important finding in the case for using an e-Nose clinically. e-Noses can be programmed or “trained” to a smaller panel of VOCs, rather than all compounds present in a breath sample, which can increase the sensitivity for a specific diagnostic situation (Dragonieri et al., 2011). As a standard, untrained, e-Nose showed concordant results with GC-MS (Lamote et al., 2017), the ability to train a device to react to a smaller set of MPM specific VOCs has the potential to increase the performance even further.

Most recently, a SpiroNose e-Nose was used to measure MPM patient breath profiles in response to immune checkpoint inhibitor (ICI) treatment as part of the

INITIATE trial (Disselhorst et al., 2021). Exhaled breath analysis using the SpiroNose was performed on MPM patients treated with nivolumab (anti PD-1) and ipilimumab (anti CTLA-4) at baseline and again after six weeks of treatment (Disselhorst et al., 2021). Statistical analysis of e-Nose data showed that baseline exhaled breath analysis was able to discriminate between responders to nivolumab plus ipilimumab and non-responders (Disselhorst et al., 2021). Previously it has been difficult to identify MPM patients that would benefit from ICI treatment due to a lack of available biomarkers (Disselhorst et al., 2021). The SpiroNose results showed that responders to ICI treatment had a distinctive breath VOC profile that was identifiable even before treatment had started (Disselhorst et al., 2021), indicating that breath analysis may be an option to determine which patients receive this treatment.

As it is still unclear what a MPM breath test, or one for any other disease, will look like in clinical practice, it is important for future studies to continue with different methodologies such as e-Nose. Comparison between different techniques will also further validate the results from a particular methodology, as seen with the similar discrimination of clinical groups in the GC-MS e-Nose comparison (Lamote et al., 2017). These methodologies can also feed into each other, informing future research. Confirming the identities of specific VOCs using GC-MS is the first step required in the development of a breath test. After that, replication of results and training with an e-Nose may lead the way for a point-of-care device to be used clinically.

1.6 *In Vitro* VOC Analysis

1.6.1 Cell Culture VOC Analysis

As with the majority of disease related research, *in vitro* models are often required to complement and inform clinical studies in order to fully comprehend an area of research. Within breath analysis, a large body of work has been published exploring VOCs identified at an *in vitro* level in comparison to those detected in exhaled breath (Table 1.6). *In vitro* populations that can be analysed include bacterial, fungal, viral, primary human and secondary human cell lines, the latter of which have found growing interest in the search for endogenously produced human VOCs (Filipiak et al., 2016). The current project focussed on MPM specific VOCs released from secondary human cell lines, therefore the remainder of this introduction will focus on compounds from secondary cell cultures.

Table 1.6: Articles published since 2018 using *in vitro* VOC analysis methods. PubMed search terms: ((cells) OR (cell line) OR (cell culture)) AND ((volatile organic compounds) OR (VOCs) OR (headspace)). TFME: thin-film microextraction.

Article Reference	Disease/Cell Type	Sample/Analysis Method
Astolfi et al., 2022	Multiple cell types	Chemo-sensor
Piqueret et al., 2022	Breast Cancer	Animal-Based (Ants)
Janssens et al., 2022	MPM & Lung Cancer	TD-GC-MS
Filipiak et al., 2021	Lung Cancer	TFME-GC-MS
Jiang et al., 2021	Breast Cancer	SPME-GC-FID
McCartney et al., 2021	Viral Infection	TD-GC-MS
Campanella et al., 2021	Hippocampal Neural Cells	SPME-GC-MS
Cassagnes et al., 2020	Epithelial Cells	PTR-MS
Chuang et al., 2020	Lung Cancer	SPME-GC-MS
Zanella et al., 2020	Lung Cancer	SPME-GCxGC-MS
Furuhashi et al., 2020	Lung Cancer	TD-GC-MS
Amaro et al., 2020	Renal Cell Carcinoma	SPME-GC-MS
Taware et al., 2020	Breast Cancer	SPME-GC-MS
Leiherer et al., 2020	Gastric Cancer	NTD-GC-MS
Traxler et al., 2019	Viral Infection	NTD-GC-MS
Liu et al., 2019	Colorectal Cancer	SPME-GC-MS
McCartney et al., 2019	CHO & T Cells	TD-GC-MS
Longo et al., 2019	Inflammation	GC-MS
Liu et al., 2019	Colorectal Cancer	SPME-GC-MS
Klemenz et al., 2019	Stem Cells	NTD-GC-MS
Yamaguchi et al., 2019	Epithelial Cells	TD-GC-MS
Liu et al., 2019	Breast Cancer	SPME-GC-MS
Wang et al., 2019	Colorectal Cancer	SPME-GC-MS
Serasanambati et al., 2019	Lung Cancer	GC-MS
Purcaro et al., 2018	Viral Infection	SPME-GCxGC-MS
Li et al., 2018	Fibroblast Cells	SPME-GC-MS
Yamaguchi et al., 2018	Epithelial Cells	TD-GC-MS
Lawal et al., 2018	Epithelial Cells	TD-GC-MS
Traxler et al., 2018	Stem Cells	NTD-GC-MS
Jia et al., 2018	Lung Cancer	SPME-GC-MS
Rodrigues et al., 2018	Bladder Cancer	SPME-GC-MS
Lima et al., 2018	Prostate Cancer	GC-MS
Thriumani et al., 2018	Lung Cancer	SPME-GC-MS & Sensor
Bischoff et al., 2018	Stem Cells	NTD-GC-MS
Purcaro et al., 2018b	Viral Infection	SPME-GCxGC-MS

The “headspace gas” above growing cell cultures contains VOCs released directly from cells that can be used as a representative model for exhaled breath analysis (Filipiak et al., 2016). *In vitro* analysis of cell cultures can avoid many of the confounding factors that influence VOC content in breath and therefore enable identification of compounds from a cell population of a single type (Filipiak et al., 2016; Jia et al., 2019). As in exhaled breath, the concentration of VOCs present in the headspace gas of cell cultures is also in the ppb-ppt range, with *in vitro* analysis also requiring a pre-concentration step. Commonly, this is performed using thermal desorption techniques such as SPME, TD tubes and NTDs which have been adapted for use with standard cell culture flasks (Table 1.6).

For example, the headspace gas of cell cultures has been drawn out of the culture vessels and onto Tenax TD tubes in order to sample VOCs (Janssens et al., 2022). In contrast to this active sampling technique, SPME has been used as a passive sampling technique to take a representative VOC sample of cell culture headspace (Table 1.6). An example of this was used to measure the effects of oxidative stress on the VOC profiles of breast cancer cells (Liu et al., 2019). As well as this, a NTD was used to sample VOCs from gastric cancer cell lines by drawing a small volume of the culture headspace gas onto a sorbent material packed micro-needle device (Leiherer et al., 2020). Other studies have also adapted e-Nose style chemo-sensors (Astolfi et al., 2022), PTR-MS (Cassagnes et al., 2020) and even animal-based sensing models (Piqueret et al., 2022).

Progression of GC-MS analysis has also been explored with the use of tandem GCxGC-MS (Zanella et al., 2020).

One of the main advantages of *in vitro* analysis systems when compared to exhaled breath studies is the ability to manipulate the experimental conditions in order to determine the effects of specific biological processes on VOC profiles. These experiments can be relatively straightforward; for example: the treatment of cells with H_2O_2 in order to induce oxidative stress and measure the subsequent change in VOCs (Baranska et al., 2015; Liu et al., 2019b). Experiments have also been focussed more on the early diagnosis of cancer, with the effects of lung cancer specific genetic mutations on VOC profiles having previously been explored (Davies et al., 2014). There is a wide scope for these experiments in the future: various biological treatments can be applied to *in vitro* models, with the measurement of VOC profile changes as the output.

1.6.2 Mesothelioma *In Vitro* Analysis

In contrast to the much more developed investigation of lung cancer, in the initial phases of the current project only one study had researched MPM cell culture headspace (Gendron et al., 2007). An e-Nose was used to analyse a panel of lung cancer and mesothelioma cell lines. The MPM cell line, REN, was differentiated from non-small cell lung carcinoma and human airway smooth muscle cell lines based on VOC pattern recognition using the e-Nose (Gendron et al., 2007). This study was restricted to just one MPM cell line and the use of an e-Nose meant that the specific identities of the discriminating VOCs were not

available (Gendron et al., 2007). Despite these limitations, this study did provide an initial proof of concept for the use of MPM cell lines as a model for breath analysis. Differences were also shown between MPM cells, lung cancer cells and normal airway cells (Gendron et al., 2007). These factors were often not considered in *in vivo* breath analysis studies and highlight the impact that *in vitro* models can have on MPM breath analysis as a whole. This research could be expanded further through the use of multiple cell lines and analysis with GC-MS to identify specific compounds and compare with *in vivo* studies. In spite of the initial promising results, *in vitro* MPM VOC analysis remained an un-researched field until the current project began, with further studies instead focussing on patient breath.

Much more recently, an *in vitro* model was used to characterise the headspace gas of six MPM cell lines and two lung cancer cell lines using TD-GC-MS (Janssens et al., 2022). The VOC profiles identified included compounds such as alkanes, aldehydes, ketones and alcohols and discrimination was achieved between MPM subtypes and the lung cancer groups (Janssens et al., 2022). This study was published in the late stages of the current project and contains many similar themes and research elements that will be discussed in more detail later in this thesis. Even with this additional study, *in vitro* MPM VOC analysis remains an under researched field which could benefit from the direction shown within lung cancer research. MPM is a cancer that is much rarer and less well understood than lung cancer, which therefore requires *in vitro* models to fully research it. The current issues with diagnosis and poor survival rate also show

that MPM is a cancer that stands to benefit greatly from the potential of VOC analysis and a non-invasive diagnostic breath test.

1.7 Development of *In Vitro* MPM VOC Analysis

Following on from the initial *in vitro* MPM VOC analysis study (Gendron et al., 2007), a number of research areas were identified for the current PhD project. These were designed to progress *in vitro* MPM VOC analysis, reflecting current research trends within MPM diagnosis and breath analysis.

The first of these was the identification of MPM associated VOCs at a cellular level, through headspace gas analysis of cell cultures using GC-MS. Identifying a panel of compounds from these experiments was designed to complement the previous patient breath analysis studies and accelerate the development of VOC biomarkers. Headspace gas analysis of 2D cell cultures also allows for the manipulation of experimental conditions and therefore changes in VOCs can be associated with specific biological processes. Within MPM, the main area for this experimentation was the induction of genetic mutations and the subsequent identification of any VOC changes through headspace gas analysis. Finally, the development of *in vitro* and pre-clinical models of breath analysis was identified as an area which could benefit from progression within the breath analysis field. For this step, 3D cell culture techniques were considered for the progression from 2D monolayer cultures.

1.8 Aims and Objectives

The aim of this project was to explore *in vitro* VOC analysis within mesothelioma in order to identify candidate VOC biomarkers at a cellular level and accelerate mesothelioma breath analysis. In order to achieve this the following objectives were investigated:

- Develop a GC-MS methodology capable of identifying VOCs released from cell cultures.

  Hypothesis: It is possible to detect and identify VOCs released into the headspace of cell cultures using a SPME GC-MS methodology.
- Use the developed methodology to identify VOCs released from a panel of MPM cell lines.

  Hypothesis: MPM cells produce distinct VOC profiles when analysed with SPME GC-MS. MPM cells can be distinguished from control cell lines and other MPM phenotypes based on VOC profiles.
- Explore the effects of specific mesothelioma associated genetic mutations on VOC profiles produced *in vitro*.

  Hypothesis: MPM associated mutations in the BAP1 gene affect VOC profiles.
- Develop the pre-clinical VOC analysis methods currently available through the use of 3D cell culture techniques.

  Hypothesis: VOCs can be detected and identified from 3D models of MPM.

2 Optimisation of a Solid-Phase Microextraction Gas Chromatography-Mass Spectrometry Method for Volatile Organic Compound Identification from Cell Cultures

2.1 Introduction

Despite the growing research interest in breath analysis and the numerous studies that have used *in vitro* models to study VOCs, a single definitive method for the analysis of these compounds has yet to be accepted (Table 1.3). GC-MS is still considered the gold standard for VOC analysis as complex mixtures of compounds can be separated and identified through spectral match to a database such as the NIST library (Sparkman et al., 2011). However, many GC-MS methodology parameters can be optimised in order to achieve the best analysis (Schafer et al., 2019). Previous studies have attempted to compare and standardise headspace gas analysis in cell cultures (Schallschmidt et al., 2015), yet differences in methodology still persist in the current literature (Table 1.3). The complex VOC profiles detected from the headspace of cell cultures (Amaro et al., 2020) means that method optimisation is required to effectively separate and detect the compounds present. Often optimisation is a balance between developing the most optimal method, the time this takes to optimise and also the time needed to analyse a single sample. For the current study, a method was required to identify VOCs that were released from MPM cell cultures.

2.1.1 Pre-concentration of Volatile Organic Compounds

VOCs in both exhaled breath and cell culture headspace are present at very low concentrations, meaning that a pre-concentration step is required to obtain a sufficient sample prior to analysis (Baranska et al., 2015; Lamote et al., 2017; Schallschmidt et al., 2015). TD tubes have been recognised as an optimal approach to VOC pre-concentration in untargeted biomarker discovery studies

(Rattray et al., 2014). TD tubes contain a combination of absorbent materials that can trap VOCs in a gaseous sample as they are actively passed through the tube (Rattray et al., 2014). The high capacity of TD tubes means they have a high sensitivity for VOC collection (Rattray et al., 2014). Experimental set-ups have been developed to flush the headspace gas of cell culture flasks onto TD tubes while at the same time maintaining the culture at 37^{o}C (Baranska et al., 2015; Janssens et al., 2022). Analysis of the VOCs was then performed with GC-MS – TD tubes were heated in a thermal desorption unit that released VOCs onto the GC-MS column for analysis (Baranska et al., 2015; Janssens et al., 2022).

A passive sampling alternative to TD tubes, SPME, has previously been used in the pre-concentration of VOCs from cell culture headspace (Liu et al., 2019; Liu et al., 2019b; Schallschmidt et al., 2015). SPME is an analytical preparation technique widely used across environmental, food, pharmaceutical and biological industries, as well as research (Sajid et al., 2019). One of the main uses of SPME is in aroma characterisation and quality control of natural and commercial products including plants and food items such as oils, coffee and cheese (Stashensko et al., 2007). The development of SPME was designed to minimise the use of organic solvents, providing a preparation technique which can directly extract analytes from a given sample either through headspace analysis or direct immersion (Sajid et al., 2019; Schafer et al., 2019). Headspace analysis involves sampling compounds from the gas above a sample in an enclosed environment such as a sample vial, whereas in direct immersion the SPME fibre is submerged in a liquid sample for extraction (Bojko, 2022).

Manual SPME fibre assemblies resemble a modified gas-tight syringe (Figure 2.1). The fibre itself is a 1-2cm section of sorbent material attached to a metal support and housed within a retractable septum piercing needle. The O-ring and adjustable needle guide can be used to set the depth of the fibre, exposing the septum piercing needle. Depressing the plunger pushes the SPME fibre out of the needle and can be held in place with the retaining screw and the Z-slot. The manual fibre assembly does not require anything additional for sampling and is therefore portable. Samples can be extracted *in situ* and the SPME fibre retracted back into the assembly before analysis. SPME fibres with different coatings can be changed in and out of the assembly depending on the properties of the target analytes. The adaptability, portability and ease of use means that SPME has seen more widespread use in cell culture headspace gas sampling than TD tubes (Table 1.3).

It was decided to use SPME as the VOC pre-concentration technique, the fibre chosen for this project was a 50/30µm divinylbenzene/Carboxen/polydimethylsiloxane (DVB/CAR/PDMS) (Supelco; Sigma Aldrich). The multi-phase coating of this fibre is designed for both absorption and adsorption, with the manufacturers recommending this for volatile and semi-volatile compounds with a range of C3-C20 (MW 40-275). A manual fibre assembly was chosen with this fibre, allowing for VOC extraction *in situ* where required and direct analysis with GC-MS. The use of SPME also meant that any additional components associated with TD tubes were not required and the sampling methodology could be optimised over a shorter period of time.

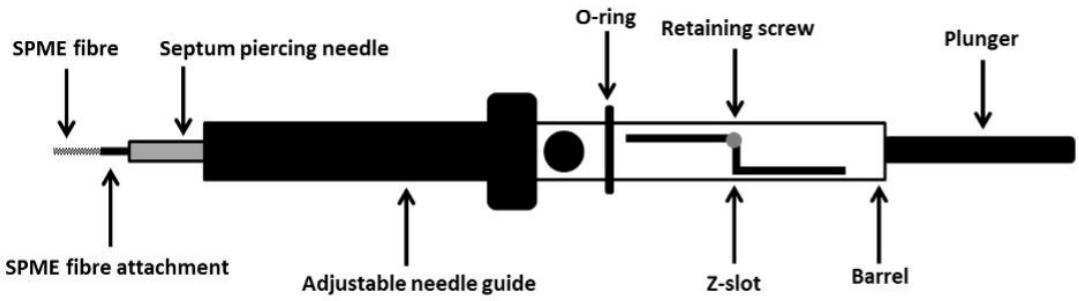

Figure 2.1: The components of a manual SPME fibre assembly with SPME fibre attached. Original figure based on a Supelco manual SPME fibre assembly and SPME fibre.

2.1.2 The Peppermint Initiative

Breath and VOC analysis has now been explored across a wide range of disease diagnosis and monitoring settings, encompassing a number of different VOC sampling and analytical techniques (Henderson et al., 2020). It has been speculated that this variability may be one of the reasons for the current lack of repeatable research findings within the breath analysis community (Henderson et al., 2020; Wilkinson et al., 2021). The peppermint initiative was therefore established within the International Association of Breath Research (IABR) with the aim of benchmarking and standardising breath analysis experiments using peppermint oil capsules (Henderson et al., 2020; Wilkinson et al., 2021). Peppermint oil contains a complex mixture of VOCs, and the majority of the peppermint initiative research focuses on exhaled breath, the ingestion of capsules and the measurement of metabolism in breath (Henderson et al., 2020). However, *in vitro* headspace analysis of peppermint capsules was also performed using TD GC-MS and direct sampling using a gas-tight syringe (Wilkinson et al., 2021). In this chapter, peppermint capsules were also analysed and compared with the previously identified compounds to assess the performance of the developed method.

2.2 Aims of the Chapter

The aim of this chapter was to develop a SPME GC-MS method that could be used to identify VOCs released from cell cultures. The first objective was to develop an initial GC flame ionisation detection (FID) method to show if this methodology was appropriate for the samples. The choice of sample preparation

was also included in this method. The second objective involved the transfer of the GC-FID method to GC-MS in order to obtain tentative identification of compounds. The next objective was to refine the GC-MS methodology so that it was capable of detecting changes in VOCs when analysing cell cultures compared to media-only controls. The final objective was to measure the performance of the method against the current literature by analysing VOCs released from peppermint capsules.

2.2.1 Hypothesis

It is possible to detect and identify VOCs released into the headspace of MPM cell cultures using a SPME GC-MS methodology.

2.3 Methods

2.3.1 Gas Chromatography-Flame Ionisation Detector (Method A)

2.3.1.1 Method A Sample Preparation

Samples were prepared in two ways: sampling in headspace vials or direct sampling in cell culture flasks. For headspace vials, complete RPMI-1640 (Thermo Fisher) was prepared by adding 10% volume/volume (v/v) foetal bovine serum (FBS) and 1% v/v penicillin/streptomycin (pen/strep) (Sigma Aldrich). Complete RPMI-1640 was incubated in standard T25 cell culture flasks for 24 hours at 37^{o}C with 5% CO_2. After incubation 5ml complete RPMI-1640 was removed and sealed in a 20ml glass headspace vial with a

polytetrafluoroethylene (PTFE)/silicone cap. Sealed headspace vials were incubated at 40°C for 30 min prior to VOC extraction. For direct sampling, either 5ml complete RPMI-1640 or $1x10^6$ MSTO-211H cells with 5ml medium were prepared in T25 flasks and incubated for 24 hours at 37°C with 5% CO_2. After incubation VOCs were extracted directly from the flask headspace.

2.3.1.2 Method A VOC Extraction

A new 50/30µm DVB/CAR/PDMS SPME fibre with a manual sampling assembly (Supelco; Sigma Aldrich) was conditioned according to the manufacturer's instructions at 270°C for 30 min prior to initial use. The SPME fibre was further conditioned for 10 min at the start of each day prior to sampling. For headspace vials, the SPME fibre assembly was inserted through the PTFE/silicone seal and secured with Parafilm. The SPME fibre was exposed to the headspace gas above samples for 20 min at 40°C. For direct sampling, the SPME fibre assembly was inserted directly through the culture flask caps and exposed to the headspace gas in the flasks for 20 min at 37°C with 5% CO_2. After VOC extraction, the SPME fibre was retracted back into the fibre assembly and analysed using GC.

2.3.1.3 Method A Gas Chromatography

An Agilent HP-6890 with a Rtx-5 column (15m x 0.32mm x 0.25µm; Restek; Saunderton, UK) was used for analysis. The inlet temperature was set to 280°C. The oven temperature programming was as follows: 40°C for 3 min, ramped to 260°C at 8°C/min and held at 260°C for 4.5 min. The total run time was 35 min.

The SPME fibre assembly was injected manually into the inlet and the fibre exposed for 1 min at the start of the oven temperature program.

2.3.1.3.1 Method A VOC Standards Mix

A mixture of VOC standards was analysed to assess the GC method performance – EPA VOC Mix 2 was purchased from Sigma Aldrich which contained 13 volatile compounds at 2000ppm (Table 2.1). 1µl of EPA VOC Mix 2 was injected directly into the GC inlet using a gas-tight syringe.

Table 2.1: Volatile components included in EPA VOC Mix 2 and the order of elution.

Elution Order	Compound
1	Benzene
2	Toluene
3	Ethylbenzene
4	m-xylene
5	Styrene
6	Bromo-benzene
7	1,3,5-trimethylbenzene
8	1,2,4-trimethylbenzene
9	p-isopropyl-toluene
10	n-butyl-benzene
11	1,2,4-trichlorobenzene
12	Naphthalene
13	1,2,3-trichlorobenzene

2.3.2 Transfer to Gas Chromatography-Mass Spectrometry (Method B)

2.3.2.1 Method B Sample Preparation

$2x10^6$ MSTO-211H cells were seeded in T25 cell culture flasks with 5ml complete RPMI-1640 and incubated at 37°C with 5% CO_2 for 24 hours. Flasks containing 5ml RPMI-1640 only were also incubated at 37°C with 5% CO_2 for 24 hours. After incubation VOCs were extracted directly from the headspace of flasks following Section 2.3.1.2.

2.3.2.2 Method B VOC Standards Mix

EPA VOC Mix 2 was diluted to a final concentration of 1ppm in dH_2O and sealed in a 20ml glass headspace vial with a PTFE/silicone cap. Sealed vials were incubated at 40°C for 30 min and VOCs extracted from headspace following Section 2.3.1.2.

2.3.2.3 Method B Gas Chromatography-Mass Spectrometry

GC-MS analysis was performed using an Agilent 7890A with a HP-5MS column (30m x 0.25mm x 0.25µm; Agilent) and a MS-5975C triple axis detector. The GC-MS inlet temperature was set to 250°C. The oven temperature programming was as follows: 40°C for 3 min, ramped to 260°C at 8°C/min and held at 260°C for 4.5 min. The total run time was 35 min. The injection mode was changed from split-less to a 1:5 split. The MS transfer line was set to 280°C and analysis was performed in full scan mode with a range of 35-300 a.m.u. After VOC extractions,

the SPME fibre assembly was injected directly into the inlet of the GC-MS and the fibre was exposed for 1 min at the start of the oven temperature program.

2.3.3 Refinement of Gas Chromatography-Mass Spectrometry (Method C)

2.3.3.1 Method C Sample Preparation

MSTO-211H and RPMI-1640 flasks were prepared as in Section 2.3.2.1.

2.3.3.2 Method C VOC Standards Mix

EPA VOC Mix 2, spiked with additional cyclopentane and cyclohexane (Fisher Scientific), was diluted to a final concentration of 500ppb in dH_2O and sealed in a 20ml glass headspace vial with a PTFE/silicone cap. Sealed vials were incubated at 40^{o}C for 30 min and VOCs extracted from headspace following Section 2.3.1.2.

2.3.3.3 Method C Gas Chromatography-Mass Spectrometry

Refinements were made to the GC-MS method presented in Section 2.3.2.3. A Rtx-VMS capillary column was used (30m x 0.25mm x 1.4µm; Restek). The GC-MS inlet temperature was set to 250^{o}C. The oven temperature programming was as follows: 35^{o}C for 5 min, ramped to 140^{o}C at 4^{o}C min^{-1} and held for 5 min, ramped again to 240^{o}C at 20^{o}C min^{-1} and held for 4 min. The total analysis time was 45.25 min. The oven temperature programming was based on a previously published SPME GC-MS method, with slightly altered initial and final temperatures (Schallschmidt et al., 2015). The MS transfer line was set to 260^{o}C

and analysis was performed in full scan mode with a range of 35-300 a.m.u. The injection mode was returned to split-less and a SPME inlet liner was used to improve peak shape. After VOC extractions, the SPME fibre assembly was injected directly into the inlet of the GC-MS and the fibre was exposed for 10 min at the start of the oven temperature program.

2.3.4 Peppermint Capsule Analysis

200mg peppermint oil food supplement capsules were purchased from Boots UK Ltd (product no. 87-61-558, batch no. 240152). One pierced capsule was sealed in a 20ml headspace vial with a PTFE/silicone cap and incubated at 40^{o}C for 30 min. After incubation, capsule headspace was sampled with SPME for 15 min at 40^{o}C. The SPME fibre was analysed following Section 2.3.3.3. Compounds identified were compared to those previously published, identified by an alternate headspace GC-MS method (Wilkinson et al., 2021).

2.4 Results

2.4.1 Gas Chromatography-Flame Ionisation Detector (Method A)

Across three replicates, GC-FID analysis of complete RPMI-1640 samples in headspace vials identified a single peak with a retention time (RT) of 5.99 min (Figure 2.2). Compound identification of this peak was not possible due to RTs from reference compounds not being available. Due to this peak only being identified once, the result was deemed irreproducible and therefore it was

concluded that GC-FID analysis did not identify any compounds from RPMI-1640 headspace samples.

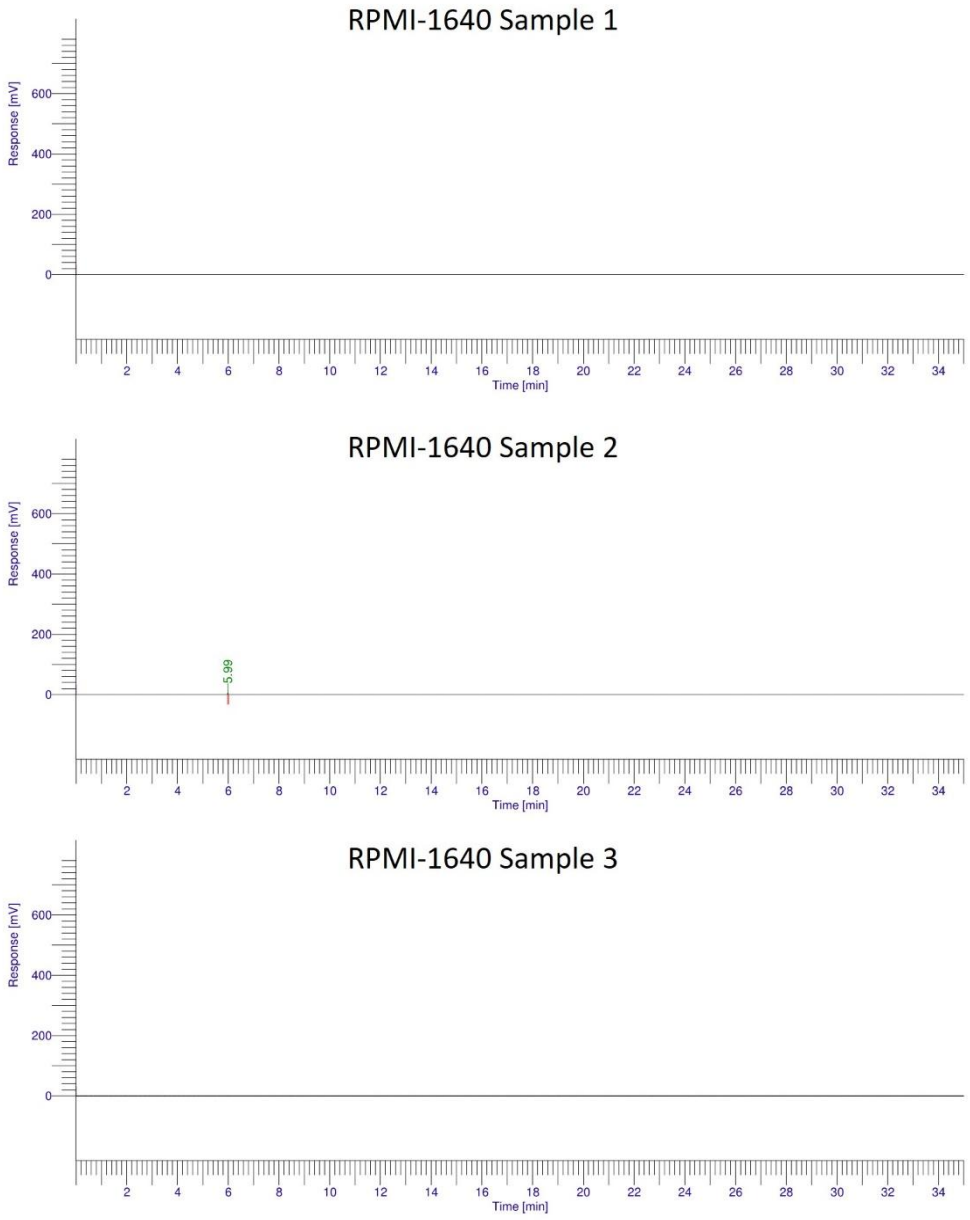

Figure 2.2: GC-FID chromatograms of RPMI-1640 samples in headspace vials, extraction performed with SPME. Out of three replicates only one peak with a RT of 5.99 min was detected in Sample 2.

When SPME was performed directly on RPMI-1640 headspace in cell culture flasks, four peaks were identified with GC-FID; three of which were identified consistently across all samples (Figure 2.3). The average RTs of these peaks were 1.014, 6.851, 10.635 and 13.875 min (Figure 2.3). Again, compound identification was not possible due to a lack of reference compounds.

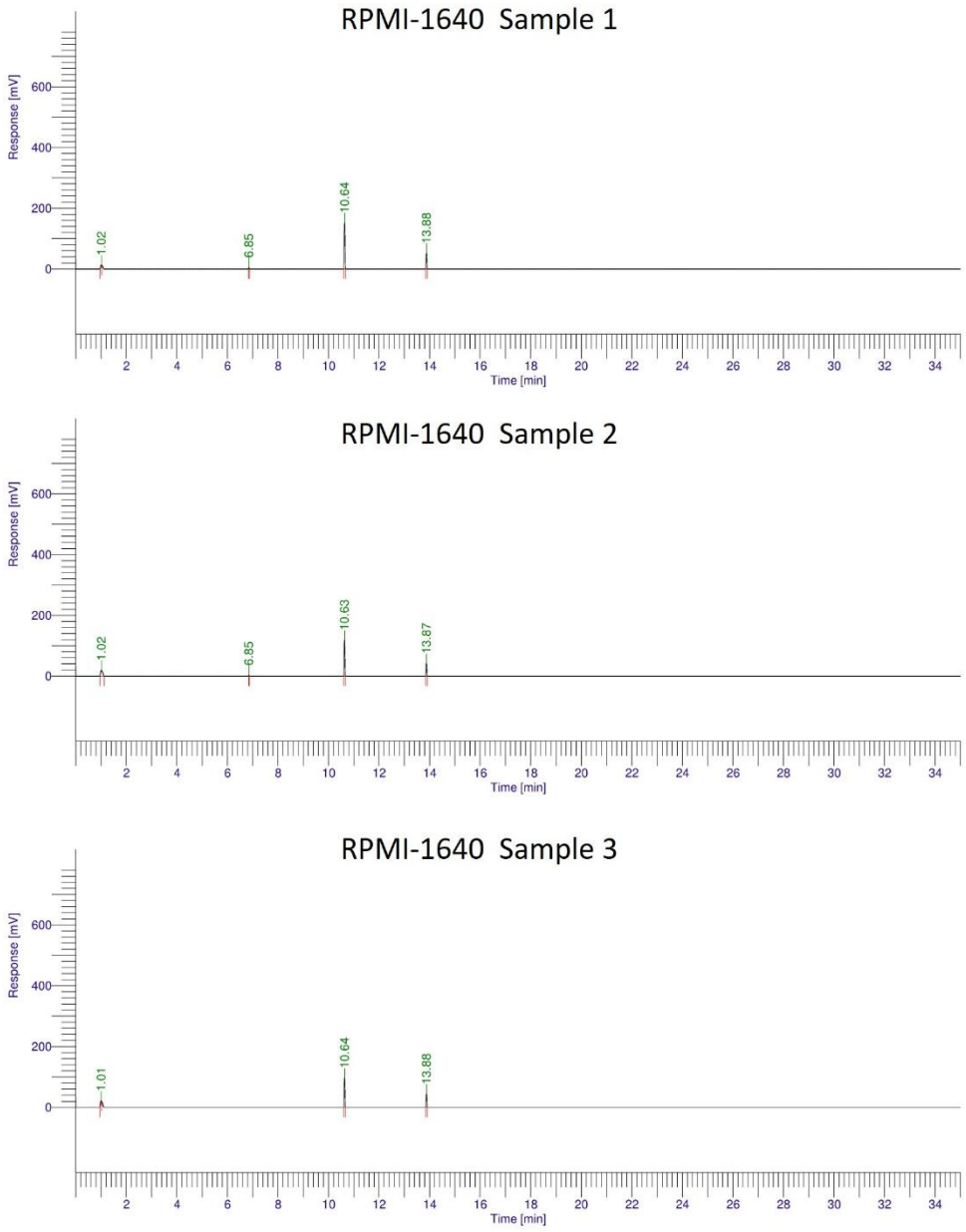

Figure 2.3: GC-FID chromatograms of RPMI-1640 samples after direct sampling in T25 cell culture flasks using SPME. Four peaks with RTs of 1.014, 6.851, 10.635 and 13.875 min were identified in sample 1 and 2, 6.851 min missing from sample 3.

Four peaks were also identified with GC-FID following direct SPME sampling of MSTO-211H cell culture headspace (Figure 2.4). These peaks had very similar RTs to those detected from RPMI-1640 flasks: 0.99, 6.843, 10.636 and 13.872 min, but again it could not be confirmed if these were the same compounds due to the lack of reference compounds (Figure 2.4). All four peaks were only detected in MSTO-211H Sample 1, with Sample 2 and Sample 3 missing the 6.843 min peak (Figure 2.4).

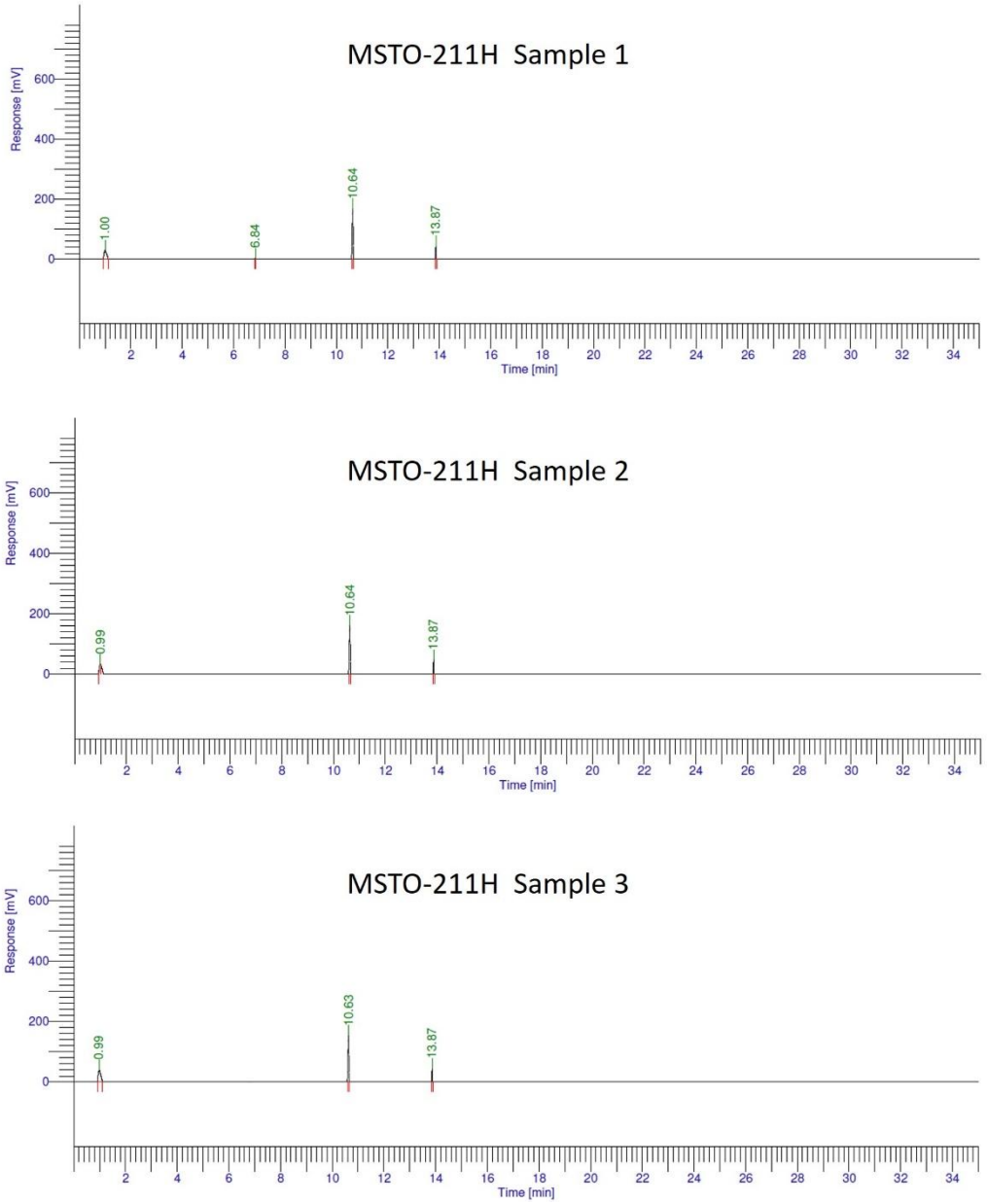

Figure 2.4: GC-FID chromatograms of MSTO-211H samples after direct sampling in T25 cell culture flasks using SPME. Four peaks with RTs of 0.99, 6.843, 10.636 and 13.872 min were identified in sample 1, 6.843 min missing from samples 2 & 3.

The direct injection of 1µl 2000ppm EPA VOC Mix 2 onto the GC-FID produced a chromatogram with a total of 13 peaks (Figure 2.5). These peaks had RTs of 0.71, 1.20, 2.04, 3.90, 4.55, 5.18, 5.34, 6.23, 6.74, 7.39, 8.01, 10.35 and 10.83 min (Figure 2.5). The detection of these 13 peaks indicated that the GC-FID methodology separated the 13 components of the EPA VOC Mix 2 (Figure 2.5).

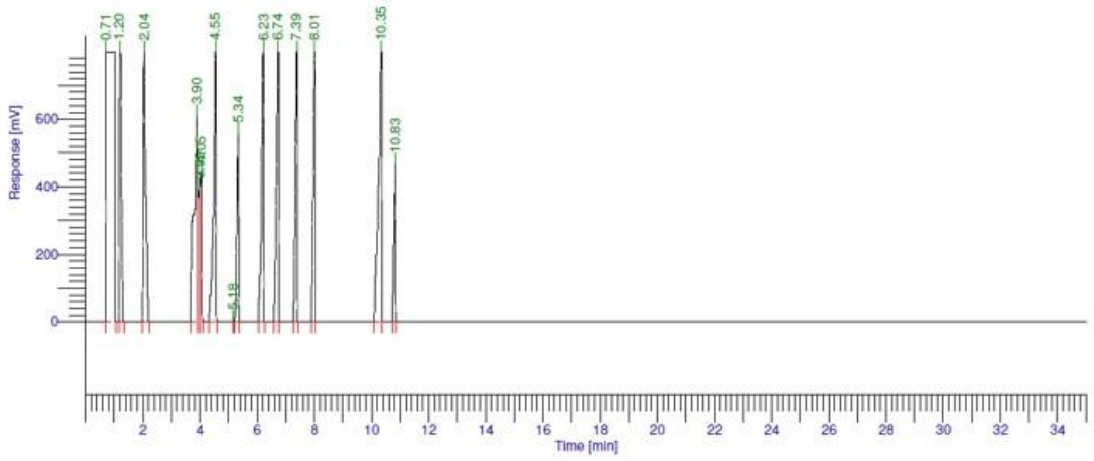

Figure 2.5: GC-FID chromatogram produced by 1µl direct injection of 2000ppm EPA VOC Mix 2. 13 main peaks were detected with RTs of 0.71, 1.20, 2.04, 3.90, 4.55, 5.18, 5.34, 6.23, 6.74, 7.39, 8.01, 10.35 and 10.83 min.

2.4.2 Transfer to Gas Chromatography-Mass Spectrometry (Method B)

As in GC-FID, GC-MS analysis produced chromatograms that separated the components of samples based on RT plotted against relative abundance. GC-MS chromatograms produced following SPME sampling of RPMI-1640 flasks were much more complex than those produced by GC-FID (Figure 2.6). Chromatograms from multiple replicates were overlaid using Agilent MassHunter software to determine if there were any differences between replicates (Figure 2.6). All RPMI-1640 replicates appeared to produce the same VOC profile, with no obvious differences in specific peaks or the pattern of compounds detected (Figure 2.6).

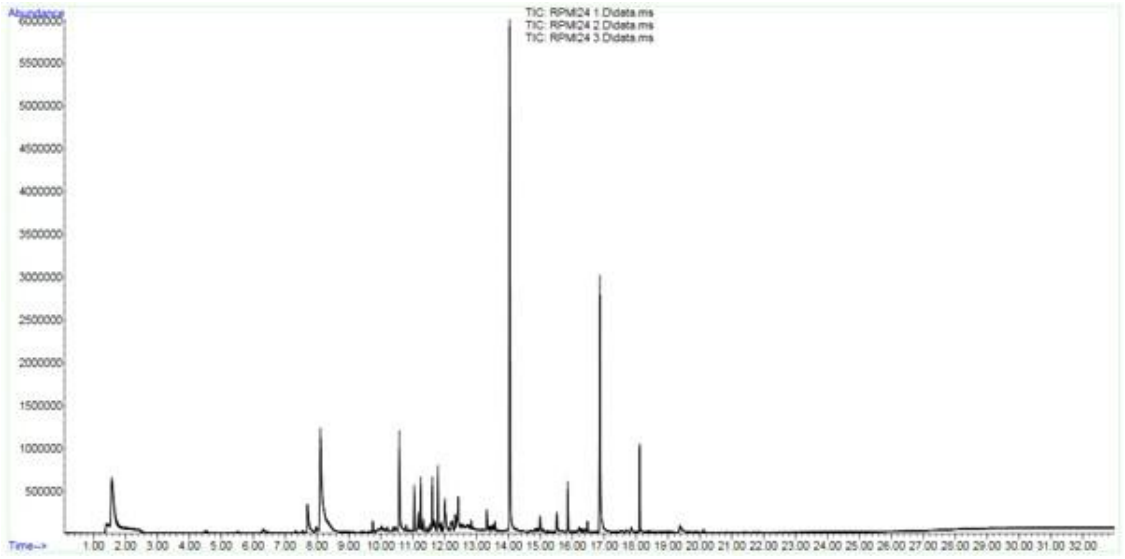

Figure 2.6: Overlaid GC-MS chromatograms produced by SPME GC-MS analysis of RPMI-1640 headspace after 24HR incubation (three replicates). All three replicates produced the same chromatogram. Chromatograms visualised in Agilent MassHunter.

The GC-MS chromatograms produced from SPME GC-MS analysis of MSTO-211H cell culture headspace were also much more complex than those produced from GC-FID (Figure 2.7). Again, multiple replicates were overlaid in MassHunter, and no differences were observed in specific peaks, or the pattern of compounds detected (Figure 2.7).

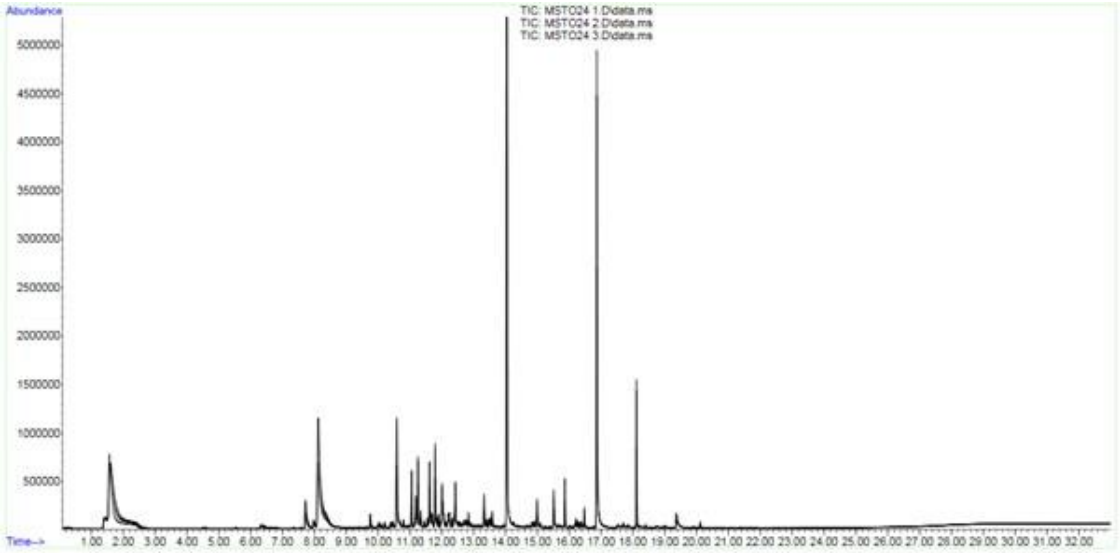

Figure 2.7: Overlaid GC-MS chromatograms produced by SPME GC-MS analysis of $2x10^6$ MSTO-211H headspace after 24HR incubation (three replicates). Chromatograms visualised in Agilent MassHunter.

It was observed that RPMI-1640 and MSTO-211H chromatograms appeared to have a very similar profile (Figure 2.6 & Figure 2.7). An overlay comparison was performed between one RPMI-1640 replicate and one MSTO-211H replicate to identify any differences between the two profiles (Figure 2.8). The overlay comparison showed that the RPMI-1640 and MSTO-211H profiles were largely the same, however it appeared that two specific peaks were increased in the MSTO-211H sample compared to the RPMI-1640 (Figure 2.8). Spectral match to the NIST library database (V11, NIH) was performed on these peaks and the compounds were tentatively identified as tetradecane with a RT of 16.9 min and a complex siloxane containing compound with a RT of 18.1 min (siloxane compounds can be detected as artefacts of SPME and GC-MS).

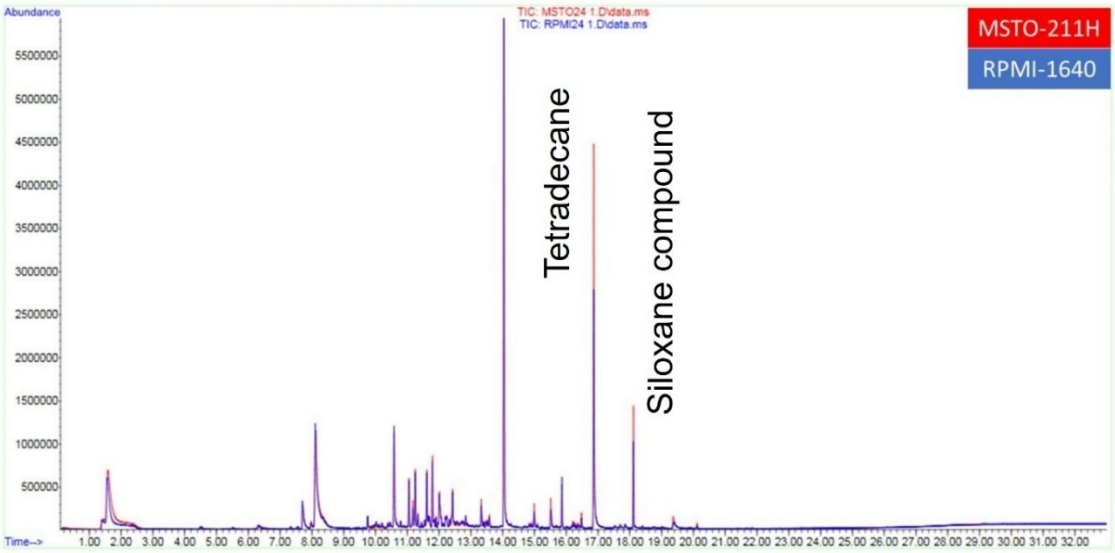

Figure 2.8: Overlay comparison between MSTO-211H and RPMI-1640 GC-MS chromatograms. Tetradecane (16.9 min) and a siloxane containing compound (18.1 min) were tentatively identified as increased in the MSTO-211H replicate compared to the RPMI-1640.

SPME GC-MS analysis of 1ppm EPA VOC Mix 2 detected 13 distinct peaks (Figure 2.9). A tentative NIST match for each peak was obtained through spectral match (Figure 2.9). Peak 7 was tentatively identified as 1,2,3-trimethylbenzene when the reference compound was 1,3,5-trimethylbenzene and p-isopropyl-toluene (peak 9) was identified as o-cymene (Figure 2.9 & Table 2.1). 1,2,3-trimethylbenzene and 1,3,5-trimethylbenzene differ only in the position of methyl groups and p-isopropyl-toluene is also known as p-cymene, which is again very similar to o-cymene. All other NIST matches, and the order of elution were as expected (Figure 2.9 & Table 2.1).

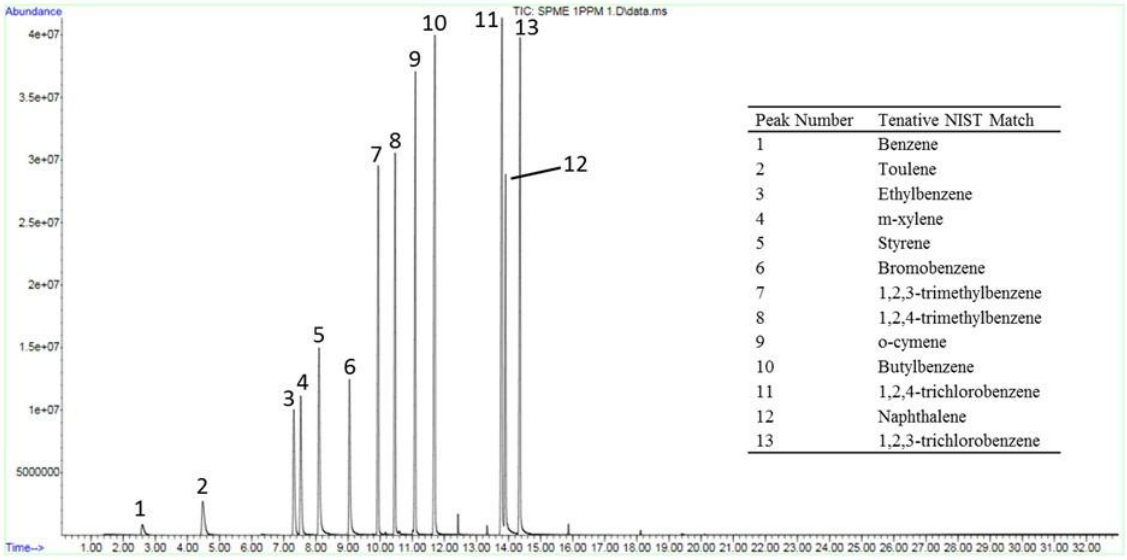

Peak Number	Tenative NIST Match
1	Benzene
2	Toulene
3	Ethylbenzene
4	m-xylene
5	Styrene
6	Bromobenzene
7	1,2,3-trimethylbenzene
8	1,2,4-trimethylbenzene
9	o-cymene
10	Butylbenzene
11	1,2,4-trichlorobenzene
12	Naphthalene
13	1,2,3-trichlorobenzene

Figure 2.9: GC-MS chromatogram produced from the headspace of 1ppm EPA VOC Mix 2 sampled with SPME. Tentative identification for each peak was performed through spectral match to the NIST library database.

2.4.3 Refinement of Gas Chromatography-Mass Spectrometry (Method C)

Chromatograms were produced from RPMI-1640 and MSTO-211H headspace following SPME and GC-MS according to Section 2.3.3.3. In summary, an Rtx-VMS capillary column was installed, and the oven temperature programming of the method was updated. The injection mode was set to split-less and a SPME inlet liner was installed to improve peak shape.

Again, an overlay comparison was performed between RPMI-1640 and MSTO-211H replicates (Figure 2.10). The general profiles of the chromatograms were similar to those produced by the previous method (Figure 2.10); however, peaks were spread across the full length of the run time, indicating an improved separation (Figure 2.10). A number of specific differences in peaks were identified from the overlay comparison; tentative identification of these compounds was performed through spectral match to the NIST library database (Figure 2.10). 2-butoxy-ethanol (21.6 min) and 2-ethyl-1-hexanol (26.6 min) were increased in MSTO-211H compared to RPMI-1640 (Figure 2.10). In contrast, benzaldehyde (24.8 min) and 2-butoxyethyl acetate (28.9 min) were reduced in MSTO-211H compared to RPMI-1640 (Figure 2.10). The spectral match for benzaldehyde was 75%, slightly less than the 80% cut-off point.

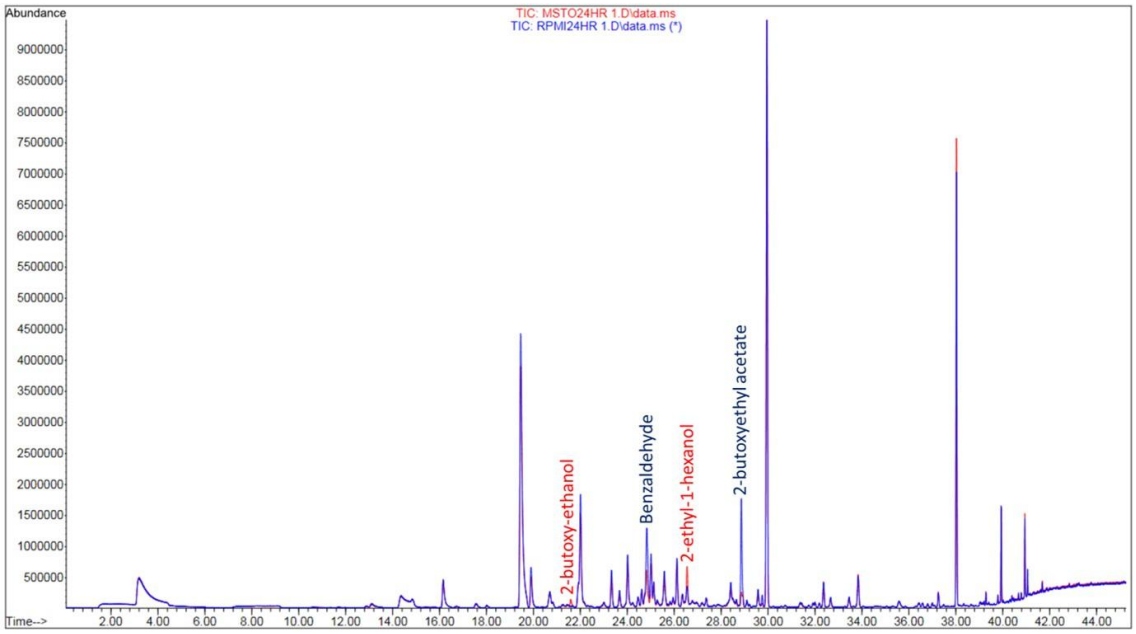

Figure 2.10: Overlaid chromatograms produced from SPME GC-MS (Method C) headspace analysis of RPMI-1640 and MSTO-211H flasks after 24HR incubation. Compounds were tentatively identified through spectral match to the NIST library database.

Cyclopentane and cyclohexane were spiked into the EPA VOC Mix 2 and headspace was analysed at a final concentration of 500ppb (Figure 2.11). The chromatogram showed 15 distinct peaks that were able to be closely matched to the reference compounds using the NIST library database (Figure 2.11). These results also showed that the most volatile compounds (those with the shortest RTs) had a much lower intensity and as volatility decreased (increasing RTs), compounds were detected at a higher intensity (Figure 2.11).

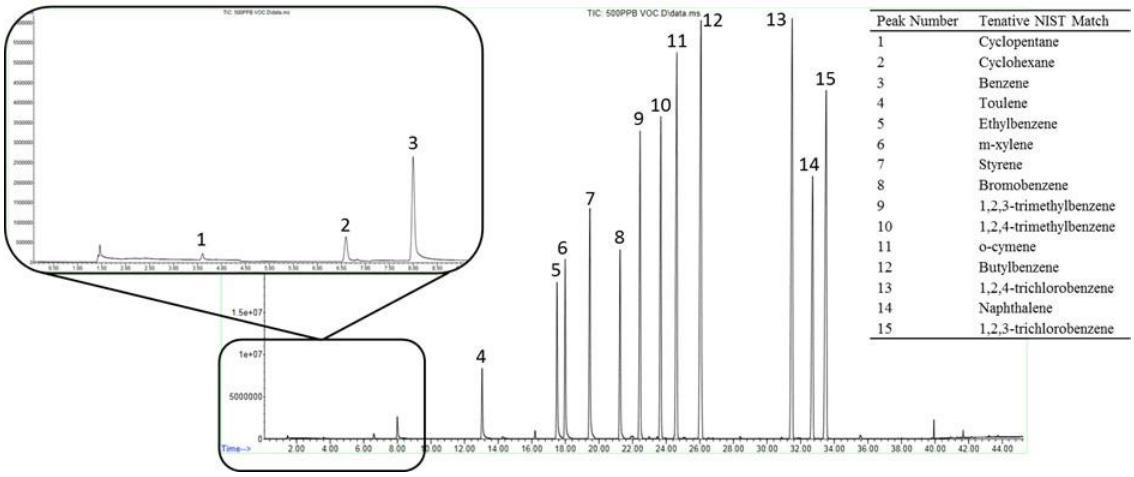

Figure 2.11: Chromatogram produced from SPME headspace analysis and GC-MS (Method C) of 500ppb EPA VOC Mix 2 spiked with cyclopentane and cyclohexane. Tentative identification was performed through spectral match to the NIST library database.

2.4.4 Peppermint Capsule Analysis

GC-MS chromatograms produced from peppermint capsules were extremely complex, consisting of a large number of peaks which were not all fully separated (Figure 2.12). Library search reports were generated to compare the compounds identified currently to those previously reported by Wilkinson *et al.,* (2021) (Table 2.2). α-Pinene, camphene, 3-carene, β-pinene, limonene, eucalyptol, menthone and carvone were identified with the currently developed methodology – this is 50% of the compounds previously reported (Wilkinson et al., 2021).

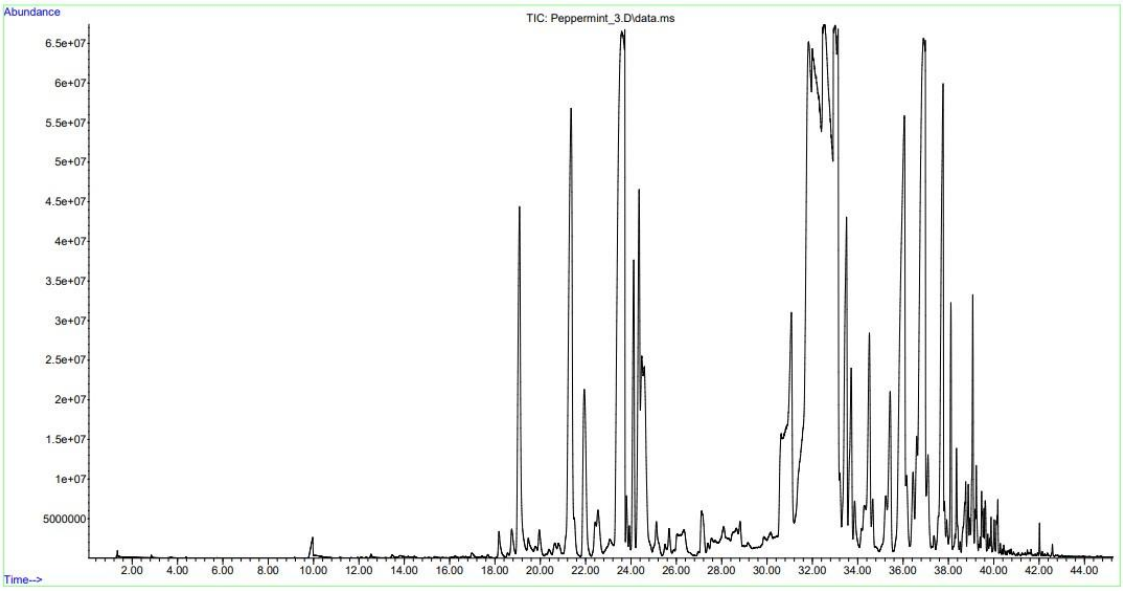

Figure 2.12: Example GC-MS chromatogram produced by SPME headspace analysis of one pierced peppermint capsule sealed in a 20ml headspace vial.

Table 2.2: Major compounds identified from headspace GC-MS analysis of peppermint capsules by Wilkinson *et al.,* (2021) and the corresponding compounds that were identified by SPME GC-MS analysis of peppermint capsules using Method C.

Identified by Wilkinson *et al.,* (2021)	Identified with Current Method C
α-pinene	✓
Camphene	✓
3-carene	✓
β-pinene	✓
α-terpine	-
p-cymene	-
Limonene	✓
Eucalyptol	✓
γ-terpine	-
Terpinolene	-
Menthone	✓
Menthofuran	-
Isomenthone	-
Menthol	-
Isomenthol	-
Carvone	✓

2.5 Discussion

The aim of this chapter was to develop a GC-MS methodology that was capable of identifying VOCs in the headspace of MPM cell cultures. To achieve this aim an initial GC-FID method was developed, transferred to GC-MS and refinements made to identify VOCs from MSTO-211H cells. Further optimisation steps were also taken by analysing a mixture of VOC standards and compounds released from peppermint capsules.

2.5.1 Gas Chromatography-Flame Ionisation Detector

Interestingly, when RPMI-1640 samples were aliquoted into headspace vials for sampling no peaks were detected (Figure 2.1Figure 2.), which suggests that VOCs may not have been at a high enough concentration to detect using GC-FID. Peaks were however detected by sampling culture flask headspace directly (Figure 2.2 & Figure 2.3), with subsequent analyses following this method. Analysis of the EPA VOC Mix 2 also showed that the GC-FID method was able to separate a more complex mixture of VOC standards (Figure 2.5). Due to the limitations of GC-FID as a technique and the lack of reference compounds available, identification of these peaks was not possible. The next stage in method development was to transfer the method conditions to GC-MS, dramatically increasing sensitivity and allowing tentative identification of compounds through spectral match to the NIST library database.

2.5.2 Gas Chromatography-Mass Spectrometry

2.5.2.1 Transfer to Gas Chromatography-Mass Spectrometry

Transfer of the methodology to GC-MS showed that the chromatograms produced by RPMI-1640 and MSTO-211H flasks were much more complex than the four peaks detected with GC-FID (Figure 2.6 & Figure 2.7). The detection of these more complex profiles was possible due to the increased sensitivity of GC-MS compared to GC-FID. These profiles were also consistent across several replicates for both RPMI-1640 and MSTO-211H results, indicating the reproducibility of the method (Figure 2.6 & Figure 2.7). An overlay comparison also highlighted differences in the intensity of tetradecane and a siloxane-containing compound, both increased in MSTO-211H compared to RPMI-1640 (Figure 2.8). These results were early indications of different VOC profiles produced by MPM cells, suggesting that MSTO-211H could potentially be identified using this analysis. The majority of the peaks detected were present in the first half of chromatograms (Figure 2.8), which showed that although some separation of compounds was present, the chromatography parameters could be adjusted to improve the separation.

2.5.2.2 Refinement of Gas Chromatography-Mass Spectrometry

The further refinement of the GC-MS methodology increased the run time but improved the separation of compounds, which meant that differences between MSTO-211H and RPMI-1640 chromatograms were clearly visible (Figure 2.10). The GC-MS column was also changed at this stage – the Rtx-VMS column used contains a proprietary cross-bond phase which is specific for VOCs. 2-butoxy-

ethanol and 2-ethyl-1-hexanol were increased in MSTO-211H compared to RPMI-1640 whereas benzaldehyde and 2-butoxyethyl acetate were decreased (Figure 2.10). The inverse relationship between 2-butoxyethyl acetate and 2-butoxy-ethanol is interesting as the two compounds are likely to be linked. Hydrolysis of ethyl acetate to produce ethanol is possible (Ahmad et al., 2013), with the same mechanism applying to 2-butoxyethyl acetate and 2-butoxyethanol. The increase of 2-butoxy-ethanol along with the simultaneous decrease of 2-butoxyethyl acetate suggests that the MSTO-211H cells hydrolysed the acetate compound to produce the alcohol. This reaction is potentially evidence of cellular metabolism of culture media identified through VOC profiles in cell culture headspace. This finding also increased the confidence in the refinements made to the SPME GC-MS methodology and it was decided to use this method in future experiments.

2.5.3 VOC Standards Mix

It was shown that the developed SPME GC-MS method was capable of separating and identifying a mixture of 15 compounds at a concentration of 500ppb (Figure 2.11). This mix of compounds was chosen as it represented multiple VOCs that had previously been identified as important in MPM breath analysis studies (de Gennaro et al., 2010; Lamote et al., 2017). Although these standards were chosen as a representation of potentially important MPM VOCs, the profiles produced by cell cultures and media controls were much more complex (Figure 2.10 & Figure 2.11). Throughout the duration of this project the VOC standards mix was therefore used more to monitor the performance of the

analysis, with regular comparisons made to ensure that the methodology was separating this group of compounds with a similar RT and detecting with the same intensity. Internal standards are also often used in GC-MS analysis as a way of measuring performance but also to quantify any VOCs identified. It was decided not to include internal standards in cell culture samples as these need to have similar properties to the analytes of interest and, as the cell cultures are living biological samples, the addition of chemical internal standards could alter cellular metabolism and the VOCs produced.

It was observed across the VOC standards chromatograms that the most volatile compounds – those with the shortest RTs – were detected at a much lower intensity, which increased with decreased volatility (Figure 2.9 & Figure 2.11). Improving the retention of the more volatile compounds represents an area where the methodology could be optimised further by reducing the starting temperature of the oven to less than 35^{o}C. This step should improve retention, but would increase the overall run time, which was already long compared to other methods in the literature (Table 1.6). Peaks with short RTs were also identified at higher intensities from the other sample types (Figure 2.10), which suggests that the preparation process of the standard mix may have caused the loss of the most volatile compounds such as cyclopentane and cyclohexane.

2.5.4 Peppermint Capsule Analysis

Headspace analysis of peppermint capsules using the developed SPME GC-MS method identified 50% of the compounds that had previously been identified

(Table 2.2). Therefore, the current method appeared to show an average performance for the separation and detection of VOCs compared to others in the literature. Complete separation of compounds was not observed when peppermint capsules were analysed (Figure 2.12) and a number of compounds were identified that were not highlighted in the previous literature. This indicates that the oven temperature programming could be optimised further leading to improved separation of the peppermint compounds and identification of the additional VOCs. Another important distinction is that TD was used to identify the benchmarking set of compounds (Wilkinson et al., 2021), whereas SPME was used currently. TD tubes have a greater capacity for VOCs than SPME and could be the reason why less compounds were identified with the current methodology. Nevertheless, the peppermint results showed that the methods developed in the chapter were somewhat comparable to methods published in the current literature.

2.6 Conclusions

The aim of the current chapter was to develop a method capable of identifying VOCs released from cell cultures; this was achieved through SPME and GC-MS. The optimisation of SPME GC-MS resulted in a method that could identify some specific differences in the VOC profiles of MSTO-211H cells compared to RPMI-1640 controls (Figure 2.10). Further optimisation of this method could have been possible. Potential areas for improvement include the better retention of the more volatile standards and pushing the limits of detection lower than 500ppb. Additional improvements to the method could also make it possible to identify more of the VOCs that had previously been identified from peppermint capsules.

The development of this method was one of the initial objectives of the overall project. As it was shown that the method was able to detect VOCs released from cell cultures, and in order to maintain the proposed timelines of the project, it was decided to use this method for all remaining analysis.

3 Identification of Volatile Organic Compounds from Secondary Malignant Pleural Mesothelioma Cell Lines

3.1 Introduction

Prior to the current investigation, a single publication had used MPM cell lines as a model for breath analysis (Gendron et al., 2007). This report only used one MPM cell line, REN, and analysed the headspace of this and lung cancer cell lines using an e-Nose (Gendron et al., 2007). The use of e-Nose meant that VOC identification could not be performed. The VOC profile of the REN cell line appeared to be different to the lung cancer cell lines (Gendron et al., 2007), however findings were still limited by the lack of VOC identification and the inclusion of just a single MPM cell line. In contrast, a panel of VOCs have however been identified in the breath of MPM patients and other clinical groups (de Gennaro et al., 2010; Di Gilio et al., 2020; Lamote et al., 2017). The proof of concept for the use of MPM cell lines presented by Gendron *et al.* can be further developed using GC-MS to allow for comparison to the MPM patient breath analysis literature.

VOCs present in exhaled breath can be representative of all cells in the body (Amann et al., 2014). This means that, despite the promising results from the patient breath analysis studies, it is not possible to be certain that the VOCs identified are specific MPM biomarkers or being released from MPM tumour cells. The profile of VOCs in exhaled breath can also be influenced by many factors including lifestyle, diet and the presence of other morbidities (Krilaviciute et al., 2019). The actual process of sampling VOCs from breath can also be influenced by other factors including the presence of exogenous compounds in the environment, the breathing rate of the patient and the phase of breath being sampled (Henderson et al., 2020). Although measures can be taken to control

these factors, they can still have some impact on the VOCs collected. Previous studies have also reported that it was difficult to find appropriately matched controls for MPM patients due to the late age of diagnosis and the co-morbidities associated with this (Lamote et al., 2017).

VOCs have been identified in the headspace of many different cell culture types, including many types of cancer (Table 1.6). Analysing the headspace of cell cultures removes many of the confounding and environmental factors that can influence breath VOC profiles (Filipiak et al., 2016). Headspace analysis of cultured cells means that essentially a “pure” population of cells can be analysed. When the correct controls are applied, for culture media background signals and control cell lines, it is then possible to more confidently associate specific VOCs with the cells being analysed. In turn, these compounds may be the more appropriate targets when searching for endogenous VOCs as their origin of production is clear. Comparisons between cell culture models and *in vivo* breath data across the same disease (MPM) or condition may then inform which VOCs are candidate biomarkers and accelerate the development of a diagnostic breath test.

The current chapter aimed to use the developed SPME GC-MS methodology (Chapter 2, Section 2.3.3). to identify MPM associated VOCs *in vitro*. This was done by performing headspace analysis on a panel of cell lines. MSTO-211H is a biphasic MPM cell line (Borchert et al., 2020). NCI-H28 is an epithelioid MPM cell line (Dell'Anno et al., 2022). MET-5A is a SV40 transformed mesothelial cell line, which was used as a control cell line (Dell'Anno et al., 2022). All cell lines

are commercially available from American Type Culture Collection (ATCC). The cell lines were chosen to initially identify VOCs that were specifically associated with MPM cells. This was performed by statistically comparing the compounds released from the MSTO-211H and NCI-H28 MPM cell lines to the MET-5A control cell line. The use of both biphasic and epithelioid cell lines also meant that a comparison could be made to determine if there were any differences in VOCs between MPM subtypes. The effects of MPM subtype on VOC profiles is not something that had been considered in the previous *in vivo* studies but has been highlighted as one of the areas for future development (Lamote et al., 2017). Together, these analyses were designed to provide a foundation for *in vitro* MPM VOC analysis and to highlight VOCs specifically associated with MPM cells for further biomarker development.

Several analysis software were used for the statistical analysis of the GC-MS data. XCMS online provides a cloud based graphical interface to process untargeted metabolomics data online (Mahieu et al., 2016). OpenChrom is a free to use software for the editing and analysis of mass spectrometric chromatographic data (Wenig & Odermatt., 2010). SIMCA is a widely used software package for discriminant analysis within the metabolomics filed (Triba et al., 2015). Finally, Metaboanalyst offers a comprehensive web-based platform for metabolomics data analysis and interpretation (Pang et al., 2021). Ensuring high cell viability is also an important control measure during VOC sampling as dying cells may cause changes in VOC profiles (Sponring et al., 2009). Viability of the cell cultures was measured after VOC sampling, to show that cells were

viable, and that the sampling procedure did not have a detrimental effect on viability.

3.2 Aims of the Chapter

The aim of this chapter was to use the developed SPME GC-MS methodology to analyse the headspace of a panel of continuous cell lines. This panel included two MPM cell lines, MSTO-211H and NCI-H28, and a non-malignant mesothelial cell line MET-5A. The secondary aim of this chapter was to analyse the cell line panel GC-MS data using XCMS online, OpenChrom, SIMCA and Metaboanalyst to compare statistical analysis methods. Data was analysed using two separate statistical pathways in order to determine the most appropriate method for VOC analysis and identify MPM specific VOCs.

3.2.1 Hypothesis

MPM cells produce distinct VOC profiles when analysed with SPME GC-MS. MPM cells can be distinguished from control cell lines and other MPM phenotypes based on VOC profiles.

3.3 Methods

3.3.1 Cell Culture

MSTO-211H, NCI-H28 and MET-5A cell lines were purchased from ATCC. MSTO-211H and NCI-H28 cell lines were maintained in RPMI-1640 (Thermo

Fisher; Loughborough, UK) supplemented with a final concentration of 10% v/v FBS and 1% v/v pen/strep (Sigma Aldrich). MET-5A cells were maintained in M199 (Sigma Aldrich) with 10% v/v FBS, 1% v/v pen/strep, 3.3nM epidermal growth factor (EGF) (Fisher Scientific; Loughborough, UK), 400nM hydrocortisone (Sigma Aldrich), 870nM zinc-free bovine insulin (Sigma Aldrich), 20mM N-2-hydroxyethylpiperazine-N-2-ethane sulfonic acid (HEPES; Sigma Aldrich) and 0.3% v/v Trace Elements B (VWR; Lutterworth, UK). All cell lines were cultured at 37°C with 5% CO_2 in a humidified incubator (standard cell culture conditions). Culture media was replaced every 2-3 days and cells sub-cultured using Trypsin-EDTA (Thermo Fisher; Loughborough, UK) for detachment when reaching 70-80% confluence. All cell lines passed routine mycoplasma testing using MycoAlert™ Mycoplasma Detection Kit (Lonza Group Ltd, Switzerland).

3.3.2 Headspace VOC Analysis

$1.8x10^6$ of MSTO-211H, NCI-H28 and MET-5A cells were seeded into T75 culture flasks and incubated at standard cell culture conditions for 72 hours. Control flasks containing complete RPMI-1640 and M199 were also prepared and incubated at standard cell culture conditions for 72 hours. After incubation, VOCs were extracted from the headspace of cell cultures and media control flasks using a 50/30µm DVB/CAR/PDMS SPME fibre. A new SPME fibre was conditioned in a GC-MS inlet at 270°C for 30 min according to manufacturer's instructions prior to initial use and injected in a GC-MS inlet at 250°C for 10 min at the start of each day before VOC extractions. For VOC extraction, the septum-piercing needle of the SPME fibre assembly was inserted directly through the filter cap of cell

cultures and control flasks and secured with Parafilm. The SPME fibre was exposed to flask headspace for 15 min under standard cell culture conditions. After extraction, the SPME fibre was retracted into the assembly and analysed directly using GC-MS.

3.3.3 Gas Chromatography-Mass Spectrometry

The SPME fibre assembly was transferred to the inlet of an Agilent 7890A with a Rtx-VMS capillary column (30m x 0.25mm x 1.4µm; Restek) and MS-5975C triple axis detector. The GC-MS inlet temperature was set to 250^{o}C. The oven temperature programming was set to: 35^{o}C for 5 min, ramped to 140^{o}C at 4^{o}C min^{-1} and held for 5 min, ramped again to 240^{o}C at 20^{o}C min^{-1} and held for 4 min. The total analysis time was 45.25 min. The MS transfer line was set to 260^{o}C and analysis was performed in full scan mode with a range of 35-300 a.m.u. The SPME fibre assembly was manually injected into the GC-MS inlet and the fibre exposed for the first 10 min of the oven temperature program; the injection mode was split-less. This 10 min exposure ensured all VOCs were desorbed from the SPME fibre onto the GC-MS column and meant that the SPME fibre was ready to be used again for another VOC extraction.

3.3.4 Cell Viability

After headspace analysis MSTO-211H, NCI-H28 and MET-5A cell viability was checked. Cell number and viability was assessed using Trypan-Blue exclusion and a Countess automated cell counting device (Invitrogen; Loughborough, UK).

3.3.5 Statistical Analysis

Statistical analysis of GC-MS data was performed in two ways: feature detection analysis using XCMS online (Scripps Research Institute) and OpenChrom (Lablicate GmbH) and multivariate statistical analysis of chromatogram peak areas using SIMCA (Umetrics, Satorius) and Metaboanalyst 5.0 (Pang et al., 2021).

3.3.5.1 Feature Detection Analysis

Raw GC-MS data were exported from Agilent MassHunter data analysis software in .CDF format and uploaded to XCMS online for feature analysis. Feature analysis in XCMS online aligned raw chromatograms and broke down the data into many smaller features which were associated with specific chromatogram peaks. Pairwise comparisons were performed between MSTO-211H and NCI-H28 groups to the RPMI-1640 group and the MET-5A group to the M199 group to identify features that were significantly altered in the cell line groups with comparison to their respective media controls. CDF files were then imported into OpenChrom, chromatograms were filtered to only include variables that were significantly altered in the cell line groups compared to their media only controls and PCA was performed on MSTO-211H, NCI-H28 and MET-5A groups to visualise the data. Further classifications were also performed between the cell line groups using orthogonal partial least squares-discriminant analysis (OPLS-DA) in OpenChrom. After data visualisation, further pairwise comparisons were performed between the MET-5A group and the MSTO-211H and NCI-H28 groups

in XCMS online to identify features that were significantly different in the two MPM groups compared to the MET-5A controls. The compounds associated with the significantly altered features were tentatively identified through spectral match to the NIST library (V11, NIH). Only variables that had a ≥80% spectral match and were significantly different in the initial cells-media pairwise comparisons were reported.

3.3.5.2 Multivariate Statistical Analysis

3.3.5.2.1 Data Pre-processing

For each chromatogram, a library search report in .CSV format was generated in MassHunter which included peak RT, peak area and the automatically assigned NIST match for each peak. The spectral match cut-off for NIST searches was set to 80%. Artefacts of SPME and GC-MS, (complex siloxane-containing compounds) were manually removed from library search reports. RTs and peak areas for all samples were used to create an aligned data matrix in .CSV format. RTs were rounded to one decimal place prior to alignment. GCalignR in R-studio (Ottensmann et al., 2018) was used to align RTs and peak areas resulting in a single aligned data matrix containing average RTs for each sample and corresponding peak area values for each RT. The aligned data matrix was manually checked to identify any discrepancies in alignment.

3.3.5.2.2 Data Normalisation and Background Filtering

The aligned data matrix was uploaded to Metaboanalyst 5.0 (Pang et al., 2021) for data normalisation and background filtering. Variables were filtered by

interquartile range, normalisation by sum and autoscaling were applied. For background filtering batch t-tests (two-sample t-tests) were performed comparing MSTO-211H and NCI-H28 groups to the RPMI-1640 group and the MET-5A group to the M199 group. The data matrix was then edited to only contain the significantly altered variables from the t-tests and RPMI-1640 and M199 groups were removed resulting in a cell line specific data matrix. The cell line matrix was used for subsequent statistical analysis.

3.3.5.2.3 Data Visualisation and Multivariate Statistical Analysis

The cell line matrix in .CSV format was imported into SIMCA (V17.0.2; Umetrics, Satorius). PCA, partial least squares-discriminant analysis (PLS-DA) and OPLS-DA were performed to visualise similarities and differences in the VOC profiles between the groups. A heat map was also generated in Metaboanalyst to show the differences between the relative, normalised peak areas for specific compounds between MSTO-211H, NCI-H28 and MET-5A groups.

3.4 Results

3.4.1 Cell Number and Viability

Cell number and viability was measured to show that cells were viable and to determine if VOC extraction had a detrimental effect on cell cultures. Differences in the number of viable cells in MSTO-211H, NCI-H28 and MET-5A cell cultures were observed (Figure 3.1). In contrast to this, the number of viable cells as a

percentage of total cells was at a consistently high level across all three groups (Figure 3.1).

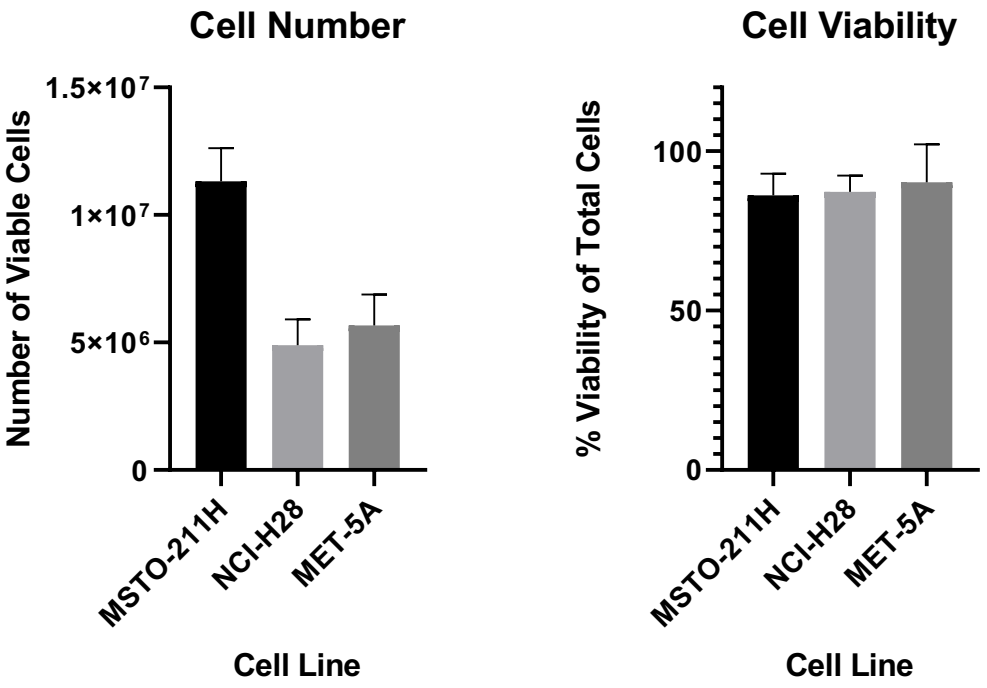

Figure 3.1: Cell number and percentage viability of MSTO-211H, NCI-H28 and MET-5A cell cultures after SPME GC-MS analysis. Measured through Trypan-Blue exclusion. Six replicates of each cell line were measured (data represent mean ± standard deviation). Data published Little et al., (2020).

3.4.2 Cell Line Chromatograms

Each chromatogram produced from MSTO-211H, NCI-H28 and MET-5A flasks showed approximately 100-200 peaks (Figure 3.2). Chromatogram profiles were very similar across all of the groups, making it difficult to identify any observable differences between the groups based solely on chromatograms (Figure 3.2).

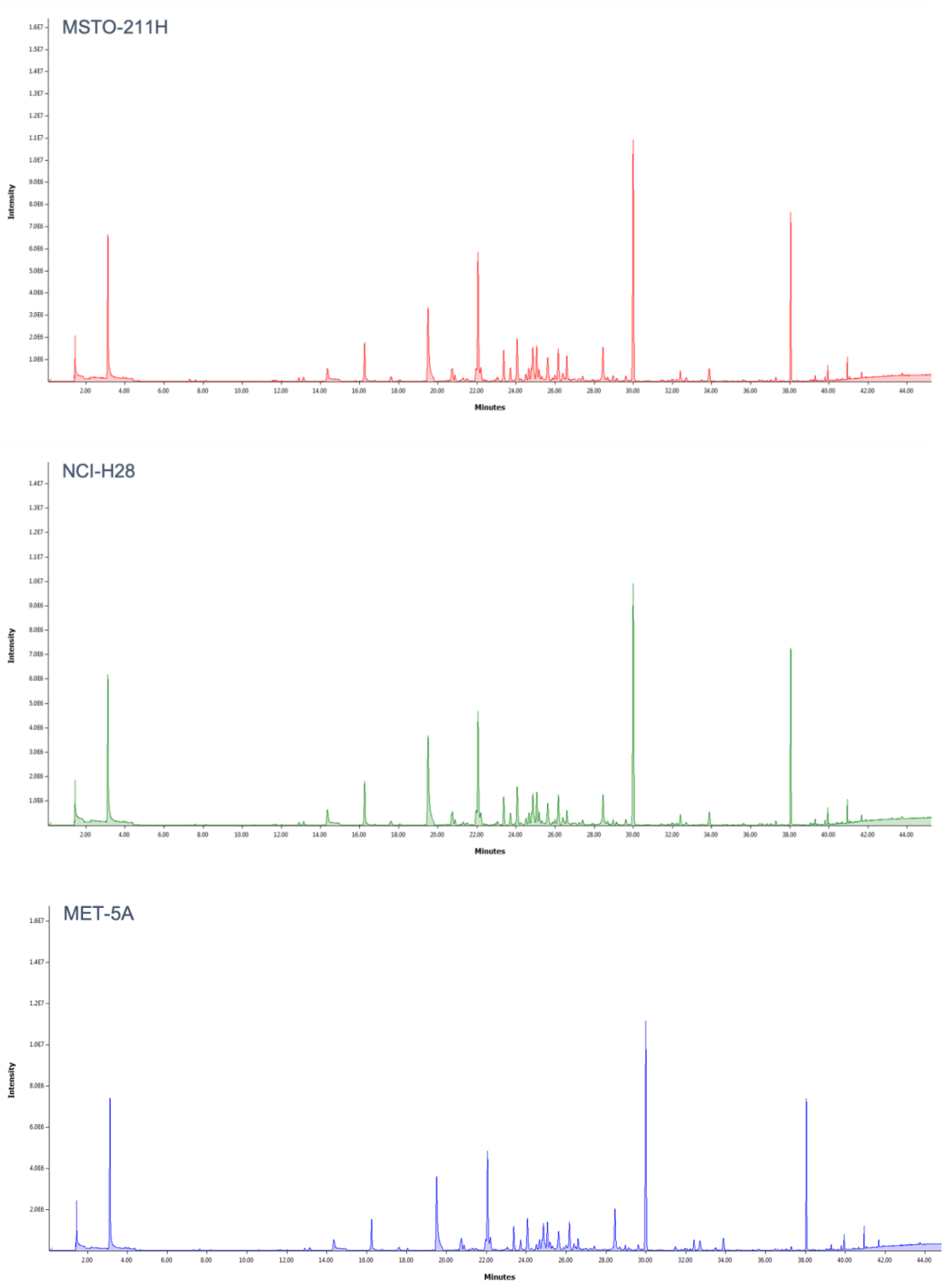

Figure 3.2: Example GC-MS chromatograms produced from MSTO-211H, NCI-H28 and MET-5A cell culture headspace after 72h incubation. Chromatograms generated in Openchrom. Data published Little et al., (2020).

3.4.3 Feature Detection Analysis

3.4.3.1 PCA and OPLS-DA

PCA was performed in OpenChrom using only the variables that were significantly different in the cell line groups compared to the media only controls. The PCA score plot showed crossover of some results between the MSTO-211H, NCI-H28 and MET-5A groups (Figure 3.3). Despite this crossover, separation was also observed between the three groups (Figure 3.3).

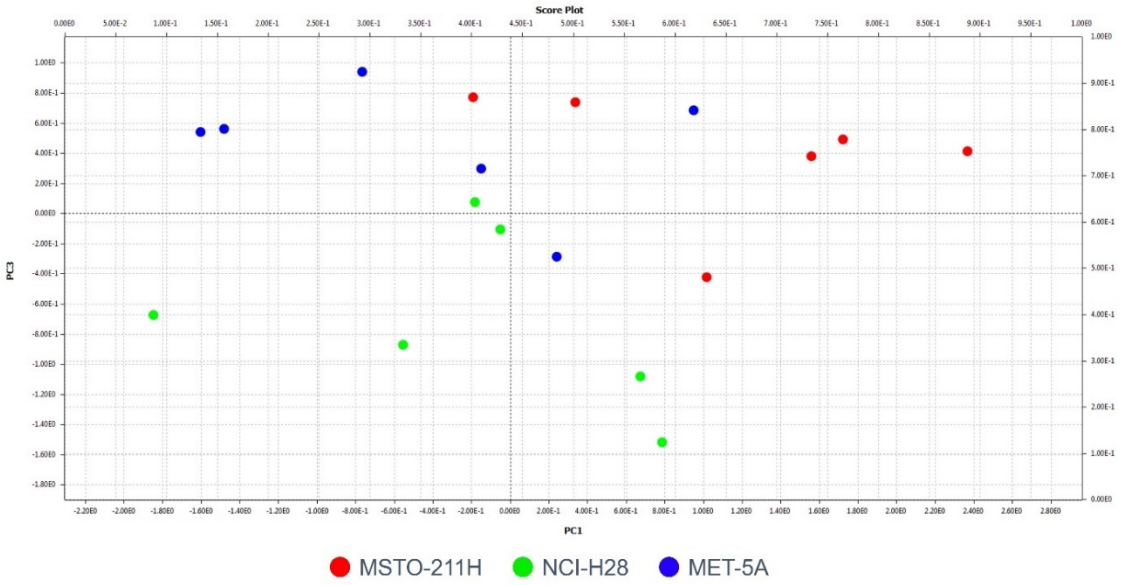

Figure 3.3: OpenChrom PCA score plot showing MSTO-211H, NCI-H28 and MET-5A groups after pairwise media reduction using XCMS online, 6x replicates per group. Data published Little et al., (2020).

The cell line profiles were further classified with OPLS-DA in OpenChrom (Figure 3.4). Using OPLS-DA both MSTO-211H and NCI-H28 were clearly separated from MET-5A and MSTO-211H and NCI-H28 were separated from each other (Figure 3.4).

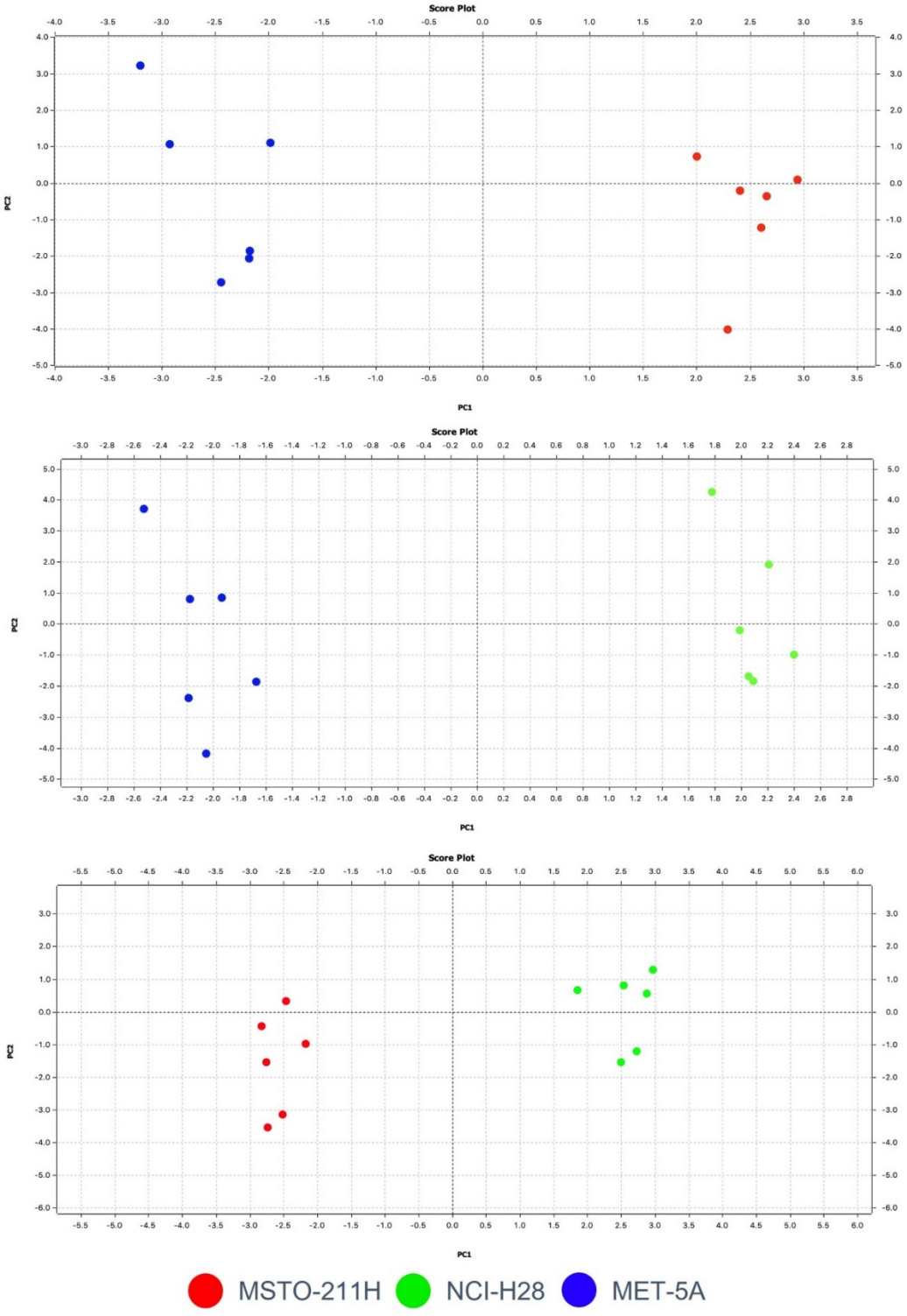

Figure 3.4: OPLS-DA score plots generated in OpenChrom, comparing MET-5A to MSTO-211H and NCI-H28 and MSTO-211H to NCI-H28, 6x replicates per group. Data published Little et al., (2020).

3.4.3.2 Significantly Altered Features

Pairwise comparisons were made in XCMS online between the MET-5A group and the MSTO-211H/NCI-H28 groups; the significantly altered features were associated with tentatively identified VOCs (Table 3.1). 2-ethyl-1-hexanol was significantly increased in both the MSTO-211H and NCI-H28 groups compared to the MET-5A group (Table 3.1). Ethyl propionate and cyclohexanol were also significantly increased in the MSTO-211H group and dodecane was significantly increased in the NCI-H28 group (Table 3.1).

Table 3.1: Significantly altered features in MSTO-211H and NCI-H28 groups with comparison to the MET-5A and their corresponding tentative NIST identification. Pairwise comparison analysis in XCMS online (Welch's t-tests) Data published Little et al., (2020).

AVG RT (min)	Tentative ID	MSTO-211H	p-value	NCI-H28	p-value
11.6	Ethyl propionate	↑	<0.01		-
20.8	Cyclohexanol	↑	<0.01		-
26.6	2-ethyl-1-hexanol	↑	<0.01	↑	0.01
30.0	Dodecane	-	-	↑	<0.01

3.4.4 Multivariate Statistical Analysis

3.4.4.1 Development of an Aligned Cell Line Matrix

Alignment of MSTO-211H, NCI-H28, MET-5A, RPMI 1640 and M199 results created an aligned data matrix consisting of 30 samples and 121 aligned RTs, 3630 individual variables in total. Batch t-tests comparing MSTO-211H to RPMI-1640, NCI-H28 to RPMI-1640 and MET-5A to M199 identified ten significantly different variables across all comparisons (Table 3.2). After the cells-media batch t-tests and removal of media groups, the resulting cell line data matrix had 18 samples and 10 aligned RTs, 180 individual variables total. The aligned, normalised cell line data matrix was used for subsequent statistical analysis.

Table 3.2: Significantly altered variables in the MSTO-211H, NCI-H28 and MET-5A cell line groups with comparison to their respective media controls, Two-sample batch t-tests (Metaboanalyst, $p<0.05$). Tentative NIST IDs in *italic* had discrepancies in identification between replicates (potential identities are included in the Appendix, Table 7.1). 2,6-bis(1,1-dimethylethyl)-2,5-cyclohexadiene-1,4-dione has been abbreviated to $C_{14}H_{20}O_2$.

		P-Value: Cells vs Media Controls		
AVG RT (min)	**Tentative ID**	**MSTO-211H**	**NCI-H28**	**MET-5A**
1.6	Carbon dioxide	-	0.049706	-
7.3	Ethyl acetate	0.001319	-	-
20.9	3-heptanone	-	0.044581	-
21.3	*Alkane*	-	-	0.032966
22.2	*Alkane*	0.044713	0.037456	-
24.9	*Alkane*	0.001939	0.00079	5.89E-05
26.6	2-ethyl-1-hexanol	5.26E-06	0.001782	0.010563
29.6	Acetophenone	0.003953	0.000873	0.000809
33.5	Trichlorobenzene	-	-	0.043095
41.1	$C_{14}H_{20}O_2$	0.000582	0.002545	0.000814

3.4.4.2 PCA, PLS-DA and OPLS-DA

The aligned, normalised cell line data matrix was imported in .CSV format into SIMCA for PCA, PLS-DA and OPLS-DA analysis. An initial comparison was made between all groups – MSTO-211H, NCI-H28 and MET-5A. The PCA score plot showed a general separation of the MSTO-211H group from the other two groups, with crossover between MET-5A and NCI-H28 results (Figure 3.5A). PLS-DA improved this separation and showed some clustering of the MET-5A and NCI-H28 groups (Figure 3.5B). OPLS-DA showed a similar pattern to PLS-DA, again with improved separation of the MSTO-211H group (Figure 3.5C). Clustering was also improved between the MET-5A and NCI-H28 groups, with the two groups starting to separate from each other (Figure 3.5C).

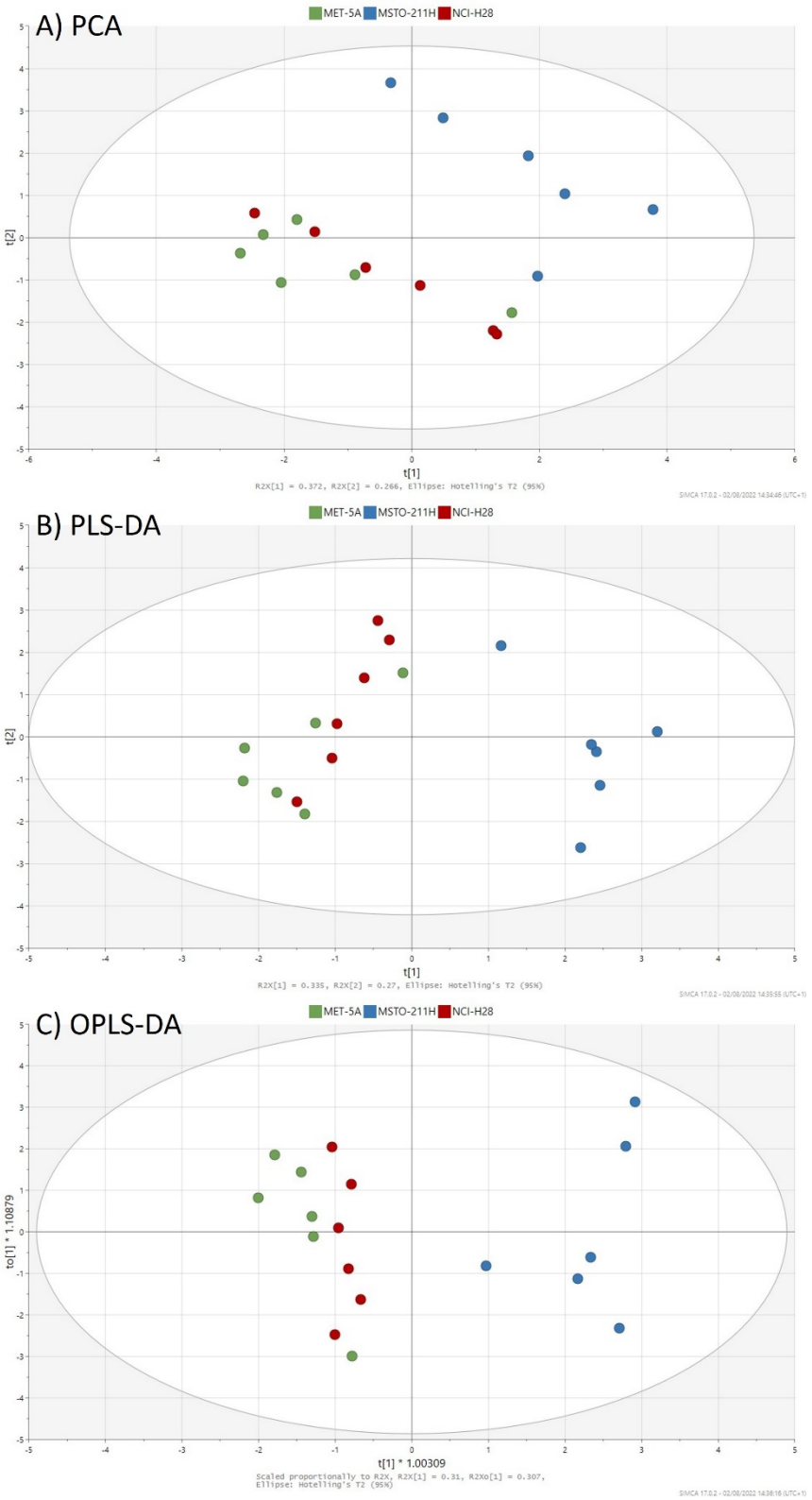

Figure 3.5: A) PCA, B) PLS-DA and C) OPLS-DA score plots (SIMCA, V17.0.2) showing MSTO-211H, NCI-H28 and MET-5A groups after normalisation and background reduction. Each point represents a single replicate, 6x replicates per group.

After the comparison between all three groups, further classification of the results was performed by comparing the MET-5A group to both the MSTO-211H and NCI-H28 groups as well as a comparison between MSTO-211H and NCI-H28 groups. The PCA, PLS-DA and OPLS-DA score plots for the MET-5A MSTO-211H comparison all showed the same general trend – separation between the two groups along the X-axis (Figure 3.6). A single outlier was observed for both the MET-5A and MSTO-211H groups on the PCA score plot (Figure 3.6A). PLS-DA improved these results (Figure 3.6B) and further classification with OPLS-DA improved the clustering of the groups even further (Figure 3.6C).

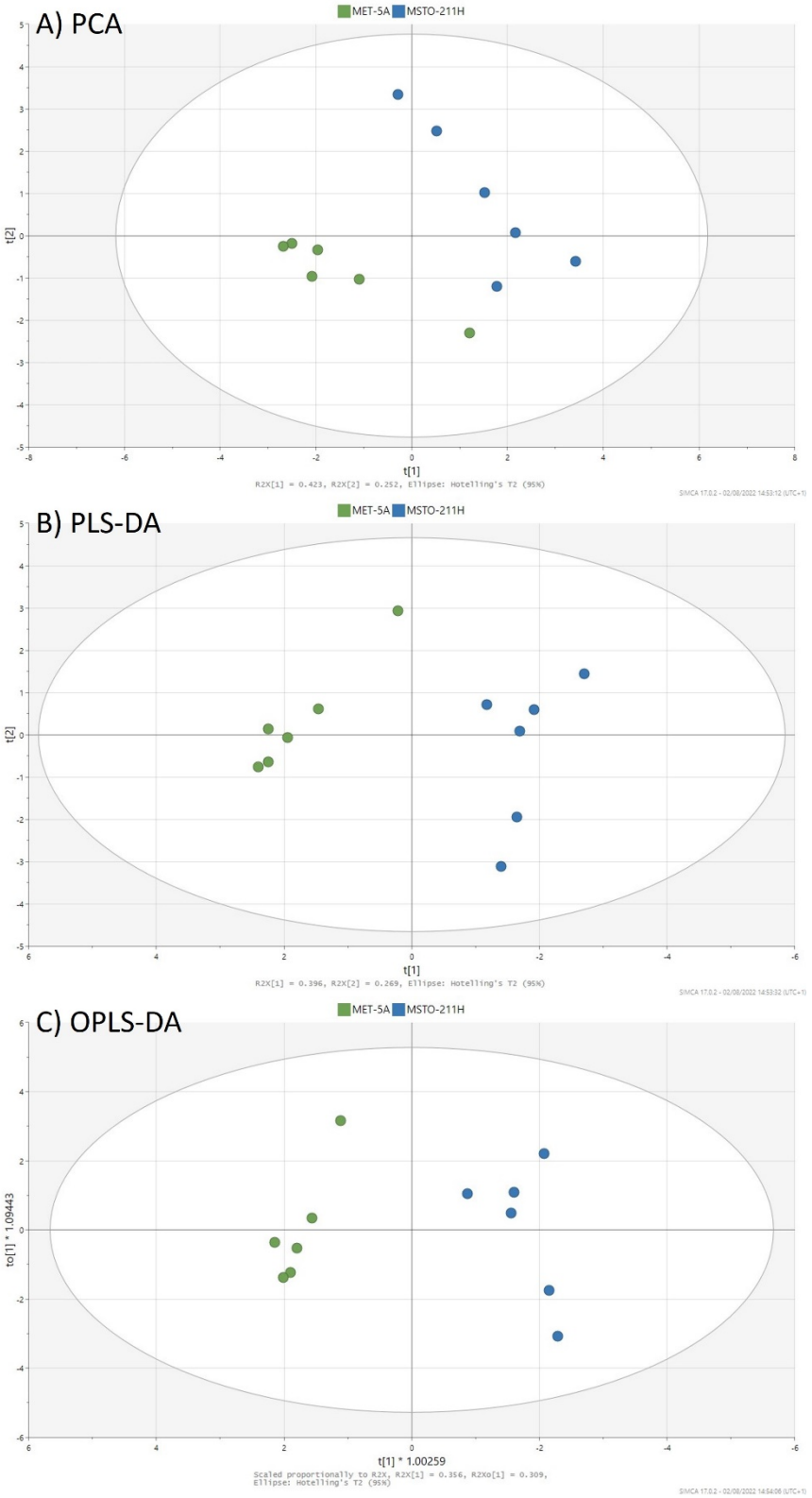

Figure 3.6: A) PCA, B) PLS-DA and C) OPLS-DA score plots (SIMCA, V17.0.2) showing MET-5A and MSTO-211H groups after normalisation and background reduction. Each point represents a single replicate, 6x replicates per group.

In contrast to MSTO-211H, when MET-5A was compared to NCI-H28, a large amount of crossover was observed on the PCA score plot and there was no real separation between the two groups (Figure 3.7A). PLS-DA showed separation between MET-5A and NCI-H28 groups along the X-axis, again with some crossover between the two groups (Figure 3.7B). OPLS-DA improved this separation, with better clustering and no crossover between MET-5A and NCI-H28 results (Figure 3.7C).

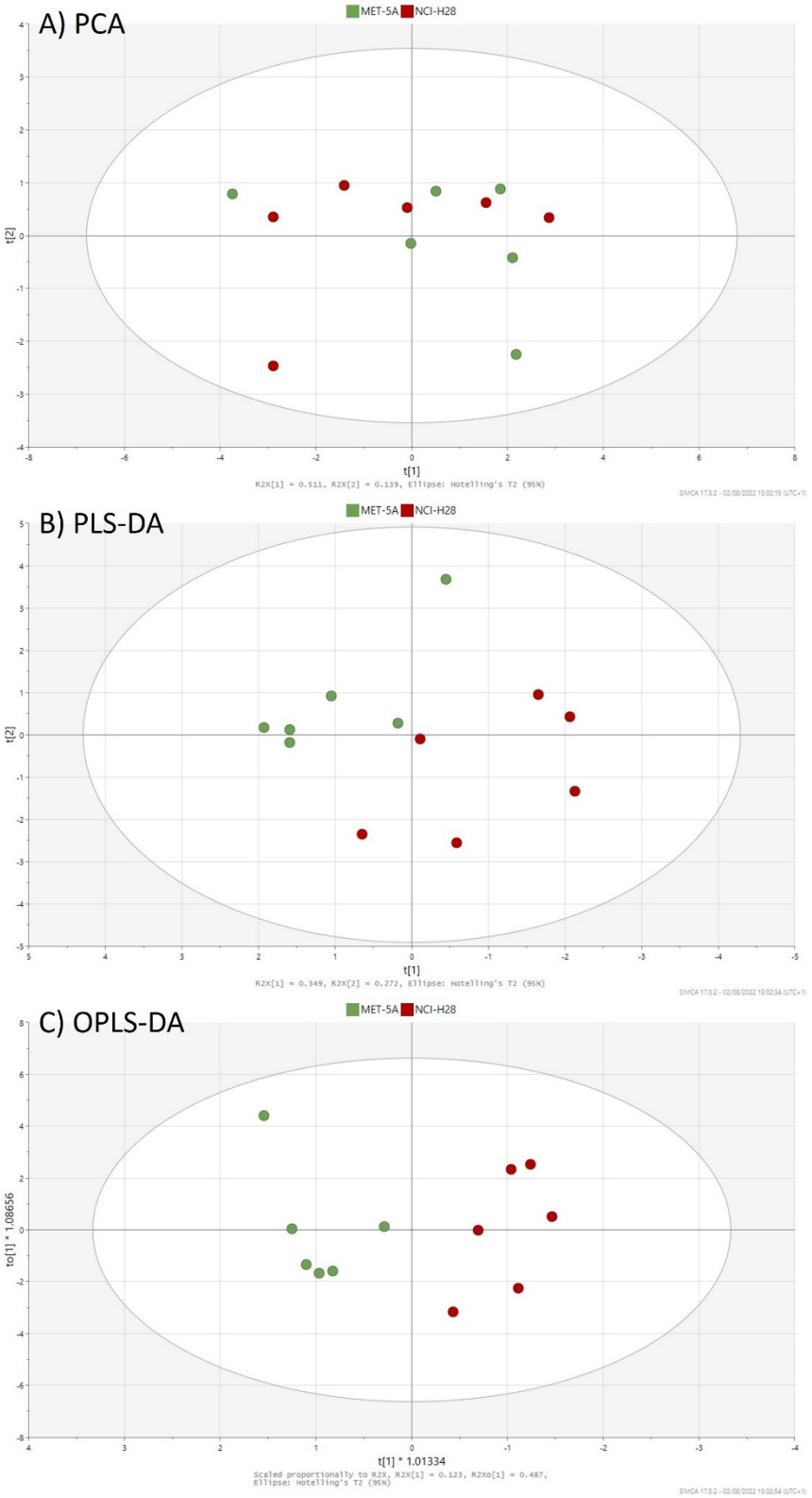

Figure 3.7: A) PCA, B) PLS-DA and C) OPLS-DA score plots (SIMCA, V17.0.2) showing MET-5A and NCI-H28 groups after normalisation and background reduction. Each point represents a single replicate, 6x replicates per group.

When the two MPM cell lines were compared, the PCA score plot showed some separation between MSTO-211H and NCI-H28 groups, with some crossover (Figure 3.8A). PLS-DA improved the separation between the two groups, removed the crossover and showed tight clustering of the NCI-H28 results (Figure 3.8B). OPLS-DA showed a very similar pattern to PLS-DA with slightly improved clustering of the MSTO-211H group (Figure 3.8C).

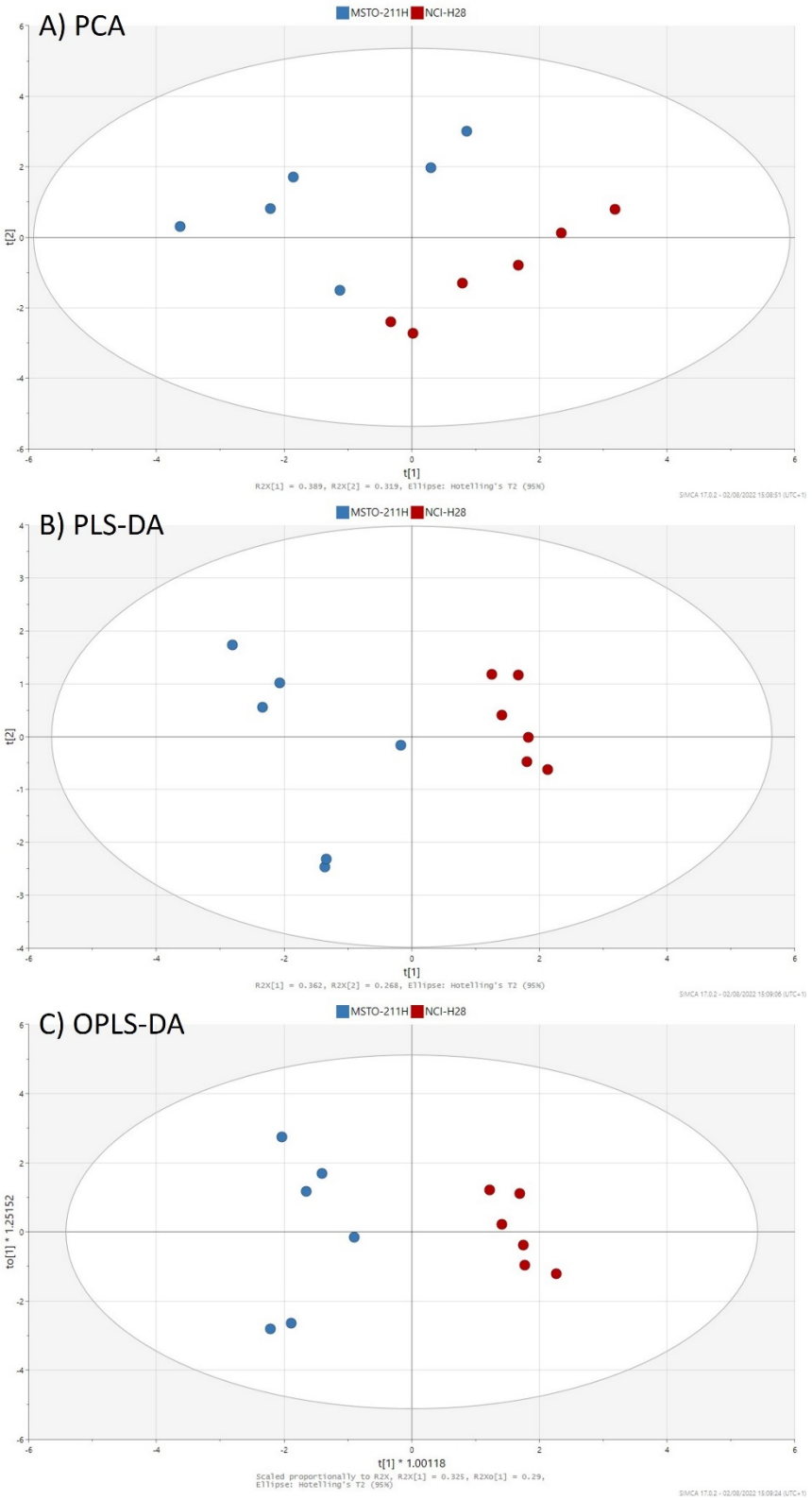

Figure 3.8: A) PCA, B) PLS-DA and C) OPLS-DA score plots (SIMCA, V17.0.2) showing MSTO-211H and NCI-H28 groups after normalisation and background reduction. Each point represents a single replicate, 6x replicates per group.

3.4.4.3 Relative Levels of Cell Line VOCs

Using Metaboanalyst, a heat-map was constructed with the normalised cell line matrix to show the relative levels of the ten compounds in MSTO-211H, NCI-H28 and MET-5A groups (Figure 3.9). The heat-map showed that the MSTO-211H profiles were clearly different from the MET-5A and NCI-H28 groups (Figure 3.9). Carbon dioxide, an alkane with a RT of 21.3 min, trichlorobenzene, ethyl acetate and 2-ethyl-1-hexanol were all at relatively higher levels in the MSTO-211H group compared to the MET-5A and NCI-H28 groups (Figure 3.9). The MET-5A and NCI-H28 groups were more similar to each other, but still showed some specific differences in the relative levels of VOCs (Figure 3.9). 2,6-bis(1,1-dimethylethyl)-2,5-cyclohexadiene-1,4-dione ($C_{14}H_{20}O_2$), an alkane with a RT of 22.2 min and acetophenone were higher in the MET-5A group, whereas 3-heptanone and an alkane with a RT of 24.9 min were relatively higher in the NCI-H28 group (Figure 3.9).

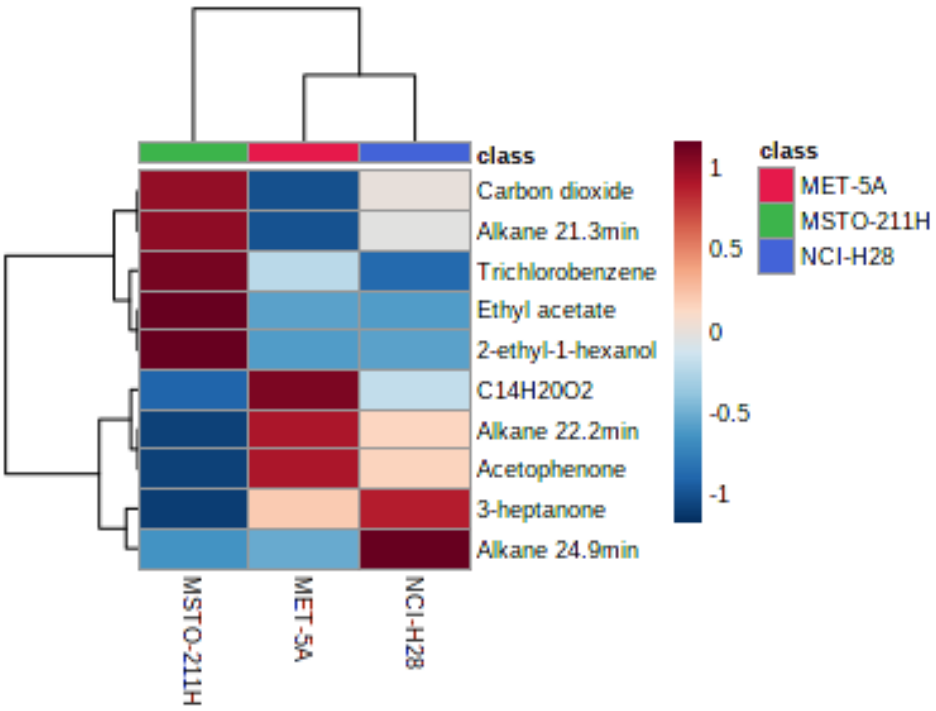

Figure 3.9: Heat-map showing the relative levels of the 10 cell line specific VOCs in MSTO-211H, NCI-H28 and MET-5A cell culture headspace. The heat-map was constructed from the normalised, background reduced cell line matrix in Metaboanalyst.

3.5 Discussion

3.5.1 Headspace Analysis and Cell Viability

The main aim of this chapter was to identify VOCs released from MSTO-211H, NCI-H28 and MET-5A cell cultures. A change in metabolism during cell death and apoptosis has the potential to influence VOC profiles (Sponring et al., 2009). The high viability of the cell cultures (Figure 3.1) indicated that the cells did not undergo detrimental levels of cell death and apoptosis during the 72-hour incubation period, suggesting that VOC profiles may not have been significantly affected by cell death processes. As the cell viability was measured after the headspace of the cultures had been sampled and analysed, the high viability results also confirm that the SPME sampling technique did not have a negative effect on cell viability. Therefore, data suggests that sampling cell culture headspace using a SPME fibre assembly was a non-destructive method of identifying VOCs released from the cell lines. Differences in the total number of viable cells were however observed (Figure 3.1), which may be a result of the differences in cell size, morphology and growth rate between the biphasic, epithelioid and non-malignant cell lines. The high viability of the cultures, and the use of media-only background controls, meant that it was more likely that the VOCs identified were coming from the cell lines, supporting the aim of this chapter.

3.5.2 VOC Statistical Analysis

Despite the increasing number of publications using GC-MS as a method for the analysis of VOCs from cell culture headspace, and many other biological matrices, there is no single unified method for statistical analysis. Data produced from GC-MS is quite complex, featuring a large number of chromatographic peaks separated based on RT and which also have associated mass spectra. The profiles produced by different experimental groups can also be very similar to each other, requiring statistical analysis to identify the subtle differences between groups – this was shown by the chromatograms produced from MSTO-211H, NCI-H28 and MET-5A cell cultures (Figure 3.2). A structured analysis pathway should include some key steps: alignment of samples and variables, data reduction or background removal and representation of data often through multivariate statistical analysis (Smolinska et al., 2014). Perhaps most importantly, any variables of interest are further contextualised within the existing data in order to draw conclusions that can form the basis of future research or have a potential clinical impact.

The current chapter used the GC-MS data obtained from the headspace of MSTO-211H, NCI-H28 and MET-5A cell cultures to explore two different methods of VOC data analysis. The feature detection method was based on the freely available software XCMS online (Mahieu et al., 2016) and OpenChrom (Wenig & Odermatt., 2010) which automatically perform much of the statistics involved in the analysis. Both software options were compatible with the raw .CDF files exported from Agilent MassHunter. XCMS online read these files and aligned the chromatograms before breakdown into many smaller “features” which were used for further analysis. Each feature only represented a small segment of the

chromatogram, rather than a RT covering a whole peak, but could be associated with a specific compound based on the NIST library searches. Background reduction was performed through pairwise analysis comparing each cell line group to its respective media only control. The RTs associated with the significantly altered features were then filtered within OpenChrom and basic PCA and OPLS-DA analyses were performed. Subsequent pairwise analyses were performed comparing MET-5A to the MSTO-211H and NCI-H28 groups, with the significantly altered features reported along with their RTs and tentative compound IDs. This analysis method was used in the publication of the data in this chapter (Little et al., 2020).

In contrast, the multivariate statistical analysis method using SIMCA and Metaboanalyst relied on the analysis of whole peak areas from the chromatograms and associated RTs, with mass spectra used for tentative identification. This method involved more steps for the user but also allowed more control over the data. Reports with RT, tentative IDs and peak areas were exported from Agilent MassHunter and alignment needed to be performed using GCAlignR in R-studio. This resulted in a single data matrix in .CSV format that could then be uploaded to Metaboanalyst for background reduction and normalisation as well as visualisation through multiple methods using SIMCA. Significantly altered variables and the representation of compounds using the heat-map were based on the normalised areas of the chromatogram peaks, rather than smaller sections in the feature analysis. SIMCA is widely used within metabolomics (Triba et al., 2015) and the combination of SIMCA and

Metaboanalyst was recently published for the analysis of the headspace of multiple cell lines (Amaro et al., 2020).

Despite differences in processing, multivariate analysis was used in both methods – PCA, PLS-DA and OPLS-DA, to visually represent the cell line profiles and observe similarities and differences between the groups. PCA is used to give an initial visualisation of the spread of the data, highlighting any potential similarities and differences (Sola Martínez et al., 2020). The feature analysis PCA score plot showed considerable crossover between the three cell line groups in the centre of the plot, however separation of the groups was still observed (Figure 3.3). The MET-5A and MSTO-211H groups separated along the X-axis; the NCI-H28 group separated along the Y-axis with slightly closer clustering to the MET-5A group (Figure 3.3). These results indicate, although they might have been subtle, the VOC profiles produced by MSTO-211H, NCI-H28 and MET-5A cells were different from each other. Comparisons can be made with the PCA score plot generated in SIMCA. This time MSTO results moved away from the other two groups, with crossover between MET-5A and NCI-H28 cell lines (Figure 3.5A). However slight clustering was still observed for some of the MET-5A results (Figure 3.5A). Interpretation of these results show that the VOC profiles used to construct the score plot showed greater differences in the MSTO-211H group in comparison to the MET-5A and NCI-H28 groups. Even with some of the differences in patterns between the two score plots, both PCA results indicated that there were some potential differences between the VOC profiles produced by the cell line panel. It is important to note that the data used for the OpenChrom

plots was not normalised whereas the data matrix used for SIMCA analysis was, which could explain some of the differences observed in analysis.

After PCA, the VOC profiles were further classified with PLS-DA and OPLS-DA. Within the feature detection analysis pathway, OpenChrom software only had the option for OPLS-DA analysis between two groups available. In contrast, SIMCA allowed for both PLS-DA and OPLS-DA of two or more groups. The PLS-DA score plot looking at all three groups amplified the spread of the data observed in PCA (Figure 3.5B). Clearly the MSTO-211H group was separated from the other two along the X-axis and improved clustering of MET-5A and NCI-H28 results also started to be observed (Figure 3.5B). OPLS-DA increased the spread of these results even further with the same separation of MSTO-211H and this time increased separation between MET-5A and NCI-H28 results (Figure 3.5C). These further analyses confirmed that the VOC profiles of the MSTO-211H cells were distinct from the other two groups and also further confirmed the possibility of slight differences between the MET-5A and NCI-H28 groups.

Further classification in the feature analysis pathway was performed using OPLS-DA in OpenChrom. These score plots showed that MET-5A results were clearly distinct from both MSTO-211H and NCI-H28 groups and that MSTO-211H and NCI-H28 groups were also distinct from each other (Figure 3.4), confirming that the VOC profiles used to construct these plots were different. Within the multivariate statistical analysis pathway, comparisons were made between MET-5A and MSTO-211H and NCI-H28 and between MSTO-211H and NCI-H28 using PCA, PLS-DA and OPLS-DA. Further classification with PLS-DA showed that

MSTO-211H and NCI-H28 groups were different from the MET-5A group (Figure 3.6B & Figure 3.7B) and MSTO-211H and NCI-H28 groups were different from each other (Figure 3.8B). As with the multiple group comparison, OPLS-DA improved the spread and clustering of these results, showing clear separation between the three cell line groups (Figure 3.6C, Figure 3.7B & Figure 3.8C). Again, these results confirmed that the cell line data matrix used to construct the plots showed differences in VOC profiles for MSTO-211H, NCI-H28 and MET-5A results.

Regardless of the specific differences discussed, it appeared that both analysis pathways concluded that there were differences in the VOC profiles of MSTO-211H, NCI-H28 and MET-5A cells. Previously, GC-MS was used to analyse MPM patient breath and differences were found when compared to other clinical groups (de Gennaro et al., 2010; Di Gilio et al., 2020; Lamote et al., 2017). Initially the breath of MPM patients was compared to that of individuals with AEx and HC (de Gennaro et al., 2010). These results were further replicated (Di Gilio et al., 2020) and a comparison with the breath of patients with benign ARD was also included (Lamote et al., 2017). The GC-MS based studies combined with breath analysis using other methods suggest that MPM patients have a VOC profile that is distinct from HCs and the other clinical groups analysed (Töreyin et al., 2020). The current chapter showed that these findings were also replicated when analysing cell culture headspace as a model for MPM breath analysis. Both MSTO-211H and NCI-H28 MPM cell lines showed different VOC profiles to the non-malignant mesothelial cell line MET-5A, showing that MPM cells themselves produced a different VOC profile to that of non-malignant cells.

The current chapter also explored additional areas in MPM breath analysis by measuring VOCs from both biphasic and epithelioid MPM cell types. Separation was observed between MSTO-211H and NCI-H28 cells and specific differences in VOCs were shown (Table 3.1 & Figure 3.9), suggesting differential VOC profiles between the two MPM subtypes. Sarcomatoid MPM has a worse prognosis than epithelioid, whilst biphasic mesotheliomas contain a combination of both cell types, with prognosis becoming increasingly worse depending upon the percentage of sarcomatoid cells present (Yap et al., 2017). Present results showed that biphasic and epithelioid MPM cell cultures produced different VOC profiles, with this *in vitro* finding providing a proof of concept for the discrimination between these two MPM subtypes based on VOC analysis. A progression of this would be the analysis of a pure sarcomatoid cell line. These initial results can also be used to inform future clinical work considering biphasic and epithelioid MPM patient breath analysis. Although there are difficulties with identifying sufficient patients with known MPM subtype at present, progression of this research could see the implementation of a breath test in clinical practice for the discrimination between these two groups.

3.5.2.1 Specific VOCs

Several compounds were found associated with significantly different features in the MPM groups compared to the MET-5A control (Table 3.1). A panel of cell line associated compounds was also identified in the multivariate statistical analysis pathway (Table 3.2). Of these compounds 2-ethyl-1-hexanol, dodecane, ethyl propionate, carbon dioxide, ethyl acetate, 3-heptanone, acetophenone and

trichlorobenzene are present on the volatilome database, indicating they have been previously identified in human breath (Pleil & Williams, 2019).

2-ethyl-1-hexanol was the only compound identified across both analyses; it was significantly increased in both MSTO-211H and NCI-H28 groups in the feature analysis (Table 3.1) and was found at relatively higher levels in MSTO-211H cells compared to MET-5A and NCI-H28 (Figure 3.9). These results suggest that the cellular production of 2-ethyl-1-hexanol may be associated with MPM. 2-ethyl-1-hexanol was used to statistically differentiate MPM patients from those exposed to a similar level of asbestos without mesothelioma development (Lamote et al., 2017), as well as distinguishing MPM patients from HCs (Di Gilio et al., 2020). The correlation between previous *in vivo* studies and the current *in vitro* model suggests that 2-ethyl-1-hexanol is a potentially endogenously produced MPM specific VOC biomarker. However, further literature searches reveal that 2-ethyl-1-hexanol has been commonly associated with other malignancies including lung (Liu et al., 2014), prostate (Jiménez-Pacheco et al., 2018) and colorectal cancer (Wang et al., 2014). Significant differences in 2-ethyl-1-hexanol levels have been reported in urine (Jiménez-Pacheco et al., 2018), blood (Wang et al., 2014), pleural effusions derived from cancer patients (Liu et al., 2014) and tumour cell line headspace (Jia et al., 2018). Recently, 2-ethyl-1-hexanol was also found to be present in the sweat of lung, prostate, gastric, kidney, head and neck cancer patients but absent from healthy controls (Monedeiro et al., 2020). The identification of altered 2-ethyl-1-hexanol levels across a range of malignancies and biological matrices suggest that this VOC is ubiquitously associated with cancer or a specific cancer-related process.

Dodecane is also a compound that has been identified in MPM breath analysis literature, having previously been used in the discrimination between MPM patients, AEx and HC (de Gennaro et al., 2010). Using SPME, dodecane was also found to be increased in cell lines derived from haematological malignancies with comparison to media-only controls (Tang et al., 2017). Among other VOCs, dodecane was highlighted as a potential biomarker for oral squamous cell carcinoma (Bouza et al., 2017). In lung cancer, dodecane has been suggested as a potential diagnostic biomarker (Handa et al., 2014; Zou et al., 2014), particularly useful in identifying adenocarcinoma patients with epidermal growth factor receptor (EGFR) mutations (Handa et al., 2014). Furthermore, dodecane was found at significantly increased levels in exhaled breath samples obtained from colorectal cancer patients with comparison to HC (Wang et al., 2014). Again, when looking at these compounds in the context of the wider literature, dodecane is another VOC that is associated with cancer in general rather than MPM specifically.

Acetophenone was part of the VOC panel used for the discrimination between MPM, AEx and HC (de Gennaro et al., 2010). 1,2,3-trichlorobenzene and 1,2,4-trichlorobenzene have also been identified in the MPM breath analysis literature (Lamote et al., 2017). 1,2,4-trichlorobenzene was used in the discrimination model between MPM and AEx, whereas 1,2,3-trichlorobenzene was used for the MPM vs AEx and ARD combined model (Lamote et al., 2017). Despite featuring in the volatilome database, acetophenone and trichlorobenzenes are not as prominent in the breath analysis literature as 2-ethyl-1-hexanol and dodecane.

The identification of compounds across multiple malignancies is an example of how a single compound will lack the specificity to diagnose MPM effectively. It is much more likely that a breath test in clinical practice will rely on the identification of multiple VOC signals, with changes in the levels and patterns of compounds indicative of a disease, rather than the presence of a single compound. This also highlights the need to contextualise any candidate VOCs identified from a single study. Multiple publications have presented a panel of compounds as biomarkers of a particular disease, only for completely different compounds to be reported in the future.

3.5.2.1.1 Cellular VOC Production

Increased ROS and oxidative stress is a major component of cancer and, more specifically, with the development of MPM caused by asbestos exposure (Røe & Stella, 2015). The production of ROS leading to an increase in oxidative stress is also thought to play an important role in the production of VOCs (Ratcliffe et al., 2020). During prolonged periods of oxidative stress, proteins and lipids are particularly susceptible to ROS-induced oxidative attack, leading to lipid peroxidation and the production of VOCs (Ratcliffe et al., 2020). Inhalation of asbestos fibres leads to rounds of frustrated phagocytosis and unresolved oxidative stress, creating an environment with high ROS (Carbone & Yang, 2017). Due to the bio-persistence of asbestos fibres (Carbone & Yang, 2017), it is likely that high levels of oxidative stress are maintained well into malignancy, with ROS initiating damage to phospholipids, proteins and other macromolecules leading to the production of VOCs (Di Gilio et al., 2020). Within MPM it has been

speculated that an increased concentration of ROS could produce a high level of oxidated organic species (Di Gilio et al., 2020).

It is possible for alkanes, such as dodecane, to arise from lipid peroxidation, with further metabolism of such alkanes leading to alcohols such as 2-ethyl-1-hexanol (Di Gilio et al., 2020). The current results reflect this, with altered levels of 2-ethyl-1-hexanol and dodecane shown in MSTO-211H and NCI-H28 cells compared to MET-5A. Headspace analysis of 2D cell cultures can be used to explore these findings further. The induction of oxidative stress in a non-malignant cell line, such as MET-5A, mimics the ROS tumourigenesis processes within MPM and allows specific VOCs to be pinpointed to a particular biological process.

3.5.3 Development of MPM *In Vitro* VOC Analysis

Very recently, a study was published that analysed the headspace of a panel of MPM and NSCLC cell lines (some of which were shared with this chapter) using TD tubes and analysis with GC-MS (Janssens et al., 2022). The cell lines analysed were from sarcomatoid MPM (NCI-H2731 and H-MESO-1), epithelioid MPM (NCI-H2795 and NCI-H2818), biphasic MPM (NK104 and MSTO-211H) and NSCLC cell lines (NCI-H2228 and NCI-H1975) were used as controls rather than a non-malignant mesothelial cell line (Janssens et al., 2022). PCA showed good separation between the different cell line groups and discrimination models were constructed comparing NSCLC to MPM, epithelioid MPM, sarcomatoid MPM and biphasic MPM; the different MPM subtypes were also compared against each other (Janssens et al., 2022).

Comparing directly to the results presented in the current chapter, it appears that both the SPME and TD tube-based methods of VOC analysis were able to show some level of discrimination between the different MPM subtypes. Other similarities were also identified. For example, many unknown compounds were reported by Janssens *et al.* and used for the discrimination models comparing the different groups (Janssens et al., 2022). There was also some crossover in the specific VOCs reported. Dodecane was reported as an important compound in the biphasic MPM vs NSCLC and the biphasic MPM vs epithelioid MPM comparisons (Janssens et al., 2022). Ethyl acetate was also reported as an important compound in the comparison between biphasic and epithelioid MPM (Janssens et al., 2022). A discussion was also included recognising these comparisons and comparing the analysis methods used in the publication of the data from this chapter (Janssens et al., 2022; Little et al., 2020). Correlations such as these between a small number of studies is important within breath analysis where reproducibility is lacking despite the growing number of publications. The observation of somewhat similar results while using slightly different sampling and analysis methods also goes some way to validating the underlying biology behind VOC analysis. The results from the current chapter and this recent study highlight that *in vitro* headspace analysis is an important tool in the development of a diagnostic MPM breath test and within breath analysis research.

3.5.4 Conclusions

Even with the growing number of publications, MPM breath analysis remains in its early stages. A key step in the development of a diagnostic breath test is the identification of endogenous VOCs. This requires the development of *in vitro* VOC analysis methods. The work presented in this chapter was the first to analyse MPM cell culture headspace using GC-MS and subsequently identify a panel of VOCs released directly from MPM cells. Two methods for the statistical analysis of VOCs were also presented. The results and the specific compounds identified are in line with the previous *in vivo* studies and the developing *in vitro* literature, highlighting 2D cell culture headspace analysis as an important part of VOC and breath analysis research.

4 The Effect of BAP1 Mutation on Volatile Organic Compound Profiles within Malignant Pleural Mesothelioma

4.1 Introduction

4.1.1 Cell Culture Headspace Analysis

Headspace analysis of cultured cells is a straightforward experimental methodology to model *in vivo* exhaled breath analysis. Cell lines from many different malignancies and other diseases have been analysed using these methods (Table 1.6). Correlation between VOCs identified at an *in vitro* level and in patient breath is designed to identify the most clinically relevant biomarkers and accelerate the development of a diagnostic breath test. However, the use of *in vitro* experiments provide one distinct advantage over measuring compounds released from a human breath – the ability to manipulate conditions and treat cell cultures that would not be possible with patient samples. Several studies have treated cell cultures with H_2O_2, to replicate high oxidative stress conditions and measure the subsequent VOC response (Baranska et al., 2015; Liu et al., 2019b). Linking specific VOC changes to biological processes such as oxidative stress is useful for understanding the production and release of these compounds. The development of cancer is fundamentally underpinned by the acquisition of genetic mutations. The control over experimental conditions in cell culture headspace analysis means that cells can be genetically modified, exploring the effects of cancer-specific mutations on VOC profiles.

4.1.1.1 Cancer Mutations and VOCs

The effects of cancer-specific genetic mutations on the VOC profiles produced by *in vitro* cell cultures have been explored. VOCs were sampled from non-small

cell lung cancer (NSCLC) cell lines with long term gene expression data; EGFR and KRAS mutants and EML4-ALK fusion cells were included in analysis (Peled et al., 2013). Analysis was performed using a combination of sorbent-based material and SPME GC-MS alongside nanomaterial-based sensor analysis (Peled et al., 2013). Triethylamine, benzaldehyde, decanal, toluene and styrene were identified as important VOCs using GC-MS (Peled et al., 2013). Nanomaterial sensor analysis also showed discrimination between EGFR mutant, KRAS mutant, EML4-ALK fusion cells and cells that were wild-type to all these mutations (Peled et al., 2013). Although this initial study suggested that cell lines with specific NSCLC mutations produced different VOC profiles, it is difficult to determine whether one of these single tumour-associated mutations had a causative effect on VOC profiles.

This methodology was further developed to assess the effects of specific mutations in TP53 and KRAS on VOC output within lung cancer (Davies et al., 2014). Non-malignant, and therefore genetically stable, human bronchial epithelial cells (HBECs) were genetically manipulated to have either TP53 knockdown or oncogenic $KRAS^{G12V}$ (Davies et al., 2014). HBECs were also engineered to have both of these mutations at once (Davies et al., 2014). The use of genetically stable HBECs is an advantage over the previous study, as results could be targeted to the specifically induced mutations. VOCs were analysed from the three mutant cell lines and the parental cell line, again with GC-MS and nano-sensor in parallel (Davies et al., 2014). Using GC-MS, the genetic manipulations performed resulted in detectable changes in HBEC VOC profiles; 2-methylpropene, benzaldehyde, tridecane and 1,2,3-trimethylbenzene

were identified as important VOCs (Davies et al., 2014). Nanomaterial sensor analysis again complimented GC-MS analysis, with discriminant factor analysis showing differences between the three mutant and parental cell lines (Davies et al., 2014).

These findings present a novel method for potentially genotyping lung cancer patients using breath-based VOC analysis. Currently, genetic analysis is used within diagnosis pathways and relies on solid tumour tissue, obtained from invasive biopsies which produce a small amount of material (Davies et al., 2014; Peled et al., 2013). Multiple tests must be performed using these small samples in order to decide relevant treatment regimens (Davies et al., 2014; Peled et al., 2013). In this situation breath analysis provides multiple distinct advantages. Firstly, collecting breath is non-invasive and therefore avoids patient biopsies. Secondly, breath provides a virtually endless supply of biological information and therefore a reliable sample source for analysis – in contrast to the small samples collected from biopsy which may be insufficient for all of the tests required. Finally, analysis of VOCs using nanomaterial sensors may translate to a point-of-care breath test (Davies et al., 2014), resulting in a more rapid turnaround time for analysis.

The impact of genetic mutations on the breath VOC profiles of breast cancer patients has also been investigated using both GC-MS and nanoarray sensors (Barash et al., 2015). Differences were observed between controls and breast cancer patients, and between HER2 positive and HER2 negative individuals, using both analysis methods (Barash et al., 2015). However, this proof of concept

needs further validation, particularly as patient breath samples are more complex than those identified *in vitro*, with VOCs originating from a number of sources and other factors affecting profiles.

4.1.2 BAP1 in Malignant Mesothelioma

BRCA1-associated protein 1 (BAP1) is a member of the de-ubiquitylase family of proteins, specifically a ubiquitin carboxy-terminal hydrolase, that was identified and named due to an association with the BRCA1 protein (Jensen et al., 1998). The BAP1 gene is located on chromosome 3p21.3 and the protein is present in both the nucleus and cytoplasm (Bononi et al., 2017). The BAP1 gene is considered a TSG because of the multiple regulatory interactions of the BAP1 protein. Nuclear activities include genome stability during DNA replication; gene expression regulation through epigenetic modifications and transcription factors; ferroptosis induction in response to ROS overproduction and double-strand DNA break repair in response to carcinogens such as asbestos (Carbone et al., 2020). Within the cytoplasm, BAP1 is also involved in the induction of apoptosis in cells with higher than physiological Ca^{2+} concentrations that would otherwise accumulate DNA damage (Bononi et al., 2017). Regulation of processes such as these, particularly ROS overproduction and asbestos-induced DNA damage, make it obvious why BAP1 is critical in the development of MPM.

Susceptibility to mesothelioma across multiple generations of families in Turkey in a hereditary style was observed and several families presented multiple mesothelioma cases in the USA (Carbone et al., 2007). Genetic screening and

sequencing studies of these populations led to the discovery of the familial BAP1 cancer syndrome (Carbone et al., 2007; Carbone et al., 2020). Germline mutations in BAP1 result in individuals being much more susceptible to the development of multiple cancer types, most frequently mesothelioma and uveal melanoma, which due to their hereditary nature can be passed down through many generations (Carbone et al., 2020). Truncating BAP1 mutations were found through sequencing of the 3p chromosome (Carbone et al., 2019). BAP1 mutations follow the traditional two-hit hypothesis of TSGs, with the initial germline mutation on one allele decreasing protein expression or function and further mutations on the second allele leading to BAP1 loss (Carbone et al., 2019). Interestingly, mesothelioma patients that also carried germline BAP1 mutations were found to have a less aggressive malignancy with an increased 5-year survival rate (Baumann et al., 2015). As well as germline mutations, 60-70% of mesotheliomas acquire somatic BAP1 mutations, which are most commonly associated with the epithelioid sub-type and therefore show a limited improvement in prognosis of a few months (Carbone et al., 2020). BAP1 immunohistochemistry is now commonplace in pleural and peritoneal diagnosis and therapeutics are emerging that could potentially target BAP1 (Carbone et al., 2019). For example, gemcitabine is used in the second line treatment of mesothelioma and other cancers, and it has been suggested that BAP1 status could be a predictor of gemcitabine sensitivity (Carbone et al., 2020).

4.1.2.1 VOC Analysis of BAP1-Mutations

BAP1 mutation is an important event in MPM tumourigenesis. As the BAP1 protein is involved in multiple biological activities, it was hypothesised that a

reduction in BAP1 expression would therefore have some impact on cellular VOC output. Experiments were designed to test this hypothesis, using the developed SPME GC-MS headspace analysis methodology (Chapter 2, Section 2.3.3). Two cell lines were kindly provided by Professor Judy Coulson and her laboratory at the University of Liverpool. The first of these, MET-5A$^{w-/KO}$ is a non-malignant mesothelial cell line that has been genetically modified with an adeno associated viral vector (AAV) to have stably reduced BAP1 expression. The MET-5A cell line was gene-edited to sequentially introduce a cancer predisposition syndrome W-mutation on one allele (Testa et al., 2011). This should truncate BAP1 and lead to its degradation; a promoter trap KO was performed on the second allele to prevent BAP1 expression. The MET-5A$^{w-/KO}$ cell line has yet to be published (publication currently in progress; Barnett *et al.,*). The second cell line provided is MET-5A$^{+/+}$, the specific parental cell line used to create MET-5A$^{w-/KO}$. This cell line should have the same characteristics as the MET-5A cell line used at Sheffield Hallam University.

The cell line panel from Chapter 3, MSTO-211H, NCI-H28 and MET-5A, were also analysed again to directly compare with MET-5A$^{w-/KO}$ and MET-5A$^{+/+}$. MSTO-211H and NCI-H28 were analysed to determine if the BAP1 mutated cells produced a VOC profile that was comparable to the two MPM cell lines. MET-5A was analysed to determine if the MET-5A$^{+/+}$ cell line did display the same characteristics as the cells currently used at Sheffield Hallam University. As MPM tumours can often be confused with lung carcinomas which leads to misdiagnosis (Yap et al., 2017), the NCI-H1975 cell line was included, to assess whether MPM

cells, MET-5A cells and the mutant MET-5A$^{w-/KO}$ BAP1 mutants could be distinguished from lung cancer cells.

This comprehensive cell line panel including biphasic MPM, epithelioid MPM, non-malignant mesothelial, BAP1 mutated mesothelial and lung cancer cell lines allows for many different comparisons to be made, which can be structured towards the diagnostic requirements of MPM. Translating clinically, the ability to detect BAP1 mutation using a VOC breath test has the potential to identify individuals susceptible to MPM development at an earlier stage, providing a greater chance of therapeutic intervention.

4.2 Aims of the Chapter

The main aim of this chapter was to investigate the effects of BAP1 mutation on VOC profiles within MPM, by using the MET-5A$^{w-/KO}$ mutant cell line, in collaboration with the University of Liverpool. The cell line panel used in this chapter was used for secondary objectives. The effect of cell culture flasks on VOCs was explored as cells were cultured in smaller cell culture flasks. The NCI-H1975 lung cancer cell line was also included to compare lung cancer to MPM and the mutant cell lines.

4.2.1 Hypothesis

MPM associated mutations in the BAP1 gene affect VOC profiles. The genetically manipulated cell line, MET-5A$^{w-/KO}$ produces a different VOC profile from controls.

4.3 Methods

4.3.1 Cell Culture

MSTO-211H, NCI-H28, MET-5A and NCI-H1975 cell lines were purchased from ATCC. MET-5A$^{+/+}$ and MET-5A$^{w-/KO}$ were kindly donated by Professor Judy Coulson at The University of Liverpool. MSTO-211H, NCI-H28 and NCI-H1975 were maintained in complete RPMI-1640 containing 10% v/v FBS and 1% v/v pen/strep. MET-5A and MET-5A$^{+/+}$ were maintained in complete M199 containing 10% v/v FBS, 1% v/v pen/strep, 3.3nM EGF, 400nM hydrocortisone, 870nM zinc-free bovine insulin, 20mM HEPES and 0.3% v/v Trace Elements B. MET-5A$^{w-/KO}$ cells were also maintained in complete M199 with additional 0.7µg/ml puromycin and 0.1mg/ml G418 (Sigma Aldrich), M119^{KO} media. All cell lines were maintained at 37^{o}C in the presence of 5% CO_2 in a humidified incubator. Cells were passaged twice weekly using Trypsin-EDTA detachment.

4.3.2 Headspace VOC Extraction

MSTO-211H, NCI-H28, NCI-H1975, MET-5A, MET-5A$^{+/+}$ and MET-5A$^{w-/KO}$ cells were prepared for headspace VOC extraction. 2x10^{6} cells were seeded into T25 cell culture flasks with their respective media and incubated under standard cell culture conditions for 24 hours. Control flasks containing only complete RPMI-1640, M199 and M199^{KO} were also prepared and incubated under standard cell culture conditions for 24 hours. After incubation headspace analysis was performed as in Section 3.3.2.

4.3.3 Gas Chromatography-Mass Spectrometry

GC-MS analysis of the SPME fibre was performed in Section 3.3.3.

4.3.4 Data Analysis

4.3.4.1 Data Pre-processing

GC-MS chromatograms were visualised using Agilent MassHunter Data Analysis; tentative peak identification was performed through spectral match to the NIST library database (V11; NIH). The spectral match cut-off point for NIST library searches was set to 80%. For each chromatogram, a library search report was generated in MassHunter which included peak RT, peak area and the automatically assigned number one NIST match for each peak that met the 80% threshold. Artefacts of SPME and GC-MS, (complex siloxane-containing compounds) were manually removed from library search reports. RTs and peak areas for all samples were used to create an aligned data matrix in .CSV format. RTs were rounded to one decimal place prior to alignment. GCalignR in R-studio (Ottensmann et al., 2018) was used to align RTs and peak areas resulting in a single aligned data matrix containing average RTs for each sample and corresponding peak area values for each RT. The aligned data matrix was manually checked to identify any discrepancies in alignment.

4.3.4.2 Data Normalisation and Background Filtering

The aligned data matrix was uploaded to Metaboanalyst 5.0 (Pang et al., 2021) for data normalisation and background filtering. Variables were filtered by

interquartile range, normalisation by sum and auto-scaling was applied. For background filtering batch t-tests (two-sample t-tests) comparing MSTO-211H, NCI-H28, NCI-H1975, MET-5A, MET-5A$^{+/+}$ and MET-5A$^{w-/KO}$ groups to their respective RPMI-1640, M199 or M199^{KO} media control groups were performed. The data matrix was then edited to only contain the significantly altered variables from the t-tests and RPMI-1640, M199 and M199^{KO} groups were removed resulting in a cell line specific data matrix. The cell line matrix was used for all subsequent statistical analysis.

4.3.4.3 Data Visualisation and Multivariate Statistical Analysis

The cell line matrix in .CSV format was imported into SIMCA (V17.0.2; Umetrics). PCA, PLS-DA and OPLS-DA were performed to visualise similarities and differences in the VOC profiles between the groups. Further batch t-tests (two-sample t-tests) were performed using Metaboanalyst to identify significantly altered variables across the cell line groups.

4.3.5 BAP1 Western Blot

MSTO-211H, NCI-H28, MET-5A, MET-5A$^{+/+}$, MET-5A$^{w-/KO}$ and NCI-H1975 cells were prepared in 6-well plates at 500,000cells/well and incubated for 24 hours. After incubation, culture media was removed, and cells washed twice with phosphate buffered saline (PBS). Cells were lysed with 1X Laemmli buffer containing 1% protease inhibitor and protein extracted through cell scraping. Protein extracts were quantified using bicinchoninic acid (BCA) assay (ThermoFisher). 20µg total protein samples were prepared in a 1X sample buffer

and incubated at 90°C for 4 min. Electrophoresis of protein samples was performed on a 10% sodium dodecyl-sulphate polyacrylamide gel electrophoresis (SDS-PAGE) gel and transferred to a nitrocellulose membrane. The membrane was blocked in blocking solution, 5% w/v non-fat milk in 1X tris-buffered saline with 0.1% Tween 20 (TBST), for 1 hour at room temperature with shaking. Primary antibodies for BAP1 (Insight Biotechnology) and GAPDH (Cell Signalling Technology) were diluted in blocking solution; 1:50 for BAP1 and 1:5000 for GAPDH. The blocking solution was removed from the membrane and replaced with the primary antibodies. The primary antibody incubation was performed at 4°C with shaking overnight. The primary antibody solution was removed, and the membrane washed 3 times with TBST for 10 min at room temperature with shaking. Both anti-BAP1 and anti-GAPDH secondary LiCor antibodies were diluted 1:10,000 in blocking solution. The membrane was incubated for 1 hour at room temperature with shaking in the secondary antibody solution. The secondary antibody solution was removed, and the membrane was washed again 3 times with TBST for 10 min at room temperature with shaking. Finally, the membrane was visualised using a LiCor Odyssey Scanner and Image Studio Lite software. BAP1 bands were quantified against GAPDH bands in comparison to MET-5A$^{+/+}$ using densitometry analysis in ImageJ.

4.4 Results

4.4.1 Development of a Cell Line VOC Matrix

After alignment with GCAlignR, the initial data matrix consisted of 81 samples and 229 aligned RTs – 18,549 individual values in total. After media background

filtering, the cell line matrix contained 54 samples and 81 aligned RTs, totalling 4374 individual values. Using the normalised cell line matrix, different comparisons were made in order to visualise the similarities and differences between the groups.

4.4.2 Multiple Group Comparisons

Before focusing on the effects of the BAP1 mutation, multiple group comparisons were made. These were used to give an overview of the dataset used in this chapter and also to compare the results from the T25 flasks to the previous T75 data (Chapter 3 Section 3.4).

4.4.2.1 All Cell Line Groups

A comparison of MSTO-211H, NCI-H28, NCI-H1975, MET-5A, MET-5A$^{+/+}$ and MET-5A$^{w-/KO}$ groups was performed; PCA, PLS-DA and OPLS-DA were applied in SIMCA. PCA and PLS-DA score plots showed poor separation between the different groups (Figure 4.1 & Figure 4.2). Improved clustering of some replicates was observed using PLS-DA, specifically NCI-H1975 and MET-5A$^{+/+}$ groups (Figure 4.2). The OPLS-DA score plot showed the most separation between groups and clustering of replicates within groups was tighter than with PCA and PLS-DA (Figure 4.3).

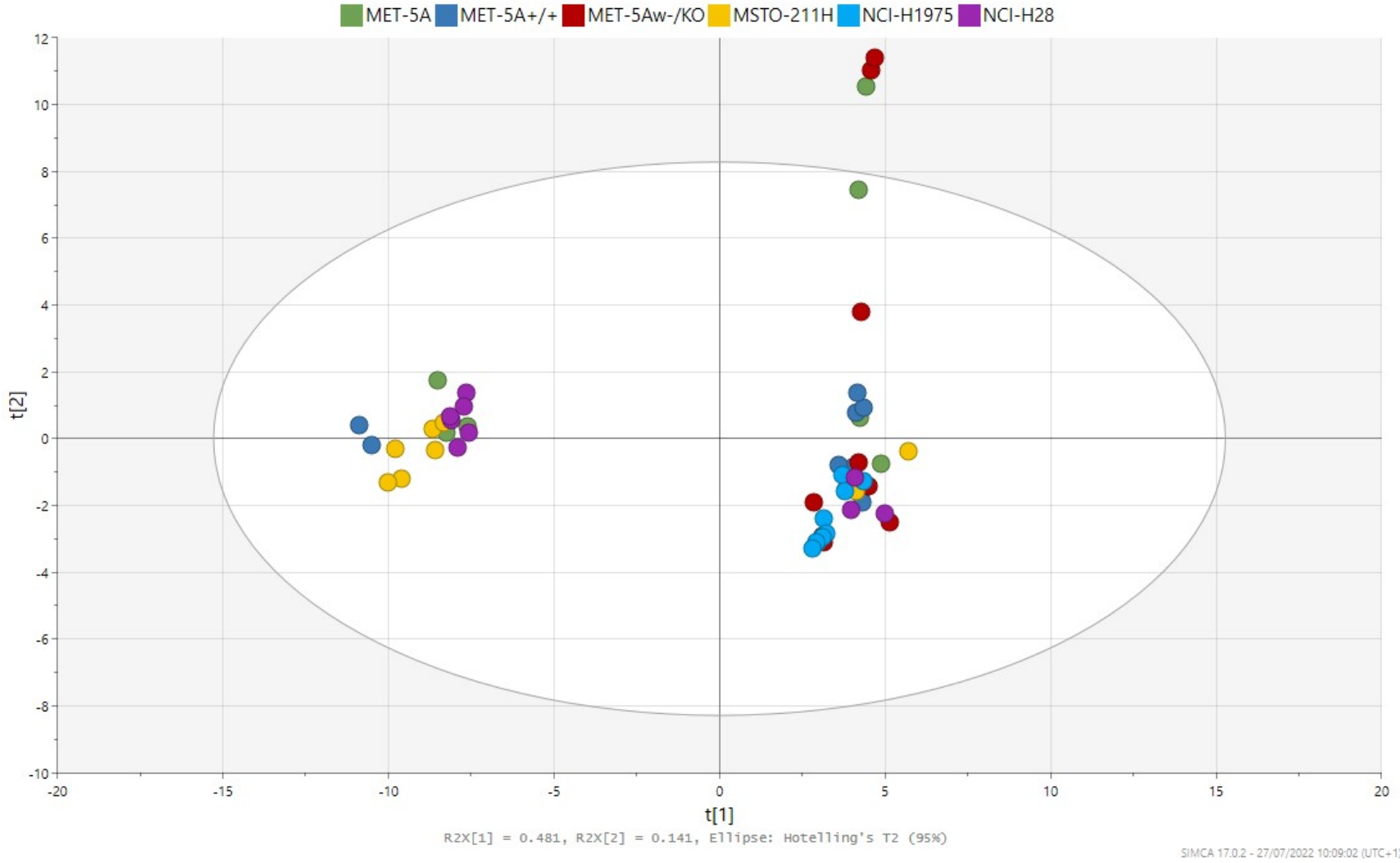

Figure 4.1: PCA score plot generated in SIMCA (V17.0.2) from MSTO-211H, NCI-H28, NCI-H1975, MET-5A, MET-5A+/+ and MET-5Aw-/KO groups. Each point represents a single replicate after data normalisation and background filtering. 9x individual replicates per group.

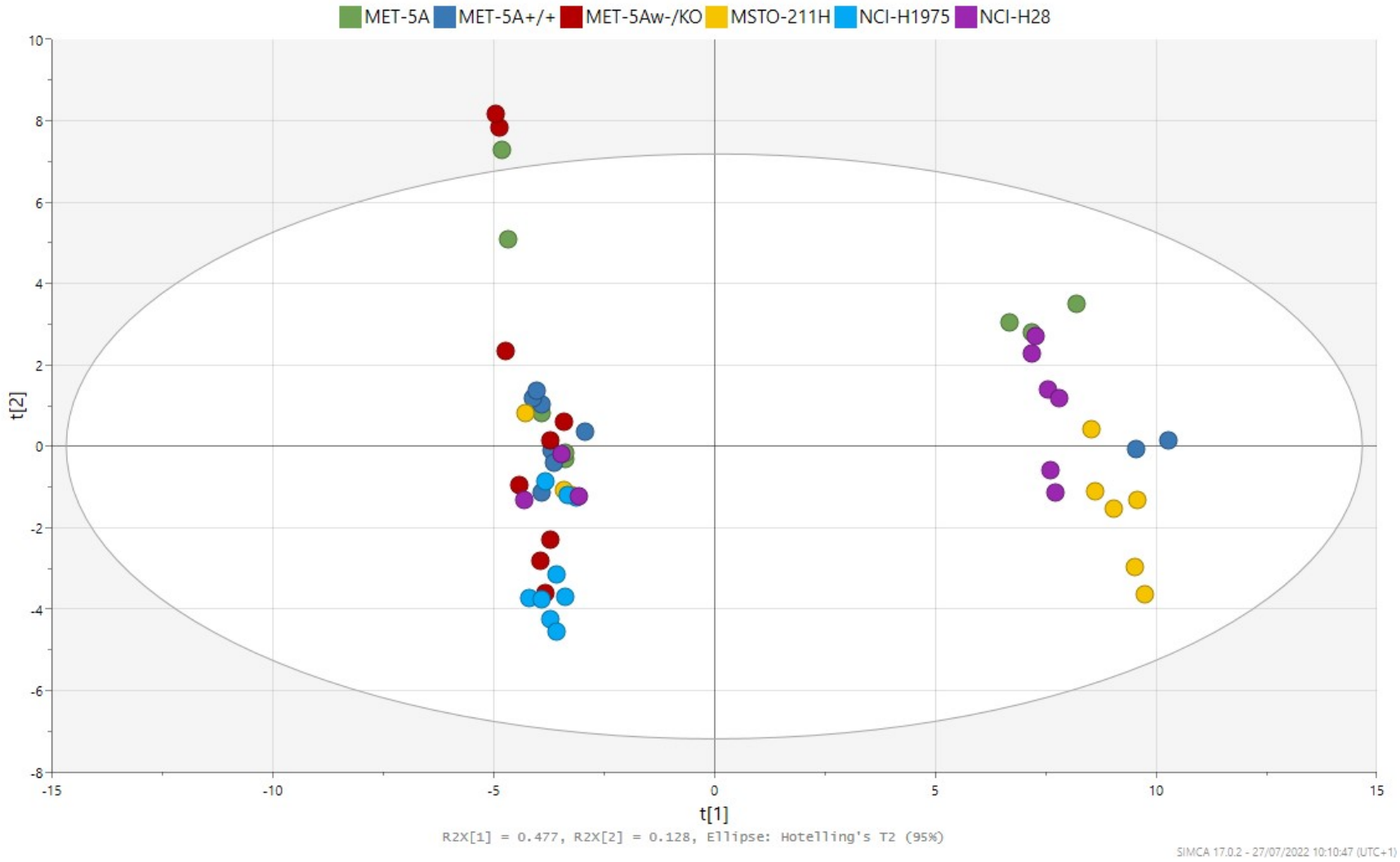

Figure 4.2: PLS-DA score plot generated in SIMCA (V17.0.2) from MSTO-211H, NCI-H28, NCI-H1975, MET-5A, MET-5A+/+ and MET-5Aw-/KO groups. Each point represents a single replicate after data normalisation and background filtering. 9x individual replicates per group.

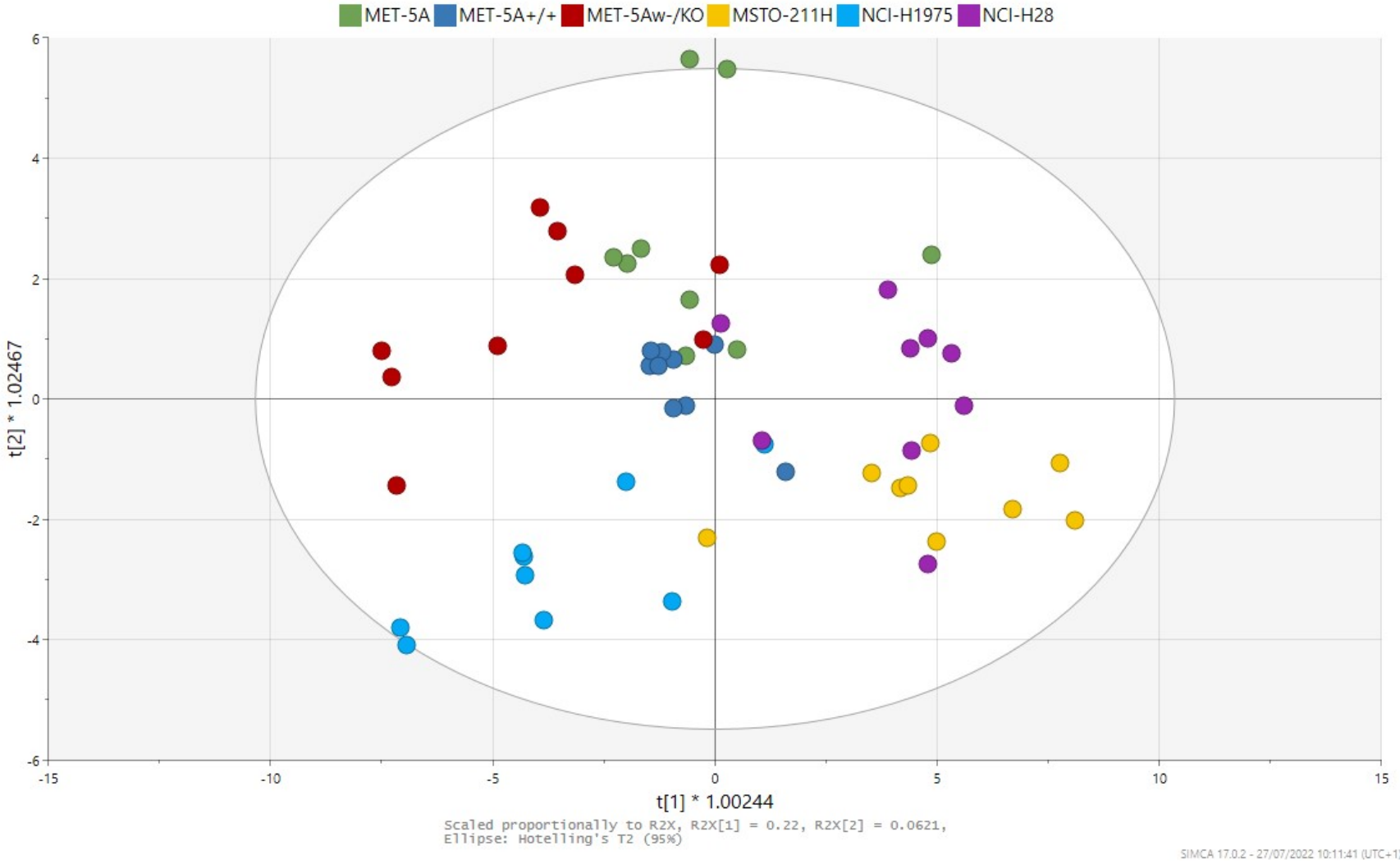

Figure 4.3: OPLS-DA score plot generated in SIMCA (V17.0.2) from MSTO-211H, NCI-H28, NCI-H1975, MET-5A, MET-5A+/+ and MET-5Aw-/KO groups. Each point represents a single replicate after data normalisation and background filtering. 9x individual replicates per group.

4.4.2.2 Malignant Pleural Mesothelioma and Lung Cancer Comparison

A comparison was made between the two MPM cell lines, MSTO-211H and NCI-H28, the non-malignant mesothelial cell line MET-5A and the lung cancer cell line, NCI-H1975. The PCA score plot showed some separation between the different groups and several of the groups showed good clustering of replicates (Figure 4.4A). The NCI-H1975 group showed tight clustering between replicates, in contrast the MET-5A group showed the poorest clustering, with results spread across the plot (Figure 4.4A). The majority of MSTO-211H and NCI-H28 replicates clustered together, however several outliers were observed (Figure 4.4A). The PLS-DA score plot showed a similar trend to the PCA plot, with slightly altered separation and clustering of the groups (Figure 4.4B). The OPLS-DA score plot showed a general separation between the two MPM groups (MSTO-211H and NCI-H28) and the NCI-H1975 group along the x-axis; The MET-5A group appeared to cluster between the MPM groups and NCI-H1975 (Figure 4.4C). Some crossover was observed between the groups, but in general replicates clustered together within their group (Figure 4.4C).

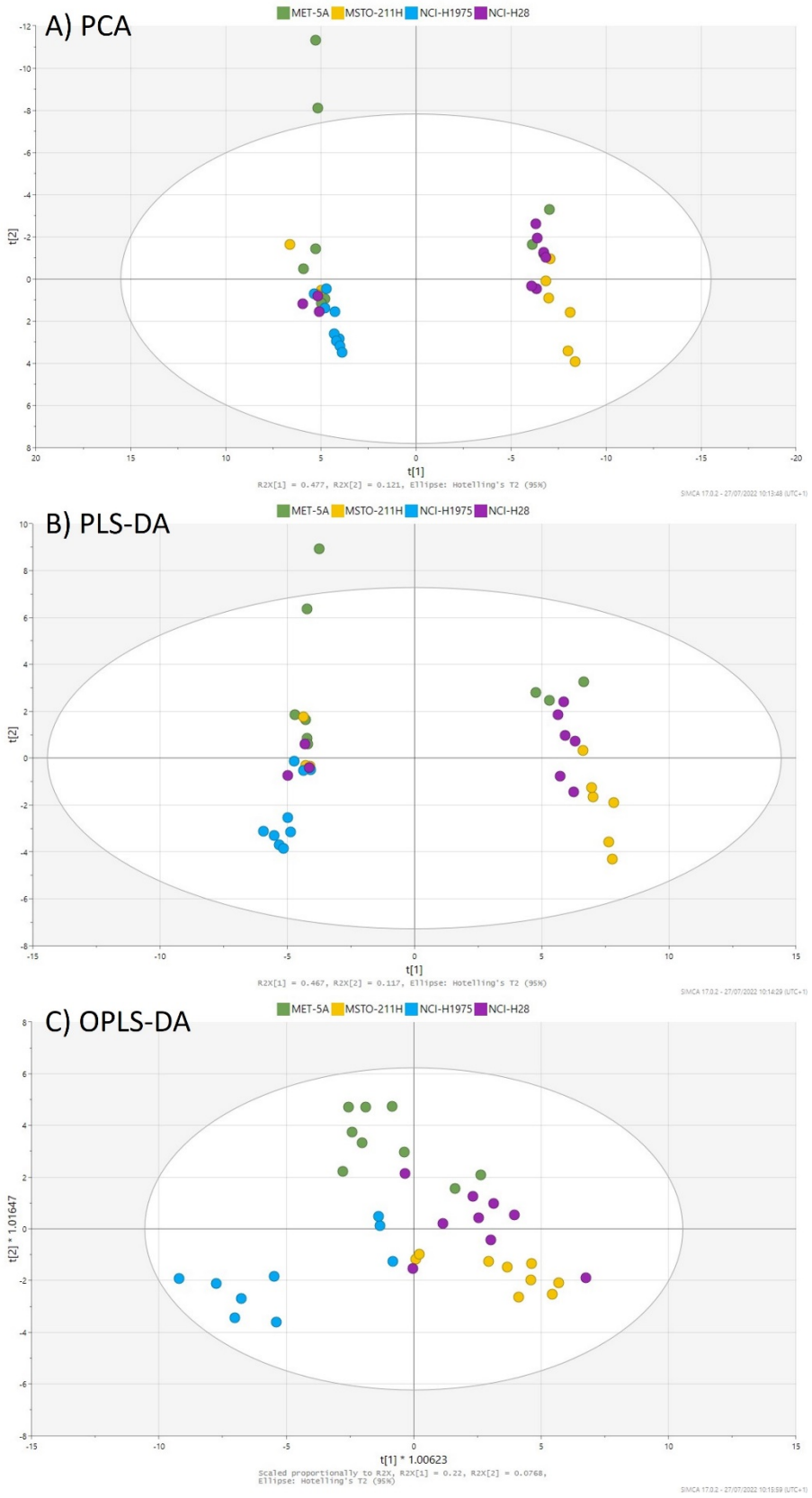

Figure 4.4: A) PCA, B) PLS-DA & C) OPLS-DA score plots generated in SIMCA (V17.0.2) from MSTO-211H, NCI-H28 and NCI-H1975 groups. Each point represents a single replicate after data normalisation and background filtering. 9x individual replicates per group.

Batch t-tests were performed in Metaboanalyst comparing MSTO-211H, NCI-H28 and NCI-H1975 profiles to the MET-5A group; a number of significantly different variables were identified (Table 4.1). Several variables had discrepancies in tentative identification through NIST library search. Some of these variables could be tentatively identified manually (Table 4.1); potential identities for the remaining variables are included in the Appendix (Table 7.2).

Table 4.1: Significantly altered VOCs in MSTO-211H, NCI-H28 and NCI-H1975 groups with comparison to the MET-5A group ($p<0.05$). *Represents compounds that had small discrepancies in identification between replicates but could be confidently identified. Tentative NIST IDs in *italic* had discrepancies in identification between replicates (potential identities are included in the Appendix, Table 7.2).

AVG RT (min)	Tentative NIST ID	MSTO-211H Trend	NCI-H28 Trend	NCI-H1975 Trend
1.3	Carbon dioxide*	-	-	Increase
6.9	Ethyl acetate	Increase	-	-
17.2	Nonane*	-	-	Decrease
17.5	m/o/p-xylene	Increase	Increase	Increase
20.3	*Alkane*	-	Increase	-
20.4	*Ketone/alkane*	-	-	Decrease
21.0	2-butoxy ethanol	Increase	-	Increase
21.4	Decane	-	-	Increase
21.6	*Alkane*	-	-	Decrease
22.8	*Alkane*	-	Decrease	Decrease
23.2	*Alkane*	-	Decrease	-
23.7	*Alkane*	-	-	Decrease
25.4	*Alkane*	-	-	Increase
25.5	Undecane*	-	-	Increase
26.0	2-ethyl-1-hexanol	-	-	Increase
26.8	*Alkane*	-	-	Increase
28.4	2-butoxyethyl acetate	Increase	Increase	Increase
28.5	*Alkane*	-	-	Increase
29.4	Dodecane	Increase	Increase	Increase
31.4	*Alkane*	-	-	Increase
35.7	*Alkane*	Increase	Increase	-
36.5	*Alkane*	-	-	Increase
39.0	*Alkane*	Increase	Increase	-
40.8	Hexadecane*	Increase	-	-
42.6	Eicosane*	Increase	-	-

4.4.3 BAP1 Mutation Comparison

4.4.3.1 BAP1 Mutant Compared to MET-5A

A comparison was performed between MET-5A (Sheffield Hallam University), MET-5A$^{+/+}$ (University of Liverpool) and MET-5A$^{w-/KO}$ (BAP1 mutant) groups to determine the effects of BAP1 mutation. The PCA score plot showed crossover between all three groups, and no real separation between the groups; several outliers were also observed (Figure 4.5A). Again, similar trends were observed when PLS-DA was applied; clustering was improved for the main set of results, but outliers were still observed for MET-5A$^{+/+}$ and MET-5A$^{w-/KO}$ groups (Figure 4.5B). OPLS-DA analysis improved the spread of the results (Figure 4.5C). MET-5A and MET-5A$^{+/+}$ groups separated from the MET-5A$^{w-/KO}$ group along the x-axis and separation was observed along the y-axis between MET-5A and MET-5A$^{+/+}$ groups (Figure 4.5C). Despite this, tight clustering was not observed in any of the groups with all results spread across the plot and crossover between the three groups (Figure 4.5C).

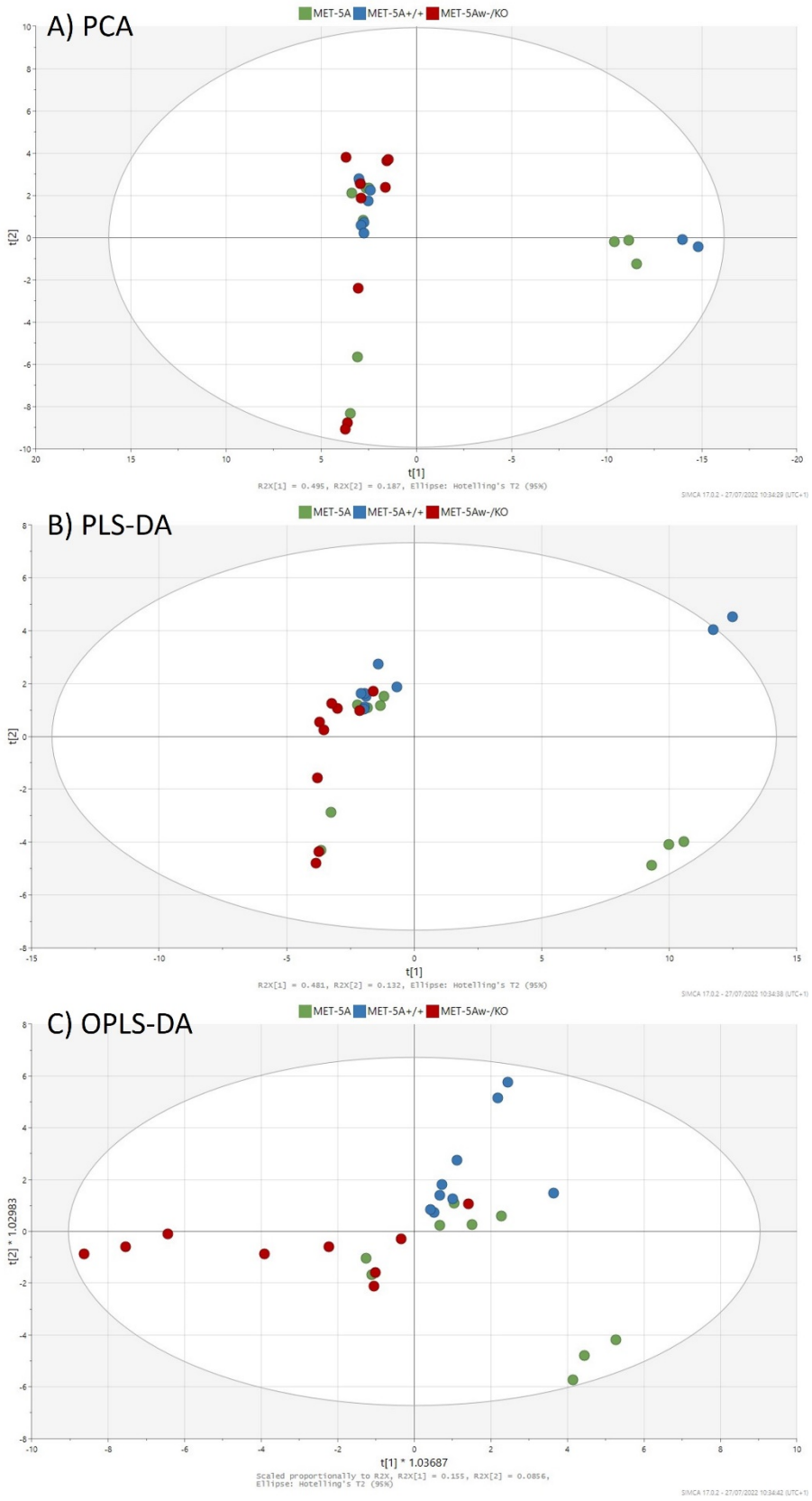

Figure 4.5: A) PCA, B) PLS-DA & C) OPLS-DA score plots generated in SIMCA (V17.0.2) from MET-5A, MET-5A$^{+/+}$ and MET-5A$^{w-/KO}$ groups. Each point represents a single replicate after data normalisation and background filtering. 9x individual replicates per group.

Batch t-tests (two-sample t-tests) were performed in Metaboanalyst comparing MET-5A and MET-5A$^{+/+}$ groups to the MET-5A$^{w-/KO}$ group. Several variables were identified as significantly different across the two comparisons (Table 4.2 & Table 4.3). CO_2 was significantly increased in the MET-5A$^{w-/KO}$ group compared to both the MET-5A and MET-5A$^{+/+}$ groups (Table 4.2 & Table 4.3). 3,7-dimethyl-nonane was also increased in MET-5A$^{w-/KO}$ compared to MET-5A$^{+/+}$ (Table 4.3). Both 1-methoxy-2-propyl acetate and tetradecane were decreased in MET-5A$^{w-/KO}$ compared to MET-5A$^{+/+}$ (Table 4.3). An alkane with an average RT of 21.6 min was decreased in MET-5A$^{w-/KO}$ compared to MET-5A, whereas an alkane with an average RT of 31.4 min was increased (Table 4.2). 2-butoxyethyl acetate was also decreased in MET-5A$^{w-/KO}$ compared to MET-5A (Table 4.2). T-tests were also performed between MET-5A and MET-5A$^{+/+}$ profiles – no significantly different variables were identified.

Table 4.2: Significantly altered variables in the MET-5Aw-/KO group with comparison to the MET-5A group (p<0.05). Tentative NIST IDs in *italic* had discrepancies in identification between replicates (potential identities are included in the Appendix, Table 7.2).

AVG RT (min)	Tentative NIST ID	Trend in MET-5A$^{w-/KO}$
1.3	Carbon dioxide	Increase
21.6	*Alkane*	Decrease
28.4	2-butoxyethyl acetate	Decrease
31.4	*Alkane*	Increase

Table 4.3: Significantly altered variables in the MET-5Aw-/KO group with comparison to the MET-5A+/+ group (p<0.05).

AVG RT (min)	Tentative NIST ID	Trend in MET-5A$^{w-/KO}$
1.3	Carbon dioxide	Increase
19.4	1-methoxy-2-propyl acetate	Decrease
24.0	3,7-dimethyl-nonane	Increase
37.6	Tetradecane	Decrease

4.4.3.2 BAP1 Mutant Compared to Malignant Pleural Mesothelioma

A comparison was made between MSTO-211H, NCI-H28 and MET-5A$^{w-/KO}$ groups to compare the BAP1 mutant to MPM cell lines. PCA showed separation between the majority of MSTO-211H/NCI-H28 results and MET-5A$^{w-/KO}$ results (Figure 4.6A). However, outliers were observed for the MET-5A$^{w-/KO}$ group and several MSTO-211H and NCI-H28 replicates clustered with the MET-5A$^{w-/KO}$ results (Figure 4.6A). Again, a similar trend was observed when PLS-DA was applied, with improved separation of the groups (Figure 4.6B). The OPLS-DA score plot showed general separation of all three groups with some crossover (Figure 4.6C).

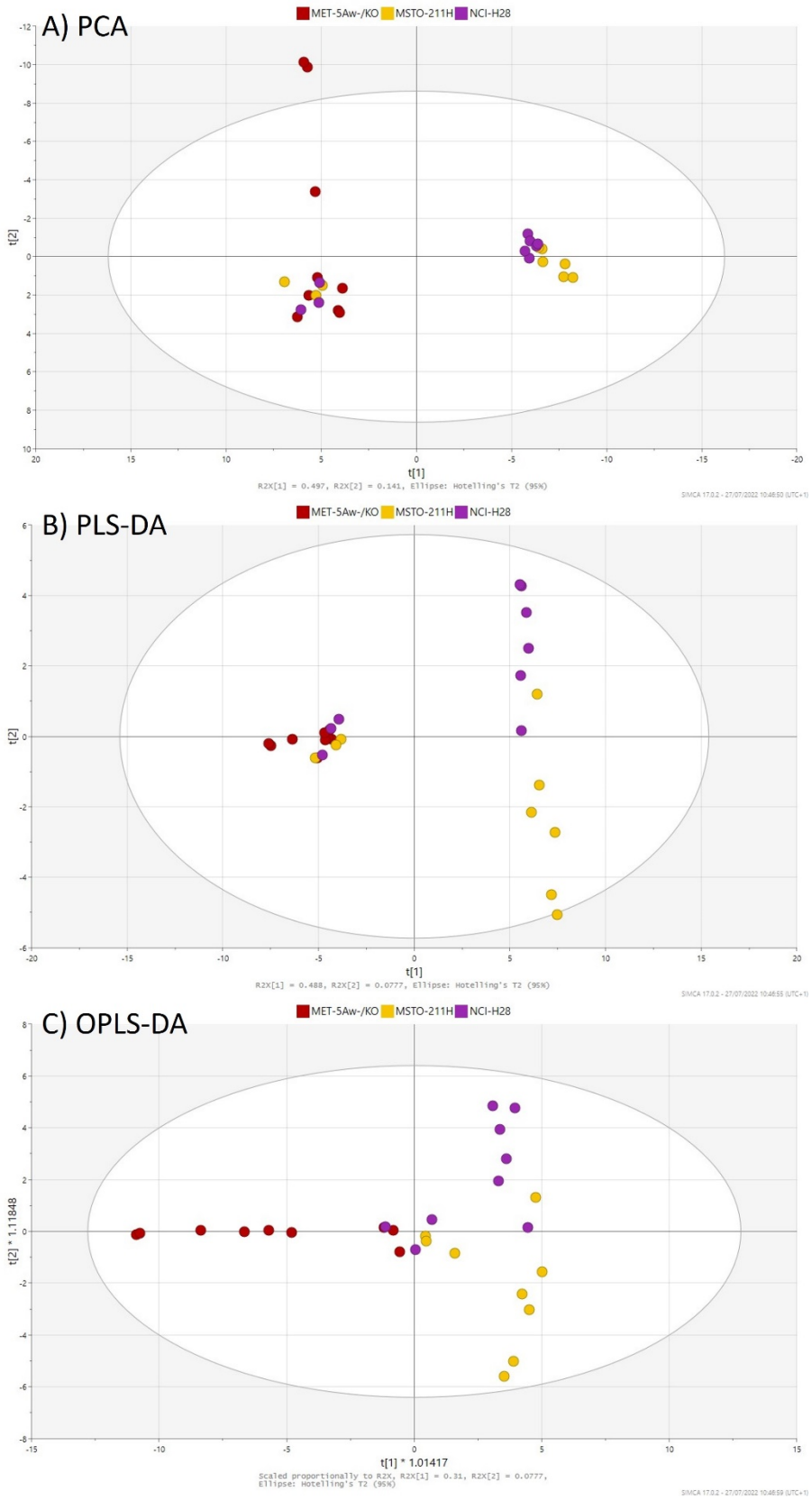

Figure 4.6: A) PCA, B) PLS-DA & C) OPLS-DA score plots generated in SIMCA (V17.0.2) from MSTO-211H, NCI-H28 and MET-5A$^{w-/KO}$ groups. Each point represents a single replicate after data normalisation and background filtering. 9x individual replicates per group.

4.4.4 BAP1 Expression

Two clear sets of bands were observed using Western blot showing BAP1 and GAPDH expression for MSTO-211H, NCI-H28, NCI-H1975, MET-5A, MET-5A$^{+/+}$ and MET-5A$^{w-/KO}$ protein extracts (Figure 4.7).

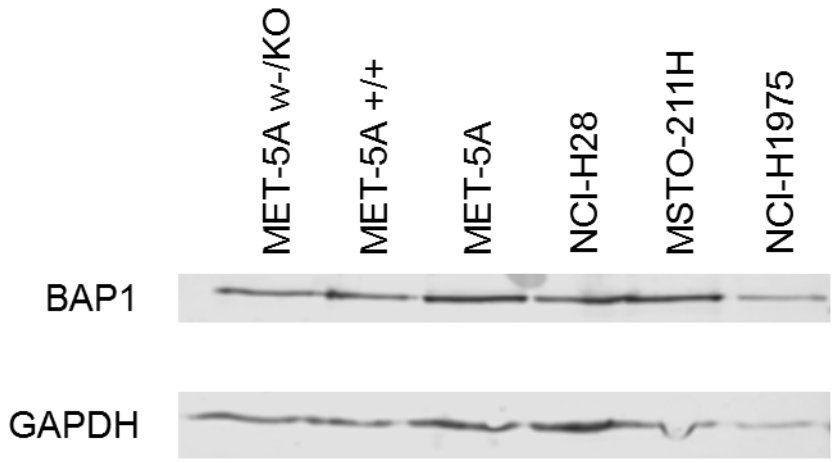

Figure 4.7: Western blot showing BAP1 and GAPDH expression in protein samples extracted from MSTO-211H, NCI-H28, NCI-H1975, MET-5A, MET-5A+/+ and MET-5Aw-/KO cells.

Relative BAP1 expression was calculated by densitometry analysis of BAP1 and GAPDH bands using ImageJ, results were normalised against MET-5A$^{+/+}$ (Figure 4.8). MET-5A$^{w/KO}$ showed approximately 50% BAP1 expression compared to MET-5A$^{+/+}$, MET-5A showed similar levels of expression (Figure 4.8). MSTO-211H showed around double the expression of MET-5A$^{+/+}$ and NCI-H28 showed around half the expression; NCI-H1975 showed a small increase in BAP1 expression (Figure 4.8).

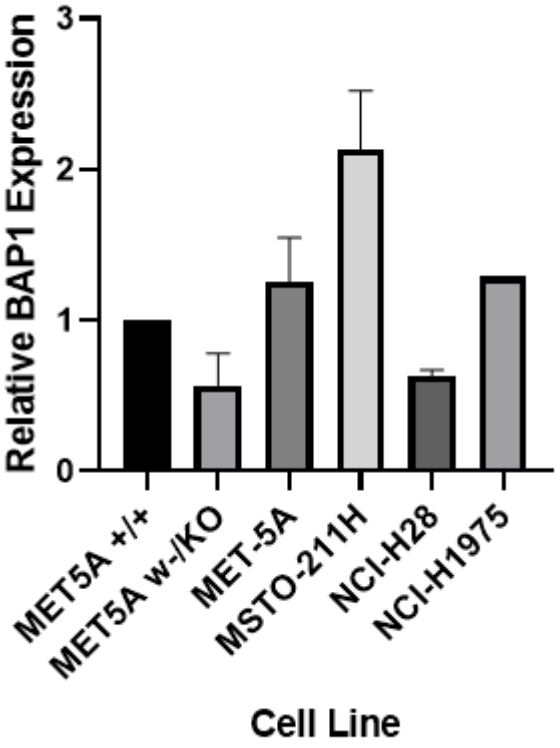

Figure 4.8: Relative BAP1 expression from MET-5A+/+, MET-5Aw-/KO, MET-5A, MSTO-211H, NCI-H28 and NCI-H1975 protein extracts. N=2 for all groups apart from NCI-H1975 (n=1).

4.5 Discussion

4.5.1 Gas Chromatography-Mass Spectrometry of Branched Alkanes

A number of variables were not able to be confidently identified in the current analyses (Table 4.1 & Table 4.2). Within an individual replicate, the NIST match cut-off of 80% was met, with these variables generally being tentatively identified as longer chain and branched alkanes. However, when comparing across multiple replicates, discrepancies in compound ID were found, which meant that confident identification was not possible. There are several possible explanations for this, and it is likely that a combination of different factors was responsible for the observed results.

Firstly, as previously mentioned, the identification of compounds using GC-MS was tentative. Identification of variables relied solely on spectral match to the NIST library database, with a cut-off point of ≥80%. Although these parameters have been used in the majority of breath analysis literature using GC-MS, it is not possible to have a 100% identification of any compound unless pure standard reference compounds are also analysed using exactly the same methodology. Due to the number of variables identified in the current analyses and the multiple possible identities of the unidentified compounds, taking these steps would result in a considerable amount of expensive experimental work. The second possible reason for the lack of identification relies on the chromatography aspect of the GC-MS methodology. Gas chromatography involves the separation of a mixture of compounds based predominantly on their volatility – within GC-MS, as the

temperature of the oven increases, compounds are gradually released from the GC column and detected by MS. VOCs in the headspace of cell cultures represent a very complex mixture of compounds, including many that are both structurally and chemically similar. Therefore each sample consists of many compounds that are difficult to separate based on their volatility and interaction with the GC-MS column, and therefore presents difficulties with GC-MS. This complexity can be addressed through optimisation of the oven temperature programming; however, it is a balance between achieving optimal chromatography and a method that can be performed in a manageable timescale. The current method was optimised to an acceptable level, with a run time of 45.25 min, which is quite long compared to the rest of the literature. Optimisation of this again may increase the GC-MS run time, which in turn would affect the number of samples able to be processed in a day. This could have a negative impact on experimental workflows which are already lengthy due to the dependence on cell cultures; ultimately reducing the amount of data that could be collected. Finally, it has been recognised that there are issues detecting longer chain and branched alkanes using GC-MS due to the ionisation patterns produced by these compounds (Sparkman et al., 2011).

A possible solution for this problem is the deconvolution of GC-MS data. In GC-MS, co-elution of compounds combined with the fragmentation of molecular ions caused by hard EI ionisation can result in a mass spectrum consisting of mass peaks from the co-eluting compounds combined (Du & Zeisel, 2013). This is a potential cause of the misidentification of a compound at a given RT. Deconvolution is the process of separating the co-eluting compounds and

obtaining a pure spectrum for each component (Du & Zeisel, 2013). In turn, this can give a more confident identification of the target compounds. Deconvolution relies on complex computational algorithms and software tools (Du & Zeisel, 2013). Limitations of the software and NIST library used in the current analyses meant that deconvolution of the data was not possible. It was therefore decided to report the potential identities of each of the variables that could not be confidently identified. As MPM VOC analysis is still in its early stage, this solution at least provides more candidate compounds until clinically relevant and viable VOC biomarkers are decided. Alternative methods of VOC analysis, such as PTR, SIFT and MCC-IMS, may also help with identifying certain compounds (Janssens et al., 2020).

The recent study that used TD GC-MS to analyse the headspace of MPM cell cultures also reported unidentified compounds (Janssens et al., 2022). In total, 277 VOC peaks were detected during analysis with 77 of these able to be identified; unidentified VOCs were reported with their corresponding RT (Janssens et al., 2022). Unidentified VOCs were chosen not to be removed from the analysis as they still have the potential to be important discriminators of MPM, this is reflected in the number of unidentified compounds used within the regression models (Janssens et al., 2022). The improvement of VOC analysis and detection methods was discussed as an area for future research in order to achieve the optimal identification of candidate biomarkers (Janssens et al., 2022).

4.5.2 Multiple Group Comparisons

To visualise the data from all groups at the same time PCA, PLS-DA and OPLS-DA score plots were generated using MSTO-211H, NCI-H28, NCI-H1975, MET-5A, MET-5A$^{+/+}$ and MET-5A$^{w-/KO}$ results (Figure 4.1, Figure 4.2 & Figure 4.3). Although some clustering of replicates was observed using PCA and PLS-DA there was a large amount of crossover between the results and defined separation between the different groups was not observed (Figure 4.1 & Figure 4.2). Only when using OPLS-DA did the separation and clustering of results improve to a point that showed clear definition between all of the groups (Figure 4.3). There was still a lot of crossover between groups but in general MPM groups separated away from MET-5A groups and the lung cancer NCI-H1975 group separated from both (Figure 4.3). Within MPM and MET-5A groups some separation was also observed between the individual groups (Figure 4.3). The improvement in clustering and separation of results as analysis progressed from PCA, to PLS-DA and finally OPLS-DA is something that was seen throughout the rest of the comparisons made. This is to be somewhat expected as it is well recognised that as analysis progresses through these different algorithms an improvement in the separation between groups will be observed, with OPLS-DA being the most optimistic technique. This indicates that, even after data normalisation and background reduction, the VOC profiles produced by the cell line groups were still quite similar, with changes in specific compounds expected to be relatively subtle.

4.5.2.1 Malignant Pleural Mesothelioma and Lung Cancer Comparison

Comparisons were made between MSTO-211H, NCI-H28, MET-5A and NCI-H1975 results (Figure 4.4). As MSTO-211H, NCI-H28 and MET-5A cells had

previously been sampled in T75 flasks (Chapter 3, Section 3.4), analysis of the same cell lines in T25 flasks meant that the effects of cell culture size on VOC profiles could be determined. General separation between these three cell lines was observed (Figure 4.4), indicating some differences in the VOC profiles produced. MSTO-211H and NCI-H28 groups appeared to be more similar to each other than the MET-5A group, although there was some crossover between NCI-H28 and MET-5A results (Figure 4.4). These results are to be expected when cell phenotype is considered. MSTO-211H and NCI-H28 are both MPM cell lines, likely to be similar to each other and distinct from the non-malignant MET-5A control. MSTO-211H is the more aggressive biphasic MPM sub-type which may also be expected to be more different to MET-5A compared to the epithelioid NCI-H28. The trends observed in the current results indicate that the VOC profiles represent these expected differences between the cell lines and also show that the analysis in T25 flasks was comparable to the previous T75 results (Chapter 3, Section 3.4).

As MPM can often be mis-diagnosed as lung carcinoma, analysis of NCI-H1975 was also performed to assess how VOC profiles produced by a lung cancer cell line compared to MPM cell lines. OPLS-DA analysis showed that NCI-H1975 separated from the MPM and mesothelial groups with clustering of the majority of replicates (Figure 4.4C). The results suggested that the VOCs produced by the NCI-H1975 cell line were different from both the MPM cell lines and the MET-5A control (Figure 4.4C). These findings were further confirmed through the identification of a number of compounds significantly altered in the NCI-H1975 group compared to the MET-5A group, which were also exclusive to NCI-H1975

(Table 4.1). Interestingly, the majority of the alkanes that could not be confidently identified were found to be significantly altered in the NCI-H1975 group (Table 4.1). A number of alkanes were found associated with lung cancer cell lines across multiple studies (Janssens et al., 2020), potentially indicating a link between this group of compounds and this tumour type.

4.5.3 BAP1 Mutation and VOC Profiles

4.5.3.1 BAP1 Mutant Compared to Mesothelial Cells

All three multivariate analysis methods, PCA, PLS-DA and OPLS-DA, showed crossover between MET-5A, MET-5A$^{+/+}$ and MET-5A$^{w-/KO}$ groups (Figure 4.5), indicating that there may have been similarities in their VOC profiles. Only with OPLS-DA did the groups begin to show some separation (Figure 4.5C). These similarities were confirmed when t-tests were performed comparing two groups. No significant differences were found in the VOC profiles between the MET-5A group and the MET-5A$^{+/+}$ group, indicating that MET-5A cells and the parental MET-5A$^{+/+}$ cells were producing the same VOCs. This result is to be somewhat expected; MET-5A is a commercially available secondary cell line and cells should therefore remain the same if they are cultured under the recommended conditions. However, it is reassuring that the parental cells used to create the mutant cell line, which were cultured at The University of Liverpool, were the same as the standard MET-5A controls. This finding also increases confidence in the experimental and statistical analysis workflow presented currently and allows for more appropriate further conclusions to be drawn.

The similarities between the MET-5A and MET-5A$^{+/+}$ cells were again shown in the western blot results; both cell lines showed similar expression of BAP1 (Figure 4.7 & Figure 4.8). In contrast to this, the MET-5A$^{w-/KO}$ cells showed a reduced BAP1 expression of approximately 50%, when compared to the MET-5A$^{+/+}$ controls (Figure 4.7 & Figure 4.8). These results confirm what was previously shown by the University of Liverpool, the MET-5A$^{w-/KO}$ cell line has stably reduced BAP1 expression (unpublished data, Barnett *et al.*). This finding also supports the main aim of the current chapter and indicates that changes in VOC profiles produced by the MET-5A$^{w-/KO}$ cell line can be more confidently linked to the presence of the BAP1 mutation. In turn, this allows for an association to be made between specifically identified VOCs and BAP1 mutation and expression.

Four variables were found to be significantly different in the MET-5A$^{w-/KO}$ group compared to both the MET-5A and MET-5A$^{+/+}$ groups, however there were differences in these variables between the two comparisons (Table 4.2 & Table 4.3). The only concordant compound across both comparisons was CO_2, which was significantly increased in MET-5A$^{w-/KO}$ compared to both MET-5A and MET-5A$^{+/+}$ (Table 4.2 & Table 4.3). It is interesting that carbon dioxide was identified as the SPME fibre manufacturer claims that the DVB/CAR/PDMS fibre is suitable for C3-C20 analysis, compounds with a molecular weight 40-275 (Supelco). CO_2 does however have a molecular weight of 44.01 and was very often the first peak identified in the current GC-MS analyses. Although CO_2 is not included in the EPA classification of VOCs, the compound is involved in some of the few clinically

approved breath tests – direct measurement of CO_2 in capnography and $^{13}CO_2$ measurement for *Helicobacter pylori* infection (Amann et al., 2014).

2-butoxyethyl acetate was found significantly decreased in MET-5A$^{w/KO}$ compared to MET-5A (Table 4.2), and 1-methoxy-2-propyl acetate was found significantly decreased in MET-5A$^{w-/KO}$ compared to MET-5A$^{+/+}$ (Table 4.3). Both of these compounds are also present on the Volatilome database (Pleil & Williams, 2019). As these compounds are both acetate compounds with similar chemical formulas, both displaying the same trend, there is the possibility that these compounds are somehow linked and are products of slight differences in metabolism between MET-5A and MET-5A$^{+/+}$ cells. Despite their presence on the volatilome database, the literature available for these two compounds is limited. VOC analysis studies have implicated 2-butoxyethyl acetate as an odour compound in grapes and juice (Liu et al., 2015; Pang et al., 2012), or as a potential chemical contaminant in plastic baby bottles (Onghena et al., 2014; Petersen & Lund, 2003). 1-methoxy-2-propyl acetate has also been identified as an odour compound associated with the plant, *Rhodobryum giganteum* (Li & Zhao, 2009). However, this compound has also been identified as part of a panel of VOCs in human plasma and urine (Fuchsmann et al., 2020). 1-methoxy-2-propyl acetate along with several other compounds was found to be highly discriminative for dietary intake of dairy or cheese (Fuchsmann et al., 2020).

The remaining significantly different compounds were all alkanes (Table 4.2 & Table 4.3). Unfortunately, the two alkanes significantly altered in MET-5A$^{w-/KO}$ compared to MET-5A were unable to be confidently identified due to the reasons

previously discussed (Section 4.5.1). However, 3,7-dimethyl-nonane was found to be increased in MET-5A$^{w-/KO}$ cells compared to MET-5A$^{+/+}$ and tetradecane was found to be decreased (Table 4.3). Neither of these compounds are present on the volatilome database however other isomers of dimethyl-nonane are. Tetradecane is a compound that has previously been associated with multiple tumour types. At an *in vitro* level, tetradecane was identified as altered in renal cell carcinoma cells compared to non-tumourgenic cells (Amaro et al., 2020). Tetradecane and other compounds were also the most frequently detected VOCs in an analysis of colorectal cancer patient breath and corresponding tissue samples (De Vietro et al., 2020). The presence of this compound has also been linked to lipid peroxidation induced during surgery of lung cancer patients (Wang et al., 2014b).

Of these two compounds, an increase in 3,7-dimethyl-nonane in the BAP1 mutant cells is the most interesting discovery. Dimethyl-nonane, along with cyclopentane and methyl-octane, was identified as significantly different in the breath of patients with long-term professional exposure to asbestos without MPM development, compared to both HC and MPM groups (de Gennaro et al., 2010). It was concluded from these results that AEx patients were therefore characterised by a breath composition different from MPM patients and healthy controls (de Gennaro et al., 2010). The results from the current chapter broadly align the MET-5A$^{w-/KO}$ BAP1 mutant group with the AEx group observed previously, with dimethyl-nonane giving a specific example where trends in VOC changes were the same in BAP1 mutant cells and AEx patients. Dimethyl-nonane therefore, appears to be associated with a “pre-MPM” VOC profile, be it through

BAP1 mutation or asbestos exposure. The BAP1 status of the AEx patients analysed was also not reported (de Gennaro et al., 2010); the dimethyl-nonane results suggest a possible link between asbestos exposure and BAP1 mutation. The potential for asbestos fibres to induce genetic mutations has been well recognised, indicating the possibility for the BAP1 gene to be affected by this, resulting in the trends observed in dimethyl-nonane across both of these groups. Regardless of any connection that may be established in the future, both AEx patients and BAP1 mutant individuals represent two populations that have an increased risk of developing MPM, with alterations in dimethyl-nonane now associated with both. Detection and monitoring of this compound in breath may therefore provide an opportunity for identifying at risk individuals and, as MPM is associated with different VOC profiles, a chance to identify if or when an individual develops MPM.

4.5.3.2 BAP1 Mutant Compared to Mesothelioma Cells

The BAP1 mutant cell line VOC profiles were also compared to the profiles produced by the two MPM cell lines, MSTO-211H and NCI-H28 (Figure 4.6). This comparison was performed as the multiple group comparison indicated that although MET-5A$^{w-/KO}$ cells appeared slightly different than the non-mutant MET-5A controls, they did not cluster together with the MPM cell lines (Figure 4.3). The further comparison confirmed these findings, with the OPLS-DA score plot showing the MET-5A$^{w-/KO}$ group separating along the X-axis from the two MPM groups, and MSTO-211H and NCI-H28 separating from each other along the Y-axis (Figure 4.6C). MET-5A$^{w-/KO}$ cells producing different VOC profiles to MPM cell lines while at the same time still showing several differences when compared

to non-mutant MET-5A is an interesting finding with potentially clinically relevant significance if explored further. These findings suggest that cells with mutated BAP1, that have yet to fully develop MPM, produce a VOC profile that is distinct from both healthy mesothelial cells and MPM tumour cells. Within MPM diagnosis, this presents an opportunity to identify individuals with BAP1 mutation before MPM development. This offers the opportunity for monitoring individuals' progression, diagnosing MPM at an earlier stage and eventually improving patient treatment options with advances in MPM therapeutics.

It is possible for the initial findings presented here to be explored further using clinical analysis of exhaled breath. The BAP1 tumour predisposition syndrome has been previously defined in families with germline mutations in the BAP1 gene (Carbone et al., 2020). Germline BAP1 mutations result in an increased sensitivity to asbestos and earlier development of MPM, most often of the less aggressive epithelioid sub-type (Carbone et al., 2020). All individuals previously genotyped and carrying a germline BAP1 mutation have also gone on to develop mesothelioma or another cancer linked to BAP1 tumour predisposition syndrome such as uveal melanoma (Carbone et al., 2020). This phenomenon presents a group of patients that could have a BAP1 mutation, likely to develop MPM, and can be identified due to the hereditary nature of the germline mutations. Analysing the breath of known BAP1 mutant individuals, compared to healthy controls and MPM patients would translate the *in vitro* work currently developed to a more clinically relevant situation. This would assess whether the VOC changes discovered at a cellular level are also observed within the more complex analysis of exhaled breath. Again, development of these findings would be an interesting

proposition for MPM diagnosis; highlighting a population that could benefit from the non-invasive monitoring potential of a MPM breath test.

Other genes have been associated with the development of MPM including NF2 and CDKN2A (Hylebos et al., 2016; Wang et al., 2016). Exploration of the effects of NF2 and CDKN2A mutations on VOC profiles would be another step that could be taken using the current methodology. The effects of single mutations could be compared to the BAP1 mutation results, but the potential of inducing multiple mutations at the same time may be of greater relevance. A cell line model with mutations in BAP1, CDKN2A and NF2 at the same time would be useful to evaluate the point at which the burden of mutations leads to a VOC profile that would be expected from MPM cells.

4.5.4 Conclusions

The main aim of this chapter was to determine whether mutations of the BAP1 gene had an effect on VOCs produced by the non-malignant mesothelial cell line MET-5A. The main results from this chapter indicated that the VOCs released into the headspace of MET-5A$^{w-/KO}$ were slightly different to those produced by both the MET-5A and MET-5A$^{+/+}$ controls. However, the mutant cell line did not appear to produce VOC profiles that were very similar to the MPM cell lines MSTO-211H and NCI-H28. Conclusions from these results suggest that the BAP1 mutation investigated had a small but measurable impact on VOC profiles but did not result in profiles that can be associated with malignant cells. Further

exploration of these initial *in vitro* findings potentially provides an opportunity where VOC and breath analysis can identify the presence of a BAP1 mutation.

The most interesting result from the current chapter is the identification of increased 3,7-dimethyl-nonane in the headspace of BAP1 mutant cells compared to non-mutant controls and the correlation of this finding to previous results regarding the breath of asbestos-exposed patients. This should be explored further due to the benefits discussed in terms of a diagnostic MPM breath test. Importantly, this discovery may have been missed if *in vitro* VOC analysis studies had not been explored, highlighting the impact that these experiments can have on *in vivo* studies and breath analysis as a whole.

5 Volatile Organic Compound Analysis of Malignant Pleural Mesothelioma Chorioallantoic Membrane Xenografts

5.1 Introduction

5.1.1 2D VOC Analysis

A large number of previous *in vitro* VOC analysis studies have analysed the headspace gas of monolayer 2D cell cultures, commonly in standard cell culture flasks (Janssens et al., 2022; Schallschmidt et al., 2015; Silva et al., 2017; Tang et al., 2017). Different cell types have showed discriminating VOC profiles when compared to controls and other cell types when using this analysis (Janssens et al., 2022; Schallschmidt et al., 2015; Silva et al., 2017; Tang et al., 2017). Many VOCs have also been collated from cell cultures to translate their impact to exhaled breath analysis; compounds identified at both a cellular level and in exhaled breath should help the discovery of the most clinically relevant biomarkers (Filipiak et al., 2016). As well as this, an advantage of cell cultures is the ability to manipulate experimental conditions and therefore explore the underlying processes associated with specific VOCs. For example, cell cultures have been exposed to oxidative stress (Liu et al., 2019b) and the effects of hypoxia (Taware et al., 2020) and cancer-associated mutations have been investigated (Davies et al., 2014). Experiments such as these would not be possible with patient breath studies. However, as seen across many fields of research that use cell lines as models, some limitations have been presented with regards to models such as these which are often now considered to be quite basic. The use of 3D cell culture models was also suggested as an area to improve tumour modelling conditions in future *in vitro* MPM VOC analysis studies (Janssens et al., 2022).

Recently, a growing body of evidence has suggested that a 2D monolayer of cells does not accurately represent the complex biological processes that occur during tumour development (Nath & Devi, 2016). In 2D cell culture, cells grow as a single, flat monolayer, elongating the cell shape and resulting in all cells receiving equal culture media - altering differentiation, proliferation and protein expression (Jensen & Teng, 2020). In contrast, cell shape is maintained within 3D culture, a nutrient gradient is formed with a hypoxic core and differentiation, proliferation and protein expression resemble more closely what is observed *in vivo* (Jensen & Teng, 2020). Secondly, an issue has been identified which is more specific to VOC analysis of 2D cell cultures and involves the use of plastic polymer cell culture flasks. It has been shown that even when completely empty, several brands of standard cell culture flasks produce complex VOC profiles, detected with GC-MS (Chu et al., 2020). This plastic background signal has the potential to overwhelm analysis of 2D cell cultures, reducing the sensitivity of the methodology and resulting in cell line-specific VOCs being missed.

Studies involving 3D cell cultures as a model of VOC breath analysis is limited. One study focussed on the analysis of volatile aldehydes in the headspace of collagen models cultured using CALU-1 lung cancer cells; an increase in the concentration of these compounds was found to be linked to ROS induction in the cells (Shestivska et al., 2017). Another study found that headspace acetaldehyde levels were increased in 3D collagen models of CALU-1 and NL20 (non-malignant lung cell line) compared to their 2D counterparts (Rutter et al., 2012). Both of these studies used SIFT-MS for headspace VOC analysis and have provided evidence that VOCs can be detected from 3D cell culture models

and the concentration of specific compounds is different when compared to 2D (Rutter et al., 2012; Shestivska et al., 2017). In contrast, 3D models have been more extensively used within metabolomics and proteomics compared to VOC analysis, or volatilomics (Avelino et al., 2021; Flint et al., 2021). These research areas are more intensively researched than volatilomics in general, but this indicates the potential for VOC analysis to follow this example and begin to use more complex models than 2D cell cultures.

5.1.2 The Chorioallantoic Membrane Model

The chorioallantoic membrane (CAM) model uses chick embryos in fertilised eggs in order to grow tissue xenografts (Ribatti, 2017). This model has gained traction within oncological research, having been used in the study of many cancer types including breast, colorectal, lung and hepatocellular (Chu et al., 2021). Within pre-clinical research, CAM models show a number of technical, biological, and ethical advantages over traditionally used murine models (Chu et al., 2021). These include but are not limited to short experiment timescales, easy handling, high vascularisation, can be prepared more economically and have less ethical implications to consider (Chu et al., 2021). CAM models potentially also address the issues raised concerning VOC analysis of 2D cell cultures. Despite this, the use of the CAM has not previously been considered as a model for the analysis of VOCs *in vitro*.

The mesoderm layers of the allantois and chorion fuse together to form the CAM during avian development – a membrane with a dense vascular network which

has a connection to the embryonic circulation (Ribatti, 2016). The transplantation of tumour cells onto the CAM and the subsequent growth of xenografts has been established as a method within the study of solid tumour types (Ribatti, 2016). A developing chick embryo is naturally immuno-deficient in the early stages, providing an environment in which foreign tumour cells are able to be successfully transplanted and proliferate (Chu et al., 2021). Vascular development in the CAM follows three defined steps: initial multiple capillary sprouts are subsequently replaced by tissue pillars which finally increase in size to form inter-capillary meshes (Ribatti, 2017). These processes provide the CAM with oxygen and essential nutrients, supplementing the growth and proliferation of transplanted tumour cells (Chu et al., 2021).

A general protocol for the CAM transplantation involves the removal of a small part of the fertilised eggshell on day three of incubation to create a window (Chu et al., 2021; Ribatti, 2017). Around 3ml of albumin is then removed to detach the CAM from the shell and on day six or seven, tumour cells can be implanted on the CAM (Chu et al., 2021; Ribatti, 2017). On day 14, chick embryos can be dissected, and CAM xenografts harvested - processing following this timeline means that a home office animal license is not required (Chu et al., 2021; Ribatti, 2017). As mentioned earlier, a number of cancer types have been successfully transplanted and xenografts grown using the CAM model. These models have been used in the study of various cancer-associated processes including tumour heterogeneity, metastasis, and angiogenesis (Chu et al., 2021). MPM xenografts generated using the CAM could therefore provide a suitable model system for the pre-clinical analysis of VOCs in a 3D setting.

5.1.3 Tissue VOC Sampling

The SPME GC-MS methodology commonly used to sample VOCs from 2D cell cultures has been adapted to analyse VOCs released from a range of different biological matrices (Aggarwal et al., 2020; Bianchi et al., 2017; Shetewi et al., 2021; Wang et al., 2014). The analysis of VOCs from tumour tissues is the most relevant to the current chapter. An initial study compared VOCs released into the headspace of both malignant and healthy lung tissue samples (Bianchi et al., 2017). The tissue samples analysed produced complex VOC profiles and following statistical analysis seven compounds were identified that were able to discriminate between the malignant and healthy groups (Bianchi et al., 2017). SPME analysis was also performed on colorectal cancer derived tissue samples and results compared to VOC profiles identified in the breath of colorectal cancer patients (De Vietro et al., 2020). A panel of compounds was identified concordantly from the tissue samples and also in exhaled breath, suggesting that the VOCs present in breath originated from the malignant tissue (De Vietro et al., 2020). As well as this, headspace needle trap extraction was used to identify VOCs released from gastric cancer tissue (Mochalski et al., 2018). Significantly different VOCs were identified in the headspace of the gastric cancer samples compared to non-cancerous tissue controls (Mochalski et al., 2018).

The sources of VOCs detected in exhaled breath have still not been fully elucidated (Issitt et al., 2022). The experiments described were designed to target *ex vivo* tissue samples in order to determine if the VOCs identified in patient

breath were also released from the corresponding tumour tissue under controlled sampling conditions. The results from these studies showed that *ex vivo* tumour tissues from a number of cancers produced detectable VOC profiles which were different from controls and also corresponded to the patient breath data (Bianchi et al., 2017; De Vietro et al., 2020; Mochalski et al., 2018). Interestingly, all of these studies used glass headspace vials for VOC extraction (Bianchi et al., 2017; De Vietro et al., 2020; Mochalski et al., 2018). Together these studies provided an alternative to the widely used 2D cell culture and patient exhaled breath analysis, establishing *ex vivo* analysis as a middle ground between the two techniques. This also highlighted the possibility of using these methods to analyse VOCs from 3D cell culture models, something which had not seen a considerable amount of research previously.

The ability to process 3D cell culture models from a tumour tissue sample removes the requirement for traditional cell culture conditions, including high oxygen (O_2) levels, when analysing. Analysing samples in glass headspace vials also reduces the use of polymer cell culture flasks, which theoretically can reduce the VOC background signal associated with disposable cell culture plastic-ware. Evidence of this was shown when analysing VOC standards in glass vials (Chapter 2, Section 2.4.3), the background signal was greatly reduced compared to analysis in cell culture flasks (Chapter 3, Section 3.4.2). In this chapter, the methods described above were applied to 3D cell culture models of MPM.

CAM models were generated and processed as though MPM tumour samples and VOCs identified through SPME GC-MS with sampling in a glass headspace

vial. Tumour xenografts were produced at the University of Liverpool using CAM models for three primary MPM cell lines: 7T biphasic and 8T and 12T, which are both epithelioid (MesobanK, Cambridge, UK). Two control CAM samples were also prepared for analysis: a mock implant control which replicated the physical methods of the tumour samples without the addition of cancer cells and a non-implant control.

5.2 Aims of the Chapter

The aims of this chapter were to develop the methods available for the identification of VOCs *in vitro* and to explore this within the context of MPM. The objectives were to analyse and identify VOCs released from a CAM model of MPM, in order to understand if this model was suitable for *in vitro* VOC analysis research. VOCs were analysed from CAM models derived from several primary MPM cell lines and controls and statistical analysis performed to determine if these CAM models were reflective of the current breath analysis literature within MPM. Research presented in this chapter was performed in collaboration with Professor Judy Coulson and her lab (Department of Cellular and Molecular Physiology, University of Liverpool).

5.2.1 Hypothesis

VOCs can be detected and identified from MPM CAM xenograft models. Therefore, CAM xenografts can provide an alternative to 2D cell cultures within pre-clinical VOC analysis research.

5.3 Methods

5.3.1 MPM Xenografts

MPM cell line xenografts were generated by Dr Sarah Barnett at Professor Judy Coulson's laboratory at the University of Liverpool. Harvested xenografts were transported on dry ice to Sheffield Hallam University for VOC extraction and analysis.

5.3.1.1 Cell Culture

MESO-7T, MESO-8T and MESO-12T primary MPM cell lines were obtained from MesobanK, authenticated by short tandem repeat (STR) profiling and were mycoplasma negative. Cells were maintained in RPMI-1640 Glutamax with 10% v/v FBS, 20ng/µl EGF (Peprotech), 1µg/ml hydrocortisone and 2µg/ml heparin at 37ºC with 5% CO_2.

5.3.1.2 Stable Cell Line Generation

MPM cell lines were transduced with lentiviral particles carrying pHIV-Luc-ZsGreen (Addgene plasmid # 39196; http://n2t.net/addgene:39196). Lentiviral particle generation and cell line transduction were performed as previously described (Reiser et al., 2009) by Dr Anne Herrmann (University of Liverpool). Transduction efficiency was assessed via fluorescent microscopy.

5.3.1.3 MPM CAM Model

Fertilised Bovan Brown eggs (Henry Stewart Co Ltd) were incubated at 37◦C and 45% humidity (embryonic day 0; E0) and windowed at E3. Prior to implantation on E7, trypsinised dual-labelled MPM cells were counted, washed in sterile PBS, and pelleted by centrifugation. Standard protocols were followed (Barnett et al, manuscript in prep) with $2x10^6$ cells implanted per egg. On E14, viability of the established tumour nodules on the CAM were assessed by bioluminescent imaging. Briefly, 250µl luciferin (Promega) was injected into the yolk sac and bioluminescent signal measured following 45min incubation using the IVIS® Spectrum In Vivo Imaging System (Perkin Elmer). Tumours were then observed under a Leica M165FC fluorescent stereomicroscope with 16.5:1 zoom optics, fitted with a Leica DFC425 C camera. Brightfield and fluorescent images were acquired both prior to and post dissection. Harvested tumours (12T n=7, 8T n=9, 7T n=5) were weighed and then placed in RNA*later* (Thermo Fisher) and frozen at -80◦C. Following removal of the tumour nodules, embryos were terminated on E14. Control (n=5) and mock (n=5) samples were collected in parallel. “Control” samples were taken from eggs that were left untreated from E3 to E14. “Mock” samples were taken from eggs that underwent a mock implant procedure, i.e. on E10 the CAM was prepared as normal but no cells were implanted.

5.3.2 VOC Extraction

Sampling of CAM xenografts was performed following a method published for the analysis of VOCs from lung cancer tissues (Bianchi et al., 2017). CAM samples were removed from -80ºC and thawed on ice prior to VOC extraction. Each CAM sample was removed from the RNAlater solution and placed in a 2ml glass

headspace vial. Headspace vials were sealed with PTFE/silicone caps. Sealed headspace vials were incubated in a heat-block for 60 min at 37^{o}C. During the incubation continuous SPME was performed to extract VOCs. A new 50/30µm DVB/CAR/PDMS SPME fibre was attached to a manual SPME fibre assembly and conditioned in the inlet of a GC-MS at 270^{o}C for 30 min prior to initial use as per the manufacturer's instructions. The SPME fibre was further conditioned in the same way at 250^{o}C for 10 min at the start of each day before the first extraction to remove any residual compounds. For SPME, the SPME fibre assembly was inserted through the cap of the headspace vials, puncturing the PTFE/silicon cap. The SPME fibre was exposed to the headspace above each CAM sample to extract VOCs for the entirety of the 60 min incubation. After extraction, the SPME fibre was retracted back into the SPME fibre assembly and analysed using GC-MS. For each CAM sample, 200µl of corresponding RNAlater solution was aliquoted and sealed in a glass 2ml headspace vial with a PTFE/silicone cap. The sealed RNAlater samples were then extracted and analysed in the same way as the CAM samples.

5.3.3 Gas Chromatography-Mass Spectrometry

After VOC extraction, the SPME fibre was analysed using GC-MS as in (Chapter 3, Section 3.3.3).

5.3.4 Data Analysis

5.3.4.1 Data Pre-Processing

GC-MS chromatograms were interpreted using Agilent MassHunter Data Analysis; tentative peak identification was able to be performed through spectral match to the NIST library database (V11, NIH). The spectral match cut-off point for NIST library searches was set to 80%. For each CAM and RNAlater chromatogram, a library search report was generated in MassHunter which included peak RT, peak area and the automatically assigned number one NIST match for each peak. Artefacts of SPME and GC-MS (complex siloxane-containing compounds) were manually removed from library search reports. RTs and peak areas for all CAM and RNAlater samples were used to create an aligned data matrix in .CSV format. RTs were rounded to one decimal place prior to alignment. GCalignR in R-studio (Ottensmann et al., 2018) was used to align RTs and peak areas for each sample resulting in a single aligned data matrix containing average RTs against samples and corresponding peak areas for each RT. The aligned data matrix was manually checked to identify any discrepancies in alignment.

5.3.4.2 Data Normalisation and Background Filtering

The aligned data matrix was uploaded to Metaboanalyst 5.0 (Pang et al., 2021) for data normalisation. Variables were filtered by inter-quartile range; data were normalised by sum and auto-scaling was applied. The normalised data matrix was downloaded in .CSV format and subsequently re-uploaded to Metaboanalyst for background filtering. For background filtering, batch t-tests (two-sample t-tests) were performed to account for signals from the RNAlater groups. 7T, 8T, 12T, Mock and Control CAM groups were compared to their respective RNAlater background group and false discovery rate (FDR) was applied to identify any

variables that were significantly different in 7T, 8T, 12T, Mock and Control groups compared to their respective RNAlater groups. The normalised data matrix was then edited to only include the normalised peak areas for the variables that were significantly altered across all groups; RNAlater groups were removed at this point. This filtered normalised data matrix was used for all subsequent statistical analysis.

5.3.4.3 Data Visualisation and Multivariate Statistical Analysis

The filtered normalised data matrix was imported in .CSV format into SIMCA (V17.0.2; Umetrics). PCA and PLS-DA were performed to visualise any similarities and differences between the groups. The filtered normalised data matrix was again re-uploaded to Metaboanalyst. ROC curves were generated: comparisons were made between combined MPM groups (7T, 8T, 12T) to combined control groups (Mock & Control) and between biphasic MPM (7T) and epithelioid MPM (8T, 12T) groups. Multivariate ROC curves were generated with PLS-DA chosen for classification and feature ranking. Multiple ROC curves were generated per comparison using 2, 3, 4, 5 and all 6 variables in order of their classified importance. A heat-map was also generated using Metaboanalyst to show the relative, normalised peak areas of the significantly altered variables across 7T, 8T and 12T groups.

5.4 Results

5.4.1 CAM Sample Characteristics

Mesothelioma cell lines 12T, 8T and 7T formed viable, vascularised tumour nodules when implanted on the CAM (Appendix, Figure 7.1). All three cell lines were modified to stably express a luciferase reporter, *in vivo* visualisation and assessment of viability was performed using bioluminescent imaging (Appendix, Figure 7.1). A total of five 7T, nine 8T, seven 12T, five Mock and five Control xenograft samples were available for GC-MS analysis (Table 5.1). Analyses were performed on all available xenograft samples and their corresponding RNAlater aliquots resulting in a total of 62 samples.

Table 5.1: CAM sample characteristics. Xenografts were successfully generated from 7T biphasic, 8T epithelioid and 12T epithelioid MPM primary cell lines. Mock and Control xenografts were also included for controls.

Group	7T Biphasic	8T Epithelioid	12T Epithelioid	Mock	Control
Sample IDs	7T_A	8T_A	12T_M	M1	C1
	7T_D	8T_B	12T_N	M2	C2
	7T_E	8T_C	12T_O	M3	C3
	7T_G	8T_D	12T_Q	M4	C4
	7T_H	8T_E	12T_R	M5	C5
		8T_F	12T_S		
		8T_G	12T_T		
		8T_H			
		8T_I			

5.4.2 GC-MS Chromatograms

GC-MS chromatograms showing retention time in min against relative peak abundance were produced for all CAM samples and their respective RNAlater samples (Figure 5.1). Some differences in VOC profiles were observable between groups (Figure 5.1), however statistical analysis was performed to confirm this and determine the significance.

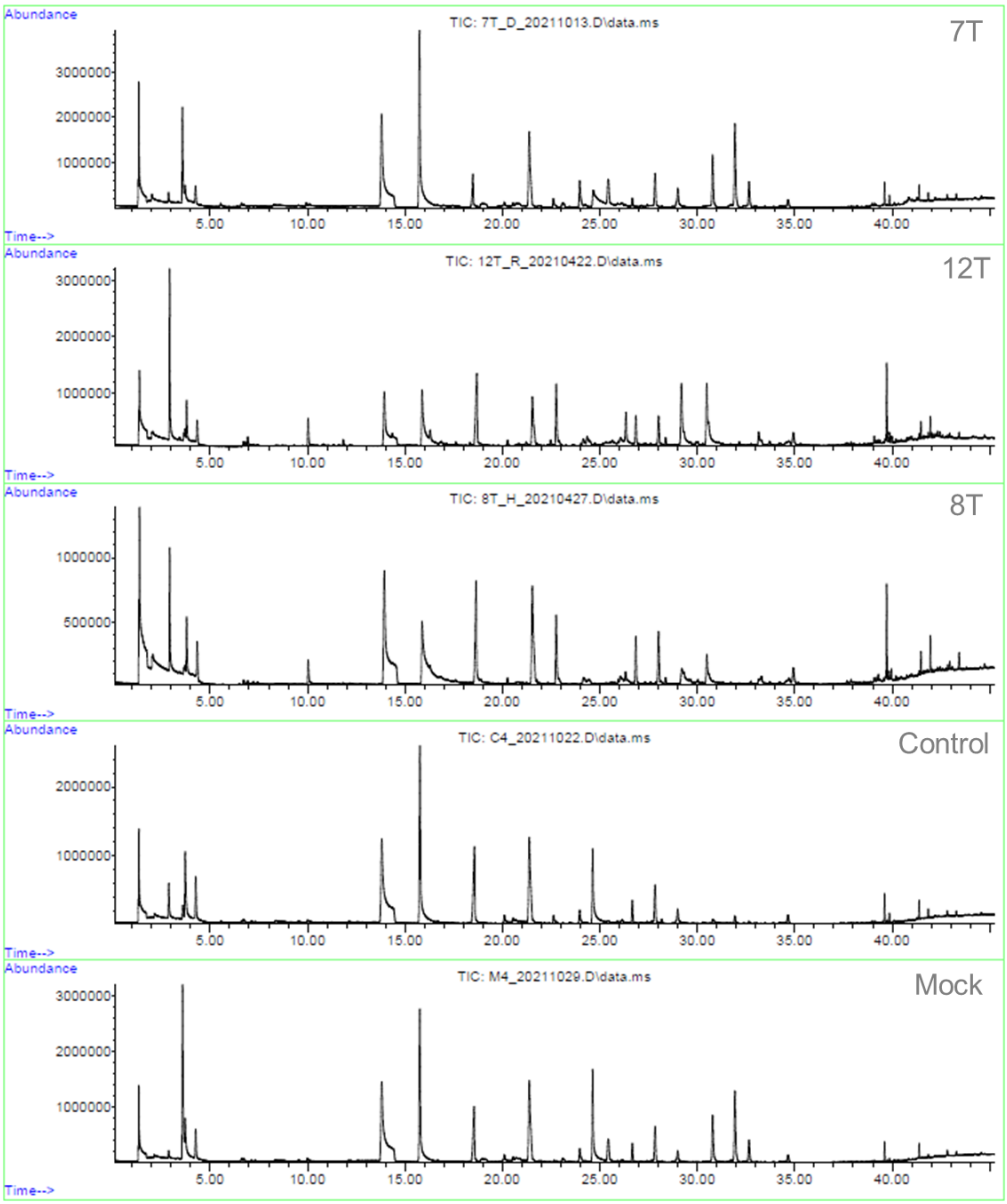

Figure 5.1: Example GC-MS chromatograms produced from the headspace of 7T, 8T, 12T, Mock and Control CAM samples.

5.4.3 Development of a Filtered Normalised Data Matrix

After alignment with GCAlignR, the initial data matrix consisted of 62 samples and a total of 216 aligned variables (RTs). After variable filtering, normalisation and scaling with Metaboanalyst, the normalised data matrix contained a total of 205 variables. Batch t-tests were performed to account for the background signal from RNAlater controls and identify variables that were significantly different (Table 5.2). Variables with average RTs of 3.69, 4.29, 18.61 and 26.70 min were significantly different in 7T; 3.78 min was significantly different in 8T; 7.10, 18.61 and 26.70 min were significantly different in the Control group (Table 5.2). No significant differences were observed in the 12T and Mock groups (Table 5.2). The normalised data matrix was filtered to include only the normalised peak areas for the six significantly altered variables across 7T, 8T, 12T, Mock and Control groups This filtered, normalised data matrix was used for all subsequent statistical analysis.

Table 5.2: Batch t-tests were performed in Metaboanalyst comparing each 7T, 8T, 12T, Mock and Control group to their respective RNAlater group. p-values indicate if a significant difference was observed in the variable between the groups and their RNAlater control.

		P-value if Significant: Group vs RNAlater				
AVG RT (min)	**Tentative ID**	**7T**	**8T**	**12T**	**Mock**	**Control**
3.69	Isopropanol	0.000576	-	-	-	-
3.78	Acetone	-	4.21E-08	-	-	-
4.29	2-methyl-2-propanol	0.000785	-	-	-	-
7.10	2-butanone	-	-	-	-	2.71E-06
18.61	2,2-dimethyl-propanoic acid	0.000147	-	-	-	0.000113
26.70	Diethylene glycol dipivalate	0.000185	-	-	-	1.46E-07

5.4.4 Multivariate Statistical Analysis

5.4.4.1 PCA and PLS-DA

The final data matrix was imported into SIMCA for multivariate statistical analysis including PCA and PLS-DA. The PCA score plot showed general separation along the X-axis between the cell line groups - 7T, 8T, 12T - and the Mock/Control groups, aside from a single outlier in the 8T group (Figure 5.2). Crossover was observed between the Mock and Control groups, with a single outlier also shown in the Control group (Figure 5.2). Within the cell line groups, 7T results appeared to cluster closely together whereas 8T and 12T groups were more spread with crossover between the two groups (Figure 5.2).

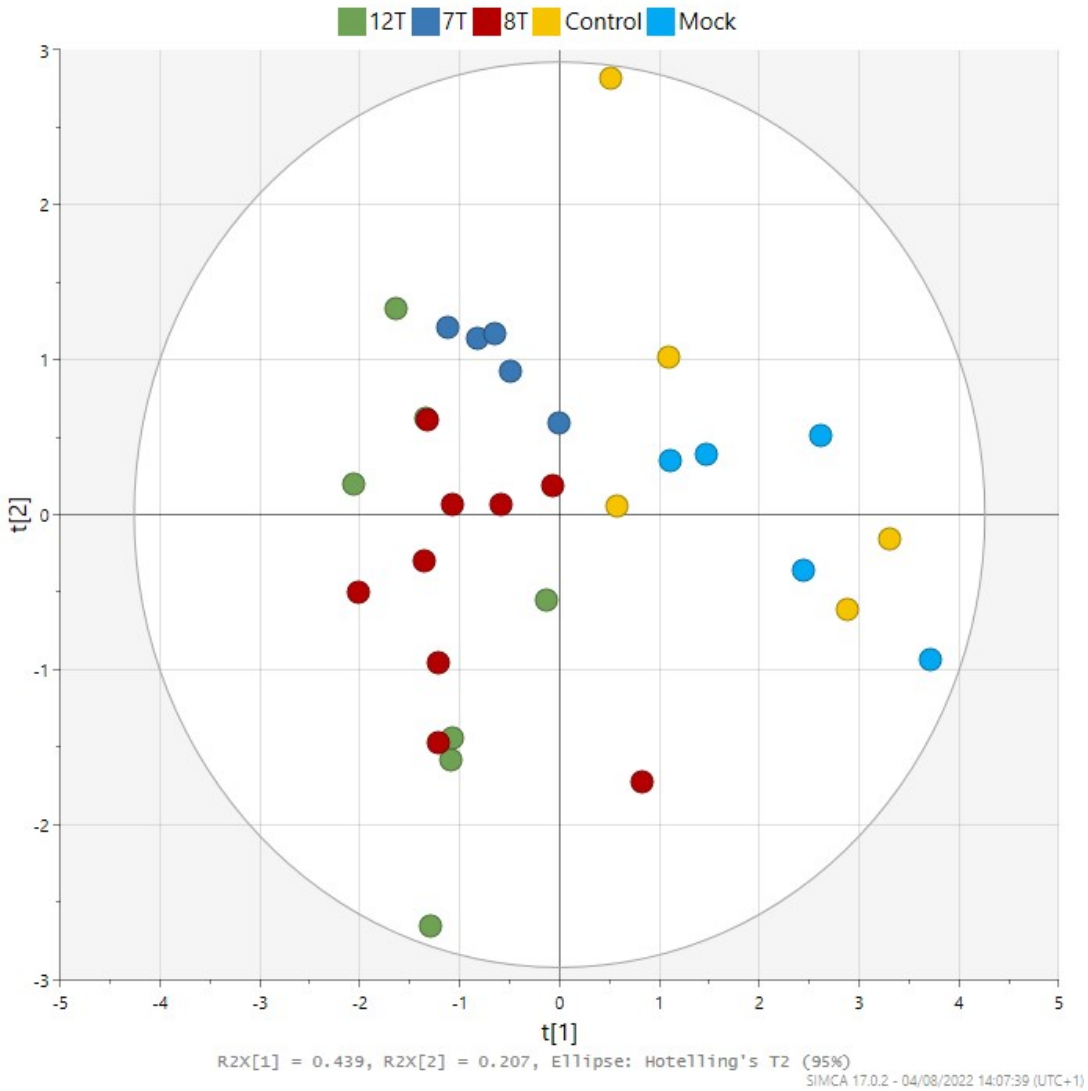

Figure 5.2: PCA score plot generated in SIMCA (V17.0.2) using the final data matrix for 7T, 8T, 12T, Mock and Control results. Each point represents the VOC profile of an individual replicate after data normalisation and background filtering.

Similar distributions were observed when further classifying the results using PLS-DA (Figure 5.3). Good separation was observed along the X-axis between cell line groups (7T, 8T, 12T) and the Mock/Control groups, again with a single outlier in the 8T group (Figure 5.3). The PLS-DA score plot showed improved clustering compared to the PCA results - the Control group outlier clustered closer to the replicates using PLS-DA (Figure 5.3). Again, within the cell line groups, clustering was tight in the 7T group whereas 8T and 12T results were more spread with some crossover (Figure 5.3).

The spread of the Mock/Control groups did not appear to be affected by Luciferin (Appendix, Figure 7.2 & Table 7.3). However, the weight of the MPM xenografts did appear to have some effect on the Y-axis distribution of results, indicating variations in tumour burden within the same phenotype (Appendix, Figure 7.3).

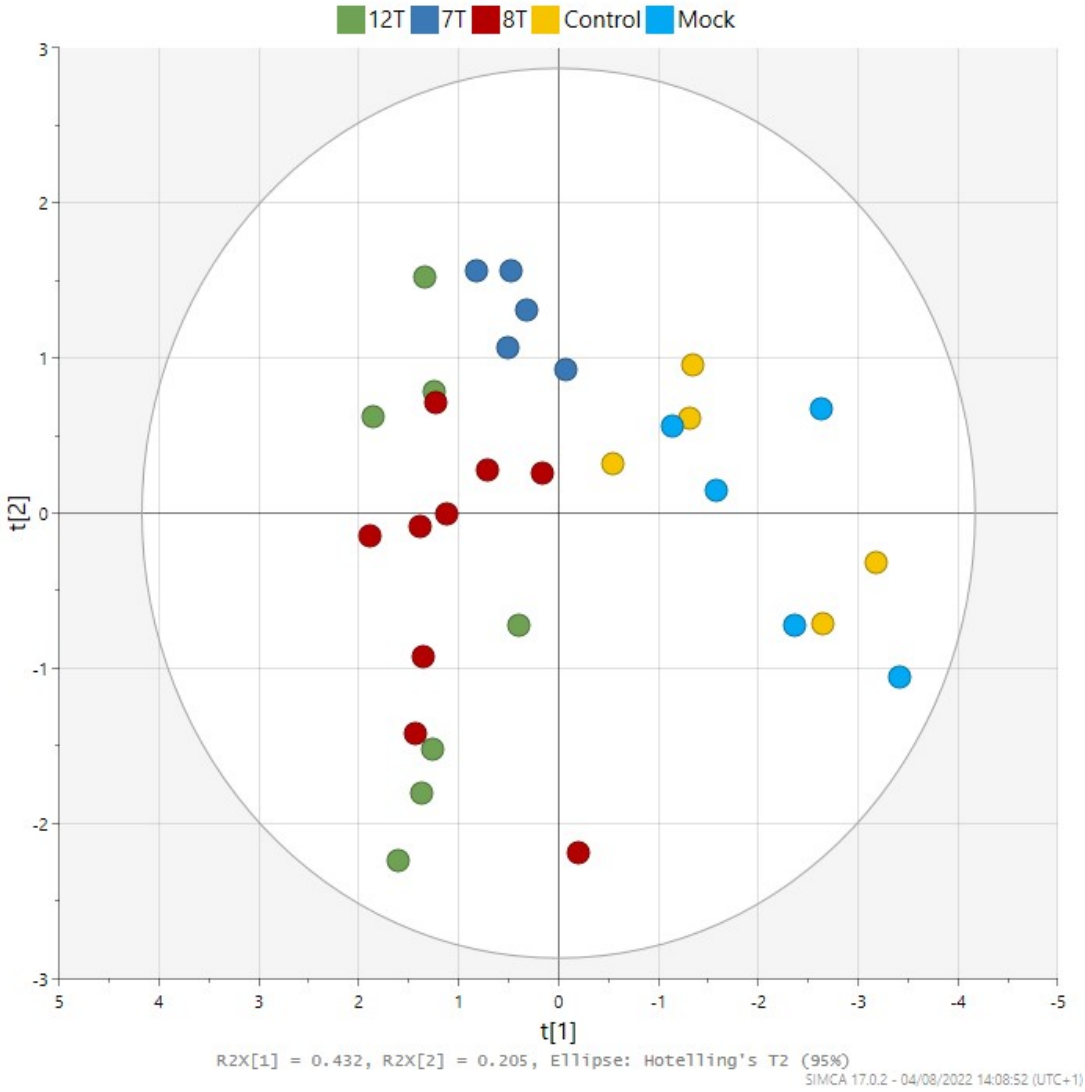

Figure 5.3: PLS-DA score plot generated in SIMCA (V17.0.2) using the final data matrix for 7T, 8T, 12T, Mock and Control results. Each point represents the VOC profile of an individual replicate after data normalisation and background filtering.

5.4.4.2 ROC Curves

Two different comparisons were made when generating ROC curves. Initially, MPM cell line groups (7T, 8T, 12T) were combined and compared to the Mock and Control groups (Figure 5.4a). When this comparison was made, the area under the curve (AUC) values for the ROC curves were between 0.991 and 1, indicating very good to perfect separation between combined MPM and Control groups (Figure 5.4a). A second comparison was made focussing only on the MPM cell line groups - 7T biphasic MPM was compared to epithelioid 8T and 12T MPM groups combined (Figure 5.4b). The AUC values when making this cell line comparison were lower at 0.839-0.95 with slightly poorer ROC curves and indicating a more average discrimination between biphasic and epithelioid MPM cell line results (Figure 5.4b).

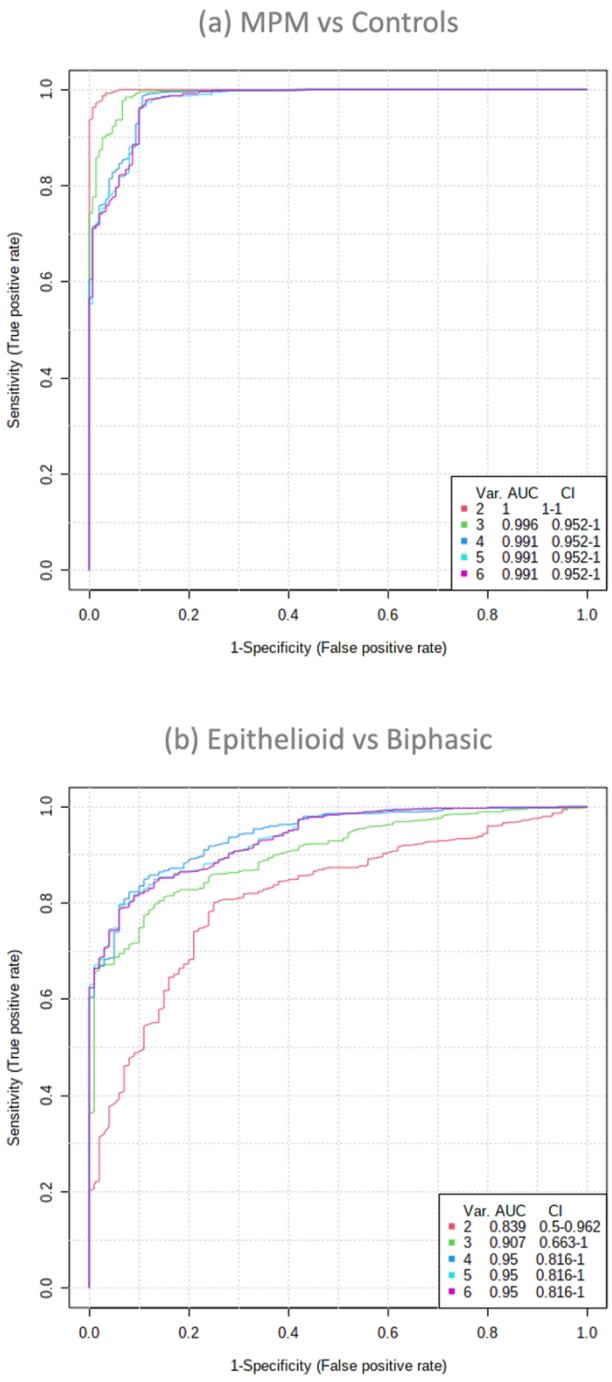

Figure 5.4: ROC Curves comparing (a) MPM groups (7T, 8T, 12T) to Controls (Mock/Control) and (b) Biphasic MPM (7T) to Epithelioid MPM (8T & 12T). Multivariate ROC curves were generated with PLS-DA chosen for classification and feature ranking. Multiple ROC curves were generated per comparison using 2, 3, 4, 5 and all 6 variables in order of their classified importance (Isopropanol, diethylene glycol dipivalate, 2-methyl-2-propanol, 2,2-dimethyl-propanoic acid, acetone and 2-butanone).

5.4.4.3 MPM Cell Lines: Relative Peak Areas

The normalised peak areas for the six significantly altered compounds were used to generate a heat-map in Metaboanalyst for 7T, 8T and 12T groups to identify the relative intensities of the compounds in the cell line groups (Figure 5.5). Isopropanol and diethylene glycol dipivalate showed a higher relative intensity in the 7T group (Figure 5.5). 8T and 12T groups were more similar to each other but still showed some differences: 2-methyl-2-propanol was high in 8T and low in 12T; 2,2-dimethyl propanoic acid (also known as pivalic acid) was similar across both groups; acetone and 2-butanone were slightly higher in the 12T group compared to the 8T group (Figure 5.5).

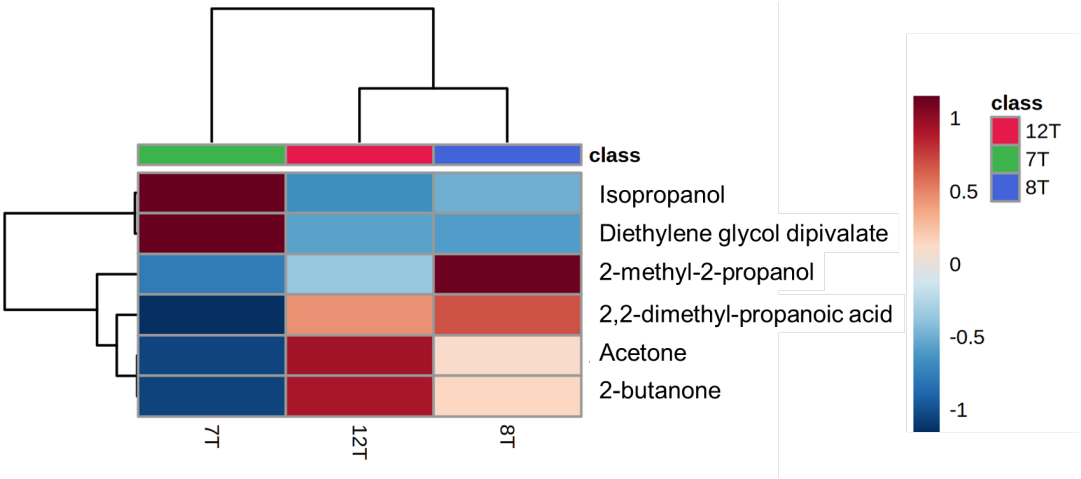

Figure 5.5: Heat-map showing relative peak areas of the six significantly altered VOCs across 7T, 8T and 12T cell line groups. Average peak areas for each group are shown.

5.5 Discussion

5.5.1 CAM Model

A large number of previous studies across a range of diseases have now used basic 2D cell cultures as a method of analysing VOCs *in vitro* (Filipiak et al., 2016). Although these studies have provided important information in the field of breath research, the limitations of 2D cell culture methods are now recognised. A lack of reproducibility in the VOCs identified from the breath of lung cancer patients and those found in the headspace above 2D lung cancer cell cultures has been suggested to be caused by the use of standard cell culture conditions (Kalluri et al., 2014). In cell culture, cells are grown in hyperoxic conditions in the presence of 5% CO_2, a contrast to the hypoxic conditions that are common during *in vivo* tumour growth (Nath & Devi, 2016). High oxygen conditions are likely to alter cellular metabolism and lead to the increased production of alcohols and other oxidised products in cell cultures compared to exhaled breath - a phenomenon that has been observed within lung cancer (Kalluri et al., 2014).

Discrepancies have also been identified when multiple groups have analysed the headspace VOC composition of the same lung cancer cell lines (Chu et al., 2020). Disposable cell culture flasks are made of polymer plastics, which themselves have the potential to release VOCs (Chu et al., 2020). It has been suggested that the discrepancies observed across lung cancer cell lines was in part due to VOC background signals released from polymer cell culture flasks (Chu et al., 2020). As well as this, several brands of completely empty cell culture flasks were shown to have quite complex VOC profiles when analysed with SPME GC-MS - methods commonly used for *in vitro* VOC analysis (Chu et al., 2020). Although these

effects can be somewhat controlled through the use of appropriate media-only controls sampled in the same flasks, any background signal from plastic cell culture-ware is likely to limit method sensitivity due to flask-derived VOCs being detected.

The CAM models presented in this chapter represent a development of current *in vitro* VOC analysis methods and address the issues raised above. The 3D tumour samples produced by the MPM cell implanted CAM methodology were much more complex and biologically representative compared to basic 2D monolayer systems. Cells were able to develop a 3D structure over the incubation period with a vasculature that more closely resembles the development of a tumour *in vivo*. By using CAM models, hyperoxic cell culture conditions can be avoided during sampling, potentially negating the effects on cellular metabolism and allowing cells to produce VOCs that you would expect to find in exhaled breath. The CAM samples were processed and analysed using a methodology previously used to identify VOCs from lung cancer tissue samples (Bianchi et al., 2017). Therefore sampling was performed in glass headspace vials, rather than polymer plastic cell culture flasks. Glass vessels have been shown to produce a negligible VOC profile, particularly compared to plastic cell culture flasks (Chu et al., 2020). This sampling procedure should go some way towards reducing the high background signal that can be produced by using plastic cell culture-ware. VOC profiles produced by CAM samples (Figure 5.1) were much less complex than those produced by 2D MPM cell cultures (Figure 3.2), indicating an improvement of the VOC sampling procedure. The ability to reduce the background VOC signals as much as possible increases the sensitivity of

methods and means that important compounds can be identified that might have otherwise been missed.

As the CAM samples in this chapter were processed in the same way as actual tumour samples, the VOCs identified no longer represent compounds directly extracted from proliferating cells. In this aspect, 2D cell culture systems may present an advantage as VOC sampling can take place without disturbing the growing culture resulting in a representative sample of VOCs produced by proliferating cells being analysed. Whether or not this is actually useful in developing a relevant VOC analysis model is another issue. A change in metabolism caused by cell death and apoptosis can potentially alter VOC production; so, if the aim of the study is to detect VOCs from living cells, a 2D cell culture may still be the most appropriate choice. However, this type of modelling may not be the most representative of tumour growth *in vivo.* So, when attempting to develop a VOC analysis model within cancer, identifying VOCs coming from living cells may not be as important as using the most biologically relevant model available, in which case the CAM model has specific advantages over 2D cell cultures. A standardised *in vitro* VOC analysis methodology has yet to be developed - the CAM model presented currently offers an alternative to usual 2D cell cultures and should therefore be considered for the study of VOCs *in vitro* in the future.

5.5.2 Multivariate Statistical Analysis

Both the PCA and PLS-DA score plots showed very similar results - aside from improved clustering using PLS-DA, both score plots showed the same distribution

and grouping of results (Figure 5.2 & Figure 5.3). This indicated that the data used to construct the two models were consistent. PCA is unsupervised, whereas PLS-DA is a supervised technique and has been previously reported to be over-optimistic within metabolomics workflows (Gromski et al., 2015). Similar trends were observed with both of these modelling systems, suggesting that the dataset used to construct them was very reliable and therefore any conclusions drawn from the results can be appropriate and relevant within the context of MPM VOC analysis.

When interpreting PCA and PLS-DA score plots, separation of results along the X-axis can be used to explain the greatest amount of variation within the dataset. All cell line groups 7T, 8T and 12T were separated from Mock/Control groups along the X-axis in both the PCA and PLS-DA score plots. Separation like this indicates a large amount of variation between the MPM cell line VOC profiles and those produced by the Mock and Control samples. To assess the discrimination of this model, ROC curves were generated comparing MPM cell line groups to Mock and Control groups combined (Figure 5.4a). The pattern of the ROC curves showed very good separation, and the AUC values were 0.991-1 (Figure 5.4a). These results confirm that there was a strong distinction between MPM cell lines and controls using the six significantly altered VOCs. A parallel can be drawn between these results and the current understanding surrounding VOC profiles within MPM breath analysis. The main concordant result from MPM breath analysis studies was that MPM patients could be distinguished from healthy controls using VOC profiles with a high degree of sensitivity and specificity (Catino et al., 2019). Differences have also been observed when comparing non-malignant mesothelial cells to MPM cell lines in 2D secondary cell cultures (Little

et al., 2020). The current CAM results are also concordant with this showing that discriminatory profiles can be identified across all levels of MPM VOC analysis - from simple 2D cultures to more complex 3D models and in the exhaled breath of MPM patients (de Gennaro et al., 2010; Di Gilio et al., 2020; Lamote et al., 2017).

CAM models were generated from three different primary MPM cell lines: 7T biphasic MPM and 8T and 12T, which are both epithelioid MPM. Previously, MPM sub-type has not been considered within patient breath analysis studies but differences in VOCs have been observed between secondary MPM cell lines with different sub-types (Janssens et al., 2022; Little et al., 2020). The multivariate analysis score plots can be interpreted in terms of MPM phenotype. All MPM results were separated from Mock/Control results - MPM samples as a whole were different from controls - however within the MPM results the 7T group appeared to cluster closely together whereas 8T and 12T results were more spread with crossover (Figure 5.2 & Figure 5.3). These results suggest that a subtly different VOC profile was produced by the 7T group compared to the 8T and 12T groups, which supports the data produced regarding these subtypes in 2D cultures. This finding was explored further, by producing ROC curves comparing biphasic CAM results to combined epithelioid groups (Figure 5.4b). The AUC values were less than observed when comparing MPM to controls but were still relatively high at 0.839-0.95, indicating good discrimination between these two groups using this model (Figure 5.4b). The combined *in vitro* results suggest that it may be possible to distinguish between biphasic and epithelioid MPM using VOC analysis. Differing prognoses caused by biphasic and epithelioid MPM sub-types has been well documented (Yap et al., 2017), with this

representing an area in which VOC analysis has the potential to make a substantial difference to current diagnosis, particularly as research towards this so far has been lacking.

5.5.3 Specific VOCs

Due to the number of compounds that have already been identified and the complex VOC profiles that can be detected in a single breath (Amann et al., 2014), it is likely that any breath test in clinical practice would analyse multiple compounds rather than relying on a single standalone VOC. The ROC curves presented in the current results were designed to reflect that - generated using the profiles from the six significant VOCs. Despite this, it is important to contextualise the significant VOCs that have been identified within the current research in order to draw appropriate conclusions and identify trends across MPM and other malignancies. The six significant VOCs identified from the CAM models have not been identified in previous MPM breath analysis studies (de Gennaro et al., 2010; Di Gilio et al., 2020; Lamote et al., 2017), however some interesting comparisons can still be made. 1-propanol, an analogue of isopropanol identified here, was previously used in a panel of VOCs to discriminate MPM patients from healthy controls (Di Gilio et al., 2020). 2-methyl-1-propanol was also found to be important in the discrimination of MPM patients from asbestos-exposed individuals (Lamote et al., 2017) - 2-methyl-2-propanol was identified currently. Examples such as 2-methyl-2-propanol could reflect the GC-MS methodology and subsequent tentative identification process that was used to identify VOCs. Compounds with a very similar molecular structure can produce very similar ionisation patterns, in turn leading to discrepancies like these

in identification. It is also possible that the metabolism underlying VOC production is capable of producing compounds with a very similar structure at the same time (Pleil & Williams, 2019). Despite this, all previous MPM breath analysis studies that used GC-MS and the one previous *in vitro* study identified VOCs from the same classes of compounds, including alcohols and ketones, as the six significant VOCs (de Gennaro et al., 2010; Di Gilio et al., 2020; Lamote et al., 2017; Little et al., 2020).

The compounds identified currently have however been previously identified across other malignancies and diseases. Acetone, isopropanol and 2-methyl-2-propanol (tert-butyl alcohol) are present on the Volatilome Database indicating that they have previously been identified in human exhaled breath (Pleil & Williams, 2019). Acetone is one of the most intensively studied VOCs and has long been associated with the sweet scent that can be present on diabetic individuals' breath (Ruzsányi & Péter Kalapos, 2017). There are a number of complex biological pathways for the production and degradation of acetone involving many enzymes associated with metabolic functions such as the cytochromes p450 (Ruzsányi & Péter Kalapos, 2017). It is not surprising then that acetone has been implicated as a potentially clinically relevant biomarker across a range of diseases including, but not limited to, the aforementioned diabetes, starvation and bacterial infection (Ruzsányi & Péter Kalapos, 2017). Within cancer, altered acetone levels have been identified across a number of lung cancer VOC analysis studies (Ruzsányi & Péter Kalapos, 2017). Following analyses with SPME GC-MS, increased levels of acetone was found in the breath of lung cancer patients compared to healthy non-smokers (Ulanowska et al., 2011). In contrast to this finding, breath acetone levels were also found to be at

a slightly lower concentration in lung cancer patients compared to healthy controls (Bajtarevic et al., 2009). These discrepancies could be attributed to the complex metabolism of acetone, combined with differences in sampling procedure which affects reproducibility in breath analysis literature as a whole (Brusselmans et al., 2018). Despite this, it is clear that acetone is an important VOC across a range of diseases, with the current results now also implicating the compound within mesothelioma.

Isopropanol was found at a higher level in the 7T group relative to the 8T and 12T groups (Figure 5.5). The oxidation of isopropanol to acetone through alcohol dehydrogenase (ADH) enzymes is considered one of the main physiological sources of acetone (Ruzsányi & Péter Kalapos, 2017). The current results therefore suggest a potential dysregulation of ADHs between biphasic and epithelioid MPM, leading to a lack of oxidation of isopropanol in the 7T samples. It has been previously observed that the activity of ADHs has been altered across a wide range of malignancies (Orywal & Szmitkowski, 2016). Much research has been performed considering isopropanol as a toxic compound from external sources, rather than a potential diagnostic biomarker (Slaughter et al., 2014). However, several studies have identified isopropanol within a VOC analysis context. Isopropanol was identified with SPME GC-MS and used in a panel of compounds for the classification of lung cancer patients from other respiratory diseases and healthy controls (Koureas et al., 2020). Similar results were achieved using needle-trap as pre-concentration rather than SPME (Monedeiro et al., 2021). Aside from exhaled breath, isopropanol has also been identified in plasma headspace associated with inflammatory bowel disease (Grove et al.,

2020) and was also used in combination with 2-butanone to distinguish breast cancer patients through VOC analysis of urine (Kure et al., 2021).

Although 2-butanone is not currently present on the Volatilome database, the above study is a good example of the breadth of research ongoing within the VOC analysis community (Kure et al., 2021). As with many compounds, 2-butanone has been found to be associated with lung cancer and was recognised as one of the most frequently identified VOCs across lung cancer studies (Saalberg & Wolff, 2016). 2-butanone was also found to be significantly different in the breath of smokers compared to non-smokers (Capone et al., 2018). There is a well-established connection between cigarette smoking and lung cancer development (Klebe et al., 2019), which may explain the increased frequency of 2-butanone in lung cancer breath analysis. A link between smoking and mesothelioma has not been established; however, asbestos exposure combined with cigarette smoking produces a synergistic effect in the development of lung cancer (Klebe et al., 2019). Despite this, it is interesting that 2-butanone was identified from the CAM samples as the literature discussed above suggests that the production and origins of this compound may be quite complex compared to other VOCs.

As previously mentioned, 2-methyl-1-propanol was identified as an important discriminatory VOC in MPM breath analysis (Lamote et al., 2017), whereas 2-methyl-2-propanol was identified from the current results. This compound appeared to be specifically increased in the 8T cell line compared to both 7T and 12T groups (Figure 5.5), indicating that the production of VOC profiles may rely on more complex processes rather than just MPM phenotype. 2-methyl-2-

propanol can also be known as tert-butyl alcohol and has been comprehensively reviewed as an inhaled toxicant (McGregor, 2010). However, at present there is a lack of available data regarding this specific compound in terms of diagnostic breath analysis.

2,2-dimethyl propanoic acid is also known as pivalic acid and has been identified as a potential breath biomarker for pre-symptomatic Alzheimer's disease (Emam et al., 2020). Aside from this, there is not much more mention of this compound in the VOC analysis literature. As with isopropanol and acetone, pivalic acid and diethylene glycol dipivalate appear to be linked metabolically; this is reflected in the relative levels of the compounds. Diethylene glycol dipivalate levels were more intense in the 7T biphasic group, whereas pivalic acid was associated with the 8T and 12T epithelioid groups, again suggesting differences in metabolism between the two MPM sub-types.

5.5.4 Conclusions

To our knowledge, this is the first time VOCs were identified from CAM-generated MPM xenografts, providing a proof of concept for this model to be used within pre-clinical VOC analysis studies. The methods presented in this chapter attempt to address the issues previously raised regarding 2D VOC analysis of cell cultures - hyperoxic cell culture conditions and the background signal from plastic flasks. The main results from the current work are in line with the previously published MPM breath analysis data: MPM samples were clearly distinct from controls and with some subtler differences between MPM sub-types. The results from this chapter show that it is possible to progress *in vitro* VOC analysis from

simple 2D cell culture models, which in turn unlocks many new possibilities within this field of research. The use of CAM models can easily be adapted to study different cancer/disease types and further experiments can be explored. Valuable information was also gained regarding MPM VOC analysis. Six candidate VOC biomarkers were identified and put into a biological context, with the potential for these compounds to form part of a MPM diagnostic breath test in the future.

6 Ongoing Work, Conclusions and Future Perspectives

6.1 Aims of the Chapter

The aim of this chapter is to provide a summary of the current PhD project, discussing the key results with regard to the original aims and objectives. An overview of the ongoing work and some future directions are included. The final discussion aims to pull together all of the main results from each chapter, with the final conclusions stating the impact that this project may have on mesothelioma diagnosis and VOC analysis.

6.2 Final Discussion

6.2.1 Malignant Mesothelioma VOC Analysis

Malignant mesothelioma remains an aggressive and devastating cancer, often diagnosed at a very late stage where 5-year survival is very poor and effective treatment options are limited (de Gooijer et al., 2020; Mutti et al., 2018). Current diagnostic methods are invasive, causing discomfort and distress to patients, and struggle to identify mesothelioma in its early stages (Figure 1.3). Analysis of VOCs in exhaled breath has shown potential within mesothelioma diagnosis, potentially providing a sensitive and specific method of diagnosis in the form of a non-invasive breath test (Di Gilio et al., 2020; Disselhorst et al., 2021; Lamote et al., 2017). The current project was the first to apply GC-MS analysis methods for the identification of VOCs released from MPM cell lines and pre-clinical tumour models. This was designed to complement patient breath analysis studies in order to progress the identification of candidate VOC biomarkers and also understand some of the underlying biology behind their production.

The aims of the first two results chapters were to develop a GC-MS methodology that could identify VOCs in cell culture headspace, and then use that method to identify VOCs released from MPM cells (Chapter 2 & Chapter 3). Chapter 2 detailed the optimisation of the methodology from initial GC-FID experiments to the final SPME GC-MS method that was used throughout the following chapters. This was an important first step in the progression of this project.

This is the first time that SPME GC-MS was used to identify VOCs from MPM cells, resulting in an original publication in The Journal of Breath Research (Little et al., 2020). Analysis using this model recapitulated results observed within the MPM breath analysis literature – *in vitro* VOC profiles were able to discriminate between MPM and non-malignant controls (Little et al., 2020). Discrimination between biphasic MSTO-211H and epithelioid NCI-H28 cells was also shown, the first-time evidence was provided for differential VOC profiles between MPM sub-types (Little et al., 2020). This initial *in vitro* finding requires further investigation with MPM patients but is a good example of how *in vitro* VOC studies can be used to inform future directions in wider clinical research.

The SPME GC-MS methodology was also used to measure the effects of BAP1 mutation on VOC profiles, using MET-5A$^{w-/KO}$ cells (Chapter 4). Mutations in the BAP1 gene have emerged as one of the most clinically relevant genetic biomarkers within mesothelioma (Carbone et al., 2020). Results from MET-5A$^{w-/KO}$ cells suggested that loss of function mutations in the BAP1 gene and decreased BAP1 expression slightly altered the VOCs produced by MET-5A cells (Table 4.2 & Table 4.3). Individuals with a BAP1 mutation represent a population that is at an increased risk of developing mesothelioma and are susceptible to

lower levels of asbestos that may not cause mesothelioma in BAP1 wild-type (Xu et al., 2014). The results from Chapter 4 indicate that at a cellular level, mesothelial cells with a BAP1 mutation produce slightly different VOCs to wild-type cells, but also produce a profile that is distinct from MPM cells. This is the first time that the effects of a BAP1 mutation has been measured on VOC profiles.

Looking forward clinically, it may be possible to identify BAP1 mutants before they have developed mesothelioma, by measuring VOCs in exhaled breath. Non-invasive breath collection would also be advantageous in this situation as long-term monitoring of BAP1 mutants could be performed without the need for uncomfortable, invasive procedures and potentially identify the signs of malignancy earlier. Again, the results presented in Chapter 4 are initial findings and further exploration is required using additional cell lines and models and also looking at patient breath – there is the possibility to identify individuals with BAP1 mutations due to the prevalence of germline mutations.

6.2.1.1 Progression of VOC Analysis Models

The initial results chapters analysed the headspace of 2D cell cultures using standard culture flasks, a method which is now widely accepted within breath analysis research (Table 1.3). Due to some of the limitations recognised with this methodology, Chapter 5 aimed to progress VOC analysis models, addressing the issues raised and still providing insight into VOCs within MPM. This was the first time that CAM xenografts had been used as a pre-clinical model for VOC analysis. It was possible to identify VOCs from the headspace of CAM xenografts and the results were in line with MPM VOC analysis in the literature and also the other experiments in this project (Figure 5.2, Figure 5.3 & Figure 5.5). Differences

in VOCs were observed between MPM xenografts and controls, and biphasic models appeared to show slight differences to epithelioid within MPM (Figure 5.2, Figure 5.3 & Figure 5.5). The differences observed in xenograft VOC profiles are reflective of the MPM breath analysis literature, which has reported differences between MPM patients and controls (de Gennaro et al., 2010; Di Gilio et al., 2020; Lamote et al., 2017). Differences between MPM sub-types also correlate with the cell culture results from the current project (Little et al., 2020) and those that have been recently published (Janssens et al., 2022). These results are the initial stages of the validation of CAM-based models within VOC analysis, with the hope that these models can be used in future studies and progress the field of breath analysis as a whole.

6.2.2 Candidate VOC Biomarkers

The overall aim of this project was to explore VOCs in *in vitro* and pre-clinical models of MPM, to identify appropriate candidate biomarkers and progress the development of a diagnostic breath test. Reproducibility is an issue in the field of breath analysis (Henderson et al., 2020; Wilkinson et al., 2021). Many studies have shown differences between specific disease types and controls, in human breath and cell line models, and presented the VOCs identified as biomarkers of that particular disease (Table 1.1 & Table 1.3). Additional studies have then observed the same patterns of results, but unfortunately the identities of the specific VOCs are often quite different. The current project attempted to not overstate the importance of any VOCs identified and instead aimed to contextualise each compound within the wider literature. This proved to be one of the most challenging aspects of the project, with thousands of compounds now

reported and nomenclature varying between studies. The volatilome database was invaluable for this, however as the resource is still relatively new, many VOCs have not been added yet. CO_2, ethyl acetate, 2-ethyl-1-hexanol and dodecane were identified as important compounds in more than one chapter in this thesis (Chapter 3 & Chapter 4).

CO_2 was used in a panel of compounds within multivariate statistical analysis comparisons between MSTO-211H, NCI-H28 and MET-5A cell lines and was also found at relatively higher levels in MSTO-211H cells compared to NCI-H28 and MET-5A (Figure 3.9). CO_2 was also found significantly increased in NCI-H1975 cells compared to MET-5A and increased in MET-5A$^{w-/KO}$ cells compared to both MET-5A and MET-5A$^{+/+}$ (Table 4.1, Table 4.2 & Table 4.3). Ethyl acetate was also part of the panel of compounds used in the comparisons between MSTO-211H, NCI-H28 and MET-5A cells and was relatively higher in MSTO-211H headspace compared to NCI-H28 and MET-5A (Figure 3.9). When analysed in smaller cell culture flasks, ethyl acetate was found at significantly increased levels in MSTO-211H compared to MET-5A (Table 4.1). 2-ethyl-1-hexanol was a compound identified in both methods of statistical analysis performed in Chapter 3 (Table 3.1 & Figure 3.9). Feature analysis detected significantly increased levels of 2-ethyl-1-hexanol in both MSTO-211H and NCI-H28 cells compared to MET-5A and was found at relatively higher levels in MSTO-211H headspace compared to NCI-H28 and MET-5A using the multivariate statistical analysis pathway (Table 3.1 & Figure 3.9). 2-ethyl-1-hexanol was also found at significantly increased levels in the headspace of NCI-H1975 cells compared to MET-5A (Table 4.1). Finally, dodecane was found at significantly increased levels in NCI-H28 compared to MET-5A using feature

detection (Table 3.1) and at significantly increased levels in MSTO-211H, NCI-H28 and NCI-H1975 headspace when analysed in smaller flasks (Table 4.1).

Correlation of results across Chapter 3 and 4 indicate some reproducibility in VOC production between different sized cell cultures. Unfortunately, the significantly altered VOCs identified in Chapter 5 did not correlate with the previous chapters. The same groups of compounds were however discovered, and comparisons could be made to VOCs identified in MPM breath analysis. As well as this, the overall trends observed in this chapter were the same as previous chapters and also in line with the key results from the literature, which may be more important due to the discrepancies already highlighted regarding reported VOC biomarker panels.

6.2.3 Development of a MPM Breath Test

Breath analysis research within MPM is not as well developed as in other tumour types such as lung cancer, even though mesothelioma patients stand to benefit greatly from a diagnostic breath test. A key area that was lacking in MPM breath research was the use of *in vitro* and pre-clinical models to complement the *in vivo* data. The current project addressed this and moving forward, MPM breath analysis should include both *in vivo* and *in vitro* studies which can feed into each other and inform the future directions in the pursuit of a diagnostic breath test. Large-scale clinical *in vivo* breath analysis studies are required comparing MPM patient breath to other clinical groups and controls, in order to increase the power of the findings. *In vitro* studies provide more targeted research to understand the

origins of VOCs and perform experiments that would not be possible with human breath. Included in this is the standardisation and the validation of results.

The most recent MPM breath analysis publications reflect these areas of development. A model was developed for the discrimination between MPM patients and healthy controls using a panel of ten VOCs identified in breath (Di Gilio et al., 2020). Validation was then performed on this model using a cohort of asbestos exposed individuals (Di Gilio et al., 2020). Another external validation was also performed on previously published data comparing MPM and AEx breath profiles, in an effort to implement a MPM in clinical practice (Janssens et al., 2022b). The accuracy of the originally published model dropped substantially when validated with an external cohort (Janssens et al., 2022b). However, after updating the model, differentiation was improved between MPM and AEx patients (Janssens et al., 2022b).

Finally, *in vitro* analysis methods have also been taken up by other research groups, with results presented analysing the headspace of MPM cell lines using TD tubes (Janssens et al., 2022). Many parallels can be drawn between Janssens' study and the current project, and it is encouraging to observe some similar results when using a different VOC sampling technique (Janssens et al., 2022). Areas for the progression of MPM *in vitro* VOC analysis were also discussed, suggesting that *in vivo* and *in vitro* MPM studies can complement each other to understand more about the discovered VOCs (Janssens et al., 2022). The current project has a place within MPM breath analysis. Novel results have been published and Chapter 4 and Chapter 5 show a development of this

research, targeting clinically relevant areas such as BAP1 and progression of VOC models with CAM xenografts.

6.3 Ongoing and Future Research Work

This section is intended to highlight relevant ongoing research questions and developments that were interrupted during the COVID-19 pandemic. Collaboration with Prof Judy Coulson's research group (University of Liverpool, facilitated by the Mesothelioma Research Network) played a substantial role in mitigating for the BAP1 objectives and providing CAM xenografts for analysis. Other avenues of research were also planned at the start of this PhD project. Here, these ongoing and future considerations are described in the context of how they would have fitted within the thesis narrative.

6.3.1 The Effects of Oxidative Stress on Mesothelial Cell VOC Profiles

6.3.1.1 Background

Increased oxidative stress and ROS plays an important role in the cellular production of VOCs and also in the development of MPM (Brusselmans et al., 2018; Ratcliffe et al., 2020). Previous studies have reported a change in VOC profiles in the headspace of cell cultures following oxidative stress induction with H_2O_2 (Baranska et al., 2015; Liu et al., 2019b). These experiments were replicated using MET-5A cells to develop a model for oxidative stress within MPM development and to determine if the non-malignant VOC profiles of MET-5A changed with an increase in ROS. Unfortunately, only the initial stages of these experiments were able to be completed.

6.3.1.2 Methods

The optimal H_2O_2 (Sigma Aldrich) concentration and treatment time was determined. MET-5A cells were set-up in 96-well plates at 5000 cells/well and incubated at 37^{o}C with 5% CO_2 overnight. After incubation, media was removed, cells washed twice with PBS and 100µl treatment media added. H_2O_2 treatment concentrations were: 0µM 100µM, 150µM, 200µM, 250µM and 300µM. Cells were incubated in treatment media for 3HR, 6HR, 9HR and 24HR time points. Blank samples without cells were also prepared for each treatment concentration to account for background absorbance. 10µL cell counting kit-8 solution (Sigma Aldrich) was added to each well 3HR before the end of the treatment time. After treatment the absorbance of the plate was measured at 450 nm using a Clariostar microplate reader (BMG Labtech).

6.3.1.3 Results

After 3 hours MET-5A cell viability appeared to be reduced by approximately 50% for all H_2O_2 concentrations (Figure 6.1). After 6 hours 100µM treatment had no effect on cell viability, 150µM showed a reduction of 50% and all other concentrations showed a reduction of 75% (Figure 6.1). At 9 hours cell viability for 100µM was less than 50% and all other concentrations were less than 25% (Figure 6.1). 24 hour incubation showed a dose-dependent reduction in cell viability: 100µM was 100%, 150µM 75%, 200µM 50%, 250µM 25% and 300µM around 10% viability (Figure 6.1).

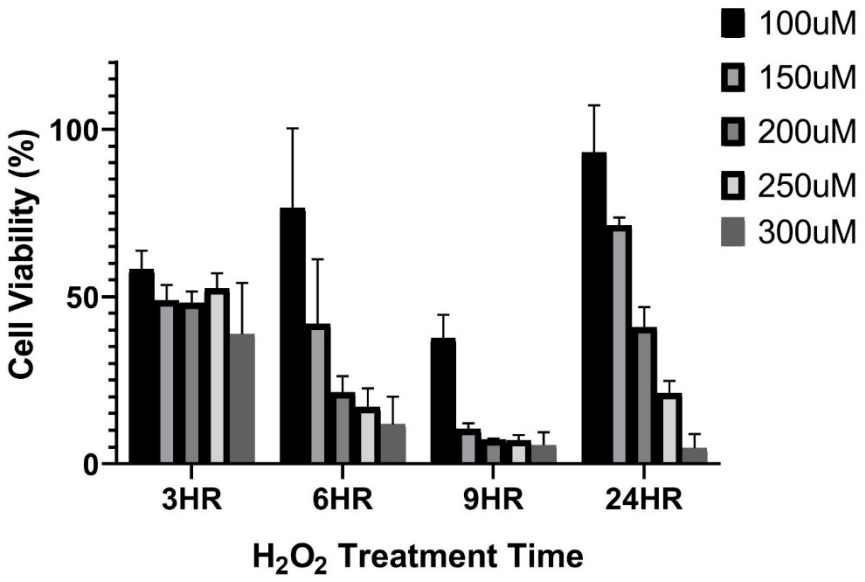

Figure 6.1: MET-5A cell viability after treatment with 100µM, 150µM, 200µM, 250µM and 300µM H_2O_2 for 3HR, 6HR, 9HR and 24HR incubation. Viability was measured using CCK-8 and absorbance read at 450nm. 3x replicates for each condition.

6.3.1.4 Discussion

Previous studies have used H_2O_2 as a way of inducing oxidative stress in cells and measuring the effects on VOC profiles (Baranska et al., 2015; Liu et al., 2019b). Replication of these experiments using MET-5A cells was attempted, unfortunately only optimisation of H_2O_2 treatment was completed (Figure 6.1). Completion of these experiments would give an idea of the effects of oxidative stress on VOC profiles in MET-5A cells, broadly modelling the early stages of MPM development in mesothelial cells.

6.3.2 VOC Analysis of 3D Cell Cultures

6.3.2.1 Background

This thesis has presented a large amount of data from 2D cell cultures (Chapter 3 & Chapter 4) and the progression of pre-clinical models using complex CAM xenografts (Chapter 5). An area identified for development was the analysis of 3D cell cultures, which would offer a more complex system than 2D cultures, but not as complex as CAM xenografts. This would provide a complete picture of pre-clinical analysis within MPM, allowing the observation of VOCs from simple 2D cultures to 3D systems and finally the more complex xenografts. This would also provide another alternative in the pursuit of standardisation within pre-clinical VOC analysis. Two methods were explored: spheroids using ultra-low adhesion (ULA) plates and alginate beads using alginic acid.

6.3.2.2 Methods

6.3.2.2.1 Ultra-Low Adhesion Plates

3D cell cultures were prepared in 96-well ULA (Corning) plates using MSTO-211H cells at 20,000 cells/well. Plates were incubated for 72 hours at 37°C with 5% CO_2, and spheroids collected for headspace analysis after incubation. MSTO-211H spheroids, along with the media they were incubated in, were transferred to 60ml glass headspace jars with PTFE/silicone caps; 96 MSTO-211H or NCI-H28 spheroids were sampled per jar. Control plates containing RPMI-1640 media only were also prepared, incubated and RPMI-1640 transferred to headspace jars. Headspace analysis was performed on spheroids and RPMI-1640 controls following Section 5.3.2. Analysis of the SPME fibre was performed with GC-MS following Section 3.3.3. Statistical analysis was performed following the pathway presented in Section 5.3.4.

6.3.2.2.2 Alginate Bead Cell Cultures

MSTO-211H cells were suspended in 1.2% w/v alginic acid in 0.15M NaCl at $1x10^6$ cells/ml. The cell suspensions were pipetted out of a 200µl pipette tip into 0.2M $CaCl_2$ solution to polymerise the beads. Alginate beads were incubated at room temperature for 3 min and then washed twice with 0.15M $CaCl_2$; washed alginate beads were cultured in complete RPMI-1640 for 72 hours. After incubation, single MSTO-211H alginate beads were transferred to RNAlater for 24 hours at room temperature and then stored at -80°C. Individual samples were defrosted on ice prior to VOC analysis.

6.3.2.3 Results

6.3.2.3.1 Ultra-Low Adhesion Plates

MSTO-211H and RPMI-1640 data were aligned, normalised and PCA was performed to determine if there were any differences between the MSTO-211H spheroid VOC profiles and the RPMI-1640 controls (Figure 6.2). Only three replicates from each group were analysed, but no real separation was observed between MSTO-211H and RPMI-1640 results, with crossover between the two groups (Figure 6.2).

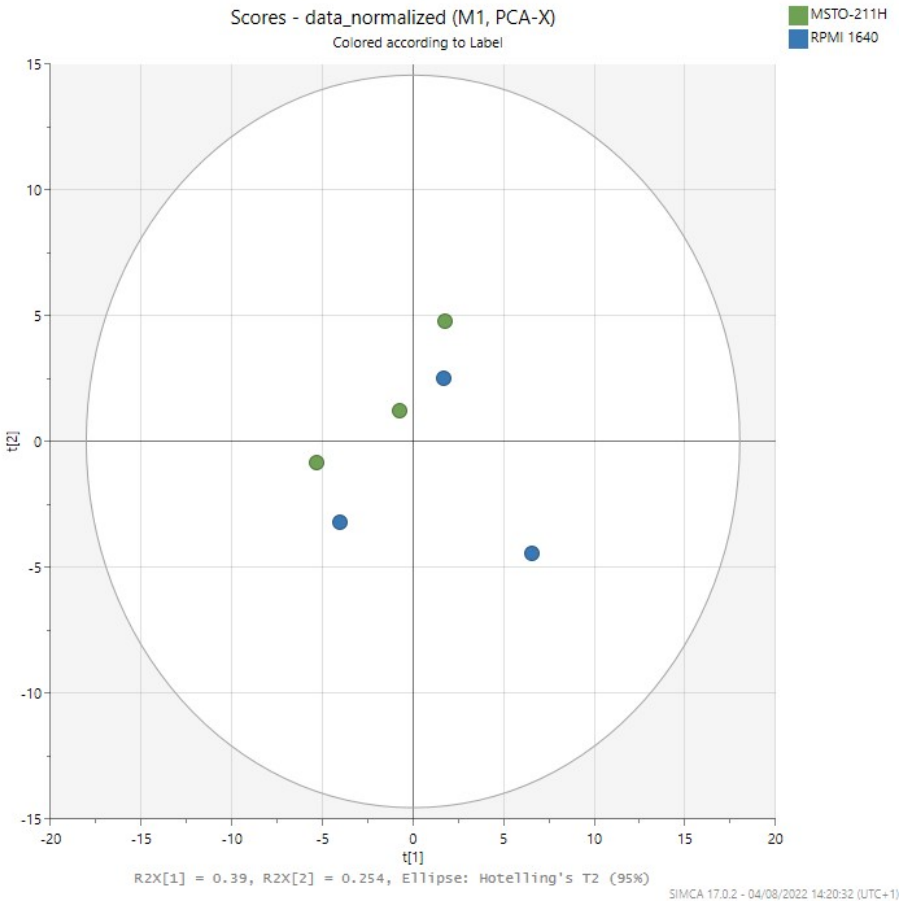

Figure 6.2: PCA score plot generated in SIMCA (V17.0.2) comparing MSTO-211H spheroids and RPMI-1640 controls. Each point represents a single replicate. For MSTO-211H this was 96 spheroids.

Batch t-tests (two-sample t-tests) were also performed between MSTO-211H and RPM-1640 groups using Metaboanalyst. A single compound, nonanal, was found

to be significantly higher in the RPMI-1640 group compared to the MSTO-211H group.

6.3.2.3.2 Alginate Bead Cell Cultures

Alginate beads were successfully grown using both MSTO-211H and NCI-H28 cell lines. Unfortunately, when alginate beads were defrosted from -80^{o}C they had dissolved into the RNAlater solution and were not able to be analysed using SPME GC-MS.

6.3.2.4 Discussion

3D MSTO-211H cell cultures were generated using both a spheroid and alginate model. The results show that VOCs were detected from MSTO-211H spheroids. However, when compared to the RPMI-1640 media controls the PCA score plot indicated that the two groups were very similar and only nonanal was found at a significantly different level in the RPMI-1640 group compared to the MSTO-211H group. For this experiment, only a small number of replicates were performed and additional parameters such as cell number and incubation time could be further optimised. Despite this, the initial results suggest that it is possible to use a spheroid model cultured with ULA plates for the study of VOCs *in vitro.* Preparation of these models is a straightforward process, and the plate-based set-up means that the effects of treatments on the cells could easily be assessed. One disadvantage may be that the ULA plates are quite expensive, with large numbers required to perform the analysis.

For the alginate beads, the next step was to culture the cells for the 72 hour incubation period and then perform headspace analysis and GC-MS on individual samples immediately. This would remove the freezing step, allow the alginate beads to remain solid and potentially identify VOCs released. Completion of these experiments would likely generate some interesting results in the development of pre-clinical VOC analysis methods within MPM.

6.3.3 Future Research: Alternative VOC Sampling Methods

Alternatives to SPME for VOC sampling of cell cultures have been published, these include NTDs and TD tubes (Table 1.3). Of these two options, TD tubes have been widely used in patient breath analysis studies (Issitt et al., 2022). Standardisation of methodologies is required to improve the reproducibility within breath analysis research (Henderson et al., 2020), this also applies to *in vitro* and pre-clinical studies. To address this, comparisons of the different sampling techniques (SPME, NTD, TD tubes) should be performed on the same panel of cell lines and a complex mixture of VOCs, such as those seen in peppermint capsules (Figure 2.12). The advantages and disadvantages of each sampling method could be identified from a direct comparison like this, resulting in the identification of the most appropriate, standardised methodology. External validation involving the wider breath analysis community and comparisons to *in vivo* breath analysis methods should also be considered. Analysis of several mesothelioma cell lines included in this thesis using TD tubes has recently been published (Janssens et al., 2022).

6.3.4 Future Research: Analysis of MPM Tumour Samples

Several studies have analysed the headspace of tumour samples taken from patient biopsies (Bianchi et al., 2017; De Vietro et al., 2020; Mochalski et al., 2018), performed using the same methods presented in Section 5.3.2. The analysis of clinically obtained tumour samples is an area of future research that would complement the work presented in this thesis and provide a full picture of *in vitro,* or pre-clinical, VOC analysis within MPM. Analysis of tissue samples can identify VOCs that are specifically released from MPM tumours which had been grown within the human body rather than under cell culture conditions. This would generate a panel of VOCs from every stage of pre-clinical analysis: 2D cell cultures, 3D cell cultures, tumour xenografts and tumour samples. This would also go towards validating the VOCs identified from the cell lines and models as potentially diagnostic biomarkers.

6.3.4.1 Final Conclusions

Analysis of VOCs in exhaled breath has the potential to revolutionise malignant mesothelioma diagnosis. However, the development of a diagnostic breath test remains in its initial stages. The current project has shown that VOC analysis models are important tools in the progression of MPM breath analysis, with novel research presented that has potentially clinically relevant impact. The aim of improving diagnostic methods within MPM is ultimately about diagnosing early to improve patient prognosis and survival. Breath analysis has the potential to do this, and it is therefore vital that VOC analysis at all levels within MPM continues.

7 Appendix

Table 7.1: Potential tentative identities of compounds that could not be confidently identified in Chapter 3, Table 3.2.

AVG RT (min)	Trends	Potential Tentative Identification
21.3	↑MET-5A compared to M199	2,2,3-trimethyl-decane 2,2,6-trimethyl-decane 2,2-dimethyl-decane 2,2,4,6,6-pentamethyl-heptane 2,2-dimethyloctadecane
22.2	↑MSTO-211H & NCI-H28 compared to RPMI-1640	2,2-dimethyl-decane 2,2,4,6,6-pentamethyl-heptane 2,2,4-trimethyl-hexane 4-ethyl-2,2,6,6-tetramethyl-heptane 2,2,6-trimethyl-octane 2,5-dimethyl-undecane 2,2-dimethyl-tetradecane 2,2-dimethyloctadecane 2,2,11,11-tetramethyl-dodecane
24.9	↑MSTO-211H & NCI-H28 compared to RPMI-1640 ↑MET-5A compared to M199	2,2-dimethyl-heptane 2,2,3-trimethyl-hexane 2,2,6-trimethyl-decane 2,2,4-trimethyl-hexane Benzaldehyde 4-ethyl-2,2,6,6-tetramethyl-heptane 2,2,5-trimethyl-hexane 2,6-dimethyl-octane 2,2,5,5-tetramethyl-hexane 5-ethyl-2,2,3-trimethyl-heptane

Table 7.2: Potential tentative identities of compounds that could not be confidently identified in Chapter 4, Table 4.1 & Table 4.2.

AVG RT(min)	Trends	Potential Tentative Identification
20.3	↑NCI-H28 compared to MET-5A	2,2,6-trimethyl-octane 2,2,5-trimethyl-hexane 2,2-dimethyl-tetradecane 2,7,10-trimethyl-dodecane 3-heptanone 4-ethyl-octane 2,9-dimethyl-undecane 3-methyl-tridecane 2,5,6-trimethyl-decane 2,4,6-trimethyl-octane
20.4	↓NCI-H1975 compared to MET-5A	3-heptanone 3-methyl-tridecane 2,2-dimethyleicosane 2,4,6-trimethyl-octane 4-ethyl-octane
21.6	↓NCI-H1975 compared to MET-5A ↓MET5Aw-/KO compared to MET-5A	Decane 3-ethyl-octane 4-methyl-decane Oxalic acid, isobutyl nonyl ester Isobutyl octadecyl ester carbonic acid 3-methyl-dodecane 4-ethyl-octane 5-ethyl-2-methyl-heptane 3,3,5-trimethyl-heptane
22.8	↓NCI-H28 & NCI-H1975 compared to MET-5A	2,2-dimethyl-decane 2,2,11,11-tetramethyl-dodecane 2,2,5-trimethyl-decane 2,5,6-trimethyl-octane 2,2,9-trimethyl-decane 2,2-dimethyl-tetradecane

		2,2,7,7-tetramethyloctane
		2,2,4,6,6-pentamethyl-heptane
23.2	↓NCI-H28 compared to MET-5A	2,2,9-trimethyl-decane
		2,2-dimethyl-undecane
		2,2-dimethyl-decane
		2,2,4,6,6-pentamethyl-heptane
		2,2,11,11-tetramethyl-dodecane
		2,2,5-trimethyl-decane
23.7	↓NCI-H1975 compared to MET-5A	3-methyl-5-propyl-nonane
		Hexadecane
		2,3-dimethyl-heptane
		3,4,5-trimethyl-heptane
		2,3,5-trimethyl-hexane
		3-ethyl-hexane
		2,3,8-trimethyl-decane
25.4	↑NCI-H1975 compared to MET-5A	3,3,8-trimethyl-decane
		4-methyl-heptadecane
		2,8,8-trimethyl-decane
		6-ethyl-2-methyl-octane
		3,7-dimethyl-decane
		3,3-dimethyl-octane
		4,8-dimethyl-undecane
		2,2,5-trimethyl-hexane
		2,2,11,11-tetramethyl-dodecane
		3,3,5-trimethyl-heptane
		3,3,5-trimethyl-decane
		2,8-dimethyl-undecane
26.8	↑NCI-H1975 compared to MET-5A	2,6,6-trimethyl-decane
		6-methyl-tridecane
		4-ethyl-2,2,6,6-tetramethyl-heptane
		2,5,6-trimethyl-decane
		2,6-dimethyl-undecane
		3-methyl-undecane

		3,7-dimethyl-nonane 6-methyl-tridecane Sulfurous acid, butyl nonyl ester 2,2,8-trimethyl-decane
28.5	↑NCI-H1975 compared to MET-5A	Sulfurous acid, di(2-ethylhexyl) ester 5-ethyl-5-methyl-decane 3,6-dimethyl-octane 3-methyl-undecane 2,6,10-trimethyl-dodecane Sulfurous acid, 2-ethylhexyl tridecyl ester
31.4	↑NCI-H1975 compared to MET-5A ↑MET5Aw-/KO compared to MET-5A	2,4-dimethyl-heptane 5-methyl-dodecane 5-methyl-tridecane 2,4-dimethyl-undecane 5,7-dimethyl-undecane 6-methyl-dodecane Hexyl octyl ether 4-methyl-dodecane 5-methyl-octadecane 5-methyl-tetradecane 4-ethyl-heptane 2,4-dimethyl-heptane 4,5-dimethyl-nonane 2,3,4-trimethyl-hexane
35.7	↑MSTO-211H & NCI-H28 compared to MET-5A	6-methyl-tridecane Sulfurous acid, decyl 2-ethylhexyl ester 2,6,11,15-tetramethyl-hexadecane 2,6-dimethyl-octadecane 9-methyl-nonadecane 5-methyl-tridecane

		5-propyl-nonane
36.5	↑NCI-H1975 compared to MET-5A	6-methyl-tridecane 2,6,10,14-tetramethyl-heptadecane Sulfurous acid, butyl dodecyl ester 2-methyl-5-propyl-nonane 3-methyl-dodecane 2-bromo dodecane 3-methyl-tridecane 2-methyl-tridecane 4,5-dimethyl-nonane Sulfurous acid, 2-ethylhexyl nonyl ester 5-propyl decane 2,6-dimethyldecane 7-methyl-heptadecane Pentacosane
39.0	↑MSTO-211H & NCI-H28 compared to MET-5A	2-bromo dodecane Sulfurous acid, butyl dodecyl ester Dodecane 3-methyl-tridecane 2-methyl-tridecane 2-methyl-tetradecane Heneicosane 10-methyl-eicosane 2,6,10,15-tetramethyl-heptadecane 9-methyl-nonadecane 2-methyl-eicosane 2,6,10,14-tetramethyl-hexadecane di-tert-dodecyl disulfide

	Pentadecane
	Eicosane
	Heptacosane
	2-methyl-ocytadecane

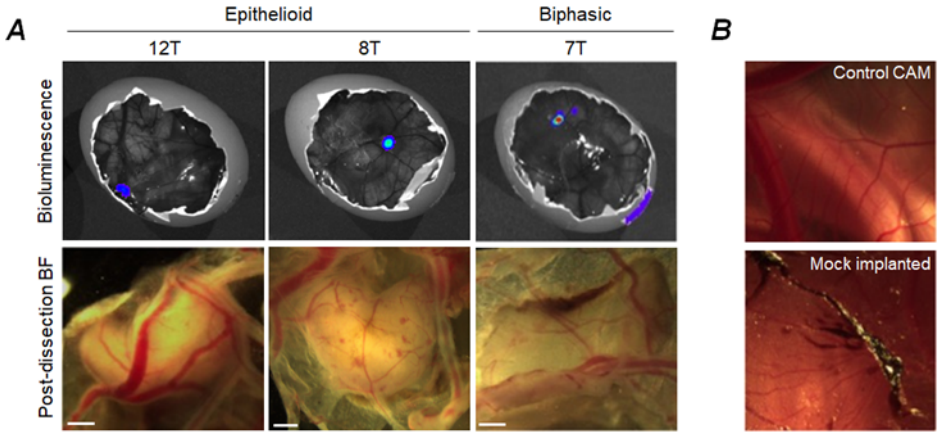

Figure 7.1: Mesothelioma xenografts generated on the CAM. A) representative tumour nodules for each mesothelioma cell line tested. Bioluminescent signal (top) and corresponding brightfield image taken post dissection (bottom). Scale bar = 500µm. B) Representative images of CAM controls acquired prior to dissection. Images acquired by Dr Sarah Barnett (University of Liverpool).

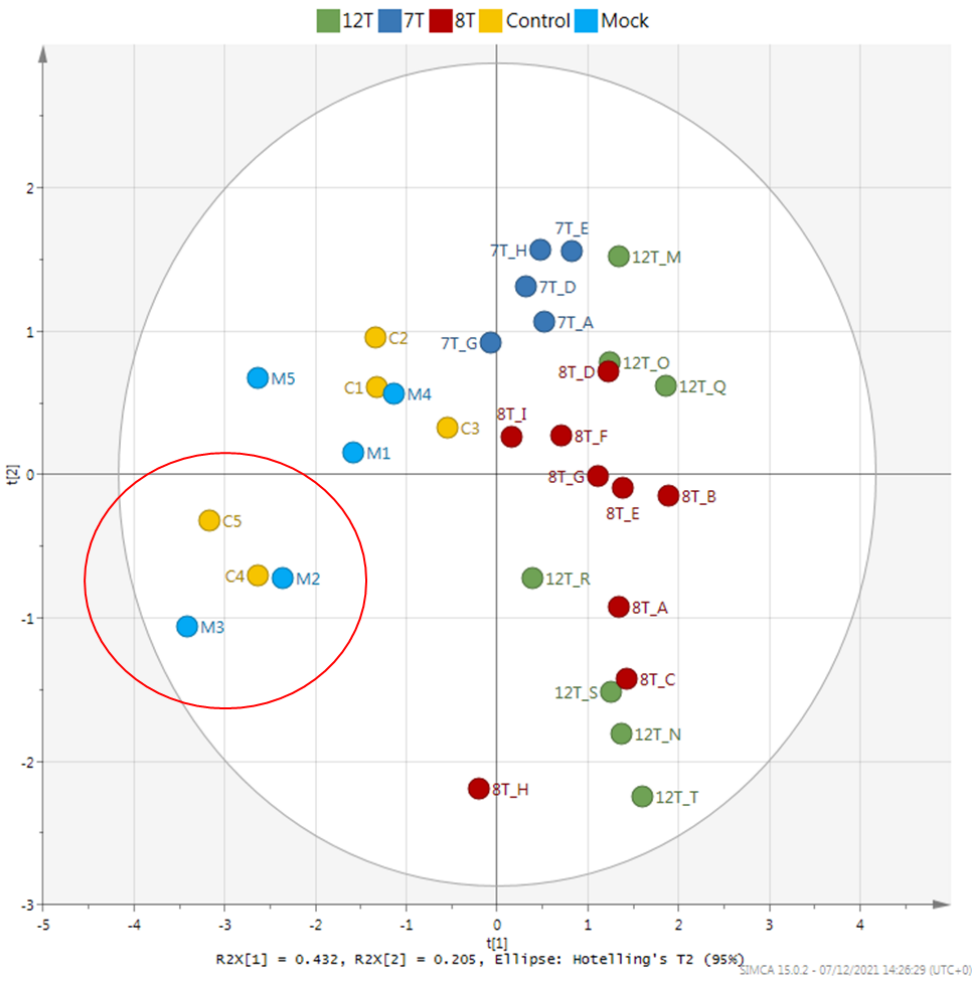

Figure 7.2: PLS-DA Score plot showing Mock, Control, 7T, 8T and 12T groups. An outlier group of Mock and Control samples was observed, which did not appear to be Luciferin related (Table 7.3). Re-analysis performed by Dr Sarah Barnett (University of Liverpool).

Table 7.3: Sample info for Mock and Control groups detailing Luciferin status. The outlier group in Figure 7.2 did not appear to be related with Luciferin. Sample info provided by Dr Sarah Barnett (University of Liverpool).

Sample info	
ID	**Description**
M1	Mock implanted
M2	Mock implanted
M3	Mock implanted
M4	Mock implanted + luciferin
M5	Mock implanted + luciferin
C1	Non-implanted
C2	Non-implanted
C3	Non-implanted + luciferin
C4	Non-implanted + luciferin
C5	Non-implanted

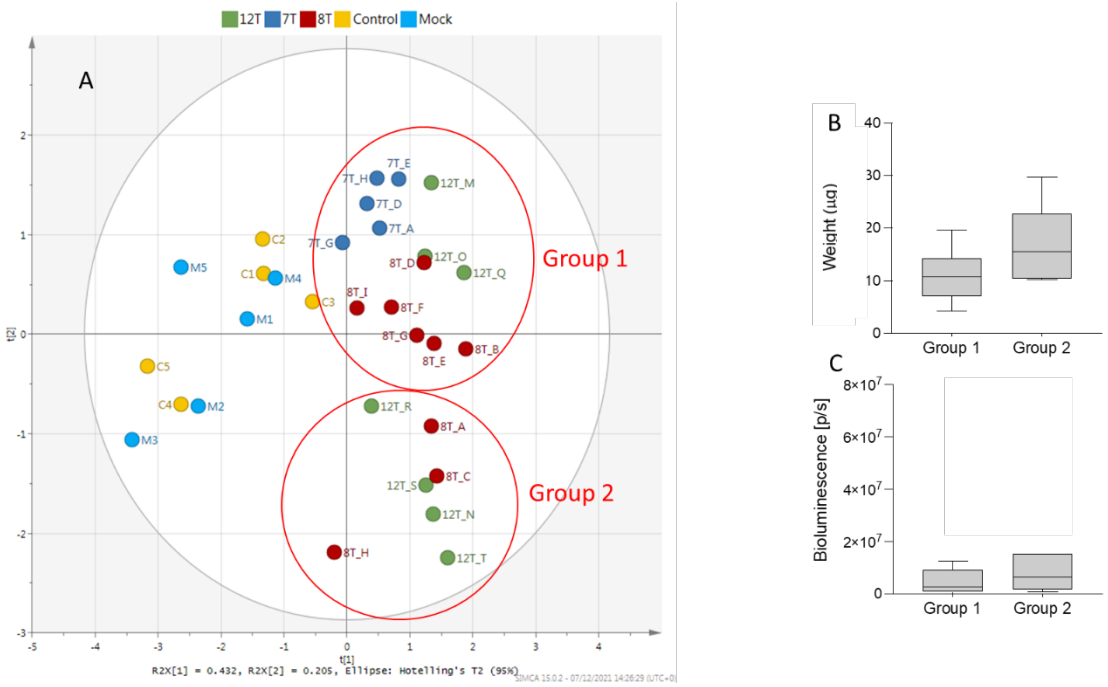

Figure 7.3: Tumour burden appeared to affect the spread of results in the same phenotype in the PLS-DA score plot (A). Two groups were observed, Group 2 was found to have an increase in tumour weight compared to Group 1 (B). Bioluminescence appeared to be the same between Group 1 and Group 2 (C). Re-analysis performed by Dr Sarah Barnett (University of Liverpool).

7.1 Publications

Little, L. D., Carolan, V. A., Allen, K. E., Cole, L. M., & Haywood-Small, S. L. (2020). Headspace analysis of mesothelioma cell lines differentiates biphasic and epithelioid sub-types. *Journal of Breath Research, 14*(4), 046011. 10.1088/1752-7163/abaaff

In preparation:

Volatile Organic Compound Analysis of Malignant Pleural Mesothelioma Chorioallantoic Membrane Xenografts

The Effect of BAP1 Mutation on Volatile Organic Compound Profiles within Malignant Pleural Mesothelioma

7.2 Research Dissemination

International Breath Summit, Pisa, Italy, June 2022

Oral Presentation (Presented by Dr Sarah Haywood-Small): Volatile Organic Compound Analysis of a Chorioallantoic Membrane Model within Malignant Pleural Mesothelioma

Mesothelioma Research Network, Virtual Webinar, UK, February 2022

Oral Presentation: Volatile Organic Compound Analysis of a CAM Model within Mesothelioma

International Society for the Study of Pleura and Peritoneum, Rome, Italy, October 2021

Oral Presentation: *In Vitro* Breath Analysis of Malignant Pleural Mesothelioma Cell Lines

Awarded prize for Best Oral Presentation

International Mesothelioma Interest Group, Brisbane, Australia (Virtual), May 2021

Poster Presentation: Headspace Analysis of Volatile Organic Compounds from Malignant Mesothelioma Cell Lines

Owlstone Medical Breath Biopsy Conference, Cambridge, UK, November 2019

Poster Presentation: Volatile Profiles of MSTO-211H Malignant Mesothelioma Cells

International Breath Summit, Loughborough, UK, September 2019

Poster Presentation: Volatile Profiles of MSTO-211H Malignant Mesothelioma Cells

8 References

Abdel-Rahman, O. (2018). Global trends in mortality from malignant mesothelioma: Analysis of WHO mortality database (1994-2013). *The Clinical Respiratory Journal, 12*(6), 2090-2100. DOI:10.1111/crj.12778

Abderrahman, B. (2019). Exhaled breath biopsy: a new cancer detection paradigm. *Future Oncology, 15*(15), 1679-1682. DOI:10.2217/fon-2019-0091

Aggarwal, P., Baker, J., Boyd, M. T., Coyle, S., Probert, C., & Chapman, E. A. (2020). Optimisation of Urine Sample Preparation for Headspace-Solid Phase Microextraction Gas Chromatography-Mass Spectrometry: Altering Sample pH, Sulphuric Acid Concentration and Phase Ratio. *Metabolites, 10*(12), 482. DOI:10.3390/metabo10120482

Ahmad, A., Ahmad, M. I., Younas, M., Khan, H., & Shah, M. U. H. (2013). A Comparative Study of Alkaline Hydrolysis of Ethyl Acetate Using Design of Experiments. *Iranian Journal of Chemistry & Chemical Engineering, 32*(4), 33-47. DOI: 10.1385/abab:121:1-3:0117

Alpert, N., Gerwen, M. v., & Taioli, E. (2020). Epidemiology of mesothelioma in the 21st century in Europe and the United States, 40 years after restricted/banned asbestos use. *Translational Lung Cancer Research, 9*(S1), S28-S38. DOI:10.21037/tlcr.2019.11.11

Altomare, D. F., Di Lena, M., Porcelli, F., Trizio, L., Travaglio, E., Tutino, M., Dragonieri, S., Memeo, V., & de Gennaro, G. (2013). Exhaled volatile organic

compounds identify patients with colorectal cancer. *British Journal of Surgery, 100*(1), 144-150. DOI:10.1002/bjs.8942

Amann, A., Costello, B. d. L., Miekisch, W., Schubert, J., Buszewski, B. a., Pleil, J., Ratcliffe, N., & Risby, T. (2014). The human volatilome: volatile organic compounds (VOCs) in exhaled breath, skin emanations, urine, feces and saliva. *Journal of Breath Research, 8*(3), 034001. DOI:10.1088/1752-7155/8/3/034001

Amaro, F., Pinto, J., Rocha, S., Araújo, A. M., Miranda-Gonçalves, V., Jerónimo, C., Henrique, R., de Lourdes Bastos, M., Carvalho, M., & de Pinho, P. G. (2020). Volatilomics Reveals Potential Biomarkers for Identification of Renal Cell Carcinoma: An In Vitro Approach. *Metabolites, 10*(5), 174. DOI:10.3390/metabo10050174

Astolfi, M., Rispoli, G., Benedusi, M., Zonta, G., Landini, N., Valacchi, G., & Malagù, C. (2022). Chemoresistive Sensors for Cellular Type Discrimination Based on Their Exhalations. *Nanomaterials, 12*(7), 1111. DOI:10.3390/nano12071111

Attanoos, R. L., Churg, A., Galateau-Salle, F., Gibbs, A. R., & Roggli, V. L. (2018). Malignant Mesothelioma and Its Non-Asbestos Causes. *Archives of Pathology & Laboratory Medicine, 142*(6), 753-760. DOI:10.5858/arpa.2017-0365-RA

Avelino, T. M., García-Arévalo, M., Torres, F. R., Goncalves Dias, M. M., Domingues, R. R., de Carvalho, M., Fonseca, M. d. C., Rodrigues, V. K. T., Leme,

A. F. P., & Figueira, A. C. M. (2021). Mass spectrometry-based proteomics of 3D cell culture: A useful tool to validate culture of spheroids and organoids. *SLAS Discovery, 27,* 167-174. DOI:10.1016/j.slasd.2021.10.013

Bajtarevic, A., Ager, C., Pienz, M., Klieber, M., Schwarz, K., Ligor, M., Ligor, T., Filipiak, W., Denz, H., Fiegl, M., Hilbe, W., Weiss, W., Lukas, P., Jamnig, H., Hackl, M., Haidenberger, A., Buszewski, B., Miekisch, W., Schubert, J., & Amann, A. (2009). Noninvasive detection of lung cancer by analysis of exhaled breath. *BMC Cancer, 9*(1), 348. DOI:10.1186/1471-2407-9-348

Baranska, A., Smolinska, A., Boots, A. W., Dallinga, J. W., & van Schooten, F. J. (2015). Dynamic collection and analysis of volatile organic compounds from the headspace of cell cultures. *Journal of Breath Research, 9*(4), 047102. DOI:10.1088/1752-7155/9/4/047102

Barash, O., Zhang, W., Halpern, J. M., Hua, Q., Pan, Y., Kayal, H., Khoury, K., Liu, H., Davies, M. P. A., & Haick, H. (2015). Differentiation between genetic mutations of breast cancer by breath volatolomics. *Oncotarget, 6*(42), 44864-44876. DOI:10.18632/oncotarget.6269

Baumann, F., Flores, E., Napolitano, A., Kanodia, S., Taioli, E., Pass, H., Yang, H., & Carbone, M. (2015). Mesothelioma patients with germline BAP1 mutations have 7-fold improved long-term survival. *Carcinogenesis, 36*(1), 76-81. DOI:10.1093/carcin/bgu227

Beauchamp, J., Herbig, J., Gutmann, R., & Hansel, A. (2008). On the use of Tedlar® bags for breath-gas sampling and analysis. *Journal of Breath Research, 2*(4), 046001. DOI:10.1088/1752-7155/2/4/046001

Bellagambi, F. G., Lomonaco, T., Ghimenti, S., Biagini, D., Fuoco, R., & Francesco, F. D. (2020). Determination of peppermint compounds in breath by needle trap micro-extraction coupled with gas chromatography-tandem mass spectrometry. *Journal of Breath Research, 15*(1), 16014. DOI:10.1088/1752-7163/abcdec

Berzenji, L., Van Schil, P. E., & Carp, L. (2018). The eighth TNM classification for malignant pleural mesothelioma. *Translational Lung Cancer Research, 7*(5), 543-549. DOI:10.21037/tlcr.2018.07.05

Bianchi, F., Riboni, N., Carbognani, P., Gnetti, L., Dalcanale, E., Ampollini, L., & Careri, M. (2017). Solid-phase microextraction coupled to gas chromatography–mass spectrometry followed by multivariate data analysis for the identification of volatile organic compounds as possible biomarkers in lung cancer tissues. *Journal of Pharmaceutical and Biomedical Analysis, 146*, 329-333. DOI:10.1016/j.jpba.2017.08.049

Bianco, A., Valente, T., De Rimini, M. L., Sica, G., & Fiorelli, A. (2018). Clinical diagnosis of malignant pleural mesothelioma. *Journal of Thoracic Disease, 10*(Suppl 2), S253-S261. DOI:10.21037/jtd.2017.10.09

Bischoff, A., Oertel, P., Sukul, P., Rimmbach, C., David, R., Schubert, J., & Miekisch, W. (2018). Smell of cells: Volatile profiling of stem- and non-stem cell proliferation. *Journal of Breath Research, 12*(2), 026014. DOI:10.1088/1752-7163/aaa111

Blyth, K. G., & Murphy, D. J. (2018). Progress and challenges in Mesothelioma: From bench to bedside. *Respiratory Medicine, 134*, 31-41. DOI:10.1016/j.rmed.2017.11.015

Bojko, B. (2022). Solid-phase microextraction: a fit-for-purpose technique in biomedical analysis. *Analytical and Bioanalytical Chemistry, 24,* 1-9 DOI:10.1007/s00216-022-04138-9

Bononi, A., Giorgi, C., Patergnani, S., Larson, D., Verbruggen, K., Tanji, M., Pellegrini, L., Signorato, V., Olivetto, F., Pastorino, S., Nasu, M., Napolitano, A., Gaudino, G., Morris, P., Sakamoto, G., Ferris, L. K., Danese, A., Raimondi, A., Tacchetti, C., . . . Carbone, M. (2017). BAP1 regulates IP3R3-mediated Ca2+ flux to mitochondria suppressing cell transformation. *Nature, 546*(7659), 549-553. DOI:10.1038/nature22798

Bononi, A., Napolitano, A., Pass, H. I., Yang, H., & Carbone, M. (2015). Latest developments in our understanding of the pathogenesis of mesothelioma and the design of targeted therapies. *Expert Review of Respiratory Medicine, 9*(5), 633-654. DOI:10.1586/17476348.2015.1081066

Borchert, S., Suckrau, P., Walter, R. F. H., Wessolly, M., Mairinger, E., Steinborn, J., Hegedus, B., Hager, T., Herold, T., Eberhardt, W. E. E., Wohlschlaeger, J., Aigner, C., Bankfalvi, A., Schmid, K. W., & Mairinger, F. D. (2020). Impact of metallothionein-knockdown on cisplatin resistance in malignant pleural mesothelioma. *Scientific Reports, 10*(1), 18677. DOI:10.1038/s41598-020-75807-x

Bouza, M., Gonzalez-Soto, J., Pereiro, R., de Vicente, J. C., & Sanz-Medel, A. (2017). Exhaled breath and oral cavity VOCs as potential biomarkers in oral cancer patients. *Journal of Breath Research, 11*(1), 016015. DOI:10.1088/1752-7163/aa5e76

Brims, F. (2021). Epidemiology and Clinical Aspects of Malignant Pleural Mesothelioma. *Cancers, 13*(16), 4194. DOI:10.3390/cancers13164194

Brinkman, P., Ahmed, W. M., Gómez, C., Knobel, H. H., Weda, H., Vink, T. J., Nijsen, T. M., Wheelock, C. E., Dahlen, S., Montuschi, P., Knowles, R. G., Vijverberg, S. J., Maitland-van der Zee, Anke H, Sterk, P. J., & Fowler, S. J. (2020). Exhaled volatile organic compounds as markers for medication use in asthma. *The European Respiratory Journal, 55*(2), 1900544. DOI:10.1183/13993003.00544-2019

Brusselmans, L., Arnouts, L., Millevert, C., Vandersnickt, J., van Meerbeeck, J. P., & Lamote, K. (2018). Breath analysis as a diagnostic and screening tool for malignant pleural mesothelioma: a systematic review. *Translational Lung Cancer Research, 7*(5), 520-536. DOI:10.21037/tlcr.2018.04.09

Bueno, R., & Opitz, I. (2018). Surgery in Malignant Pleural Mesothelioma. *Journal of Thoracic Oncology, 13*(11), 1638-1654. DOI:10.1016/j.jtho.2018.08.001

Campanella, A., De Summa, S., & Tommasi, S. (2019). Exhaled breath condensate biomarkers for lung cancer. *Journal of Breath Research, 13*(4), 044002. DOI:10.1088/1752-7163/ab2f9f

Campanella, B., Colombaioni, L., Nieri, R., Benedetti, E., Onor, M., & Bramanti, E. (2021). Unraveling the Extracellular Metabolism of Immortalized Hippocampal Neurons Under Normal Growth Conditions. *Frontiers in Chemistry, 9*, 621548. DOI:10.3389/fchem.2021.621548

Capone, S., Tufariello, M., Forleo, A., Longo, V., Giampetruzzi, L., Radogna, A. V., Casino, F., & Siciliano, P. (2018). Chromatographic analysis of VOC patterns in exhaled breath from smokers and nonsmokers. *Biomedical Chromatography, 32*(4), e4132 DOI:10.1002/bmc.4132

Carbone, M., Adusumilli, P. S., Alexander, H. R., Baas, P., Bardelli, F., Bononi, A., Bueno, R., Felley-Bosco, E., Galateau-Salle, F., Jablons, D., Mansfield, A. S., Minaai, M., Perrot, M., Pesavento, P., Rusch, V., Severson, D. T., Taioli, E., Tsao, A., Woodard, G., . . . Pass, H. I. (2019). Mesothelioma: Scientific clues for prevention, diagnosis, and therapy. *CA: A Cancer Journal for Clinicians, 69*(5), 402-429. DOI:10.3322/caac.21572

Carbone, M., Emri, S., Dogan, A. U., Steele, I., Tuncer, M., Pass, H. I., & Baris, Y. I. (2007). A mesothelioma epidemic in Cappadocia: scientific developments and unexpected social outcomes. *Nature Reviews. Cancer, 7*(2), 147-154. DOI:10.1038/nrc2068

Carbone, M., Harbour, J. W., Brugarolas, J., Bononi, A., Pagano, I., Dey, A., Krausz, T., Pass, H. I., Yang, H., & Gaudino, G. (2020). Biological Mechanisms and Clinical Significance of BAP1 Mutations in Human Cancer. *Cancer Discovery, 10*(8), 1103-1120. DOI:10.1158/2159-8290.CD-19-1220

Carbone, M., & Yang, H. (2017). Mesothelioma: recent highlights. *Annals of Translational Medicine, 5*(11), 238. DOI:10.21037/atm.2017.04.29

Cassagnes, L. E., Leni, Z., Håland, A., Bell, D. M., Zhu, L., Bertrand, A., Baltensperger, U., El Haddad, I., Wisthaler, A., Geiser, M., & Dommen, J. (2020). Online monitoring of volatile organic compounds emitted from human bronchial epithelial cells as markers for oxidative stress. *Journal of Breath Research, 15*(1), 16015. DOI:10.1088/1752-7163/abc055

Catino, A., de Gennaro, G., Di Gilio, A., Facchini, L., Galetta, D., Palmisani, J., Porcelli, F., & Varesano, N. (2019). Breath Analysis: A Systematic Review of Volatile Organic Compounds (VOCs) in Diagnostic and Therapeutic Management of Pleural Mesothelioma. *Cancers, 11*(6), 831. DOI:10.3390/cancers11060831

Chapman, E. A., Thomas, P. S., Stone, E., Lewis, C., & Yates, D. H. (2012). A breath test for malignant mesothelioma using an electronic nose. *The European Respiratory Journal, 40*(2), 448-454. DOI:10.1183/09031936.00040911

Chapman, E. A., Thomas, P. S., & Yates, D. H. (2010). Breath analysis in asbestos-related disorders: a review of the literature and potential future applications. *Journal of Breath Research, 4*(3), 034001. DOI:10.1088/1752-7155/4/3/034001

Cherrie, J. W., McElvenny, D., & Blyth, K. G. (2018). Estimating past inhalation exposure to asbestos: A tool for risk attribution and disease screening. *International Journal of Hygiene and Environmental Health, 221*(1), 27-32. DOI:10.1016/j.ijheh.2017.09.013

Christiansen, A., Davidsen, J. R., Titlestad, I., Vestbo, J., & Baumbach, J. (2016). A systematic review of breath analysis and detection of volatile organic compounds in COPD. *Journal of Breath Research, 10*(3), 034002. DOI:10.1088/1752-7155/10/3/034002

Chu, P., Koh, A. P., Antony, J., & Huang, R. Y. (2021). Applications of the Chick Chorioallantoic Membrane as an Alternative Model for Cancer Studies. *Cells, Tissues, Organs, 211*(2) 1-16. DOI:10.1159/000513039

Chu, Y., Zhou, J., Ge, D., Lu, Y., Zou, X., Xia, L., Huang, C., Shen, C., & Chu, Y. (2020). Variable VOCs in plastic culture flasks and their potential impact on cell

volatile biomarkers. *Analytical and Bioanalytical Chemistry, 412*(22), 5397-5408. DOI:10.1007/s00216-020-02756-9

Chuang, H., Tsai, S., Shie, R., Lu, Y., Song, S., Huang, S., Peng, H., & Yang, H. (2020). A novel lung alveolar cell model for exploring volatile biomarkers of particle-induced lung injury. *Scientific Reports, 10*(1), 15700. DOI:10.1038/s41598-020-72825-7

Crosby, D., Bhatia, S., Brindle, K. M., Coussens, L. M., Dive, C., Emberton, M., Esener, S., Fitzgerald, R. C., Gambhir, S. S., Kuhn, P., Rebbeck, T. R., & Balasubramanian, S. (2022). Early detection of cancer. *Science, 375*(6586), eaay9040. DOI:10.1126/science.aay9040

Davies, M. P. A., Barash, O., Jeries, R., Peled, N., Ilouze, M., Hyde, R., Marcus, M. W., Field, J. K., & Haick, H. (2014). Unique volatolomic signatures of TP53 and KRAS in lung cells. *British Journal of Cancer, 111*(6), 1213-1221. DOI:10.1038/bjc.2014.411

de Gennaro, G., Dragonieri, S., Longobardi, F., Musti, M., Stallone, G., Trizio, L., & Tutino, M. (2010). Chemical characterization of exhaled breath to differentiate between patients with malignant pleural mesothelioma from subjects with similar professional asbestos exposure. *Analytical and Bioanalytical Chemistry, 398*(7-8), 3043-3050. DOI:10.1007/s00216-010-4238-y

de Gooijer, C. J., Borm, F. J., Scherpereel, A., & Baas, P. (2020). Immunotherapy in Malignant Pleural Mesothelioma. *Frontiers in Oncology, 10*, 187. DOI:10.3389/fonc.2020.00187

de la Hoz, R. E., Weber, J., Xu, D., Doucette, J. T., Liu, X., Carson, D. A., & Celedón, J. C. (2019). Chest CT scan findings in World Trade Center workers. *Archives of Environmental & Occupational Health, 74*(5), 263-270. DOI:10.1080/19338244.2018.1452712

De Vietro, N., Aresta, A., Rotelli, M. T., Zambonin, C., Lippolis, C., Picciariello, A., & Altomare, D. F. (2020). Relationship between cancer tissue derived and exhaled volatile organic compound from colorectal cancer patients. Preliminary results. *Journal of Pharmaceutical and Biomedical Analysis, 180*, 113055. DOI:10.1016/j.jpba.2019.113055

Dell'Anno, I., Melani, A., Martin, S. A., Barbarino, M., Silvestri, R., Cipollini, M., Giordano, A., Mutti, L., Nicolini, A., Luzzi, L., Aiello, R., Gemignani, F., & Landi, S. (2022). A Drug Screening Revealed Novel Potential Agents against Malignant Pleural Mesothelioma. *Cancers, 14*(10), 2527. DOI:10.3390/cancers14102527

Di Gilio, A., Catino, A., Lombardi, A., Palmisani, J., Facchini, L., Mongelli, T., Varesano, N., Bellotti, R., Galetta, D., de Gennaro, G., & Tangaro, S. (2020). Breath Analysis for Early Detection of Malignant Pleural Mesothelioma: Volatile Organic Compounds (VOCs) Determination and Possible Biochemical Pathways. *Cancers, 12*(5), 1262. DOI:10.3390/cancers12051262

Di Gilio, A., Palmisani, J., Ventrella, G., Facchini, L., Catino, A., Varesano, N., Pizzutilo, P., Galetta, D., Borelli, M., Barbieri, P., Licen, S., & de Gennaro, G. (2020b). Breath Analysis: Comparison among Methodological Approaches for Breath Sampling. *Molecules, 25*(24), 5823. DOI:10.3390/molecules25245823

Disselhorst, M. J., de Vries, R., Quispel-Janssen, J., Wolf-Lansdorf, M., Sterk, P. J., & Baas, P. (2021). Nose in malignant mesothelioma—Prediction of response to immune checkpoint inhibitor treatment. *European Journal of Cancer, 152*, 60-67. DOI:10.1016/j.ejca.2021.04.024

Dragonieri, S., Pennazza, G., Carratu, P., & Resta, O. (2017). Electronic Nose Technology in Respiratory Diseases. *Lung, 195*(2), 157-165. DOI:10.1007/s00408-017-9987-3

Dragonieri, S., van der Schee, M. P, Massaro, T., Schiavulli, N., Brinkman, P., Pinca, A., Carratú, P., Spanevello, A., Resta, O., Musti, M., & Sterk, P. J. (2011). An electronic nose distinguishes exhaled breath of patients with Malignant Pleural Mesothelioma from controls. *Lung Cancer, 75*(3), 326-331. DOI:10.1016/j.lungcan.2011.08.009

Du, X., & Zeisel, S. H. (2013). Spectral deconvolution for gas chromatography mass spectrometry based metabolomics: Current status and future perspectives. *Computational and Structural Biotechnology Journal, 4*(5), e201301013. DOI:10.5936/csbj.201301013

Dweik, R. A., & Amann, A. (2008). Exhaled breath analysis: the new frontier in medical testing. *Journal of Breath Research, 2*(3), 030301. DOI:10.1088/1752-7163/2/3/030301

Einoch Amor, R., Nakhleh, M. K., Barash, O., & Haick, H. (2019). Breath analysis of cancer in the present and the future. *European Respiratory Review, 28*(152), 190002. DOI:10.1183/16000617.0002-2019

Emam, S., Nasrollahpour, M., Colarusso, B., Cai, X., Grant, S., Kulkarni, P., Ekenseair, A., Gharagouzloo, C., Ferris, C. F., & Sun, N. (2020). Detection of presymptomatic Alzheimer's disease through breath biomarkers. *Alzheimer's & Dementia: Diagnosis, Assessment & Disease Monitoring, 12*(1), e12088. DOI:10.1002/dad2.12088

Filipiak, W., Jaroch, K., Szeliska, P., Żuchowska, K., & Bojko, B. (2021). Application of Thin-Film Microextraction to Analyze Volatile Metabolites in A549 Cancer Cells. *Metabolites, 11*(10), 704. DOI:10.3390/metabo11100704

Filipiak, W., Mochalski, P., Filipiak, A., Ager, C., Cumeras, R., Davis, C. E., Agapiou, A., Unterkofler, K., & Troppmair, J. (2016). A Compendium of Volatile Organic Compounds (VOCs) Released By Human Cell Lines. *Current Medicinal Chemistry, 23*(20), 2112-2131. DOI:10.2174/0929867323666160510122913

Flint, L. E., Hamm, G., Ready, J. D., Ling, S., Duckett, C. J., Cross, N. A., Cole, L. M., Smith, D. P., Goodwin, R. J. A., & Clench, M. R. (2021). Comparison of Osteosarcoma Aggregated Tumour Models with Human Tissue by Multimodal

Mass Spectrometry Imaging. *Metabolites, 11*(8), 506. DOI:10.3390/metabo11080506

Fuchsmann, P., Tena Stern, M., Mu̇nger, L. H., Pimentel, G., Burton, K. J., Vionnet, N., & Vergères, G. (2020). Nutrivolatilomics of Urinary and Plasma Samples to Identify Candidate Biomarkers after Cheese, Milk, and Soy-Based Drink Intake in Healthy Humans. *Journal of Proteome Research, 19*(10), 4019-4033. DOI:10.1021/acs.jproteome.0c00324

Furuhashi, T., Ishii, R., Onishi, H., & Ota, S. (2020). Elucidation of Biochemical Pathways Underlying VOCs Production in A549 Cells. *Frontiers in Molecular Biosciences, 7*, 116. DOI:10.3389/fmolb.2020.00116

Galateau-Salle, F., Churg, A., Roggli, V., & Travis, W. D. (2016). The 2015 World Health Organization Classification of Tumors of the Pleura: Advances since the 2004 Classification. *Journal of Thoracic Oncology, 11*(2), 142-154. DOI:10.1016/j.jtho.2015.11.005

Gaude, E., Nakhleh, M. K., Patassini, S., Boschmans, J., Allsworth, M., Boyle, B., & van der Schee, Marc P. (2019). Targeted breath analysis: exogenous volatile organic compounds (EVOC) as metabolic pathway-specific probes. *Journal of Breath Research, 13*(3), 032001. DOI:10.1088/1752-7163/ab1789

Gendron, K. B., Hockstein, N. G., Thaler, E. R., Vachani, A., & Hanson, C. W. (2007). In vitro discrimination of tumor cell lines with an electronic

nose. *Otolaryngology-Head and Neck Surgery, 137*(2), 269-273. DOI:10.1016/j.otohns.2007.02.005

Goossens, N., Nakagawa, S., Sun, X., & Hoshida, Y. (2015). Cancer biomarker discovery and validation. *Translational Cancer Research, 4*(3), 256-269. DOI:10.3978/j.issn.2218-676X.2015.06.04

Gromski, P. S., Muhamadali, H., Ellis, D. I., Xu, Y., Correa, E., Turner, M. L., & Goodacre, R. (2015). A tutorial review: Metabolomics and partial least squares-discriminant analysis – a marriage of convenience or a shotgun wedding. *Analytica Chimica Acta, 879*, 10-23. DOI:10.1016/j.aca.2015.02.012

Grove, D., Miller-Atkins, G., Melillo, C., Rieder, F., Kurada, S., Rotroff, D. M., Tonelli, A. R., & Dweik, R. A. (2020). Comparison of volatile organic compound profiles in exhaled breath versus plasma headspace in different diseases. *Journal of Breath Research, 14*(3), 036003. DOI:10.1088/1752-7163/ab8866

Hanahan, D. (2022). Hallmarks of Cancer: New Dimensions. *Cancer Discovery, 12*(1), 31-46. DOI:10.1158/2159-8290.CD-21-1059

Hanahan, D., & Weinberg, R. (2011). Hallmarks of Cancer: The Next Generation. *Cell, 144*(5), 646-674. DOI:10.1016/j.cell.2011.02.013

Handa, H., Usuba, A., Maddula, S., Baumbach, J. I., Mineshita, M., & Miyazawa, T. (2014). Exhaled breath analysis for lung cancer detection using ion mobility spectrometry. *PLoS ONE, 9*(12), e114555. DOI:10.1371/journal.pone.0114555

Henderson, B., Ruszkiewicz, D. M., Wilkinson, M., Beauchamp, J. D., Cristescu, S. M., Fowler, S. J., Salman, D., Francesco, F. D., Koppen, G., Langejürgen, J., Holz, O., Hadjithekli, A., Moreno, S., Pedrotti, M., Sinues, P., Slingers, G., Wilde, M., Lomonaco, T., Zanella, D., . . . Thomas, C. L. P. (2020). A benchmarking protocol for breath analysis: the peppermint experiment. *Journal of Breath Research, 14*(4), 46008-046008. DOI:10.1088/1752-7163/aba130

Hiriart, E., Deepe, R., & Wessels, A. (2019). Mesothelium and Malignant Mesothelioma. *Journal of Developmental Biology, 7*(2), 7. DOI:10.3390/jdb7020007

Hylebos, M., Van Camp, G., van Meerbeeck, J. P., & Op de Beeck, K. (2016). The Genetic Landscape of Malignant Pleural Mesothelioma: Results from Massively Parallel Sequencing. *Journal of Thoracic Oncology, 11*(10), 1615-1626. DOI:10.1016/j.jtho.2016.05.020

Issitt, T., Wiggins, L., Veysey, M., Sweeney, S. T., Brackenbury, W. J., & Redeker, K. (2022). Volatile compounds in human breath: critical review and meta-analysis. *Journal of Breath Research, 16*(2), 024001. DOI:10.1088/1752-7163/ac5230

Janssens, E., Mol, Z., Vandermeersch, L., Lagniau, S., Vermaelen, K. Y., van Meerbeeck, J. P., Walgraeve, C., Marcq, E., & Lamote, K. (2022). Headspace Volatile Organic Compound Profiling of Pleural Mesothelioma and Lung Cancer Cell Lines as Translational Bridge for Breath Research. *Frontiers in Oncology, 12*, 851785. DOI:10.3389/fonc.2022.851785

Janssens, E., Schillebeeckx, E., Zwijsen, K., Raskin, J., Van Cleemput, J., Surmont, V. F., Nackaerts, K., Marcq, E., van Meerbeeck, J. P., & Lamote, K. (2022b). External Validation of a Breath-Based Prediction Model for Malignant Pleural Mesothelioma. *Cancers*, *14*(13), 3182. DOI:10.3390/cancers14133182

Janssens, E., van Meerbeeck, J. P., & Lamote, K. (2020). Volatile organic compounds in human matrices as lung cancer biomarkers: a systematic review. *Critical Reviews in Oncology/Hematology, 153*, 103037. DOI:10.1016/j.critrevonc.2020.103037

Jensen, C., & Teng, Y. (2020). Is It Time to Start Transitioning From 2D to 3D Cell Culture? *Frontiers in Molecular Biosciences, 7*, 33. DOI: 10.3389/fmolb.2020.00033

Jensen, D. E., Proctor, M., Minna, J., Borodovsky, A., Schultz, D. C., Wilkinson, K. D., Maul, G. G., Barlev, N., Berger, S. L., Prendergast, G. C., Rauscher, F. J., Marquis, S. T., Gardner, H. P., Ha, S. I., Chodosh, L. A., Ishov, A. M., Tommerup, N., Vissing, H., & Sekido, Y. (1998). BAP1: a novel ubiquitin hydrolase which binds to the BRCA1 RING finger and enhances BRCA1-mediated cell growth suppression. *Oncogene, 16*(9), 1097-1112. DOI:10.1038/sj.onc.1201861

Jia, Z., Zhang, H., Ong, C. N., Patra, A., Lu, Y., Lim, C. T., & Venkatesan, T. (2018a). Detection of Lung Cancer: Concomitant Volatile Organic Compounds and Metabolomic Profiling of Six Cancer Cell Lines of Different Histological Origins. *ACS Omega, 3*(5), 5131-5140. DOI:10.1021/acsomega.7b02035

Jiang, X., Yu, L., Sun, Y., Li, Y., Li, H., & Lv, Y. (2021). Hollow zeolitic imidazolate framework-7 coated stainless steel fiber for solid phase microextraction of volatile biomarkers in headspace gas of breast cancer cell lines. *Analytica Chimica Acta, 1181*, 338901. DOI:10.1016/j.aca.2021.338901

Jiménez-Pacheco, A., Salinero-Bachiller, M., Iribar, M. C., López-Luque, A., Miján-Ortiz, J. L., & Peinado, J. M. (2018). Furan and p-xylene as candidate biomarkers for prostate cancer. *Urologic Oncology, 36*(5), 243.e21-243.e27. DOI:10.1016/j.urolonc.2017.12.026

Kalluri, U., Naiker, M., & Myers, M. A. (2014). Cell culture metabolomics in the diagnosis of lung cancer-the influence of cell culture conditions. *Journal of Breath Research, 8*(2), 027109. DOI:10.1088/1752-7155/8/2/027109

Klebe, S., Leigh, J., Henderson, D. W., & Nurminen, M. (2019). Asbestos, Smoking and Lung Cancer: An Update. *International Journal of Environmental Research and Public Health, 17*(1), 258. DOI:10.3390/ijerph17010258

Klemenz, A., Meyer, J., Ekat, K., Bartels, J., Traxler, S., Schubert, J. K., Kamp, G., Miekisch, W., & Peters, K. (2019). Differences in the Emission of Volatile

Organic Compounds (VOCs) between Non-Differentiating and Adipogenically Differentiating Mesenchymal Stromal/Stem Cells from Human Adipose Tissue. *Cells, 8*(7), 697. DOI:10.3390/cells8070697

Koureas, M., Kirgou, P., Amoutzias, G., Hadjichristodoulou, C., Gourgoulianis, K., & Tsakalof, A. (2020). Target Analysis of Volatile Organic Compounds in Exhaled Breath for Lung Cancer Discrimination from Other Pulmonary Diseases and Healthy Persons. *Metabolites, 10*(8), 317. DOI:10.3390/metabo10080317

Krilaviciute, A., Leja, M., Kopp-Schneider, A., Barash, O., Khatib, S., Amal, H., Broza, Y. Y., Polaka, I., Parshutin, S., Rudule, A., Haick, H., & Brenner, H. (2019). Associations of diet and lifestyle factors with common volatile organic compounds in exhaled breath of average-risk individuals. *Journal of Breath Research, 13*(2), 026006. DOI:10.1088/1752-7163/aaf3dc

Kure, S., Satoi, S., Kitayama, T., Nagase, Y., Nakano, N., Yamada, M., Uchiyama, N., Miyashita, S., Iida, S., Takei, H., & Miyashita, M. (2021). A prediction model using 2-propanol and 2-butanone in urine distinguishes breast cancer. *Scientific Reports, 11*(1), 19801. DOI:10.1038/s41598-021-99396-5

Lagniau, S., Lamote, K., van Meerbeeck, J. P., & Vermaelen, K. Y. (2017). Biomarkers for early diagnosis of malignant mesothelioma: Do we need another moonshot? *Oncotarget, 8*(32), 53751-53762. DOI:10.18632/oncotarget.17910

Lamote, K., Brinkman, P., Vandermeersch, L., Vynck, M., Sterk, P. J., van Langenhove, H., Thas, O., van Cleemput, J., Nackaerts, K., & van Meerbeeck, J.

P. (2017). Breath analysis by gas chromatography-mass spectrometry and electronic nose to screen for pleural mesothelioma: a cross-sectional case-control study. *Oncotarget, 8*(53), 91593-91602. DOI:10.18632/oncotarget.21335

Lamote, K., Vynck, M., Thas, O., Van Cleemput, J., Nackaerts, K., & van Meerbeeck, J. P. (2017b). Exhaled breath to screen for malignant pleural mesothelioma: a validation study. *The European Respiratory Journal, 50*(6), 1700919. DOI:10.1183/13993003.00919-2017

Lamote, K., Vynck, M., Van Cleemput, J., Thas, O., Nackaerts, K., & van Meerbeeck, J. P. (2016). Detection of malignant pleural mesothelioma in exhaled breath by multicapillary column/ion mobility spectrometry (MCC/IMS). *Journal of Breath Research, 10*(4), 046001. DOI:10.1088/1752-7155/10/4/046001

Lansley, S. M., Searles, R. G., Hoi, A., Thomas, C., Moneta, H., Herrick, S. E., Thompson, P. J., Mark, N., Sterrett, G. F., Prêle, C. M., & Mutsaers, S. E. (2011). Mesothelial cell differentiation into osteoblast- and adipocyte-like cells. *Journal of Cellular and Molecular Medicine, 15*(10), 2095-2105. DOI:10.1111/j.1582-4934.2010.01212.x

Lawal, O., Knobel, H., Weda, H., Bos, L. D., Nijsen, T. M. E., Goodacre, R., & Fowler, S. J. (2018). Volatile organic compound signature from co-culture of lung epithelial cell line with Pseudomonas aeruginosa. *Analyst, 143*(13), 3148-3155. DOI:10.1039/C8AN00759D

Leiherer, A., Ślefarska, D., Leja, M., Heinzle, C., Mündlein, A., Kikuste, I., Mezmale, L., Drexel, H., Mayhew, C. A., & Mochalski, P. (2020). The Volatilomic Footprints of Human HGC-27 and CLS-145 Gastric Cancer Cell Lines. *Frontiers in Molecular Biosciences, 7*, 607904. DOI:10.3389/fmolb.2020.607904

Li, J., Chen, N., Tian, Y., & Xu, H. (2018). Solid-phase microextraction of volatile organic compounds in headspace of PM-induced MRC-5 cell lines. *Talanta, 185*, 23-29. DOI:10.1016/j.talanta.2018.03.041

Li, L., & Zhao, J. (2009). Determination of the Volatile Composition of Rhodobryum giganteum (Schwaegr.) Par. (Bryaceae) Using Solid-phase Microextraction and Gas Chromatography/Mass Spectrometry (GC/MS). *Molecules, 14*(6), 2195-2201. DOI:10.3390/molecules14062195

Lima, A. R., Araújo, A. M., Pinto, J., Jerónimo, C., Henrique, R., Bastos, M. d. L., Carvalho, M., & Guedes de Pinho, P. (2018). Discrimination between the human prostate normal and cancer cell exometabolome by GC-MS. *Scientific Reports, 8*(1), 5539-12. DOI:10.1038/s41598-018-23847-9

Little, L. D., Carolan, V. A., Allen, K. E., Cole, L. M., & Haywood-Small, S. L. (2020). Headspace analysis of mesothelioma cell lines differentiates biphasic and epithelioid sub-types. *Journal of Breath Research, 14*(4), 046011. DOI:10.1088/1752-7163/abaaff

Liu, D., Ji, L., Li, M., Li, D., Guo, L., Nie, M., Wang, D., Lv, Y., Bai, Y., Liu, M., Wang, G., Li, Y., Yu, P., Li, E., & Wang, C. (2019). Analysis of volatile organic

compounds released from SW480 colorectal cancer cells and the blood of tumor-bearing mice. *Translational Cancer Research, 8*(8), 2736-2751. DOI:10.21037/tcr.2019.10.21

Liu, D., Gao, Y., Li, X., Li, Z., & Pan, Q. (2015). Attenuated UV Radiation Alters Volatile Profile in Cabernet Sauvignon Grapes under Field Conditions. *Molecules, 20*(9), 16946-16969. DOI:10.3390/molecules200916946

Liu, H., Wang, H., Li, C., Wang, L., Pan, Z., & Wang, L. (2014). Investigation of volatile organic metabolites in lung cancer pleural effusions by solid-phase microextraction and gas chromatography/mass spectrometry. *Journal of Chromatography. B, Analytical Technologies in the Biomedical and Life Sciences, 945-946*, 53-59. DOI:10.1016/j.jchromb.2013.11.038

Liu, M., Li, Y., Wang, G., Guo, N., Liu, D., Li, D., Guo, L., Zheng, X., Yu, K., Yu, K., & Wang, C. (2019). Release of volatile organic compounds (VOCs) from colorectal cancer cell line LS174T. *Analytical Biochemistry, 581*, 113340. DOI:10.1016/j.ab.2019.06.011

Liu, Y., Li, W., & Duan, Y. (2019b). Effect of H 2 O 2 induced oxidative stress (OS) on volatile organic compounds (VOCs) and intracellular metabolism in MCF-7 breast cancer cells. *Journal of Breath Research, 13*(3), 036005. DOI:10.1088/1752-7163/ab14a5

Mahieu, N. G., Genenbacher, J. L., & Patti, G. J. (2016). A roadmap for the XCMS family of software solutions in metabolomics. *Current Opinion in Chemical Biology, 30*, 87-93. DOI:10.1016/j.cbpa.2015.11.009

McCartney, M. M., Linderholm, A. L., Yamaguchi, M. S., Falcon, A. K., Harper, R. W., Thompson, G. R., Ebeler, S. E., Kenyon, N. J., Davis, C. E., & Schivo, M. (2021). Predicting influenza and rhinovirus infections in airway cells utilizing volatile emissions. *The Journal of Infectious Diseases, 224*(10), 1742-1750 DOI:10.1093/infdis/jiab205

McGregor, D. (2010). Tertiary-Butanol: A toxicological review. *Critical Reviews in Toxicology, 40*(8), 697-727. DOI:10.3109/10408444.2010.494249

Meyerhoff, R. R., Yang, C. J., Speicher, P. J., Gulack, B. C., Hartwig, M. G., D'Amico, T. A., Harpole, D. H., & Berry, M. F., (2015). Impact of mesothelioma histologic subtype on outcomes in the Surveillance, Epidemiology, and End Results database. *The Journal of Surgical Research, 196*(1), 23-32. DOI:10.1016/j.jss.2015.01.043

Mezei, G., Chang, E. T., Mowat, F. S., & Moolgavkar, S. H., (2017). Epidemiology of mesothelioma of the pericardium and tunica vaginalis testis. *Annals of Epidemiology, 27*(5), 348-359.e11. DOI:10.1016/j.annepidem.2017.04.001

Mochalski, P., Leja, M., Gasenko, E., Skapars, R., Santare, D., Sivins, A., Aronsson, D. E., Ager, C., Jaeschke, C., Shani, G., Mitrovics, J., Mayhew, C. A., & Haick, H. (2018). Ex vivo emission of volatile organic compounds from gastric

cancer and non-cancerous tissue. *Journal of Breath Research, 12*(4), 046005. DOI:10.1088/1752-7163/aacbfb

Monedeiro, F., Dos Reis, R. B., Peria, F. M., Sares, C. T. G., & De Martinis, B. S. (2020). Investigation of sweat VOC profiles in assessment of cancer biomarkers using HS-GC-MS. *Journal of Breath Research, 14*(2), 026009. DOI:10.1088/1752-7163/ab5b3c

Monedeiro, F., Monedeiro-Milanowski, M., Ratiu, I., Brożek, B., Ligor, T., & Buszewski, B. (2021). Needle Trap Device-GC-MS for Characterization of Lung Diseases Based on Breath VOC Profiles. *Molecules, 26*(6), 1789. DOI:10.3390/molecules26061789

Murgia, A., Ahmed, Y., Sweeney, K., Nicholson-Scott, L., Arthur, K., Allsworth, M., Boyle, B., Gandelman, O., Smolinska, A., & Ferrandino, G. (2021). Breath-Taking Perspectives and Preliminary Data toward Early Detection of Chronic Liver Diseases. *Biomedicines, 9*(11), 1563. DOI:10.3390/biomedicines9111563

Mutti, L., Peikert, T., Robinson, B. W. S., Scherpereel, A., Tsao, A. S., de Perrot, M., Woodard, G. A., Jablons, D. M., Wiens, J., Hirsch, F. R., Yang, H., Carbone, M., Thomas, A., & Hassan, R. (2018). Scientific Advances and New Frontiers in Mesothelioma Therapeutics. *Journal of Thoracic Oncology, 13*(9), 1269-1283. DOI:10.1016/j.jtho.2018.06.011

Nath, S., & Devi, G. R. (2016). Three-dimensional culture systems in cancer research: Focus on tumor spheroid model. *Pharmacology & Therapeutics, 163*, 94-108. DOI:10.1016/j.pharmthera.2016.03.013

Onghena, M., van Hoeck, E., Vervliet, P., Scippo, M. L., Simon, C., van Loco, J., & Covaci, A. (2014). Development and application of a non-targeted extraction method for the analysis of migrating compounds from plastic baby bottles by GC-MS. *Food Additives & Contaminants. Part A, Chemistry, Analysis, Control, Exposure & Risk Assessment, 31*(12), 2090-2102. DOI:10.1080/19440049.2014.979372

Orywal, K., & Szmitkowski, M. (2016). Alcohol dehydrogenase and aldehyde dehydrogenase in malignant neoplasms. *Clinical and Experimental Medicine, 17*(2), 131-139. DOI:10.1007/s10238-016-0408-3

Ottensmann, M., Stoffel, M. A., Nichols, H. J., & Hoffman, J. I. (2018). GCalignR: An R package for aligning gas-chromatography data for ecological and evolutionary studies. *PloS One, 13*(6), e0198311. DOI:10.1371/journal.pone.0198311

Pang, X., Guo, X., Qin, Z., Yao, Y., Hu, X., & Wu, J. (2012). Identification of Aroma-Active Compounds in Jiashi Muskmelon Juice by GC-O-MS and OAV Calculation. *Journal of Agricultural and Food Chemistry, 60*(17), 4179-4185. DOI:10.1021/jf300149m

Pang, Z., Chong, J., Zhou, G., de Lima Morais, D. A., Chang, L., Barrette, M., Gauthier, C., Jacques, P., Li, S., & Xia, J. (2021). MetaboAnalyst 5.0: narrowing the gap between raw spectra and functional insights. *Nucleic Acids Research, 49*(W1), W388-W396. DOI:10.1093/nar/gkab382

Papaefstathiou, E., Stylianou, M., Andreou, C., & Agapiou, A. (2020). Breath analysis of smokers, non-smokers, and e-cigarette users. *Journal of Chromatography. B, Analytical Technologies in the Biomedical and Life Sciences, 1160*, 122349. DOI:10.1016/j.jchromb.2020.122349

Pauling, L., Robinson, A. B., Teranishi, R., & Cary, P. (1971). Quantitative Analysis of Urine Vapor and Breath by Gas-Liquid Partition Chromatography. *Proceedings of the National Academy of Sciences - PNAS, 68*(10), 2374-2376. DOI:10.1073/pnas.68.10.2374

Peled, N., Barash, O., Tisch, U., Ionescu, R., Broza, Y. Y., Ilouze, M., Mattei, J., Bunn, P. A., Hirsch, F. R., & Haick, H. (2013). Volatile fingerprints of cancer specific genetic mutations. *Nanomedicine, 9*(6), 758-766. DOI:10.1016/j.nano.2013.01.008

Petersen, J. H., & Lund, K. H. (2003). Migration of 2-butoxyethyl acetate from polycarbonate infant feeding bottles. *Food Additives and Contaminants, 20*(12), 1178-1185. DOI:10.1080/02652030310001605970

Piqueret, B., Bourachot, B., Leroy, C., Devienne, P., Mechta-Grigoriou, F., d'Ettorre, P., & Sandoz, J. (2022). Ants detect cancer cells through volatile organic compounds. *iScience, 25*(3), 103959. DOI:10.1016/j.isci.2022.103959

Pleil, J. D., & Williams, A. (2019). Centralized resource for chemicals from the human volatilome in an interactive open-sourced database. *Journal of Breath Research, 13*(4), 040201. DOI:10.1088/1752-7163/ab2fa2

Purcaro, G., Rees, C. A., Wieland-Alter, W. F., Schneider, M. J., Wang, X., Stefanuto, P., Wright, P. F., Enelow, R. I., & Hill, J. E. (2018). Volatile fingerprinting of human respiratory viruses from cell culture. *Journal of Breath Research, 12*(2), 026015. DOI:10.1088/1752-7163/aa9eef

Purcaro, G., Stefanuto, P., Franchina, F. A., Beccaria, M., Wieland-Alter, W. F., Wright, P. F., & Hill, J. E. (2018b). SPME-GC×GC-TOF MS fingerprint of virally-infected cell culture: Sample preparation optimization and data processing evaluation. *Analytica Chimica Acta, 1027*, 158-167. DOI:10.1016/j.aca.2018.03.037

Ratcliffe, N., Wieczorek, T., Drabi ska, N., Gould, O., Osborne, A., & De Lacy Costello, B. (2020). A mechanistic study and review of volatile products from peroxidation of unsaturated fatty acids: an aid to understanding the origins of volatile organic compounds from the human body. *Journal of Breath Research, 14*(3), 034001. DOI:10.1088/1752-7163/ab7f9d

Rattray, N. J. W., Hamrang, Z., Trivedi, D. K., Goodacre, R., & Fowler, S. J. (2014). Taking your breath away: metabolomics breathes life in to personalized medicine. *Trends in Biotechnology, 32*(10), 538-548. DOI:10.1016/j.tibtech.2014.08.003

Reiser, J., Kutner, R. H., & Zhang, X. (2009). Production, concentration and titration of pseudotyped HIV-1-based lentiviral vectors. *Nature Protocols, 4*(4), 495-505. DOI:10.1038/nprot.2009.22

Ribatti, D. (2016). The chick embryo chorioallantoic membrane (CAM). A multifaceted experimental model. *Mechanisms of Development, 141*, 70-77. DOI:10.1016/j.mod.2016.05.003

Ribatti, D. (2017). The chick embryo chorioallantoic membrane (CAM) assay. *Reproductive Toxicology, 70*, 97-101. DOI:10.1016/j.reprotox.2016.11.004

Rodrigues, D., Pinto, J., Araújo, A. M., Monteiro-Reis, S., Jerónimo, C., Henrique, R., de Lourdes Bastos, M., de Pinho, P. G., & Carvalho, M. (2018). Volatile metabolomic signature of bladder cancer cell lines based on gas chromatography–mass spectrometry. *Metabolomics, 14*(5), 62-15. DOI:10.1007/s11306-018-1361-9

Røe, O. D., & Stella, G. M. (2015). Malignant pleural mesothelioma: history, controversy and future of a manmade epidemic. *European Respiratory Review, 24*(135), 115-131. DOI:10.1183/09059180.00007014

Rutter, A. V., Chippendale, T. W. E., Yang, Y., Špan l, P., Smith, D., & Sulé-Suso, J. (2012). Quantification by SIFT-MS of acetaldehyde released by lung cells in a 3D model. *Analyst, 138*(1), 91-95. DOI:10.1039/c2an36185j

Ruzsányi, V., & Péter Kalapos, M. (2017). Breath acetone as a potential marker in clinical practice. *Journal of Breath Research, 11*(2), 024002. DOI:10.1088/1752-7163/aa66d3

Saalberg, Y., & Wolff, M. (2016). VOC breath biomarkers in lung cancer. *Clinica Chimica Acta, 459*, 5-9. DOI:10.1016/j.cca.2016.05.013

Sajid, M., Khaled Nazal, M., Rutkowska, M., Szczepańska, N., Namieśnik, J., & Płotka-Wasylka, J. (2019). Solid Phase Microextraction: Apparatus, Sorbent Materials, and Application. *Critical Reviews in Analytical Chemistry, 49*(3), 271-288. DOI:10.1080/10408347.2018.1517035

Schafer, M., Gachanja, A., Turner, D. C., Lancaster, S., Janmohamed, I., & Creasey, J. (2019). *Gas chromatography-mass spectrometry: how do I get the best results?* London, UK: Royal Society of Chemistry.

Schallschmidt, K., Becker, R., Jung, C., Rolff, J., Fichtner, I., & Nehls, I. (2015). Investigation of cell culture volatilomes using solid phase micro extraction: Options and pitfalls exemplified with adenocarcinoma cell lines. *Journal of Chromatography. B, Analytical Technologies in the Biomedical and Life Sciences, 1006*, 158-166. DOI:10.1016/j.jchromb.2015.10.004

Schillebeeckx, E., van Meerbeeck, J. P., & Lamote, K. (2021). Clinical utility of diagnostic biomarkers in malignant pleural mesothelioma: a systematic review and meta-analysis. *European Respiratory Review, 30*(162), 210057. DOI:10.1183/16000617.0057-2021

Sementino, E., Menges, C. W., Kadariya, Y., Peri, S., Xu, J., Liu, Z., Wilkes, R. G., Cai, K. Q., Rauscher, F. J., Klein-Szanto, A. J., & Testa, J. R. (2018). Inactivation of Tp53 and Pten drives rapid development of pleural and peritoneal malignant mesotheliomas. *Journal of Cellular Physiology, 233*(11), 8952-8961. DOI:10.1002/jcp.26830

Serasanambati, M., Broza, Y. Y., Marmur, A., & Haick, H. (2019). Profiling Single Cancer Cells with Volatolomics Approach. *iScience, 11*, 178-188. DOI:10.1016/j.isci.2018.12.008

Shestivska, V., Rutter, A. V., Sulé-Suso, J., Smith, D., & Španěl, P. (2017). Evaluation of peroxidative stress of cancer cells in vitro by real-time quantification of volatile aldehydes in culture headspace. *Rapid Communications in Mass Spectrometry, 31*(16), 1344-1352. DOI:10.1002/rcm.7911

Shetewi, T., Finnegan, M., Fitzgerald, S., Xu, S., Duffy, E., & Morrin, A. (2021). Investigation of the relationship between skin-emitted volatile fatty acids and skin surface acidity in healthy participants-a pilot study. *Journal of Breath Research, 15*(3), 37101. DOI:10.1088/1752-7163/abf20a

Siegel, R. L., Miller, K. D., Fuchs, H. E., & Jemal, A. (2022). Cancer statistics, 2022. *CA: A Cancer Journal for Clinicians, 72*(1), 7-33. DOI:10.3322/caac.21708

Silva, C. L., Perestrelo, R., Silva, P., Tomás, H., & Câmara, J. S. (2017). Volatile metabolomic signature of human breast cancer cell lines. *Scientific Reports, 7*(1), 43969. DOI:10.1038/srep43969

Slaughter, R. J., Mason, R. W., Beasley, D. M. G., Vale, J. A., & Schep, L. J. (2014). Isopropanol poisoning. *Clinical Toxicology, 52*(5), 470-478. DOI:10.3109/15563650.2014.914527

Smolinska, A., Hauschild, A., Fijten, R. R. R., Dallinga, J. W., Baumbach, J., & van Schooten, F. J. (2014). Current breathomics-a review on data pre-processing techniques and machine learning in metabolomics breath analysis. *Journal of Breath Research, 8*(2), 027105. DOI:10.1088/1752-7155/8/2/027105

Sola Martínez, R. A., Pastor Hernández, J. M., Lozano Terol, G., Gallego-Jara, J., García-Marcos, L., Cánovas Díaz, M., & de Diego Puente, T. (2020). Data preprocessing workflow for exhaled breath analysis by GC/MS using open sources. *Scientific Reports, 10*(1), 22008. DOI:10.1038/s41598-020-79014-6

Solbes, E., & Harper, R. W. (2018). Biological responses to asbestos inhalation and pathogenesis of asbestos-related benign and malignant disease. *Journal of Investigative Medicine, 66*(4), 721-727. DOI:10.1136/jim-2017-000628

Sparkman, O. D., Penton, Z., & Kitson, F. G. (2011). *Gas Chromatography and Mass Spectrometry*. Amsterdam, Netherlands: Elsevier Science & Technology.

Sponring, A., Filipiak, W., Mikoviny, T., Ager, C., Schubert, J., Miekisch, W., Amann, A., & Troppmair, J. (2009). Release of Volatile Organic Compounds from the Lung Cancer Cell Line NCI-H2087 In Vitro. *Anticancer Research, 29*(1), 419-426.

Stashenko, E. E., & Martínez, J. R. (2007). Sampling volatile compounds from natural products with headspace/solid-phase micro-extraction. *Journal of Biochemical and Biophysical Methods, 70*(2), 235-242. DOI:10.1016/j.jbbm.2006.08.011

Sugita, K., & Sato, H. (2021). Sample Introduction Method in Gas Chromatography. *Analytical Sciences, 37*(1), 159-165. DOI:10.2116/analsci.20SAR19

Sung, H., Ferlay, J., Siegel, R. L., Laversanne, M., Soerjomataram, I., Jemal, A., & Bray, F. (2021). Global Cancer Statistics 2020: GLOBOCAN Estimates of Incidence and Mortality Worldwide for 36 Cancers in 185 Countries. *CA: A Cancer Journal for Clinicians, 71*(3), 209-249. DOI:10.3322/caac.21660

Tang, H., Lu, Y., Zhang, L., Wu, Z., Hou, X., & Xia, H. (2017). Determination of volatile organic compounds exhaled by cell lines derived from hematological malignancies. *Bioscience Reports, 37*(3), BSR20170106, DOI:10.1042/BSR20170106

Taware, R., Taunk, K., Kumar, T. V. S., Pereira, J. A. M., Câmara, J. S., Nagarajaram, H. A., Kundu, G. C., & Rapole, S. (2020). Extracellular volatilomic alterations induced by hypoxia in breast cancer cells. *Metabolomics, 16*(2), 21. DOI:10.1007/s11306-020-1635-x

Testa, J. R., Carbone, M., Cheung, M., Pei, J., Below, J. E., Tan, Y., Sementino, E., Cox, N. J., Dogan, A. U., Pass, H. I., Trusa, S., Hesdorffer, M., Nasu, M., Powers, A., Rivera, Z., Comertpay, S., Tanji, M., Gaudino, G., & Yang, H. (2011). Germline BAP1 mutations predispose to malignant mesothelioma. *Nature Genetics, 43*(10), 1022-1025. DOI:10.1038/ng.912

Thriumani, R., Zakaria, A., Hashim, Y. Z. H., Jeffree, A. I., Helmy, K. M., Kamarudin, L. M., Omar, M. I., Shakaff, A. Y. M., Adom, A. H., & Persaud, K. C. (2018). A study on volatile organic compounds emitted by in-vitro lung cancer cultured cells using gas sensor array and SPME-GCMS. *BMC Cancer, 18*(1), 362. DOI:10.1186/s12885-018-4235-7

Töreyin, Z. N., Ghosh, M., Göksel, Ö, Göksel, T., & Godderis, L. (2020). Exhaled Breath Analysis in Diagnosis of Malignant Pleural Mesothelioma: Systematic Review. *International Journal of Environmental Research and Public Health, 17*(3), 1110. DOI:10.3390/ijerph17031110

Torre, L. A., Siegel, R. L., Ward, E. M., & Jemal, A. (2016). Global Cancer Incidence and Mortality Rates and Trends--An Update. *Cancer Epidemiology, Biomarkers & Prevention, 25*(1), 16-27. DOI:10.1158/1055-9965.EPI-15-0578

Traxler, S., Barkowsky, G., Saß, R., Klemenz, A., Patenge, N., Kreikemeyer, B., Schubert, J. K., & Miekisch, W. (2019). Volatile scents of influenza A and S. pyogenes (co-)infected cells. *Scientific Reports, 9*(1), 18894-12. DOI:10.1038/s41598-019-55334-0

Traxler, S., Bischoff, A., Trefz, P., Schubert, J. K., & Miekisch, W. (2018). Versatile set-up for non-invasive in vitro analysis of headspace VOCs. *Journal of Breath Research, 12*(4), 041001. DOI:10.1088/1752-7163/aaccad

Triba, M. N., Le Moyec, L., Amathieu, R., Goossens, C., Bouchemal, N., Nahon, P., Rutledge, D. N., & Savarin, P. (2015). PLS/OPLS models in metabolomics: the impact of permutation of dataset rows on the K-fold cross-validation quality parameters. *Molecular bioSystems, 11*(1), 13-19. DOI:10.1039/C4MB00414K

Ulanowska, A., Kowalkowski, T., Trawińska, E., & Buszewski, B. (2011). The application of statistical methods using VOCs to identify patients with lung cancer. *Journal of Breath Research, 5*(4), 046008. DOI:10.1088/1752-7155/5/4/046008

van Zandwijk, N., Reid, G., & Frank, A. L. (2020). Asbestos-related cancers: the 'Hidden Killer' remains a global threat. *Expert Review of Anticancer Therapy, 20*(4), 271-278. DOI:10.1080/14737140.2020.1745067

Wagner, J. C., Sleggs, C. A., & Marchand, P. (1960). Diffuse Pleural Mesothelioma and Asbestos Exposure in the North Western Cape

Province. *British Journal of Industrial Medicine, 17*(4), 260-271. DOI:10.1136/oem.17.4.260

Wang, A., Papneja, A., Hyrcza, M., Al-Habeeb, A., & Ghazarian, D. (2016). BAP1: gene of the month. *Journal of Clinical Pathology, 69*(9), 750-753. DOI:10.1136/jclinpath-2016-203866

Wang, C., Li, P., Lian, A., Sun, B., Wang, X., Guo, L., Chi, C., Liu, S., Zhao, W., Luo, S., Guo, Z., Zhang, Y., Ke, C., Ye, G., Xu, G., Zhang, F., & Li, E. (2014). Blood volatile compounds as biomarkers for colorectal cancer. *Cancer Biology & Therapy, 15*(2), 200-206. DOI:10.4161/cbt.26723

Wang, C., Dong, R., Wang, X., Lian, A., Chi, C., Ke, C., Guo, L., Liu, S., Zhao, W., Xu, G., & Li, E. (2014b). Exhaled volatile organic compounds as lung cancer biomarkers during one-lung ventilation. *Scientific Reports, 4*(1), 7312. DOI:10.1038/srep07312

Wang, G., Li, Y., Liu, M., Guo, N., Han, C., Liu, D., Li, D., Yang, M., Peng, Y., Liu, Y., Yu, K., & Wang, C. (2019). Determination of volatile organic compounds in SW620 colorectal cancer cells and tumor-bearing mice. *Journal of Pharmaceutical and Biomedical Analysis, 167*, 30-37. DOI:10.1016/j.jpba.2019.01.050

Wenig, P., & Odermatt, J. (2010). OpenChrom: a cross-platform open source software for the mass spectrometric analysis of chromatographic data. *BMC Bioinformatics, 11*(1), 405. DOI:10.1186/1471-2105-11-405

Wilk, E., & Krówczyńska, M. (2021). Malignant mesothelioma and asbestos exposure in Europe: Evidence of spatial clustering. *Geospatial Health, 16*(1), 91-102. DOI:10.4081/gh.2021.951

Wilkinson, M., White, I., Hamshere, K., Holz, O., Schuchardt, S., Bellagambi, F. G., Lomonaco, T., Biagini, D., Di, F. F., Fowler, S. J., Beauchamp, J. D., Cristescu, S. M., Focant, J. F., Franchina, F. A., Grassin-Delyle, S., Hadjithekli, A., Henderson, B., Koppen, G. F., Langejürgen, J., . . . Zenobi, R. (2021). The peppermint breath test: A benchmarking protocol for breath sampling and analysis using GC-MS. *Journal of Breath Research, 15*(2), 26006. DOI:10.1088/1752-7163/abd28c

Wu, S., Zhu, W., Thompson, P., & Hannun, Y. A. (2018). Evaluating intrinsic and non-intrinsic cancer risk factors. *Nature Communications, 9*(1), 3490-12. DOI:10.1038/s41467-018-05467-z

Xu, J., Kadariya, Y., Peng, H., Karar, J., Rauscher, F. J., Testa, J. R., Cheung, M., Pei, J., Talarchek, J., Sementino, E., Tan, Y., Menges, C. W., Cai, K. Q., & Litwin, S. (2014). Germline mutation of Bap1 accelerates development of asbestos-induced malignant mesothelioma. *Cancer Research, 74*(16), 4388-4397. DOI:10.1158/0008-5472.CAN-14-1328

Yamaguchi, M. S., McCartney, M. M., Falcon, A. K., Linderholm, A. L., Ebeler, S. E., Kenyon, N. J., Harper, R. H., Schivo, M., & Davis, C. E. (2019). Modeling cellular metabolomic effects of oxidative stress impacts from hydrogen peroxide

and cigarette smoke on human lung epithelial cells. *Journal of Breath Research, 13*(3), 036014. DOI:10.1088/1752-7163/ab1fc4

Yamaguchi, M. S., McCartney, M. M., Linderholm, A. L., Ebeler, S. E., Schivo, M., & Davis, C. E. (2018). Headspace sorptive extraction-gas chromatography–mass spectrometry method to measure volatile emissions from human airway cell cultures. *Journal of Chromatography. B, Analytical Technologies in the Biomedical and Life Sciences, 1090*, 36-42. DOI:10.1016/j.jchromb.2018.05.009

Yap, T. A., Aerts, J. G., Popat, S., & Fennell, D. A. (2017). Novel insights into mesothelioma biology and implications for therapy. *Nature Reviews. Cancer, 17*(8), 475-488. DOI:10.1038/nrc.2017.42

Zalcman, G., Mazieres, J., Margery, J., Greillier, L., Audigier-Valette, C., Moro-Sibilot, D., Molinier, O., Corre, R., Monnet, I., Gounant, V., Rivière, F., Janicot, H., Gervais, R., Locher, C., Milleron, B., Tran, Q., Lebitasy, M., Morin, F., Creveuil, C., . . . Scherpereel, A. (2015). Bevacizumab for newly diagnosed pleural mesothelioma in the Mesothelioma Avastin Cisplatin Pemetrexed Study (MAPS): a randomised, controlled, open-label, phase 3 trial. *The Lancet, 387*(10026), 1405-1414. DOI:10.1016/S0140-6736(15)01238-6

Zanella, D., Henket, M., Schleich, F., Dejong, T., Louis, R., Focant, J., & Stefanuto, P. (2020). Comparison of the effect of chemically and biologically induced inflammation on the volatile metabolite production of lung epithelial cells by GC×GC-TOFMS. *Analyst, 145*(15), 5148-5157. DOI:10.1039/d0an00720j

Zou, Y., Zhang, X., Chen, X., Hu, Y., Ying, K., & Wang, P. (2014). Optimization of volatile markers of lung cancer to exclude interferences of non-malignant disease. *Cancer Biomarkers: Section A of Disease Markers, 14*(5), 371-379. DOI:10.3233/CBM-140418